NANOBIOTECHNOLOGY

Editors:
Professor David Andrew Phoenix
London South Bank University, United Kingdom

Professor Waqar Ahmed
University of Central Lancashire (UCLAN), United Kingdom

Contents

Preface

Nanotechnology is one of the most exciting and dynamic fields to emerge over the last 100 years. Governments, industry and academia have invested huge amounts of effort and large sums of money on fundamental research in the search for new or improved applications. New insights have emerged and applications have been developed in semiconductor, automotive, aerospace, textile and cosmetics industries. Nanotechnology is widely expected to have a massive impact on commercial applications in the near future.

Nobel Laureate Richard P. Feynmans' vision, outlined in his famous lecture 'There is Plenty of Room at the Bottom', is finally being realised due to developments in the revolutionary 'microchip' technology that is clearly seen in devices that are now commonly found in electronics shops all over the world. Almost everyone is carrying around a supercomputer in their pockets in the form of a smart phone or tablet.

The academic impact of nanotechnology after Feynman has been recognised with Nobel Prizes being awarded to Curl, Kroto and Smalley for the discovery of C_{60} in 1996 and to Geim and Novoselov (2010) for their ground breaking work on the two-dimensional material Graphene. These and other developments provide a firm foundation for investigating the way in which these nanostructures can be adapted for use in medicine through the development of new electronic interfaces, coatings for medical devices and through the development of new drug delivery mechanisms to name but a few.

Nanomedicine and nanobiomaterials will revolutionise medical treatments and healthcare when interfaced with appropriate control electronics. Over the last 10 years the number of papers in nanomedicine and nanobiomaterials have exploded exponentially from all over the world, particularly from China. The interdisciplinary nature of nanotechnology brings people together from various disciplines, facilities and regions with the common objective of improving lives of everyone regardless of their background, culture and geographical location. It provides not only great scientific potential in terms of output but also provides a framework through which we can shape some of the most dynamic and exciting multidisciplinary research currently in practice

Nanotechnology is so broad that this work only presents a *'small'* perspective on nanotechnology with authors with interdisciplinary backgrounds coming together to provide important insights in nanobiomaterials. We hope that you find this book stimulating, useful and enjoyable and that it sparks your interest to explore this field further.

Professor Waqar Ahmed
Head: Institute of Nanotechnology and Bioengineering, University of Central Lancashire, UK

Professor David A. Phoenix OBE, AcSS, DUniv, DSc.
Vice Chancellor, London South Bank University, UK

Editors

Dave Phoenix – Bio

Professor David Andrew Phoenix, OBE, AcSS, DSc studied Biochemistry at degree and doctoral level at Liverpool University which in 2009 awarded him a Doctor of Science for his impact on the field. In 2000 he was appointed Professor of Biochemistry, at the University of Central Lancashire (UCLan) and has held visiting chairs in Canada, China and Russia. He has over 200 publications as well as a number of edited collections and monographs focused on the structure function relationships of bioactive amphiphilic molecules. He is a Fellow of the Royal Society of Chemistry, The Society of Biology, The Institute of Mathematics and Its Applications and the Royal Society of Medicine. He was elected to Fellowship of the Royal College of Physicians (Edinburgh) for his contribution to medical research and education in 2013 and in 2013 was also appointed Vice Chancellor of London South Bank University. He was made an Officer of the Most Excellent Order of the British Empire in 2010 for services to Science and Higher Education and recognized as an Academician by the Academy of Social Sciences in 2012.

Waqar Ahmed – Bio

Currently **Professor Waqar Ahmed**, CEng FIMMM FRSC is the head of UCLAN Institute of Nanotechnology and Bioengineering, holds the Chair in Nanotechnology and Advanced Manufacturing and is the Divisional Leader for Nanomedicine in the new School of Medicine and Dentistry. Educated at UK Universities of Salford, Strathclyde and Warwick he has established himself as a leading international authority in the emerging and exciting field of Nanotechnology. He has authored over 500 research papers and articles, over a dozen books and been an invited keynote speaker at international conferences throughout the world. Prof Ahmed has served as founding editor-in-chief of several journals including International Journals of Nanomanufacturing; Nano and Biomaterials; and Nanoparticles and is on the advisory board of the Oxford University Press Book Series on Nanomanufacturing with Prof. Jackson from Purdue University. He has also chaired numerous conferences, committees and sessions in the USA, China, Europe, Russia and Middle East. Professor Ahmed is a Fellow of both learned societies Royal Society of Chemistry and the Institute of Materials, Minerals and Mining. He holds honorary and visiting Professorship worldwide at prestigious Universities including Sichuan University (China), Purdue University (USA), Tenessee Technological University (USA), Manchester Metropolitan University (UK), University Roma Torvagata (Italy). His research interests include thin films and nanoparticles and their applications in medicine, dentistry, engineering and energy generation.

1

Chitin Nanofibrils: a Natural Multifunctional Polymer *Physicochemical characteristics, effectiveness and safeness.*

Pierfrancesco Morganti[1*], Francesco Carezzi[2], Paola Del Ciotto[2], Gianluca Morganti[2], Maria Luisa Nunziata[2], XH Gao[3], Hong Duo-Chen[4], Galina Tishenko[5] and Vladimir E. Yudin[6]

[1]Prof. of Skin Pharmacology, Dermatology Depart, 2nd University of Naples, Italy. Visiting Professor, China Medical University, Shenyang, China. Head of R&D, Centre of Nanoscience Mavi Sud s.r.l, Italy
[2]R&D, Centre of Nanoscience Mavi Sud s.r.l, Italy
[3]Prof. of Dermatology, Director, Key Lab of Immunodermatology, Ministry of Health, No 1 Hospital of China Medical University, Shenyang, China
[4]Prof. of Dermatology, Head Depart Dermatology No 1 Hospital of China Medical University Shenyang, China
[5]Institute of Macromolecular Chemistry AS CR, v.v.i., Prague 6, 162 06, Czech Republic
[6]Head Department, Institute of Macromolecular Compounds, Russian Academy of Sciences, St. Petersburg, Russia; St. PetersburgPolytechnic University, 195251, Polytechnicheskaya ul. 29, St. Petersburg, Russia

Outline:

Introduction

Every year about 300 billion tons of industrial and agricultural waste are generated, deriving from processing of plant raw materials into intermediates or final products [1]. Only 3% (13 billion tons/year) of world plant biomass is used for making goods, whilst 20% of 154 billion tons/year of fishery and crustacean's processing are transformed into chitin, chitosan and oligosaccharides, producing waste of 30 million/tons [2, 3]. Hence, a comprehensive overview of the amount of by-products generated in different industrial and agricultural sectors in each country is timely and much needed [4] in order to transform the waste in useful goods by means of environmentally friendly processes (Figure 1.1).
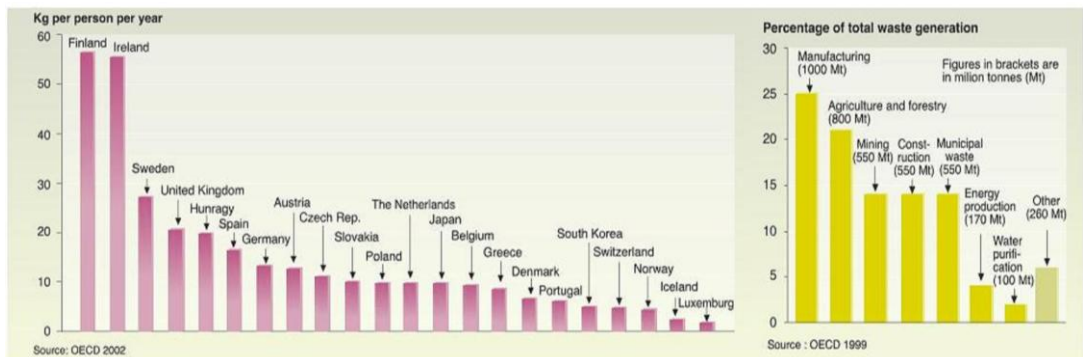
FIGURE 1.1
Waste generated by person per year in different Industrial Sectors and in different Countries.

The recycling and reuse of waste using green technologies will reduce water consumption, greenhouse gas emissions and worldwide pollution without impoverishing of the environment with precious and fundamental materials whilst saving the biodiversity of the Earth [5].
Natural ingredients play an important role in consumer culture, and knowledge and ethic of traditional sourcing of biodiversity have increased strongly, particularly in emerging economies like Brazil and China (Figure 1.2) [5]. In China, 98% of consumers buy cosmetic products based on natural ingredients, and 94% pay close attention to the source of the ingredients for food. A significant increase in the amount of waste resulting from the industrial processing of seafood has became a problem for environmental and processing plants. About 45% of processed seafood consists of 50-70% of shrimps exoskeleton and cephalothorax waste. Naturally, the amount of the discarded raw material depends on the processing conditions, species, body parts, and season's changes [3, 6-8].
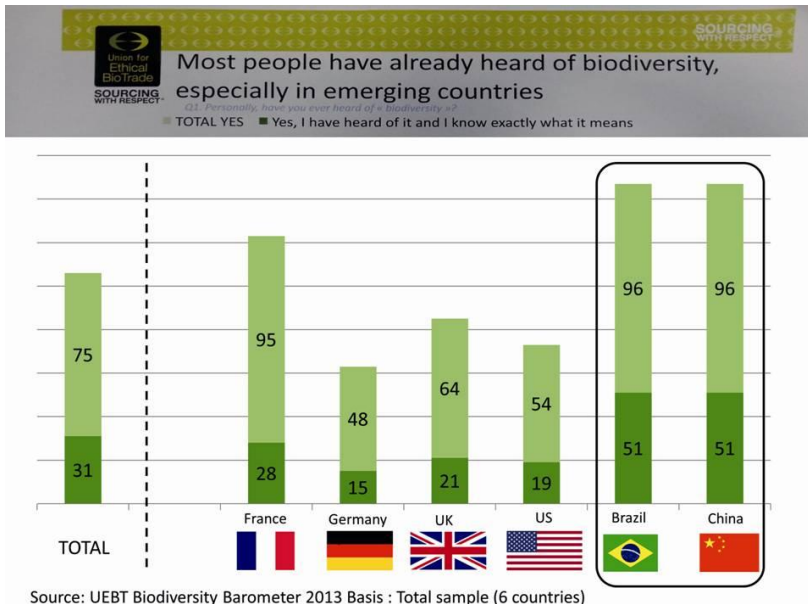
FIGURE 1.2

Chitin is the main structural polysaccharide of arthropods and fungal cell walls containing of about 50-100% of N-acetyl-D-glucosamine and 50-0% of D-glucosamine together with mineral salts and proteins. It is the second most abundant natural biopolymer on Earth after cellulose. Owing to its sugar-like character, this natural polymer is promising in several areas due to its biocompatibility, biodegradability, antimicrobial properties and high tensile strength. The deacetylated form of chitin refers to chitosan (Figure 1.3).
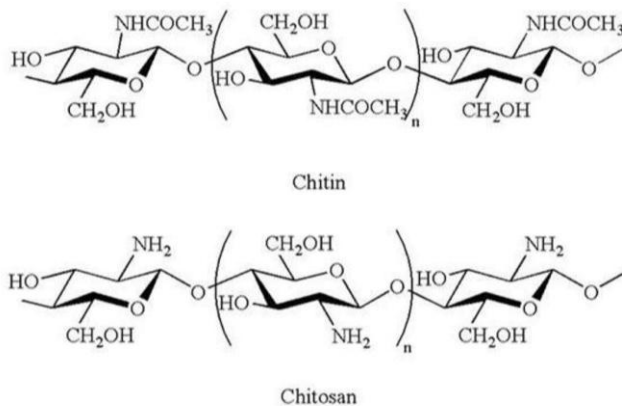
Chitin

Chitosan

FIGURE 1.3
Chemical structures of Chitin and Chitosan. When the degree of N-acetylation (DA) is greater than 50%, the polysaccharide is considered to be chitin. When the DA is less that 50% , the polysaccharide is considered to be chitosan.

However, contrary to chitosan, only recently, chitin received little industrial attention due to its poor solubility. Chitin Nanofibrils (CN) have been already used in interesting delivery systems, goods and biomaterials [9-13].

CN being positively charged polymeric nanoparticles of crystal nature, easily form complexes with any natural or synthetic electronegative polymer containing entrapped active ingredients of different kind inside or outside their structure [14-16]. In addition to solve the delivery problems associated with poorly soluble substances, CN are promising carriers for controlled delivery and release of active ingredients by offering new nanotechnological solutions safe for both human and environment [17-19]. Nanobiotechnology is a multidisciplinary science acquiring knowledge from physical sciences, molecular engineering, biology, chemistry, and biotechnology that gives a great advantage for advanced pharmaceutical, healthcare and food products [20-22].

Chitin Nanofibrils

Physicochemical characteristics

Chemistry

Chitin Nanofibrils, known also as nanowhiskers or CN, are slender rods with diameter and length of about 30-40 nm and 600-800 nm, respectively (Figure 1.4).
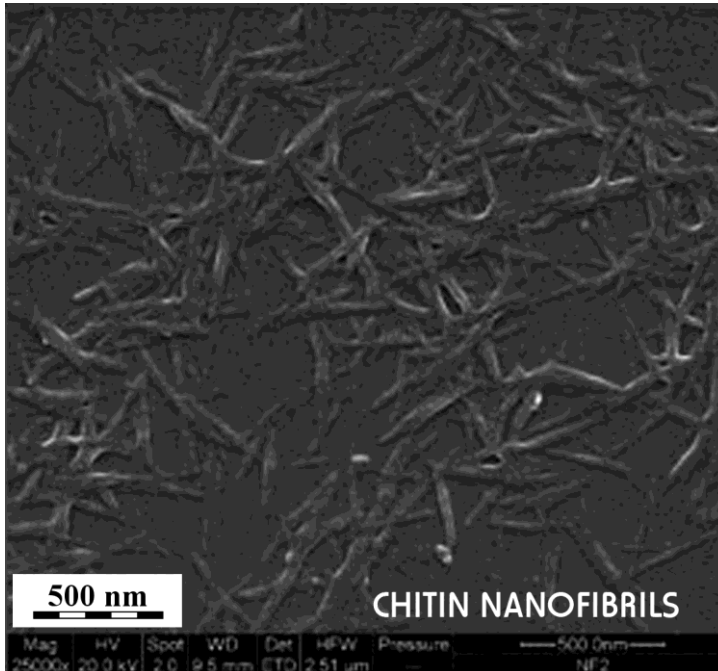
FIGURE 1.4
Chitin Nanofibrils at SEM.

They are the purest crystal form of chitin. This natural, renewable and biodegradable block copolymer consists of N-glucosamine and N-acetyl-D-glucosamine units attached to each other through β-(1-4) glycosidic bonds. Each chitin nanofiber is composed of linear intertwined chitin chains containing about 18-25 units.

Hyaluronic acid, (HA) [23] is an amorphous substance (Figure 1.5) with the same structural unit (N-acetyl-D-glucosamine) similarly to chitin but N-glucosamine units in HA are displaced with glucuronic acid ones.
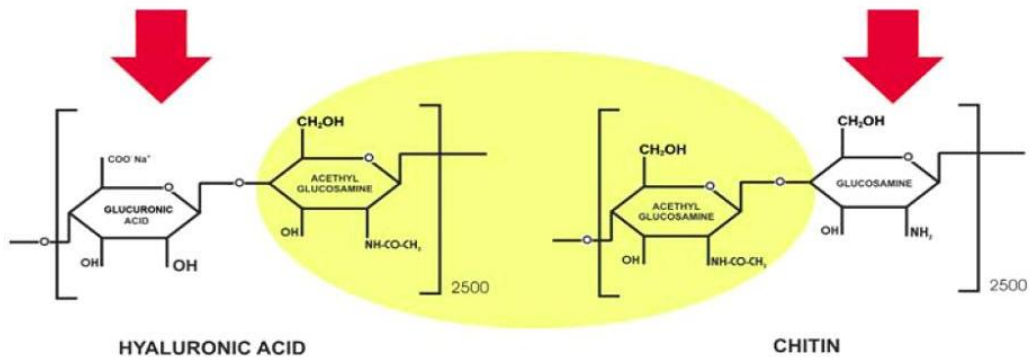
FIGURE 1.5
Chitin has the same backbone of hyaluronic acid.

Despite its accessibility, chitin is still an under utilized natural renewable resource due its insolubility in water and common organic solvents. Recently, the crystalline chitin nanofibrils have been obtained as a stable aqueous suspension from commercial chitin using the green process patented world wide [24]. CN have been used in making innovative cosmetics, drug delivery systems, and advanced medications [25-27]. In the dry form, CN [27] were obtained using a spray-dryer (Buchi-190, Flawil, Switzerland), at the following operation conditions: (the feed rate of 10ml/min; the air inlet and outlet temperature of 148°C and 90° C, respectively; the air flow of 600 l/h). Their structure was analyzed using SEM (SEM/EDY, Philips XL30).

A single chitin nanofibril appears as needle-like crystal with the medium dimensions of 240×7×5 nanometers (nm) (Figure 1.6), Its medium weight is evaluated to be equal to 0.074×10^6 ng and the water uptake achieves of about 400 wt% At pH interval (2-4), one ml of the aqueous colloidal CN dispersion contains of about 2×10^{14} (i.e. 300 trillions!) nanocrystals, which are enveloped with water molecules preventing CN from flocculation. Protonation of free amino groups on the CN surface provides the positive charge. The diluted colloidal CN dispersion is stabilized owing to electrostatic repulsive forces between chitin nanofibrils bearing the same electrostatic charge [27-29]. The surface charge density can be evaluated from the values of the average particle volume (1.1×10^5 nm^3), the crystal surface (2.0×10^4 nm^2), and the chitin density (1.425g ×cm^3). If the content of amino groups per 1 nm^3 of a CN nanocrystal is equal to ~15,000 [27-29], then 10 nm^3 is occupied with about 7.6 charges. As a rule, CN suspension also contains fragments of chitin nanocrystals having irregular shape and associated or collapsed micro/nanocrystals. The size distribution, width of distribution, and zeta potential of dried CN dispersion re-suspended in distilled water, were determined using a Zetasizer (Nano ZS model Zen 3600, Malvern Instruments, Worchestershire, UK) (Figure 1.6). Their length and width usually ranged from 100 nm up to 600 nm, and from 4 to 40 nm [28], respectively. More than

75% of the CN crystals obtained have an average length and width of about 240 and 7 -5 nm (Figure 1.7) respectively.
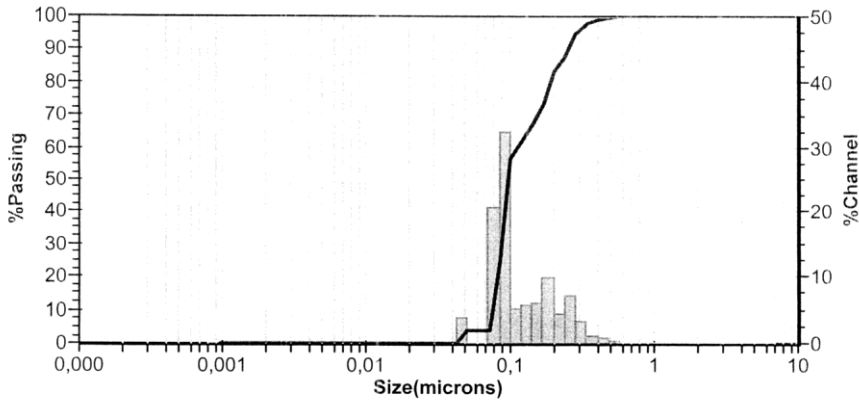
FIGURE 1.6
Size distribution of Chitin Nanofibrils in water suspension.
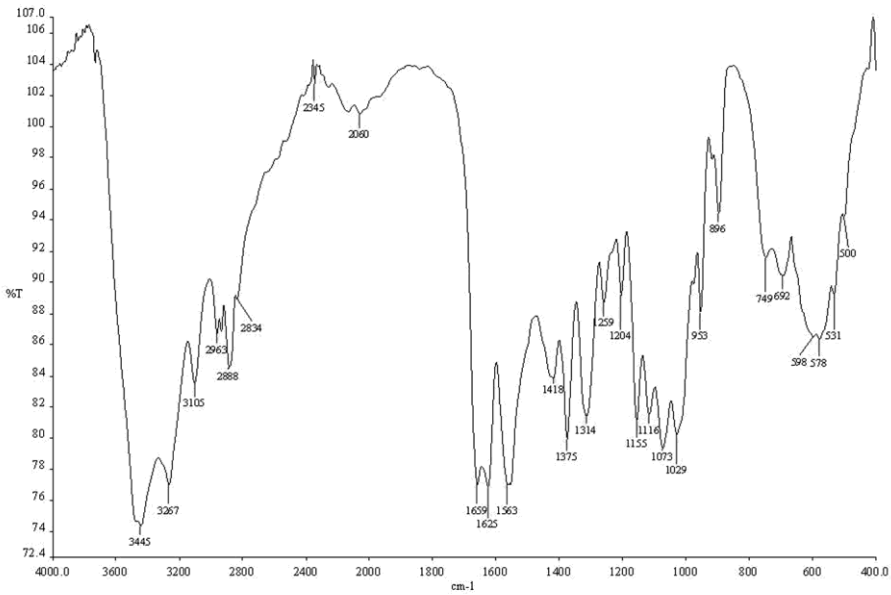
Fourier transform infrared spectrum of spray-dried chitin nanofibrils

FIGURE 1.7
Chitin Nanofibril crystal form, compared with the commercial chitin, has shown a superior quality, as evident by the obtained Infrared bands 1375,1155.

X-ray diffraction and infrared spectroscopy

CN samples dried using spray-drying have been characterized with FT-IR spectroscopy and X-ray diffraction. [27,28]. X-ray measurements were performed using a Bruker AXS General Area Detector

Diffraction System equipped with a two-dimensional gas-filled sealed multi-wire detector (scattering-angle resolution of 0.02°) mono-chromatized by CuK α-radiation (λ= 0.154 nm). The powder samples were placed in 0.8-diameter Lindmann glass capillaries at a distance to detector of 10 cm. The spectra of intensity *vs* scattering-angle were obtained after radial average of the measured 2D isotropic diffraction patterns.

The Attenuated Total Reflection (ATR) spectra were recorded using a Perkin Elmer Spectrometer GX FT-IR equipped with a multiscope system of an infrared microscope with a movable 75×50 mm X-Y stage (MCT-SL detector) [27, 28]. Small amount of the dried CN powder was cooled in liquid nitrogen and ground with KBr to obtain the spectra using a Spectra Tech with a Diffuse Reflectance (DRIFT) accessory.

The spectrum obtained (Figure 1.8) was the results of 16 scans with a resolution of 4 cm^{-1}, which were treated using a Grams/32 Galactic Co. Software package.
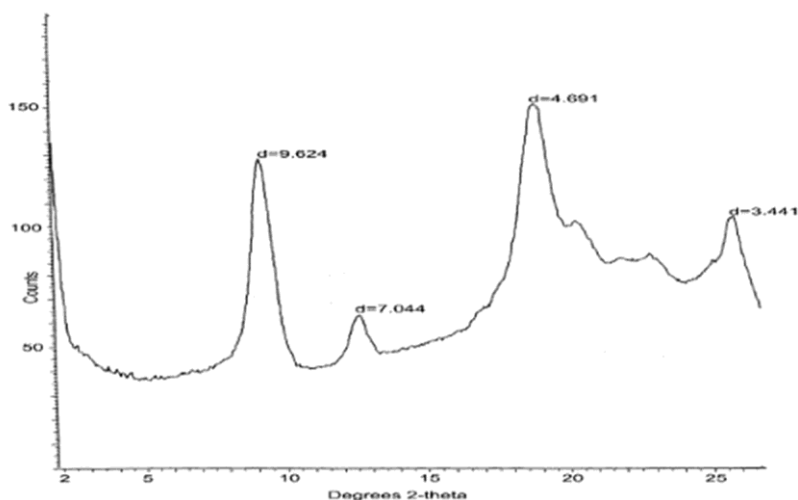
Wide angle X-ray diffraction spectrum of spray-dried chitin nanofibrils

FIGURE 1.8
Chitin Nanofibril crystal form, compared with the commercial chitin, has shown a superior quality as evident by the high intensity of the 9. 624 X-Ray diffraction spectrum.

Typical bands of chitin are present in the spectrum of CN (Figure 1.7): bands at 3445 cm^{-}1 and 3267 cm-1, which are assigned to vibration of N-H, O-H groups and N-H group of the secondary amide in trans-configuration, respectively; the band at 3110 cm^{-1} confirms the vibration of NH-CO grouping in chitins; the bands at 2963 cm^{-1} and 2888 cm^{-1} reflect the vibration of methylene (-CH$_2$-) in –CH$_2$OH and in pyranose ring and methyl (CH$_3$-) in CH$_3$CONH-groupins, respectively. The vibrations at 1625 cm^{-1} and 1659 cm^{-1} are attributed to C-N of the later grouping of chitin in crystalline and amorphous states, respectively. The presence of acetylated and deacetylated amine groups is confirmed by the bands at 1375 cm^{-1} and 1563 cm^{-1}, which are assigned to vibration of CH$_3$ group and N-H in amine, respectively. Finally, the absence of the vibration band at 1540 cm^{-1}, which is assigned to proteins, is an evidence of high purity of CN obtained by the patented process [24]. The absence of any trace of proteins, being possible cause of allergic and sensitizing phenomena, ensures safety of CN for medical applications. The structure of α-chitin with aniparallel chains packing has been determined by using X-ray diffraction analysis based on the intensity data (8) [27, 28].

The chains form hydrogen-bonded sheets linked by C=O...H–N bonds approximately parallel to the α-axis. Each chain has an O-3'–H...O.5 intra-molecular hydrogen bond, similar to that in cellulose. The results indicate also that a statistical mixture of CH_2OH orientations is present, equivalent to half oxygen on each residue, each forming inter- and intra-molecular hydrogen bonds. As a result, the structure contains two types of amide groups, which differ in their hydrogen bonding, and account for the splitting of the amide I band in the infrared spectrum. The inability of this chitin polymorph to swell on soaking in water is explained by the extensive intermolecular hydrogen bonding [27, 29].

The type of crystallinity with its strong intermolecular hydrogen bonding determines the structure and morphology of chitin nanofibrils. They are perfect crystals with uni-planar orientation [30]. In fact, CN, as α-chitin, contains two anti-parallel chains, which are held tightly by a number of strong C=O...H-N inter-chain hydrogen bonds.

Biodegradability

Biodegradability, non-toxicity, biocompatibility and ability to promote the synthesis of hyaluronan are the main specific characteristics of natural chitin-derived polymers in general and of CN in particular. Metabolism of chitin in nature is controlled by enzymatic systems, which produce and break down its molecule by chitin synthases and chitinases. Thus, chitin and chitosan are easily degraded not only by enzymes such as lysozyme [31], N-acetyl-D-glucosaminidase and lipases [32], but also by chitotriosidase (HCHT) belonging to 18 family of chitinases secreted by humans [33].

It is interesting to underline that the level of HCHT in blood is up-regulated in a series of human diseases such as cardiovascular risk and coronary artery disease [34], prostatic hyperplasia [35], and other medical conditions or antiparasite responses [36] and can be considered as a biomarker. It seems that HCHT represents better defence against chitin-containing pathogens. It is primarily expressed in human macrophages [37, 38] and activated by human microbiota [39].

This specific enzyme degrades chitin and chitosan primarily via the endo-processive mechanism showing an absolute preference for acetylated polymers compared with the deacetylated ones because of a relative weak preference for an acetylated unit in the -2, -1, and +1 subsites, respectively [40, 41]. Thus, CN are easily degraded because of higher content of acetylated glucosamine groups in comparison to chitosan resulting in enhancing the production of hyaluronan and collagen glycosaminoglycans which are the fundamental components of extracellular matrix (ECM) [22]. As a result, a risk of hypertrophic formations of scars and keloid and a slowdown of intra-peritoneal adhesion and intestinal structures are considerably reduced [42, 43]. A probable reason could be the increase of chito-oligosynthase DG42 protein, which has been recovered, for example, during the embryo genetic process and acted as primer in the synthesis of hyaluronan [44]. Another reason may be associated with contemporary activity the chitin oligosaccharides shown in modulating the collagen synthesis [22, 28].

Formation of scars depends on the continued synthesis and catabolism of collagen, which has to be balanced for preventing the formation of keloids and hypertrophic scars during the wound-healing process [43, 45]. Therefore, CN acts as a template for both the synthesis of hyaluronan and glycosaminoglycan and as a carrier capable to modulate the collagen production by disposition of its fibers during the healing process [43-46].

Studies in chitin-treated lesions suggest that N-acetylglucosamine serve as a substratum for reinforcement of wounded tissues, while the histiocytes induced by chitin, are activated to produce fine collagen fibres [45-47]. It is clearly seen that chitin can stimulate the activity of fibroblasts to balance its synthesis. In turn, the production of fine collagen fibres increases in the early wound healing stage. In the subsequent healing stages, an appropriate amount of synthesized collagen is degraded by

collagenase produced from macrophages, epidermal cells, neutrophils and fibroblasts to balance its synthesis [48-50].
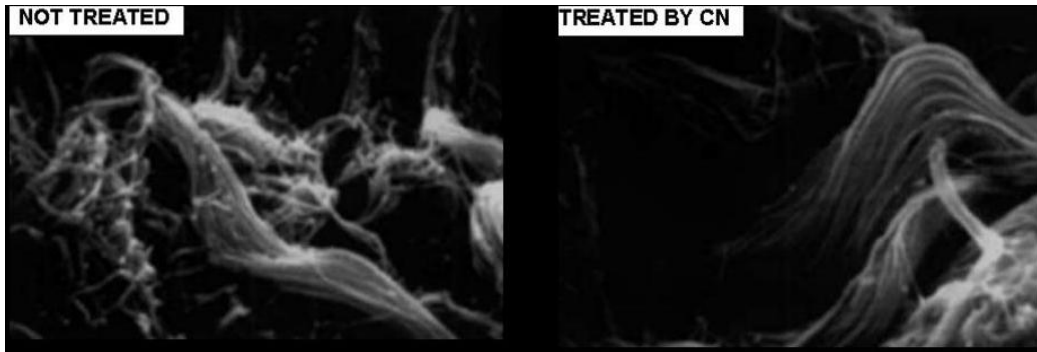
FIGURE 1.9
Chitin Nanofibrils activity to faster the skin granulation phenomena accompanied by angiogenesis and regular deposition of collagen fibers.

Wound healing, consists of a complex series of biochemical processes regulated by hormonal factors and anti-inflammatory mediators, resulting in the rebuilding of tissue and protection against infections [45-50]. Regulating factors include some biochemical substances, growth factors and immunological mediators, whose influence can be decisive, particularly during the early phase of tissue rebuilding [51, 52]. Skin cells interact with the extracellular environment via surface proteins such as integrins, defensins and fibronectin, which trigger various metabolic pathways of important roles in processing their shape, mobility, and proliferation [53, 54]. Owing to purity and polysaccharide nature, CN can constitute a cell micro-environmental stimulus, influencing the correct trophism of the skin and its appendages, and control the molecular relationship of the mesenchymal epithelium and the hair follicle cycle [52, 54]. While, adequate extracellular signalling inputs prompt a local and diffuse cellular response, their extracellular adhesion, cell proliferation and migration leads to the cell dynamic rearrangement [55]. These hyaluronan-mediated signals induced by CN are transmitted partially by activation of protein phosphorylation cascades, cytokine release and stimulation of cell cycle proteins. In this way, CN exhibits an enormously developed surface interacting with the signalling cell enzymes, platelets, and other cell compounds present in living tissue to regulate the cell life continuously. Thus, the recovered peculiarity of wound healing with CN consists in the ability for the faster formation of an adequate granulation tissue accompanied by angiogenesis and regular deposition of collagen fibers, with the consequently enhanced and correct repair of derma-epidermal lesions [52-55] (Figures 1.9 & 1.10).

FIGURE 1.10
Cicatrizing activity of Chitin Nanofibrils on skin wounds.

The main functions characterizing the activity of chitin/chitosan are: (a) chemo-attraction and activation of macrophages and neutrophils to initiate the healing process; (b) promotion of granulation tissue and riepithelization; (c) limitation of scar formation and retraction; (d) analgesic and haemostatic activities; (e) activation of immunocytes; (f) release of glucosamine, N-acetylglucosamine, and oligomers that stimulate cellular activities being used as building blocks in the synthesis of the ECM; (g) own antimicrobial activity [55-58].

Studies from our group [20-22] show the nanocrystalline form of chitin enhances all these functions with relevant biological significance, favouring extremely high cells migration, activating polymorphonuclear cells and fibroblasts, modulating cytokine release and collagenase, metallo proteinases activity and ATP synthesis.

Amongst the cumulative environmental and endogenous skin damages, a decrease of hyaluronan synthase and mitochondrial ATP production takes place together with elevation of level of proteolytic enzymes such as collagenase, elastase and other matrix metallo proteinases [59, 60]. Figure 1.11 shows that CN alone influence the hyaluronan synthase a boosting activity when complexed with vitamin E, melatonin, and B-glucan probably stimulating the HAS-2 gene expression of fibroblasts. CN also inhibit the collagenase activity (Figure 1.12), and increase the ATP production of irradiated keratinocytes (Figure 1.13).
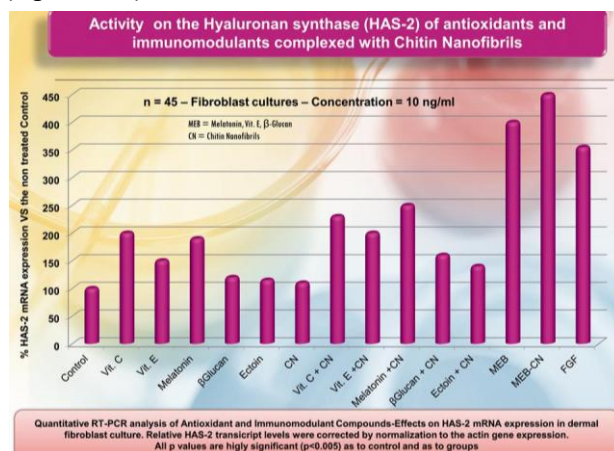
FIGURE 1.11
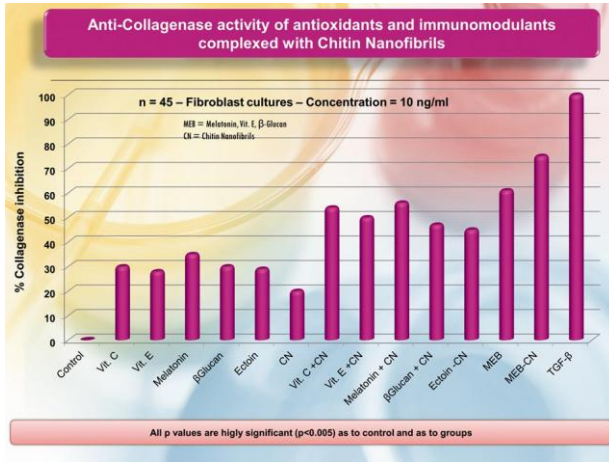
FIGURE 1.12
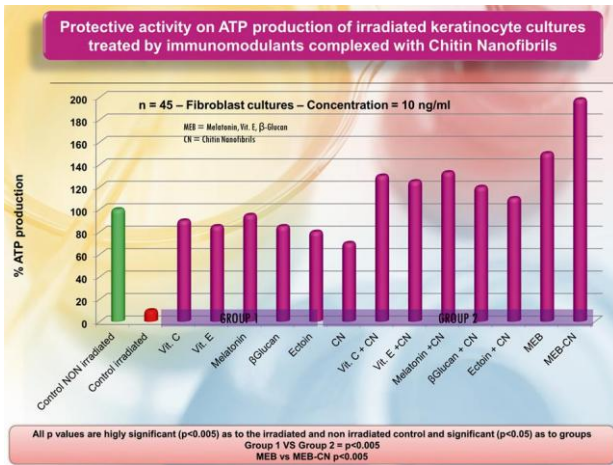
FIGURE 1.13

Biocompatibility

Biocompatibility is the ability of a biomaterial to perform desired function with respect to a medical therapy without eliciting undesirable local or systemic effects in the recipient or patient.

A further characteristic of a biocompatible material is the ability to generate the most appropriate beneficial cellular or tissue response in a specific context [61, 62]. As shown in Figures 1.14 and 15 [16], the biocompatibility of CN was verified for the cultures of keratinocytes and fibroblasts by the MTT method on culture of keratinocytes and fibroblasts.
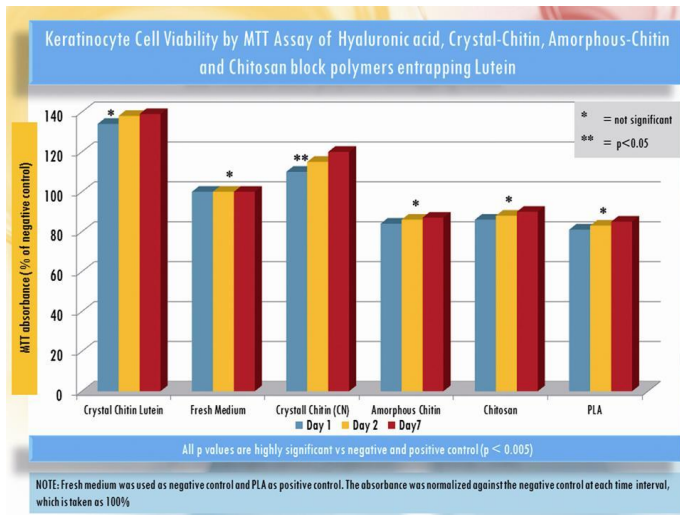
FIGURE 1.14
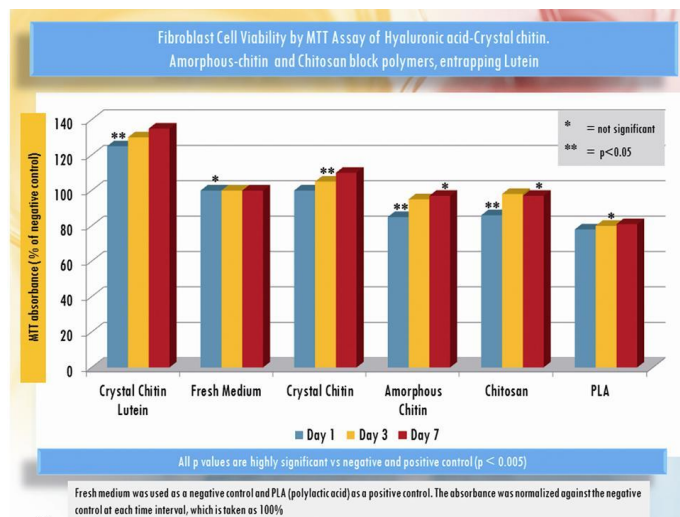
FIGURE 1.15

Block copolymeric nanoparticles

CN have a reactive surface, on which hydroxyl, amine and possibly some acetylated amine groups belonging to polysaccharide chitin chains are exposed. They are able to participate in multiple interactions via van der Waals attractions and hydrogen bonds. The functionality of the surface of CN can be changed by involving the most reactive amine groups in chemical reactions.

These modifications create specific functions, for expanding applications of this natural compound. Owing to protonation of amine groups the CN surface acquires the positive charge and simply interacts with different synthetic or electronegative polymers obtained from animal or vegetal wastes [63-65]. In

this way and without using any chemical ingredients or toxic solvents, complexes can be made from the used block copolymeries (BCC) capable to entrap or encapsulate different kind of physiologically *active* substances [66, 67]. These CN-based complexes can be easily prepared in the form of micro/nano particles.

Combining of CN and other natural lignocellulosic polymers, such as cellulose, hemicellulose and pectin, the compounds obtained are biodegradable, biocompatible, and environmentally friendly.

By forming these complexes through gelation of aqueous CN dispersions with hyaluronan as negatively charged polymer (Figure 1.16) it is possible to obtain micro/nanolamellae or globular nanoparticles with a mean size between 250 and 400 nm (Figure 1.17). They can contain the entrapped different active ingredients able to regularly release them in time, as was demonstrated for carotenoid lutein (Figure 1.18) [20, 66-68].
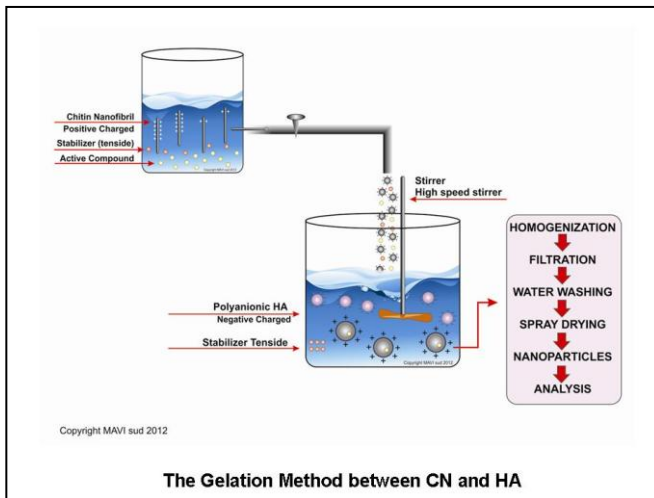
FIGURE 1.16
Chitin Nanofibrils form block-copolymeric nanoparticles with electro-negative polymers, such as Hyaluronic Acid (HA), by the gelation method.
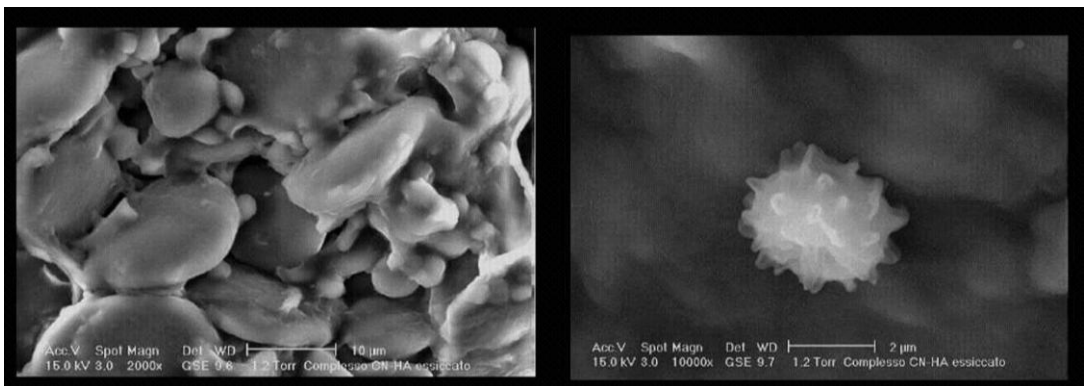
FIGURE 1.17
Nanolamellae and Nanoparticles of Chitin Nanofibrils (CN)–Hyaluronic Acid (HA) at SEM.
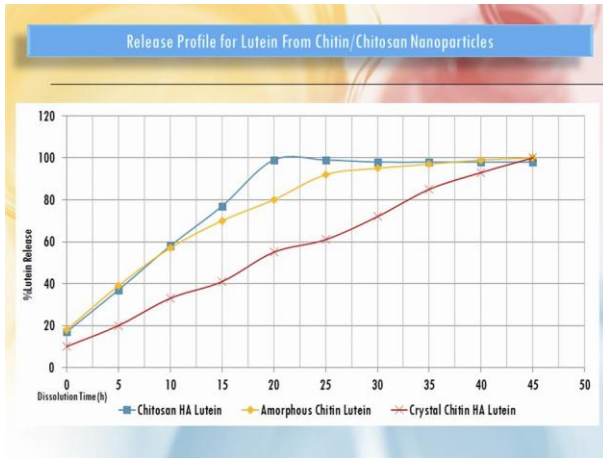
FIGURE 1.18

As the design of complexes based on polyelectrolyte polymers (PEPs), some important aspects should be taken into considerations such as their water solubility, the possibility of controlling anionic and cationic BCC assembley and reversibility of their functionality by changing pH, ionic strength, type of counterions and the solvent effects. Naturally, the quality of the BCC obtained plays an important role in their self-assembly and the ability to disintegrate in living organisms.

The driving force for the spontaneous adsorption of the negatively charged PEPs onto a positively changed surface is primarily the entropically favoured release of small counterions into solution.

The process of dipping a cationic (as CN) polymeric polyelectrolyte substrate into a suspension of anionic (e.g. hyaluronic acid) one, rinsing with water and then dipping the negatively charged complex obtained into a oppositely charged polymer (e.g. cationic) may be referred to as the layer-by-layer deposition shown schematically in Figure 1.19.
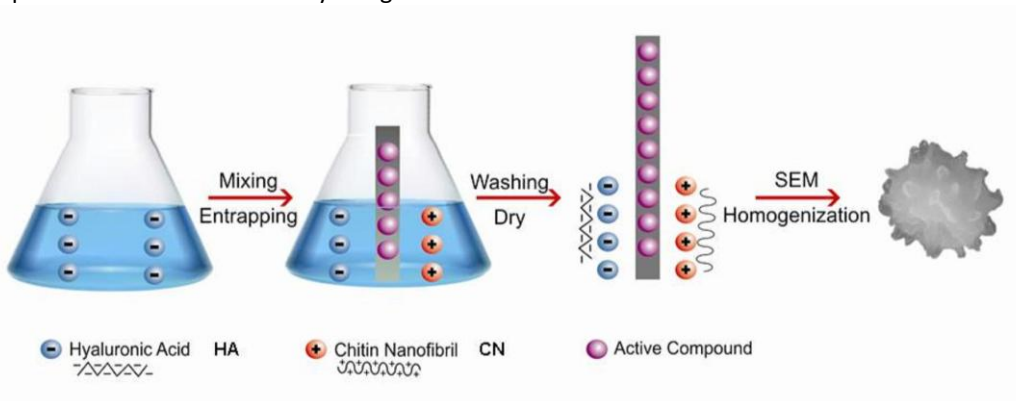
FIGURE 1.19
Method for producing CN-HA block polymeric nanoparticles.

Our studies show that the entrapment efficacy of a component, its loaded content, and the release of active ingredients depend on the crystallinity, size, and the electrical charge covering the CN surface (Table I) [14-16, 66-68]. Positive charges of nanoparticles seem to have the interesting ability to disturb the tight lamellar layers of the *stratum corneum*, enabling a better diffusion of the entrapped active compounds through the skin, (Figure 1.20), by using the stripping method *in vivo* [16].
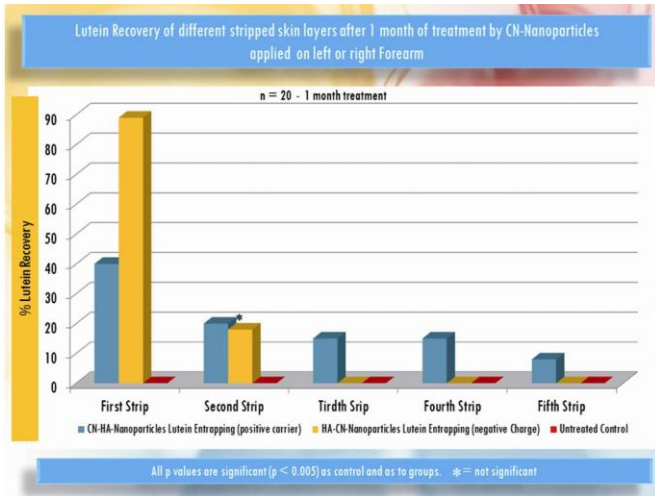
FIGURE 1.20

Naturally, the electrical charge, size, the balance of hydrophilicity/hydrophobicity of CN as *carrier* and the used *active ingredients* determined in advance by the *designed formulation,* will control the release of the *active substances* during the predicted time for obtaining the expected efficacy of the final product. On the one hand, the choice of CN as *active* nanoparticles for preparation of polyelectrolyte complexes has to be based on the reason of administration and the properties of the selected *active ingredients* (their stability, hydrophilicity/hydrophobicity and etc.) [60, 66-68]. On the other hand, the release of the *active ingredients* from these BCC‑nanoparticles can occur through either outer absorption (burst release) or a continuous release, depending on the type of the polymer materials and the nature of the entrapped active ingredients [69] including the electrical charge of nanoparticles (Figure 1.21).
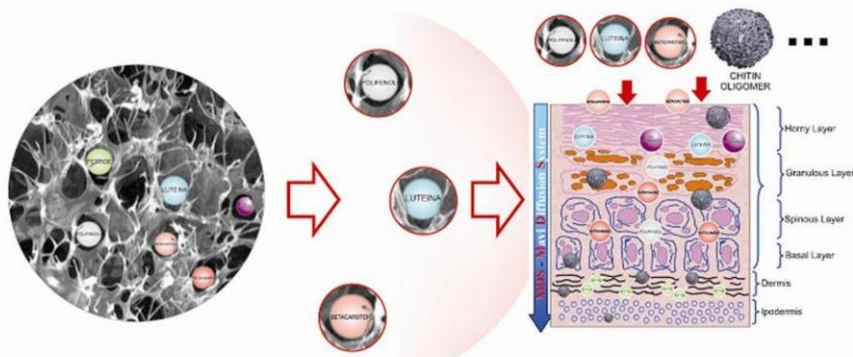
FIGURE 1.21
Skin penetrability of nanoparticles depends on their size, superficial charge and type and polymer used.

Active ingredients can be dissolved, absorbed, entrapped and/or encapsulated into/or onto the selected BCC whilst the rate limiting step of the kinetics of release could be doubled: a) diffusion of active ingredient and carrier and/or b) dissolution of the carrier itself [70].

The appropriate choice of the carrier material together with the methods adopted to encapsulate the active ingredients are the decisive factors for regulating the release of active ingredients and achieving the effective dosage.

Finally, the influence of positively charged CN on cell biology seems to be related also to the osmotic stress induced by the particular hydrophilicity of the BCC obtained e.g. from CN and hyaluronic acid or collagen [13-16]. When skin cells contact with these complexes, they initially swell up with water, and subsequently shrink back to close their previous volume due to an inflow of ions and osmolytes, which induce an outflow of water and skin hydration.

BCC with different entrapped active ingredients and obtained by the interaction of chitin nanofibrils with hyaluronic acid (CN-HA), have shown interesting activities both *in vitro* and *in vivo* when introduced into cosmetic emulsions. These emulsions have been tested *in vitro* on keratinocytes and fibroblast cultures and *in vivo* on 60 healthy women showing signs of photoaging in the multicenter randomized study [22].

The BCC with different *activate ingredients*; have accelerated the collagen formation *in vitro* (Figure 1.22), and the synthesis of chaperon HSP-47 (Figure 1.23) at the level of fibroblasts' culture. An interesting antioxidative activity, re-equilibrating its imbalance, occurs during the oxidative stress (Figure 1.24, 25) [16, 22].
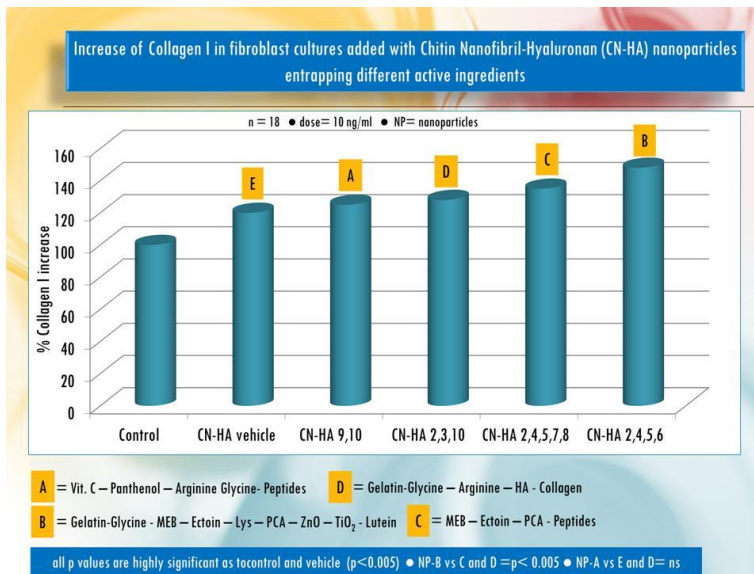
FIGURE 1.22
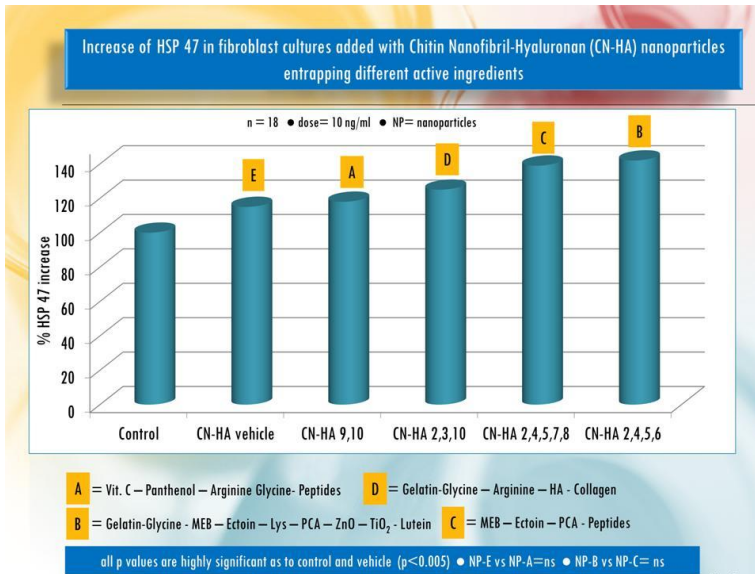
FIGURE 1.23
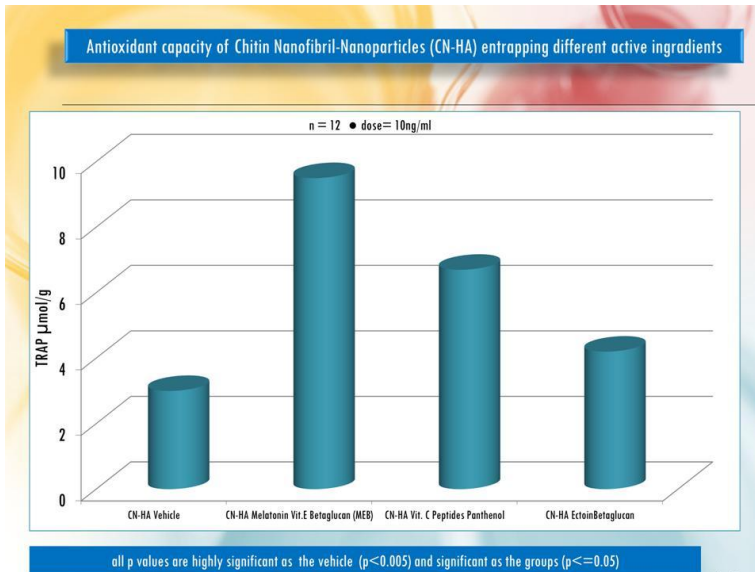
FIGURE 1.24
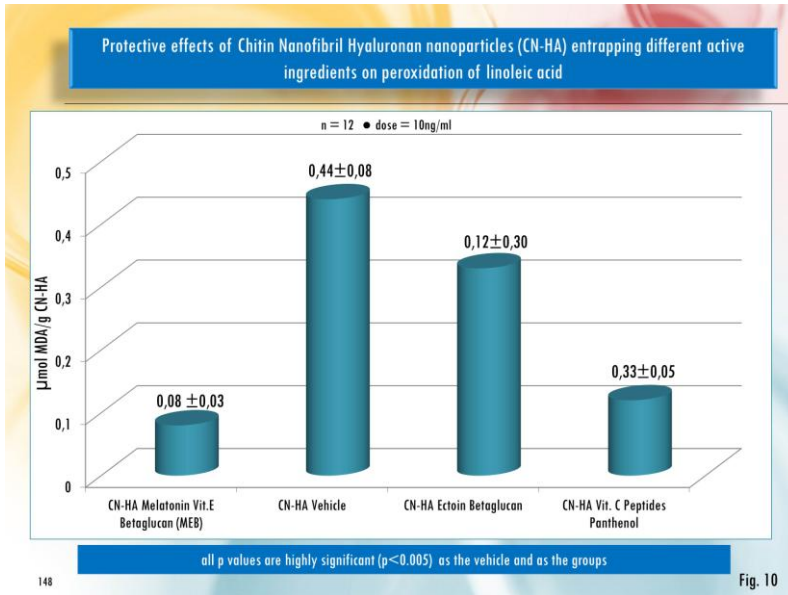
FIGURE 1.25

Furthermore, the topical *in vivo* application of the different daily-used emulsions in the multicenter randomized vehicle controlled preliminary study has shown increase in the skin hydration (Figure 1.26) with a contemporary decrease of both TEWL (Figure 1.27) and black spots (Figure 1.28) for the treated voluntary women. These results supported the previous data reported by our group [10, 20, 28, 67].
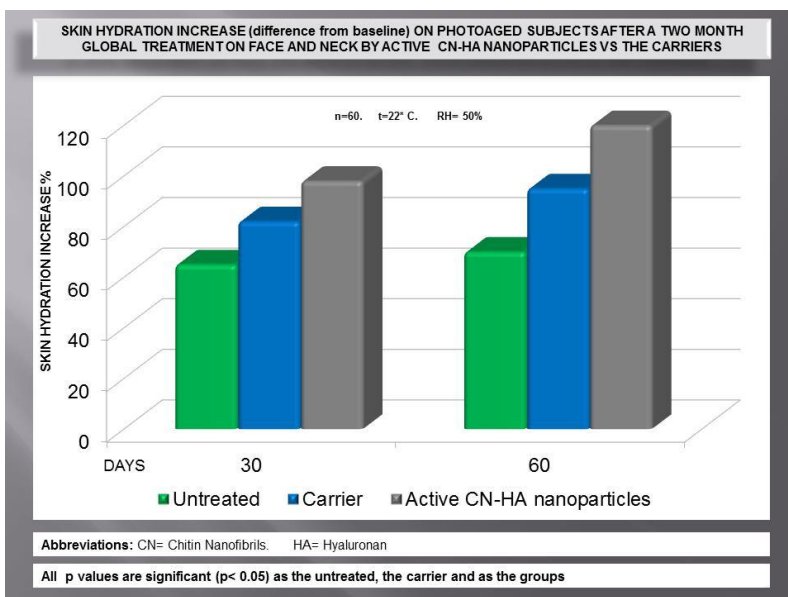
FIGURE 1.26
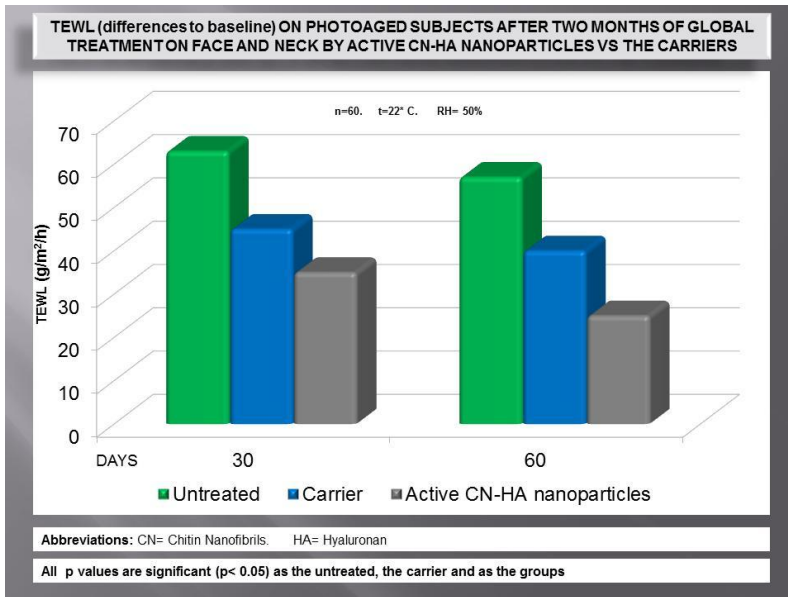
FIGURE 1.27
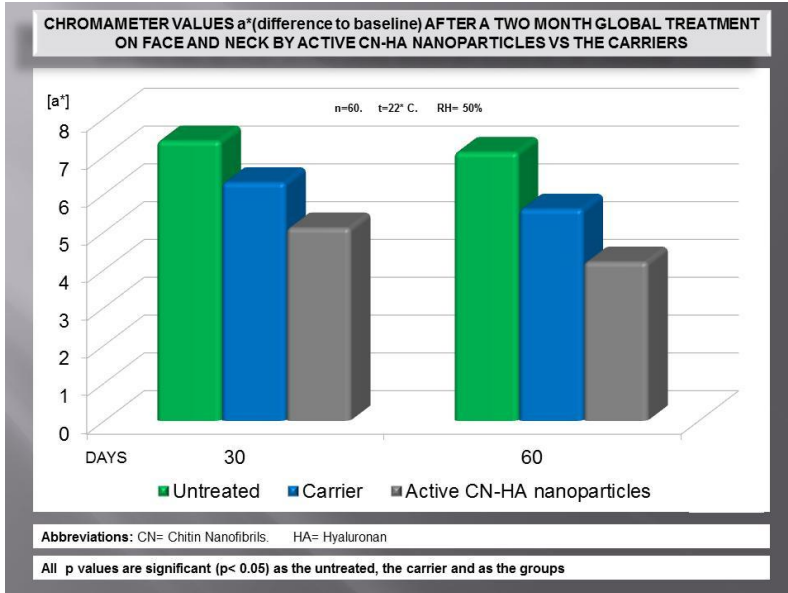
FIGURE 1.28

The exposure to either UV or other aggressive agents generate reactive oxygen or nitrogen species (ROS and RNS) resulting in premature entry of the skin into the senescent state [71]. Thus, in photoaged skin (extrinsic aging), collagen fibres become disorganized, abnormally cross-linked with elastin-containing material [72]. In genetic aging (intrinsic aging), the decline in signalling molecules

(cytokines and chemiokines) and cell receptors induce fibroblast senescence and alteration in the synthesis and maturation of both collagen and scaffold-stress proteins, as HSP-47. Hence, they play a key role in the formation of the adaptive immune system [73] and regulation of the collagen folding [74]. Moreover, BCC have stimulating activity on ATP production (Figure 1.29) and Langerhans cell density (Figure 1.30) due to UVB irradiation and on fibroblasts proliferation (Figure 1.31) [15, 75]. It is interesting to underline also that CN increase the antidandruff activity of zinc pyrithione (Table II) improving also the mechanical properties of UV-damaged hairs (Figure 1.32) [76]. This natural polysaccharide seems to possess a boosting activity in comparison with zinc ions and pyrithione by increasing their antidandruff activity. It is also able to repair the hair's cortex proteins, ameliorating its modulus and surface gloss (Figure 1.33).
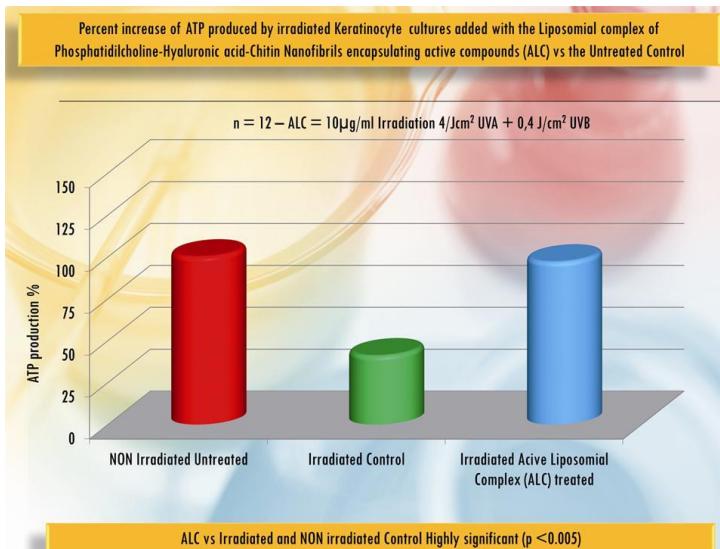
FIGURE 1.29
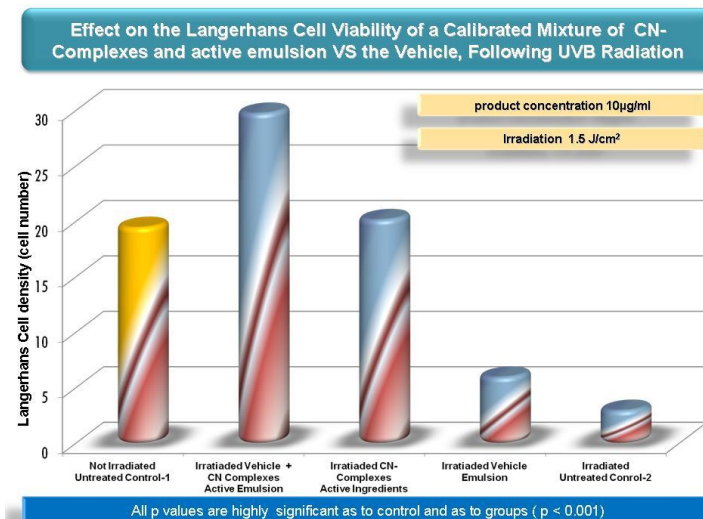
FIGURE 1.30
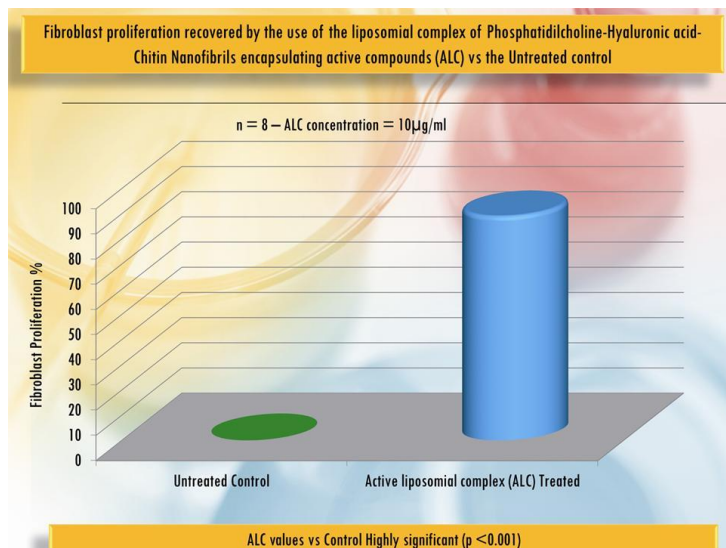
FIGURE 1.31

TABLE I

Polymer	Nanoparticle yield (%)	Lutein loading content (%)	Entrapment efficacy (%)	Particle mean size (nm)
Chitosan -HA- Lutein	33 ± 9	10 ± 3	32 ± 5	458 ± 14
Amorphous Chitin -HA- Lutein	31 ± 10	18 ± 3	40 ± 5	355 ± 13
Crystal-Chitin HA (CN) Lutein	42 ± 9	35 ± 3	66 ± 6	185 ± 13

NOTE: all measurements were performed in triplicate
ABBREVIATIONS: CN = Chitin Nanofibrils; HA = Hyaluronic acid

TABLE II

Dandruff scales on the scalp of subjects affected by oily scalp with dandruff treated by Zn-CN Shampoo and conditioner VS traditional treatment and unaffected

RH = 50% - t = 22° C		n = 10 +20 + 20 + 20			60 days of treatment
	SUBJECT	**0**	**30**	**60**	**TREATMENT**
Control unaffected	10	$855.384 \pm 4 \times 10^4$	$832.500 \pm 7 \times 10^4$	$861.721 \pm 6 \times 10^4$	NO treatment
Dandruff affected	20	$1,356.821 \pm 1.56 \times 10^5$	$915.743 \pm 1.88 \times 10^4$	$878.903 \pm 3 \times 10^4$	Product B Zn Shampoo CN-ZPT Conditioner
Dandruff affected	20	$1,512.300 \pm 5 \times 10^4$	$1,117.281 \pm 5 \times 10^4$	$972.333 \pm 5 \times 10^4$	Commercial antidandruff products (shampoo+conditioner)
Oily scalp	20	$955.764 \pm 3 \times 10^4$	$871.615 \pm 5 \times 10^4$	$863.487 \pm 4 \times 10^4$	Zn-Shampoo + CN-&Cationic-LPO Conditioner

all p values are significant as to groups and as untreated ($p < 0.05$)

Decrease in elastic modulus of hair exposed to UV and treated by Zn-CN shampoo and conditioner

RH = 50%   t = 22° C   n = 30   UV Exposed 36 hours (500 W/m²)

- 1S Control Untreated
- 2S Control untreated UV exposed
- 3S UV exposed treated by shampoo A
- 4S UV exposed treated by shampoo B
- 5S UV exposed treated by shampoo & conditioner A
- 6S UV exposed treated by shampoo & conditioner B
- 7S UV exposed treated by commercial shampoo & conditioner
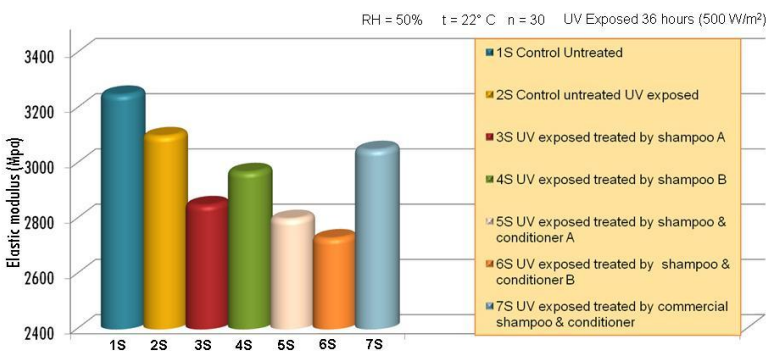
all p values are significant ($p < 0.05$) VS untreated
5S and 6S are very significant ($p < 0.005$) VS untreated and significant ($p < 0.05$) VS 5S vs 6S

FIGURE 1.32

Gloss measurements of hair UV exposed and treated by Zn-CN shampoo and conditioner

RH = 50%   t = 22° C   n = 30   UV Exposed 36 hours (500 W/m²)

- 1S Control Untreated
- 2S Control untreated UV exposed
- 3S UV exposed treated by shampoo A
- 4S UV exposed treated by shampoo B
- 5S UV exposed treated by shampoo & conditioner A
- 6S UV exposed treated by shampoo & conditioner B
- 7S UV exposed treated by commercial shampoo & conditioner

all p values are significant (p<0.05) VS as baseline untreated sample
3S VS 4S and 7S = ns ; 5S and 6S are highly significant (p<0.005) VS 3S and 4S

FIGURE 1.33

Non-woven tissues and films

Chitin nanofibrils are obtained as aqueous suspension and may be used for reinforcing of water-soluble polymers in preparation of the environmentally friendly biodegradable nanocomposite materials with high performance.

CN-based biomedical nanocomposites can be used for drug/gene delivery, for tissue engineering as scaffolds and cosmetic orthodontics [25, 26, 77] because they are able to support the growth of cells inducing tissue regeneration. Best results are obtained when a scaffold or non-woven tissue has a proper architecture, which is designed in such a way that the cellular response desirable for biological function of specific organs is triggered [78-80].

One of the most versatile techniques of polymer processing for this purpose is electrospinning. It allows generating micro- and nano- fibers for production of nonwoven tissues (scaffolds) [78]. During the electrospinning process, a jet of a polymer is formed from a viscous solution/suspension in the presence of the high voltage. Electrospinning seems to have high potential efficacy to produce various nonwoven fibers with high surface/volume ratio. If different active ingredients are incorporated into the fiber, the scaffolds prepared have better healing effect. The structural features of scaffolds influence on their therapeutic effect. When the structure of scaffolds made from electrospun fibers are comparable with that of native extra cellular matrix (ECM) of the skin, the cellular adhesion, proliferation, and guide cell differentiation increase (Figure 1.34) (unpublished data). It has been shown that the antimicrobial activity (Figure 1.35) [63] and enhanced effect on healing of human skin is observed if Ag-ions have been entrapped into both a CN-containing gel emulsion [43] and nanocomposite chitosan films made by casting.
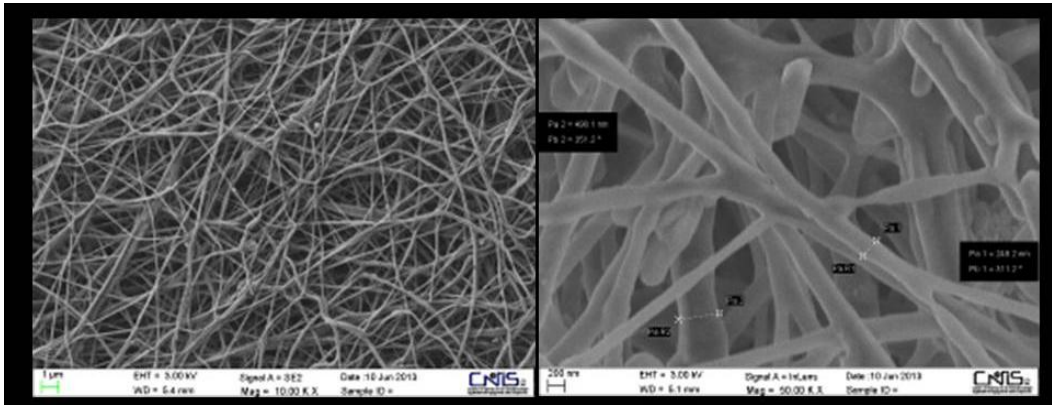
FIGURE 1.34
Non-woven tissue made by Chitin Nanofibrils at SEM.
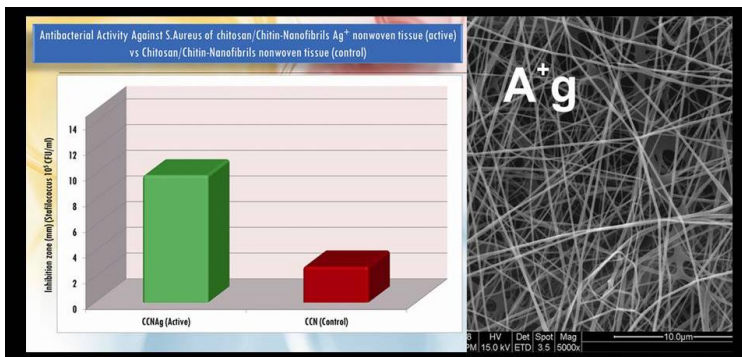
FIGURE 1.35

A polymer composite from ligninocellulosic compounds and CN having the same ECM architecture of skin may also form the multifunctional medical tissues or beauty masks with the entrapped antiseptic mineral ions (e.g. Ag+) or with other kind of *active ingredients* useful for ameliorate skin appearance. As usual, the addition of fillers in a fiber- or film-forming polymer is a standard method for improving the mechanical behaviour of a composite material. The CN-filled chitosan films (Figure 1.36a,b) exhibit enhanced tensile strength, thermal stability and water resistance [81], which increase with increasing CN content. Since CN has capability to bind ions and other polymers by electrostatic interactions they can store and deliver them for long period of time. Their antimicrobial and antifungal effectiveness for different microorganisms was found out. Investigations, which were supported by the projects BIOMIMETIC (www.biomimetic-eu-project.eu) and n-CHITOPACK (www.n-chitopack.eu), have revealed the viability of both keratinocytes and fibroblasts on the non-woven tissues and nanocomposte films (unpublished data). Both non-woven tissues and films made by electrospinning (Figure 1.37) [82] or casting [83], respectively, are in progress to use CN with entrapped different ions and active ingredients as storage matrix in skin care.

For medical applications, various composite fibers, nonwoven tissues, films or gels can be prepared on the basis of homogeneous aqueous CN suspension and cellulosic polymers or chitosan by using environmentally friendly processes. A huge diversity of different nanocarriers able to penetrate in certain human tissues owing to their physicochemical properties can be also developed be means of different technical methodologies.
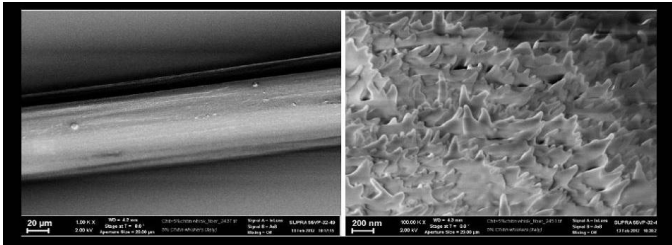
FIGURE 1.36a
The smooth surface of chitosan/CN composite fibers (a) shows a regular disposition of CN into its inner structure (b). The fiber contains 1 wt.% of CN.
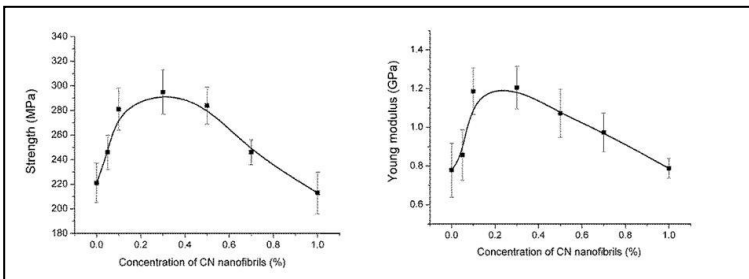
FIGURE 1.36b
Dependences of tensile strenght (a) and Young Modulus (b) of the chitosan/CN composite fibers on the content of the chitin nanofibrils.
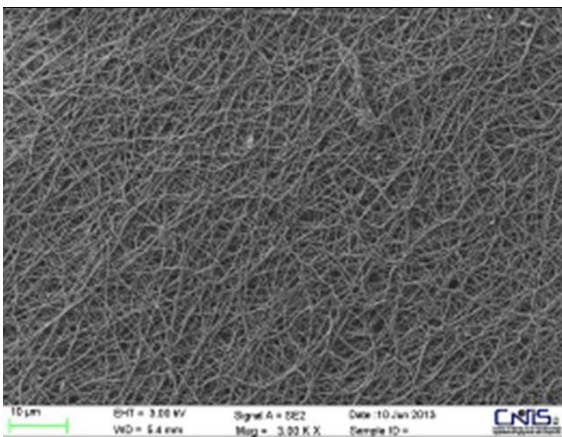
FIGURE 1.37
Non woven Tissue obtained by electrospinning at SEM.

Conclusions

Engineered nanomaterials constitute a large number of classes and subclasses of diverse materials having features in common: one, two or three of their dimensions are within the interval of 1-100 nm [84]. If only one dimension equals or less than 100 nm, everyone deals with nanoflakes. Materials with fibrous as CN or tubular structures or those having cubic shape are characterized with two or three nanodimensions, respectively.

CN providing numerous advantages including their easy availability, non-toxicity, renewability, biodegradability, good biocompatibility, reproducibility, and easy chemical and mechanical modification [16, 23, 26, 81] are much better choice for using as nanofillers than the traditional inorganic ones in fabrication of the various so called *green composites* [1-8, 63-65], i.e. environmentally friendly biopolymers such as e.g. CN and different ligninocellulosic compounds [1-8, 63-65].

According to innovative BioEconomy, green compounds have advantages not only from the ecological but also from the economical point of view [85]. This is the reason why in its 2020 strategy the European Union highlights nanotechnology as one of the fundamental basis of BioEconomy and sustainable technology, capable of providing prosperity and social stability to its citizens [85, 86]. Being multifunctional compounds, CN act, first of all, as reinforcing agents giving to polymeric nanocomposites some additional properties.

If CN are incorporated to biopolymers, the formed innovative biomaterials (templates) ensure the successful tissue development in the process of skin regeneration owing high cyto-compatibility of CN with human cells. Nanocomposite films for food packaging prepared from CN-filled chitosan slurries are safety for humans because of antimicrobial activity and non-toxicity of both CN and chitosan. The same effect can be expected for CN-based biotexiles [87] for production of both sportswear and various hygienic and medical biomaterials. The latter are highly advantageous for patients suffering from dermatitis or psoriasis because the risk of secondary infections is remarkable reduced.

Being produced from low cost raw chitin by using the environmentally friendly process of CN fabrication, the ultrafine nanofibril-based porous membranes prepared by electrospinning may surpass conventional membranes in-water purification owing to the impressive high flux efficiency.

A new class of thin CN-based films and membranes with barrier permeability for gases can be manufactured by using casting [64] owing to excellent film-forming properties of chitosan. The chains are bound with each other and CN through multiple hydrogen bonds and hydrophobic interactions. The porous CN-based polymeric membranes can be prepared by electrospinning.

Drug delivery with CN is highly effective since the positively charged CN surface, due to protonation of glucosamine groups is able to attract and complex many negatively charged polymers. The formed nano-lamellae or nanoparticles entrap water- or lipo-soluble active ingredients, which are used for pharmaceutical and cosmetic purposes. Moreover, due to their biological and safe characteristics, CN may be used for the production of innovative and advanced medications using both the Electrospinning and the Casting technology.

As previously reported, the physicochemical properties of the cosmetic nanoparticles, tissue-nanofibers, and/or casting-films made of CN and other natural polymers, may be predicted and designed at the molecular level, whilst their real shape, size, and electrical charges can be controlled and optimized for each specific application.

There is also a tendency to predict the physicochemical properties of the CN-containing cosmetic nanoparticles, nanofibers for tissue engineering and films from chitosan and other natural polymers with the aim of designing them at the molecular level and comparing the obtained theoretical calculations with experimentally determined characteristics (shape, size, electrical charge and etc.) of the prepared CN complexes.

Interestingly, chitin being a fishery waste, is the second most abundant polysaccharide existing in nature as component of the invertebrates' exoskeleton, proceeded only by cellulose obtained from the vegetable biomass. As a consequence, polymers obtained from these waste materials using green processes, will reduce the worldwide pollution, ameliorating the quality of our life.

Many interesting possibilities exist in different fields of nanotechnology, especially when raw materials used are classified as natural or possibly obtained from the waste and by-products such as CN. It is important to underline the possibility of using the same raw material for producing, for example, innovative cosmetics, advanced medications, dedicated textiles, and also in air and water filtration, or drug delivery, to reduce pollution and transform waste materials into goods.

In conclusion, it is imperative requirement to develop new strategies for designing effective and possibly low cost biomaterial for practical usage [78, 80, 88] in order to enter into a real *green era*.

References

1. Morganti P. Saving the Environment by Nanotechnology and Waste Raw Material: Use of Chitin Nanofibril by EU research Projects. J Appl Cosmetol., 2013; 31, 89-96.
2. UNEP DTIE. Converting Waste Agricultural Biomass into a Resource. Compendium of Technologies. Osaka, United Nations Environment Programme, 2009.
3. FAO yearbook. 2010 Fishery and Aquaculture Statistics. Rome, 31 December, 2011; pp 1-80.
4. Baker E, Bournay E, Harayama A, and Rekacewicz P. Vital Waste Graphics. UNEP, Nairobi, 2004; October 12.
5. UNEP. Convention on Biological Diversity. The Biodiversity Barometer 2013, Paris/Montreal, 2013; April 19.
6. Kurita K. Chitin and chitosan: Functional biopolymers from marine crustaceans. Marine Biotechnology 2006; 8(3) 203-226.
7. Bruck WM, Slater JW, and Carney BF. Chitin and Chitosan from Marine Organisms. In: SK Kim Ed, Chitin, Chitosan, Oligosaccharides and their Derivatives, New York, CRC-Press, 2011; pp 11-23.
8. Gortari MC and Hours RA. Biotechnological processes for chitin recovery out crustacean waste: A mini-review. Electronic J Biotechnol., 2013 16(3).
9. Morganti P, Li YH, Morganti G. Nanostructured products: technology and future. J Plastic Dermatology 2008 4(3):253-260.
10. Morganti P, Chen HD, Gao XH, Li YH, Jacobson C, Arct J, Fabianowski W. Nanoscience Challenging Cosmetics, Healthy Food & Biotextiles. SOFW-Journal 2009 135(4):32-41.
11. Morganti P, Fabrizi G, Palombo P, Palombo M, Ruocco E, Cardillo A, and Morganti G. Chitin Nanofibrils: a new cosmetic carrier. J Appl Cosmetol. 2008 26:113-128.
12. Morganti P, Morganti G. Chitin Nanofibrils for Advanced Cosmeceuticals. Clinics in Dermatology 2008 26(4):334-340.
13. Morganti P, Del Ciotto P, Gao XH. Skin Delivery and Controlled Release of Active Ingredients Nanoencapsulated by Chitin Nanofibrils: A new Approach. Cosmetic Science Technology, 2012 20:136-142.
14. Morganti P. Chitin Nanofibrils and Their Derivatives as Cosmeceuticals. In: SK Kim Ed Chitin, Chitosan, and Their Derivatives. Biological Activities and Application, New York, CRC-Press, 2010 pp 531-542.

15. Morganti P, Del Ciotto P, Morganti G, and Fabien-Soulé V. Application of Chitin Nanofibrils and Collagen of Marine Origin as Bioactive Ingredients. In: SK Kim Ed, Marine Cosmeceuticals: Trends and Prospects, New York, CRC-Press, 2012 pp 267-289.

16. Morganti P, Tishchenko G, Palombo M, Kelnar L, Brozova L, Spirkova M, Pavlova E, Kobera L, Carezzi F. Chitin Nanofibrils for biomimetic products: Nanoparticles and nanocomposite chitosan films in health-care. In SK Kim Ed Marine Biomaterials: Isolation, Characterization and Application, New York, CRC-Press, 2013 pp 681-715.

17. Morganti P, Chen HD, Gao XH, Del Ciotto P, Carezzi F, Morganti G. Nanoparticles of Chitin Nanofibril-Hyaluronan block polymer entrapping lutein as UVA Protective compound. In Carotenoids: Food Source, Production and Health Benefits, Nova Science Publishers Inc, 2013 pp 237-259.

18. Morganti P. To improve quality of life minimizing the environmental impact. SOFW-Journal 2013 139(10):66-72.

19. Morganti P, Palombo M, Fabrizi G, Guarneri F, Svolacchia F, Cardillo A, Del Ciotto P, Carezzi F, Morganti G. New insights on Anti-aging activity of Chitin Nanofibril-Hyaluronan block copolymers entrapping active ingredients: in vitro and in vivo study. J Appl Cosmetol. 2013 31:1-29.

20. Morganti P. Use and potential of nanotechnology in cosmetic dermatology. Clinical Cosmetic and Investigational Dermatology, 2010 3:5-13.

21. Firdos Alam Khan. Biotechnology Fundamentals. New York, CRC-Press, 2013.

22. Morganti P. Innovation, Nanotechnology and Industrial Sustainability by the use of Underutilized Byproducts: The EU support to SMEs. J Mol Biochem. 2013 2(3):137-141.

23. Morganti P. Chitin Nanofibrils in skin treatment. J Appl Cosmetol. 2009 27:251-270.

24. Mavi Sud (2006/2013) PCT No: WO 2006/048829; US 8, 383, -57B2 26 Feb. 2013.

25. Morganti P. Chitin Nanofibrils for Cosmetic Delivery. Cosmetic & Toiletries 2009 125(4):36-393.

26. Mincea M, Negrulescu A, Ostafe V. Preparation, Modification, and Application of Chitin Nanowiskers: A Review. Rev Adv Mater Sci. 2012 30:225-242.

27. Muzzarelli RAA, Morganti P, Morganti G, Palombo P, Palombo M, Biagini G, Mattioli-Belmonte M, Giantomassi F, Orlandi F, Muzzarelli C. Chitin nanofibril/chitosan composites as wound medicaments. Carbohydrate Polymers. 2007 70:274-284.

28. Morganti P, Del Ciotto P, Carezzi F, Morganti G, Chen HD. From waste Material a New Anti Aging Compound: A Chitin Nanofiber Complex. SOFW-journal 2012 138(7):30-36.

29. Muzzarelli RAA, Muzzarelli C. Chitin Nanofibrils. In: Chitin and Chitosan. Opportunities and Challenges,. PM Dutta Ed, New Dehli, India, New Age international, 2005.

30. Raabe D, Romano P, Sachs C, Fabritius H, Al-SawalmiH A, Yi SB, Servos G, Hartwig HG. Microstructure and crystallographic texture of the chitin-protein network in the biological composite material of the lobster Homarus Americanus. Materials Science Engineering, 2006 A 421:143-153.

31. Tokura S, Azuma I. Chitin derivatives in life sciences. Japan Soc Chitin, Sapporo, 1992.

32. Sashiwa H, Saito K, Saimoto H, Minami S, Okamoto Y, Mstsuhashi A, Shigemasa Y. Enzymatic degradation of chitin and chitosan. In: RAA Muzzarelli (Ed) Chitin Enzymology, Atec, Grottammare, Italy, 1993 pp 177-186.

33. Eide KB, Norberg AL, Heggset EB, Lindbom AR, Varum KM, Eijsink VGH, Sorlie M. Human Chitotriosidase-Catalyzed Hydrolysis of Chitosan. Biochemistry. 2012 51: 487-495.

34. Karadag B, Kucur M, Isman FK, Hacibekiroglu M, Vural VA. Serum chitotriosidase activity in patients with coronary artery disease. Circ J. 2008 72:71-75.

35. Kucur M, Isman FK, Balci C, Onal B, Hacibekiroglu M, Ozkan F, Ozkan A. Serum YKL-40 levels and chitotriosidase activity as potential biomarker in primary prostate cancer and benign prostatic hyperplasia. Urol. Oncol. 2008 26: 47-52.

36. Van Eijk M, Scheij SS, van Roomen C, Speijer D, Boot RG, Aerts J. TRL- and NOD2-dependent regulation of human phagocyte-specific chitotriosidase. FEBS Lett. 2007 581:5389-5395.

37. Artieda M, Cenarro A, Ganan A, Lukic A, Moreno E, Puzo J, Pocovi M, Civeira F. Serum chitotriosidase activity, a marker of activated machrophage, predicts new cardiovascular events indipendently of C-reactive protein. Cardiology 2007 108:297-306.

38. Hollak CEM, Vanweely S, Vanoers MHJ, Aerts J. Marked Elevation of Plasma Chitotriosidase Activity: A novel Hallmark of Gaucher Disease. J Clin Invest. 1994 93:1288-1292.

39. Morganti P, Cornelli U, Gazzaniga G. Probiotic & Prebiotic to save Human Microbiota Enhancing Health and Wellbeing. In print on AgroFood

40. van Aalten DMF, Komander D, Synstad B, Gaseidnes S, Peter MG, Eijsink VGH. Structural insights into the catalytic mechanism of a family 18 exo-chitinase. Proc Natl Acad Sci. USA, 2001 98:8979-8984.

41. Terwisscha van Scheltinga AC, Armand S, Kalk KH, Isogai A, Henrissat B, Dijkstra BW. Stereochemistry of chitin hydrolysis by a plant chitinase/lysozime and X-ray structure of a complex with allosamidin: Evidence for substrate assisted catalysis. Biochemistry. 1995 34:15619-15623.

42. McCarthy MF. Glucosamine for wound healing. Med Hypoth. 1996 47:273-275.

43. Mezzana P. Clinical efficacy of a new nanofibrils-based gel in wound healing. Acta Chirurgiae Investig Dermatol. 2008 3:5-13.

44. Bakkers J, Semino CE, Stroband H, Kune JW, Robbins PW. An important developmental role for oligosaccharides during early embryogenesis of cyprinid fish. Proc Natl Acad Sci. USA 1997 94:7982-7986.

45. Muzzarelli RAA, Mattioli-Belmonte M, Pugnaloni A, Biagini G. Biochemistry hystology and clinical uses of chitins and chitosans in wound healing. In: P Jolles and RAA Muzzarelli (Eds) Chitin and Chitinases, Birkhauser Verlag, Basel/ Switzerland, 1999 pp. 251-264.

46. Biagini G, Gabbanelli F, Giantomassi F, Virgili L, and Mattioli-Belmonte M. Natural Cosmetology; Innovative Approach to Ameliorate the Skin Barrier. J Appl Cosmetol. 2003 21:47-52.

47. Hano H, Iriyama K, Nishiwaki H, Kifune K.Effects on N-acetyl-D-glucosamine on wound healing in rats. Mie Med J. 1985 35: 53-56.

48. Werb Z, Gordon S. Secretion of a specific collagenase by stimulated macrophages. J Exp Med. 1975 142: 346-360.

49. Mattioli-Belmonte M, Zizzi A, Lucarini G, Giantomassi F, Biagini G, Tucci G, Orlando F, Provinciali M, Carezzi F, Morganti P. Chitosan-linked to chitosan glycolate as Spray, Gel, and Gauze Preparations for Wound Repair. J Bioactive and Compatible Polymers 2007 22: 525-538.

50. Morganti P, Mattioli-Belmonte M, Tucci MG, Ricotti G, Biagini G. New Prospects for Cutaneous Wound Healing and Keloid Treatment. J Appl Cosmetol 2000 18:125-130.

51. Clark RAF. The molecular and cellular biology of wound repair. New York, Plenum Press, 1996.

52. Tucci MG, Belmonte-Mattioli M, Ricotti G, Biagini G. Polysaccharides: Health-Environment Binomial. J Appl Cosmetol. 1999 17:94-101.

53. Toh YC, Ng S, Khong YM, Zhang X, Zhu Y, Lin PC, Te CM, Sun W, Yu H. Cellular response to nanofibrous environment. Nano Today 2006 1:34-43.

54. Biagini G, Zizzi A, Giantomassi F, Orlando F, Lucarini G, Mattioli-Belmonte M, Tucci MG. Cutaneous absorption of nanostructured chitin associated with natural Synergstic molecules (lutein). J Appl Cosmetol. 2008 26:69-80.

55. Tran H, Pankov R, Tran SD, Hampton B, Burgess WH, Yamada KM. Integrin clustering induces kinectin accumulation. J Cell Sci. 2002 115:2031-2040.

56. Ravi Kumar MNV, Muzzarelli RAA, Muzzarelli C, Sashiwa H, Domb AJ. Chitosan chemistry and pharmaceutical perspectives. Chemical Reviews 2004 104:6017-6084.

57. Muzzarelli RAA, Boudrant J, Meyer D, Manno N, De Marchis M, Paoletti MG. A tribute to Henri Braconnot precursor of the carbohydrate polymers science on the chitin bicentennial. Carbohydrate Polymers 2012 87:995-1012.

58. Busilacchi A, Gigante A, Mattioli-Belmonte M, Manzotti S, and RAA Muzzarelli(2013) Chitosan stabilizes platelet growth factors and modulate stem cell differentiation toward tissue regeneration. Carbohydrate Polymers 98:665-676.

59. Fisher GJ, Datta S, Wang Z, Li Y, Quan T, Chung J, Kang S, Voerhees J. C-Jung dependent inhibition of cutaneous procollagen transcription following ultraviolet irradiation is reversed by all trans retinoic acid. J Clin Invest, 2000 106: 661-668.

60. Krutmann J, Schroeder P. Role of mithocondria in photoaging of human skin. J Invest Dermatol, 2009 14:44-49.

61. Williams DF. On the mechanisms of biocompatibility. Biomaterials 2008 29:2941-2953.

62. Simak J. The effects of engineered Nanomaterials on Platelets. In: Dobrovolskaia MA and McNeil SE. Handbook of Immunological Properties of Engineered Nanomaterials, London, World Scientific, 2013 pp. 293-356.

63. Morganti P, Morganti G, Morganti A. Transforming nanostructured chitin from crustacean waste into beneficial health products: a must for our society. Nanotechnology, Science and Application, 2011 4: 123-129.

64. Morganti P, Yuan-Hong Li. From Waste Materials Skin-Friendly Nanostructured Products to Save Humans and the Environment. Journal of Cosmetics. Dermatological Sciences and Applications (JCDSA), 2011 1: 99-105.

65. Morganti P, Morganti A. Chitin Nanofibrils. A natural nanostructured compound to save the environment. NBT (Nutraceutical, Business & Technology), 2011 7(5): 50-52.

66. Morganti P, Carezzi F, Del Ciotto P, Morganti G. Chitin Nanoparticles as Innovative Delivery System. Personal Care Europe 2012 5(2):95-98.

67. Morganti P, Del Ciotto P, Fabrizi G, Guarneri F, Cardillo A, Palombo M, and Morganti G. Safety and Tolerability of Chitin Nanofibrils-Hyaluronic acid Nanoparticles Entrapping Lutein. Note I: Nanoparticles Characterization and Bioavailability. SOFW-Journal 2013 139(1/2):12-23.

68. Morganti P, Di Massimo G, Cimini C, Del Ciotto P. Characterization of Chitin nanofibril-Hyaluronan Block Polymer. Personal Care Europe 2013 6(9):61-66.

69. Ulrich KE, Cannizzaro SM, Langer RS, Shakesheff KM. Polymeric Systems for controlled drug release. Chem Rev, 1999 99:3181-3198.

70. Nishiyama N. Nanomedicine: Nanocarriers shape Ag for long life. Nat Nanotechnol, 2007 233:51-59.

71. Von Zglinicki T. Role of oxidative stress in telomere length regulation and replicate senescence. Ann NY Acad Sci, 2000 928:79-86.

72. Yaar M. Clinical and histological features of intrinsic versus extrinsic aging. In: BA Gilchrest and Krutmann (Eds.) Skin aging, Berlin, Springer, 2006 pp.9-21.

73. Nasume T, Koide T, Yokoya S, Hirayoshi K, Nagata K.Interaction between collagen-binding stress protein HSP-47 and collagen. Analysis of kinetic parameters by surface Plasmon resonance biosensor. J Biol Chem, 1994 269 (49): 31224-28.

74. Getting PG. Serpin structure, mechanism, and function. Chem Rev, 2003 102(12):4751-4804.

75. Morganti P, Palombo M, Palombo P, Fabrizi G, Cardillo A, Carezzi F, Morganti G, Ruocco E, Dziergowski S. Cosmetic Science in Skin Aging: Achieving the efficacy by the chitin Nano-Structured Crystallites. SOFW-Journal 2010 136(3): 14-24.

76. Morganti P., Palombo M., Cardillo A., Del Ciotto P., Morganti G, Gazzaniga G. Anti-dandruff and anti-oily Efficacy of Hair formulations with a Repairing and Restructuring activity. The Positive Influence of the Zn-Chitin Nanofibrils Complexes. J. Appl. Cosmetol. 2012 30: 149-159.

77. Rosen Y, Elman N. Biomaterial Science. An integrated Clinical and Engineering Approach. New York, CRC-Press, 2012.

78. Palsson BO, Bathia SN. Tailoring biomaterials. In: Tissue Engineering, Upper Saddle River, NJ, Pearson Prendice Hall, 2004 pp. 270-287.

79. Keeney M, Han LH, Onyiah S, Yang F. Tissue Engineering: Focus on the Musculoskeletal System. In: Y. Rosen and N. Elman (Eds.), Biomaterial Science, New York, CRC-Press, 2012 pp. 191-221.

80. Agarwal S, Greiner A, Wendorff JH. Progress in Polymer Science. Review 2013 38: 963.

81. Yudin VE, Dobrosvolskaya IP, Neelov IM, Dreswanina EN, Popryadukhin PN, Ivankova EM, Elochoysky V, Kasatkin IM, Okrugin B, Morganti P. Wet spinning of fibers made of chitosan and chitin nanofibrils. Carbohydrate Polymers, 2014 108: 176-182.

82. Bhardwas N, Kundu SC. Electrospinning: a fascinating fiber fabrication technique. Biotechnology Advances 2010 28:325-347.

83. Kramadhati S, Thyagarajan K. Optical properties of pure and doped polyvinyl alcohol polymer thin films. Int J Engineering Research and Development 2013 6(8): 15-18.

84. Savolainen K. Responsive Development of Nanotechnology. Newsletter Nanotech It, 2011 1: 27-30.

85. Morganti P, Morganti G, Morganti A. Nanobiotecnologia e Bioeconomia Verde.ICF 2014 V (1): 26-30.

86. EU Strategy 2020. Communication from Commission: EUROPE 20020. A strategy for smart, sustainable and inclusive growth. EU Commission, 2010.

87. Mantovani E, Zappelli P, Conde J, Sitja R, Pierales. ObservatoryNANO. Report on Nanotechnology & Textiles. AIRI/NANOTECH IT and Bax & Willems Consulting Ed, Bruxelles, April, 2010.

88. Zotarelli Filho IJ, Frascino LF, Greco OT, de Araújo JD, Bilaqui A, Kassis EN, Ardito RV and Bonilla-Rodriguez GO. Chitosan-Collagen scaffold s can regulate the biological activities of adipose mesenchymal stem cells for tissue engineering. Regenerative Medicine & Tissue Engineering, ISSN 2050-1218, 2013 Herbert open access Journals, http://creativecommons.org/licenses/by/3.0

2

Materials for Drug & Gene Delivery

Syed Zia Ul Quasim[1], Abdul Naveed[2], Mohd Moheed Athar[2], Syed Irfan[3], Mohd Irfan Ali[4], Dr. Mohd Muqtader Ahmed[5], R. Balaji Reddy[5]

[1]Dept of Chemistry, Texas A&M University commerce, Texas City of Commerce, U.S.
[2]Dept of Pharmacy Practice, Malla Reddy College of Pharmacy, Hyderabad, India
[3]Department of Chemistry, Long Island University, New York
[4]Department of Pharmaceutics, Long Island University, New York
[5]Department of Pharmaceutics, Deccan School of Pharmacy, Hyderabad, India

Outline:

Introduction

International Union of Pure and Applied Chemistry (IUPAC) has defined nanomaterials as materials having sizes smaller than 100 nanometers (1 nm = 10^{-9} m) along at least one dimension (length, width, or height) [1]. Nanomaterials are a new step in the evolution of understanding and utilization of materials. They are investigated as promising tools for the advancement of diagnostic biosensors, drug/gene delivery and biomedical imaging for their unique physicochemical and biological properties. Many properties of nanomaterials, such as size, shape, chemical composition, surface structure, surface charge, aggregation, agglomeration, and solubility can greatly influence their interactions with biomolecules and cells [2]. The uniqueness of the structural characteristics, energetics, response, dynamics, and chemistry of nanostructures constitutes the basis of nanoscience [3]. Suitable control of these properties and responses of nanostructures can lead to new devices and technologies.

Although it is basically impossible to cover all the areas where nanoscale materials are involved, we have made a choice of topics for this book that will provide the reader not only with a broad overview of current hot topics in materials chemistry, but also with specific examples of the special properties of these materials and some particular applications of interest.

Nanoparticles

Nanoparticles may be defined as ultra dispersed solid supramolecular structures, generally (but not necessarily) made of polymers and displaying a sub-micrometer size, preferably smaller than 500 nm [4]. Polymers used in controlled drug delivery, including nanoparticles, may be classified as either (*i*) synthetic and natural, or (*ii*) biodegradable and nonbiodegradable. Synthetic biodegradable polymers used to prepare nanoparticles include: poly lactide-co-glycolide (PLGA), poly-ε-caprolactone, polylactic acid (PLA), Polyglycolic acid (PGA), polyanhydrides, and polyphosphazene. Synthetic nonbiodegradable polymers used in drug delivery include polymethyl methacrylate. Naturally occurring biodegradable and biocompatible polymers include: chitosan, gelatin, alginate, cellulose, pullulan, and gliadin [5].

Synthesis

Methods used in synthesis of nanoparticles can be divided into two groups (*i*) those based on polymerization (*ii*) those taking advantage of preformed polymers. The choice of the method for the preparation of nanoparticulate formulation depends upon various factors including (a) size of nanoparticles required (b) inherent properties of drug, e.g., aqueous solubility and stability (c) surface characteristics such as charge and permeability (d) degree of biodegradability, biocompatibility and toxicity (e) drug release profile desired (f) Antigenicity of the final product [6].

Solvent Evaporation

This method can be used for preparation of particles with sizes varying from a few nanometers to micrometers by controlling the stirring rates and conditions, showing high efficiency in incorporation of lipophillic drugs [6]. Polymer solution is prepared in volatile solvents and emulsion is formulated (either oil in water or water in oil in water). Earlier dichloromethane and chloroform preformed polymer were widely used, which is now replaced with ethyl acetate, having better toxicological profile. High speed homogenization or ultrasonication are utilized to reduce the particle size followed by evaporation of

the solvent, either by continuous magnetic stirring at room temperature or under reduced pressure. The emulsion is converted into a nanoparticle suspension on evaporation of the solvent. Afterwards, the solidified nanoparticles can be collected by ultracentrifugation and washed with distilled water to remove additives such as surfactants. Finally, the product is lyophilized. The Schematic representation of solvent evaporation technique is shown in Figure 2.1 [7, 8].
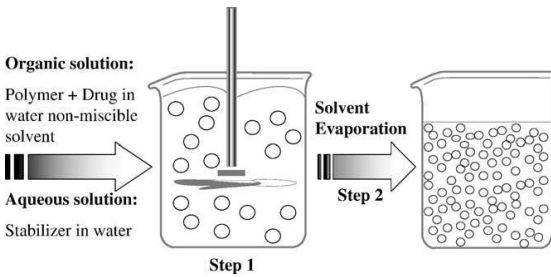
FIGURE 2.1
Solvent Evaporation technique [8].

Emulsification /solvent diffusion method

This is a modified version of solvent evaporation method. The polymer is dissolved in a partially water soluble solvent such as propylene carbonate and saturated with water to ensure the initial thermodynamic equilibrium of both liquids. To produce the precipitation of the polymer and the consequent formation of nanoparticles, it is necessary to promote the diffusion of the solvent by diluting with excess of water or other organic solvent. Subsequently, the polymer-water saturated solvent phase is emulsified in an aqueous solution containing stabilizer, leading to solvent diffusion to the external phase and the formation of nanoparticles. Finally, the solvent is eliminated by evaporation or filtration, according to its boiling point [8].
Emulsification /solvent diffusion method is efficient in encapsulating lipophilic drugs.
Several drug-loaded nanoparticles were produced by the ESD technique, including mesotetra(hydroxyphenyl)porphyrin-loaded PLGA (p-THPP) nanoparticles, doxorubicin-loaded PLGA nanoparticles, plasmid DNA-loaded PLA nanoparticles, coumarin-loaded PLA nanoparticles, indocyanine, cyclosporine (Cy-A)-loaded gelatin and cyclosporin (Cy-A)-loaded sodium glycolate nanoparticles [5, 9-15].
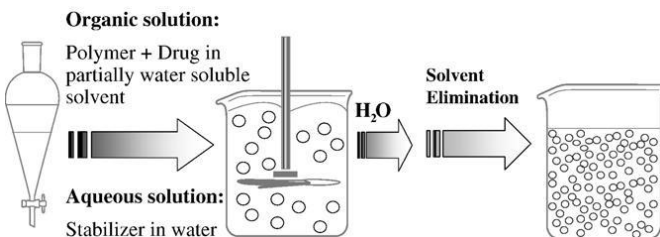
FIGURE 2.2
Emulsification /solvent diffusion method [8].

Salting Out

Salting out is based on the separation of a water miscible solvent from aqueous solution via a salting out effect. Polymer and drug are initially dissolved in a solvent such as acetone, which is subsequently emulsified into an aqueous gel containing the salting-out agent (electrolytes such as magnesium chloride, calcium chloride and magnesium acetate or non- electrolytes such as sucrose) and a colloidal stabilizer such as polyvinylpyrrolidone or hydroxyethylcellulose. This oil/water emulsion is diluted with a sufficient volume of water to enhance the diffusion of acetone into the aqueous phase, thus inducing the formation of nanospheres. Both the solvent and the salting out agent are then eliminated by cross-flow filtration [8].
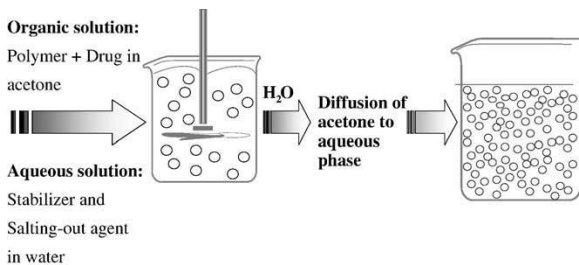
FIGURE 2.3
Salting out technique [8].

Solvent Displacement/ Nanoprecipitation

Nanoprecipitation is also called solvent displacement method. It involves the precipitation of a preformed polymer from an organic solution and the diffusion of the organic solvent in the aqueous medium in the presence or absence of a surfactant [16-19].
The polymer is dissolved in a water-miscible solvent of intermediate polarity, leading to the precipitation of nanoparticles. Acetone, dichloromethane are used to dissolve and increase the entrapment of drugs. The dichloromethane increases the mean particle size [20]. This phase is injected into a stirred aqueous solution containing a stabilizer as a surfactant. When both phases are in contact the solvent diffuses from the organic phase into the water and carries with it some polymer chains which are still in solution. As the solvent diffuses further into the water the associated polymer chains aggregate forming nanoparticles. Polymer deposition on the interface between the water and the organic solvent, caused by fast diffusion of the solvent, leads to the instantaneous formation of a colloidal suspension [6, 18].
This method is basically applicable to lipophilic drugs because of the miscibility of the solvent with the aqueous phase, and it is not an efficient means to encapsulate water-soluble drugs. It has been applied to various polymeric materials such as PLGA, PLA, PCL, and poly (methyl vinyl ether-comaleic anhydride) (PVM/MA) [17, 21-24]. Nanoprecipitation is well adapted for the incorporation of cyclosporin A, because entrapment efficiencies as high as 98% were obtained [25].
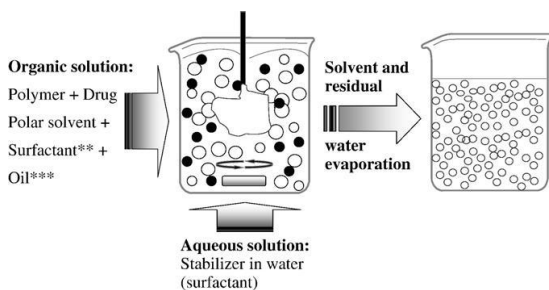
FIGURE 2.4
Solvent Displacement [8].

Emulsion-Diffusion-Evaporation

This method incorporates both evaporation and diffusion process in nanoparticles formation. Polymer is dissolved in a volatile, slightly miscible organic solvent, like ethyl acetate, which is added to the aqueous phase under continuous stirring. The resulting emulsion is slowly diluted by sufficient water under continuous stirring resulting in nanoparticle formation. The basic methodology involves the dispersion of organic phase as globules in equilibrium with external aqueous phase due to continuous stirring. The emulsion is stabilized by adsorption of stabilizer at the interface. The globule size is further lowered by homogenization. Addition of water destabilizes the equilibrium and diffusion of organic solvent to aqueous phase causes local super-saturation near the interface resulting in nanoparticles formation. The organic phase is removed from the preparation by evaporation at 400°C [26].

Spray Drying

In spray drying technique polymer solution is obtained by dissolving polymer and drug in dilute acetic acid at room temperature. The polymer solution is then added to the aqueous medium containing cross linking agent with magnetic stirring at room temperature. The resulting colloidal solution was stirred for 30 minutes before spray-dried at a feed rate of 6.0 ml/min. The spray-drying conditions were inlet temperature 128–132°C, outlet temperature 68–71°C, aspirator 90% and pump feed 20% [27]. The nature of solvent used, temperature of the solvent evaporation and feed rate affects the morphology of the microspheres. The main disadvantage of this process is the adhesion of the microparticles to the inner walls of the spray-dryer [28-30].

Materials

Poly (Lactide-Co-Glycolide) (PLGA)

PLGA, copolymer of poly lactic acid (PLA) and poly glycolic acid (PGA), is widely used for DDS development because of its biodegradability, biocompatibility and ease of processing [31]. It is the best defined biomaterial available for drug delivery with respect to design and performance. Poly lactic acid contains an asymmetric carbon which is typically described as the D or L form in classical stereochemical terms and sometimes as R and S form, respectively. PLGA is generally an acronym for poly D,L-lactic-co-glycolic acid where D- and L- lactic acid forms are in equal ratio [32].

PLGA, which is hydrophobic in nature [32], can be processed into almost any shape/size, and can encapsulate molecules of virtually any size. It is soluble in wide range of common solvents including chlorinated solvents, tetrahydofuran, acetone and ethyl acetate [33, 34]. Crystalline PGA, when co-polymerized with PLA, reduces the degree of crystallinity of PLGA hence a higher content of PGA leads to quicker rates of degradation with an exception of 50:50 ratio of PLA/PGA, which exhibits the fastest degradation. Properties of PLGA like glass transition temperature (Tg), moisture content and molecular weight, changes during polymer biodegradation and has influences on the release and degradation rates of incorporated drug molecules. Properties like molecular weight and polydispersity index also affect the ability to be formulated as a drug delivery device and may control the device degradation rate and hydrolysis [32].

Sustained intracellular retention suggest that nanoparticles containing encapsulated plasmid DNA could serve as an efficient sustained release gene delivery system [35]. Therapeutic proteins and peptides can be encapsulated into nanoparticles using double emulsion solvent evaporation techniques. Adjuvant properties of PLGA nanoparticles containing encapsulated vaccines and drug have been extensively studied [36].

Polymethyl methacrylate (PMMA)

PMMA is a non-biodegradable synthetic homopolymer of methylmethacrylate monomer (MMA). It is classified as a hard, rigid but brittle material with a glass transition temperature of 105°C [37]. PMMA is rather hydrophobic but becomes slightly more hydrophilic after contact with water. The best organic solvents for PMMA are partly substituted hydrocarbons as trichloroethylene. At present, it is generally accepted that PMMA is a non-toxic polymer as it possesses a very good toxicological safety record in biomedical applications [38].

PMMA used as the carrier for daptomycin, non-steroidal anti-inflammatory drugs (NSAID) like indomethacin, tolmetin and mefenamic acid, antineoplastic and antiresorptive agents as methotrexate, doxorubicin and pamidronate and anti-fungal drugs as amphotericin B [39-43].

Poly-ε-Caprolactones (PCL)

Poly (ε-caprolactone) (PCL) is biodegradable industrial polyester with excellent mechanical strength, non-toxicity, and biocompatibility. It has been frequently used as implantable carriers for drug delivery systems or as surgical repair materials. It is hopeful to combine chitosan with the biodegradable polyester to create amphiphilic copolymer applicable to drug delivery systems.

Dextran-PCLn was prepared by coupling between carboxylic function present on preformed PCL monocarboxylic acid and the hydroxyl groups on dextran [44, 45]. The modification of the surface with dextran significantly reduced the cytotoxicity [46].

Poly-ε-caprolactone nanoparticles have been used as vehicles to deliver a wide range of drugs including tamoxifen, retinoic acid, and griseofulvin [47]. Bovine serum albumin and lectin were incorporated in the nanoparticles. Lectins could also be adsorbed onto the surface of the nanoparticles. Surface-bound lectin conserved its hemagglutinating activity, suggesting the possible application of this type of surface-modified nanoparticles for targeted oral administration [48].

Poly glycolic acid (PGA)

PGA is biocompatible and has been known since 1954 to be a potentially low-cost tough fibre forming polymer. PGA is the simplest aliphatic polyester. It has a glass transition temperature between 35–40˚C

and melting point ranging from 224– 227˚ C. Because of its simple chemical structure and stereoregularity, it occurs with different degree of crystallinity from completely amorphous to a maximum of 52% crystallinity. The crystallinity of PGA in Dexon Suture is typically in the range of 46–52% and it tend to lose mechanical strength rapidly, typically over a period of 2–4 weaks after implantation [49].

Poly Lactic Acid (PLA)

PLA is a synthetic, bioabsorbable, non-toxic and biodegradabile polymer [50]. PLA is chiral in nature, the chirality is seen in the carbon with four different substituents (hydrogen, oxygen, carbonyl, and methyl), and it is this that causes two different PLA polymers – PDLA and PLLA. PLLA has a crystallinity of 37%, a glass transition temperature between 50 and 80°C, and a melting temperature of 173-178° C. A polymerization of the racemic mixture produces PDLLA, which, due to the interference of stereochemistry in the chain alignment, is amorphous [51].

Chitosan

Chitason is a natural polymer obtained by deacetylation of chitin, a component of crab shells. It is a cationic polysaccharide composed of linear β (1,4)-linked d-glucosamine [52]. Chitosan is produced commercially by deacetylation of chitin, which is the structural element in the exoskeleton of crustaceans (such as crabs and shrimp) and cell walls of fungi [53-55]. Chitin is highly basic polysaccharides due to presence of primary amino group in its structure.

The main factors which may affect the chitason properties are its molecular weight and degree of deacetylation. The molecular weight of the chitason depends on viscosity, solubility, elasticity and tears strength. In alkaline or neutral medium, free amino group of chitosan is not protonated and therefore it is insoluble in water, while in acidic pH, it gets solubilized due to protonation of free amino groups and the resultant soluble polysaccharide is positively charged. Chitosan forms water-soluble salts with inorganic and organic acids includes glyoxylate, pyruvate, tartarate, malate, malonate, citrate, acetate, lactate, glycolate, ascorbate [56].

Chitosan used as carrier material for various drugs by numerous mechanisms including chemical cross-linking, ionic cross-linking, and ionic complexation [57]. Chitosan also used as a carrier for antibodies [58].

Alginates

Alginate is a water-soluble linear, polyanionic, polysaccharide extracted from brown seaweed and is composed of alternating blocks of 1–4 linked α-L-guluronic and β-D-mannuronic acid residues [59]. Alginate exhibits a pH-dependent anionic nature and has the ability to interact with cationic polyelectrolytes and proteoglycans [60]. In aqueous media, the sodium ions from salts of this anionic polymer exchange with divalent cations, such as calcium, to form water-insoluble gels [5]. Therefore, delivery systems for cationic drugs and molecules can be obtained through simple electrostatic interactions.

The molecular weight (MW) of alginate influences the degradation rate and mechanical properties of alginate-based biomaterials. Basically, higher MW decreases the number of reactive positions available for hydrolysis degradation, which further facilitates a slower degradation rate [60].

Alginates are ideal carriers for oligonucleotides, peptides, proteins, water-soluble drugs, or drugs that degrade in organic solvents [5].

Gelatin

Gelatin is a natural, biodegradable protein obtained by acid- or base-catalyzed hydrolysis of collagen. It is a heterogenous mixture of single- or multi-stranded polypeptides composed predominantly of glycine, proline, and hydroxyproline residues and is degraded in vivo to amino acids. Gelatin is a polyampholyte having both cationic and anionic groups along with hydrophobic group [61]. PEGylation of the particles significantly enhances their circulation time in the blood stream and increases their uptake into cells by endocytosis [62].

Gelatin nanoparticles have been used to deliver paclitaxel, methotrexate, doxorubicin, DNA, double-stranded oligonucleotides, and genes [62]. Antibody-modified gelatin nanoparticles have been used for targeted uptake by lymphocytes [63].

Nanocapsules

Nanocapsules are defined as nano-vesicular systems that exhibit a typical core-shell structure in which the drug is confined to a reservoir or within a cavity surrounded by a polymer membrane or coating. The cavity can contain the active substance in liquid or solid form or as a molecular dispersion. Likewise, this reservoir can be lipophilic or hydrophobic according to the preparation method and raw materials used. Nanocapsules can also carry the active substance on their surfaces or imbibed in the polymeric membrane.

Synthesis

Generally, there are five classical methods for the preparation of nanocapsules: nanoprecipitation, emulsion–diffusion, double emulsification, emulsion-coacervation and layer by layer.

Nanoprecipitation method

Nanocapsule synthesis needs both solvent and non-solvent phases. The solvent phase (usually organic phase) essentially consisting of a solution in a solvent or in a mixture of solvents (i.e. ethanol, acetone, hexane, methylene chloride or dioxane) of a film-forming substance such as a polymer (synthetic, semi-synthetic or naturally occurring polymer), the active substance, oil, a lipophilic tensioactive and an active substance solvent. On the other hand, the non-solvent phase (usually aqueous phase) consisting of a non-solvent or a mixture of non-solvents for the film-forming substance, supplemented with one or more naturally occurring or synthetic surfactants.

In the nanoprecipitation method, the polymer is dissolved in a water-miscible solvent of intermediate polarity, leading to the precipitation of nanospheres. This phase is injected into a stirred aqueous solution containing a stabilizer as a surfactant. The process of particle formation in the nanoprecipitation method comprises three stages: nucleation, growth and aggregation. The rate of each step determines the particle size and the driving force of these phenomena is supersaturation. The separation between the nucleation and the growth stages is the key factor for uniform particle formation. The key variables of the procedure are those associated with the conditions of adding the organic phase to the aqueous phase, such as organic phase injection rate, aqueous phase agitation rate, the method of organic phase addition and the organic phase/aqueous phase ratio.

The polymers commonly used are biodegradable polyesters, especially poly-e-caprolactone (PCL), poly(lactide) (PLA) and poly(lactide-co-glicolide) (PLGA). Synthetic polymers have higher purity and better reproducibility than natural polymers.
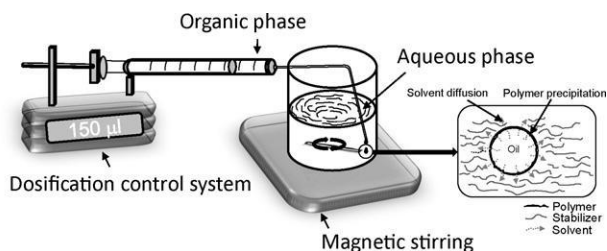
FIGURE 2.5
Nanoprecipitation.

Emulsion–diffusion method

Preparation of nanocapsules by the emulsion–diffusion method allows both lipophilic and hydrophilic active substance nanoencapsulation. The experimental procedure performed to achieve this requires three phases: organic, aqueous and dilution. The organic phase contains the polymer, the active substance, oil and an organic solvent (partially miscible with water). The aqueous phase comprises the aqueous dispersion of a stabilizing agent. Dilution phase is usually water.

For preparation of nanocapsules using the emulsion–diffusion method, the organic phase is emulsified under vigorous agitation in the aqueous phase. The subsequent addition of water to the system causes the diffusion of the solvent into the aqueous phase, resulting in nanocapsule formation. This can be eliminated by distillation or cross-flow filtration depending on the boiling point of the solvent.

The nanocapsule formation mechanism is based on the theory that each emulsion droplet produces several nanocapsules and that these are formed by the combination of polymer precipitation and interfacial phenomena during solvent diffusion. Consequently, solvent diffusion from the globules carries molecules into the aqueous phase forming local regions of supersaturation from which new globules or polymer aggregates are formed and stabilized by the stabilizing agent, which prevents their coalescence and the formation of agglomerates. If the stabilizer remains at the liquid–liquid interface during the diffusion process and if its protective effect is adequate, the nanocapsules will be formed after the complete diffusion of the solvent. The nanocapsule size is related to the shear rate used in the emulsification process, chemical composition of the organic phase, polymer concentration, oil-to-polymer ratio and the drop size of the primary emulsion.

The polymers commonly used are biodegradable polyesters, especially PCL, PLA and eudragit. Poly(hydroxybutyrate-co-hydroxyvalerate) (PHBHV) may also be used. Ethyl acetate is the first option as a solvent though propylene carbonate, benzyl alcohol and dichloromethane can also be used. In regarding to the aqueous phase, the solvent used is water and poly(vinyl alcohol) (PVA) is preferred as the stabilizing agent. Other stabilizing agents such as poloxamer and ionic emulsifiers have been used. The dilution phase is often water.
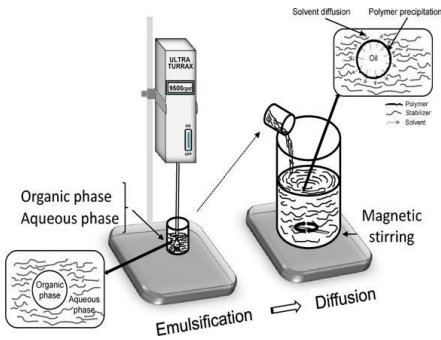
FIGURE 2.6
Emulsion–diffusion method.

Double emulsification method

Double emulsions are complex heterodisperse systems called "emulsions of emulsions", that can be classified into two major types: water-oil-water emulsion (w/o/w) and oil-water-oil emulsion (o/w/o). Double emulsions are usually prepared in a two step emulsification process using two surfactants: a hydrophobic one designed to stabilize the interface of the w/o internal emulsion and a hydrophilic one to stabilize the external interface of the oil globules for w/o/w emulsions.

In the primary w/o emulsion the oil is changed by an organic phase containing a solvent that is totally or partially miscible in water, film-forming polymer and a w/o surfactant. Then the water containing a stabilizing agent is added to the system to obtain the water in organic in water emulsion.

For the preparation of nanocapsules by double emulsification, the primary emulsion is formed by ultrasound and the w/o surfactant stabilizes the interface of the w/o internal emulsion. The second emulsion is also formed by ultrasound and nanocapsule dispersion is stabilized by the addition of the stabilizing agent. Finally, the solvents are removed by evaporation or extraction by vacuum, leaving hardened nanocapsules in an aqueous medium.

In the organic phase ethyl acetate, methylene chloride and dichloromethane have been used as solvents. Biodegradable polyesters such as PCL, PLA and PLGA have been frequently used. Sorbitan esters are preferred as o/w surfactants. PVA and polysorbates are used as stabilizing agents in external aqueous phase.
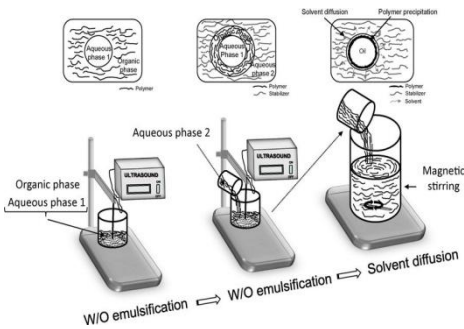
FIGURE 2.7
Double emulsification method.

Emulsion-coacervation method

The emulsion-coacervation process is mainly presented as a strategy for nanocapsules preparation from naturally occurring polymeric materials. Up to now, sodium alginate and gelatin have been used though synthetic polymeric materials could be used for this purpose.

The procedure involves the o/w emulsification of an organic phase (oil, active substance and active substance solvent if necessary) with an aqueous phase (water, polymer, stabilizing agent) by mechanical stirring or ultrasound. Then, a simple coacervation process is performed by using either electrolytes (sodium alginate–calcium chloride system) with the addition of a water miscible non-solvent or a dehydration agent with a gelatin–isopropanol–sodium sulfate system or by temperature modification with the application of triblock terpolymer in gold nanocapsule synthesis. Finally the coacervation process is complemented with additional crosslinked steps that make it possible to obtain a rigid nanocapsule shell structure.

Nanocapsule formation by the emulsion-coacervation method uses the emulsion as a template phase and the formation of a coacervate phase that causes polymer precipitation from the continuous emulsion-phase to form a film on the template forming the nanocapsule. Additionally, it can be stabilized by physical intermolecular or covalent cross-linking, which typically can be achieved by altering pH or temperature, or by adding a cross-linking agent.
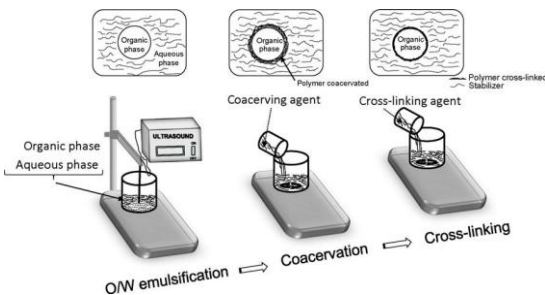
FIGURE 2.8
Emulsion-coacervation method.

Layer-by-layer method

The layer-by-layer assembly process developed for colloidal particle preparation makes it possible to obtain vesicular particles, called polyelectrolyte capsules, with well-defined chemical and structural properties. The layer by layer technique is based on alternate adsorption of oppositely charged materials, mostly linear polyelectrolytes, via electrostatic interactions. Multilayer ultrathin films can be developed with "molecular architecture" design with precise control of thickness and molecular composition

The mechanism of nanocapsule formation is based on irreversible electrostatic attraction that leads to polyelectrolyte adsorption at supersaturating bulk polyelectrolyte concentrations. This method requires a colloidal template onto which is adsorbed a polymer layer either by incubation in the polymer solution, subsequently washed, or by decreasing polymer solubility by drop-wise addition of a miscible solvent. This procedure is then repeated with a second polymer and multiple polymer layers are deposited sequentially. The solid form of the active substances, biological cells, compact forms of DNA, protein aggregates and gel beads can be used as a template.

The polycations used in layer-by-layer method are polylysine, chitosan, gelatin B, poly(allylamine) (PAA), poly(ethyleneimine) (PEI), aminidextran and protamine sulfate. The polyanions are poly(styrene sulfonate) (PSS), sodium alginate, poly(acrylic acid), dextran sulfate, carboxymethyl cellulose, hyaluronic acid, gelatin A, chondroitin and heparin [64, 3].
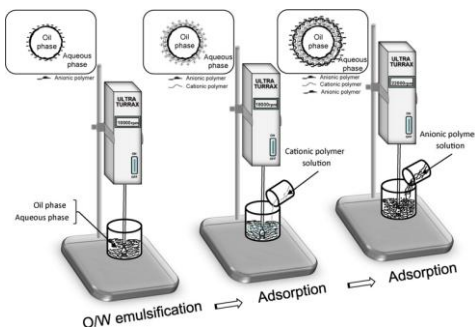
FIGURE 2.9
Layer-by-layer method.

Materials

The polymers commonly used are poly-e-caprolactone (PCL), poly(lactide) (PLA), poly (lactide-co-glicolide) (PLGA), poly(alkyl cyanoacrylate) (PACA) and Eudragit [64]. PCL, PLA and PLGA are discussed earlier in this chapter.

Poly alkyl cyanoacrylate (PACA)

Alkyl cyanoacrylate monomers are highly reactive and polymerized via anionic, zwitterionic or radical mechanism in suitable polymerization medium to form various types of nanocarriers - nanospheres, core-shell nanoparticles (with covalently attached hydrophilic polymers on the surface), nanocapsules (with oily or aqueous core), hybrid nanoparticles with magnetic core etc [65].

Nanoparticles of PACA homopolymers have relatively hydrophobic surfaces and adsorb larger amounts of proteins [65]. The PEGylation concept, either via a simple adsorption of PEG chains onto the

nanoparticles or by a covalent linkage of PEG chains with PACA polymers, allows different types of hydrophilic molecules to anchor on to the surface of PACA nanoparticles [66].

Different types of PACA-based nanocarriers incorporate a great variety of drugs, such as cytostatics, antibiotics, antiviral agents, anti-fungal drugs, non-steroidal anti-inflammatory drugs etc [65].

Eudragit

Eudragit is a trade name of Poly(meth)acrylates prepared by the polymerization of acrylic and methacrylic acids or their esters, e.g., butyl ester or dimethylaminoethyl ester [67]. Eudragit polymers are available in a wide range of different physical forms (aqueous dispersion, organic solution granules and powders). The flexibility to combine the different polymers enables to achieve the desired drug release profile by releasing the drug at the right place and at the right time and, if necessary, over a desired period of time [68].

Eudragit has a glass transition temperature 48˚C. It is soluble in gastric fluid to pH=5 [67]. Eudragit L and S polymers are preferred choice of coating polymers. They enable targeting specific areas of the intestine [68].

Eudragit used in delivery of drugs like Ibuprofen, Acetaminophen, Morphine HCl, Roxithromycin, Nizatidine, Cetraxate HCl, Ciprofloxacin, Ibuprofen, Bifemelane HCl etc [67].

Fullerenes

Fullerenes are closedcage carbon molecules with three-coordinate carbon atoms tiling the spherical or nearly-spherical surfaces, the best known example being C60, with a truncated icosahedral structure formed by twelve pentagonal rings and twenty hexagonal rings. Subsequent studies have shown that fullerenes actually represent a family of related structures containing 20, 40, 60, 70, or 84 carbons.

A key attribute of the fullerene molecules is their numerous points of attachment, allowing for precise grafting of active chemical groups in 3D orientations. This attribute, the hallmark of rational drug design, allows for positional control in matching fullerene compounds to biological targets [69].
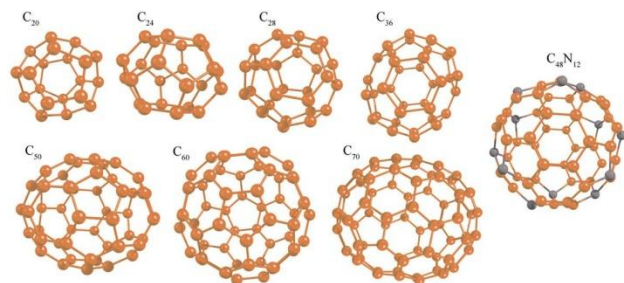
FIGURE 2.10
Structure of fullerenes [70].

Synthesis

Two high purity graphite rods are clamped to the high current feedthrougs. The chamber is then pumped down to ≤ 10^{-3} torr and refilled with He gas to a pressure of 150-250 torr. Because both oxygen and water significantly inhibit the formation of fullerenes, it is important to evacuate the chamber carefully and refill it using purified helium. The electrides are positioned so that the carbon rods are just touching, and then the vaporization is initiated by passing a high current through the rods. For 6.25mm diameter rods, current between 100-200A leads to efficient fullerene formation. Under these conditions, the 6.25mm rods are consumed at a rate of about 5-10 mm/min. The crude carbon product or soot produced by this vaporization collect on the water cooled inner surface of the fullerene apparatus and is readily removed from the walls and collected using a stiff brush. This soot contains a variety of carbon products including C_{60} and larger fullerenes [71].

Properties

The diameter of a C60 molecule is about 7 Å. The C60 molecule, also termed as 'buckminsterfullerene' and 'buckyball' has two bond lengths. The 6:6 ring bonds (between two hexagons) can be considered 'double bonds' and are shorter than the 6:5 bonds (between a hexagon and a pentagon). The carbon atoms in fullerene are in sp2 and sp3 hybridized state. The free electrons on the cage build a strong localized p-electron system. This electron system influences the chemical reactions of the fullerenes. In chemical reactions, these molecules do not exhibit aromatic behavior. Instead, they show aliphatic behavior.
Fullerenes are insoluble in water. However, they are soluble in other solvents like carbon disulphide, toluene and o-dichlorobenzene. Solutions of pure C60 have a deep purple color [72]. The solubility in a solvent generally increases with increasing molecular weight of the solvent [73].

Applications

Fullerenes have potential applications in the treatment of diseases where oxidative stress plays a role in the pathogenesis. These include Degenerative diseases of the CNS including PD, AD, and amyotrophic lateral sclerosis, Multiple sclerosis, Ischemic cardiovascular diseases, Atherosclerosis, Major long-term complications of diabetes, Sun-induced skin damage and physical manifestations of aging etc [69].
Fullerenes are used in treatment of cancer cells, the surface of fullerenes can be 'decorated' with chemotherapeutic agents. An antibody is attached, which serves as a guidance system. metallo fullerenes are being investigated for loading radioactive atoms and then firing them like guided missiles at diseased cells [72].

Nanotubes

The Major Colloidal drug delivery system includes liposome and polymeric nanoparticles [74]. The increase in therapeutic range of the targeted delivery with the help of nanoparticles helped in decreasing the toxicity and side effects [75]. Carbon nanotubes have become the most popular candidates in the field of biomedical engineering, biotechnology, defense research and pharmaceutical

industry after their discovery in 1991 [76]. The introduction of DNA, proteins or drug molecules into the living cells is important to therapeutics. Nanotubes have advanced physical and chemical properties which make them highly promising for biological applications [77].
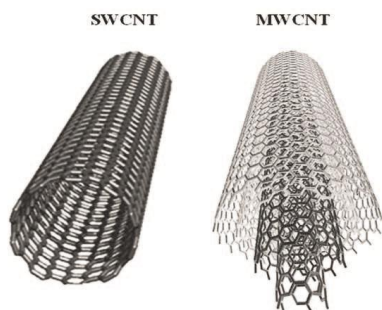
FIGURE 2.11
Single-wall and Multi-wall Carbon Nanotubes [78].

Synthesis

Among the various nanomaterials being currently developed carbon nanotubes (CNTs) have attracted considerable interest due to their great properties and potential benefits in many industrial applications (from materials engineering and electronics to medical devices and drug delivery systems). [79].

Arc-vaporization

The arc vaporization technique generally involves the use of two high-purity graphite electrodes. The anode is either pure graphite or contains metals and cathode is made of metals, mixed with the graphite powder. Cathod is introduced in a hole made in the anode center. The electrodes are momentarily brought into contact and an arc is struck. The synthesis is carried out at low pressure (30-130 torr or 500 torr) in controlled atmosphere composed of inert and/or reactant gas. The distance between the electrodes is reduced until the flowing of a current (50–150 A). The temperature in the inter-electrode zone is so high (>3000°C) that carbon sublimes from the positive electrode (anode) that is consumed. A constant gap (1mm) between the anode and cathode is maintained by adjusting the position of the anode. Plasma is formed between the electrodes which can be stabilized for a long reaction time by controlling the distance between the electrodes by means of the voltage (25–40 V) control. The reaction time varies from 30–60 seconds to 2–10 minutes [80].

Laser ablation

In the laser ablation technique, a high power laser was used to vaporize carbon from a graphite target at high temperature. In order to generate nanotubes, metal particles as catalysts must be added to the graphite targets similar to the arc discharge technique. The quantity and quality of produced carbon nanotubes depend on several factors such as the amount and type of catalysts, laser power and wavelength, temperature, pressure, type of inert gas, and the fluid dynamics near the carbon target. The laser beam (532 nm) is focused onto a carbon targets containing 1.2 % of cobalt/nickel with 98.8 % of graphite composite, placed in a 1200°C quartz tube furnace under the argon atmosphere (~500

Torr). The laser beam scans across the target surface under computer control to maintain a smooth, uniform face for vaporization. The soot produced by the laser vaporization was swept by the flowing Ar gas from the high-temperature zone, and deposited onto a water-cooled copper collector positioned downstream just outside the furnace. The nanotubes will self-assemble from carbon vapors and condense on the walls of the flow tube. The diameter distribution of SWNTs from this method varies about 1.0 - 1.6 nm. Carbon nanotubes produced by laser ablation were purer (up to 90 % purity).
The targets were uniformly mixed composite rods made by the following three-step procedure: (i) a paste produced from mixing high-purity metal or metal-oxide with graphite powder and carbon cement at room temperature was placed in a mold; (ii) the mold was placed in a hydraulic press equipped with heating plates and baked at 130°C for 4–5 h under constant pressure (iii) the baked rod was then cured at 810°C for 8 h under Ar flow. Fresh targets were heated at 1200°C under flowing Ar for 12 h. Subsequent runs with the same target proceeded after two additional hours heating at 1200 °C. The following metals were used: Co, Cu, Nb, Ni, Pt, Co/Ni, Co/Pt, Co/Cu, Ni/Pt [80-82].

Chemical Vapor Deposition

The process involves passing a hydrocarbon vapor (typically for 15-60 minutes) through a tube furnace in which a catalyst material is present at sufficiently high temperature (600-1200°C) to decompose the hydrocarbon. CNTs grow over the catalyst and are collected upon cooling the system to room temperature. For liquid hydrocarbon (benzene, alcohol, *etc*.), the liquid is heated in a flask and an inert gas purged through it to carry the vapor into the reaction furnace. The vaporization of a solid hydrocarbon (camphor, naphthalene, *etc*.) can be conveniently achieved in another furnace at low temperature before the main, high temperature reaction furnace. The catalyst material may also be solid, liquid, or gas and can be placed inside the furnace or fed in from outside. Pyrolysis of the catalyst vapor at a suitable temperature liberates metal nanoparticles [83].

Applications

- Single-walled carbon nanotubes are molecular transporters or carriers with very high optical absorbance in the where biological systems are transparent. This intrinsic property stems from the electronic band structures of nanotubes and is unique among transporters.
- Carbon nanotube (CNT) membranes present the opportunity to create a transdermal patch that can vary its rate of delivery throughout its application to the skin to attain therapeutic plasma levels and plasma profiles of a specific drug [84].
- Cisplatin is a platinum based anticancer drug which is used to treat a wide range of tumors, despite its adverse side effects. It is expected that this form of targeted nanoscale drug delivery will significantly reduce these adverse side effects. The most ideal delivery capsule in terms of minimizing the amount of material required for encapsulation, thus providing the least toxicity. This technique, used to represent the encapsulation of cisplatin entering carbon, boron nitride, boron carbide and silicon nanotubes, can be extended to any number of drug molecules or alternative nanotube materials [85].

Lipid Based Carriers

Encapsulating drugs began in 1970`s with different level of success with vesicles such as liposome that a entrap a solvent core and separate it from the surrounding. Depending on the method of

preparation, lipid vesicles can be multi-, oligo- or unilamellar, containing many, a few, or one bilayer shell(s) respectively. The diameter of the lipid vesicles may vary between about 20 nm and a few hundred micrometers. Small unilamellar vesicles (SUVs) are surrounded by single lipid layer (25–50 nm), whereas several lipid layers separated by intermittent aqueous layer surround large unilamellar vesicles (LUV) (100–200 μm). Giant unilamellar vesicles (GUV) have a mean diameter of 1–2 μm, multilamellar vesicles (MLV) have a mean diameter between 1 μm and 2 μm (10 layers). Multivesicular vesicles are liposomes with lots of vesicles inside [86]. Vesicles are composed of various lipids such as phospatidylcholines, phosphotidylglycerols, and cholesterols. These lipids aggregates, fuses and releases their contents [87]. Lipid based drug delivery system has the advantage of being modified according to the requirement by adjusting the content of different lipid excipients and additives. Increase interest in the lipid base system is due to the versatility of the lipidic excipients, formulation versatility, enhanced permeation capacity, better characterization [88]. The important parameters that defines the oral drug delivery is solubilization of the drug and absorption, drugs which have poor solubility can be overcome using lipid based systems and due to the lipidic nature the absorption can be increased [89].

Type of Lipid Carrier Materials

There are many type of lipid carrier materials few of them includes:

a) **Lipophilic liquid:** Drugs like steroids have good solubility in triacylgylcerols, therefore such drugs can be encapsulated in for delivery. The drawback of this type system is that it limits the use of complex formulation.
b) **Micro-emulsifying systems:** Micro-emulsion systems are essentially surfactant micelles with oil and drug.
c) **Liposomes:** They are spherical bilayered structures consisting of a fatty acid component. the hydrophilic components are entrapped in the internal spaces of the system. They have to ability to penetrate through and delivery the drug, that is the reason they are popular among the lipid based system.
d) **Modified Lipoproteins:** The use of apoprotiens and recognition markers can be helpful in modifying the lipoprotein by using LDL and HDL [90].
e) **Solid Liquid Nanoparticles:** Developed in 1990s produced by replacing the liquid from the emulsion with a solid lipid or blended solid lipid. These are the stable nano-lipid carriers in which the drug is either dissolved or displaced.
f) **Nano-structured lipids:** They are produced by blending solid and liquid lipids. The use of this system is to improve the poor loading of the drug while preserving controlled release features [91].
g) **Lipospheres:** First reported by Domb as water dispersible solid micro-particles composing of solid hydrophobic fat core stabilized by a monolayer of phospholipid molecule embedded in a microparticle surface. The core contains the active ingredient [92].

Synthesis

Melt dispersion technique

In this method, drug is dissolved or dispersed in the molten lipidic phase. Aqueous phase is composed of water or suitable buffer which is heated to the same temperature as lipid phase. The aqueous phase is kept under stirring during which emulsifier is added. To the aqueous phase containing emulsifier, lipid phase containing drug is added drop wise while maintaining the temperature and stirring speed. The temperature of the mixture is rapidly brought down to room temperature or below room temperature by adding ice cold water or ice under continuous stirring. This cold resolidification results in the formation of discrete lipospheres which can be filtered.

Several drugs like bupivacaine, glipizide, aceclofenac, retinyl acetate, progesterone, sodium cromglycate, diclofenac, carbamazepine, C14-diazepam, proteins like somatostatin, thymocartin, casein, bovine serum albumin, R32NS1 malaria antigen, tripalmitin based lipospheres for labon-chip applications have been prepared by melt dispersion methods.

Lipids carrying antigens exert their adjuvant effect to immunogenicity of antigens and the effect was found to decrease in the following order for the lipids studied: ethyl stearate> olive oil> tristearin> tricaprin> corn oil> stearic acid. Also inclusion of negatively charged lipids like dimyristoyl phosphotidyglycerol in the lipid core was found to improve the antibody response to encapsulated malaria antigen [93].
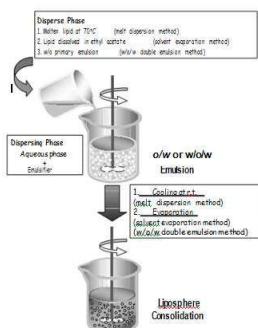
FIGURE 2.12
Melt dispersion technique.

Detergent removal method

Detergents can be defined as a subgroup of surfactants that are able to solubilize lipid membranes. Sufficient amount of detergents lead to the reorganization of lipid bilayers to form smaller, soluble detergent–lipid aggregates of various shapes.

The lipids and lipophilic substances, to be incorporated into the liposomal membrane, are dissolved together with the detergent in an organic solvent or solvent mixture to obtain a clear solution. In most cases methanol, ethanol, or mixtures with chloroform are used as solvent. The solvent is then removed in a rotary evaporator by reduced pressure at a moderate temperature. Residual solvent should be removed by high vacuum for at least 1hr. The dry film is normally clear when bile salts are used as detergent but with nonionic detergents the film will be turbid. A suitable buffer, optionally together with hydrophilic substances to be encapsulated, is added to yield the desired lipid concentration and

the temperature is adjusted. With octylglucoside, after adding the buffer, the dispersion may be opalescent for some seconds before clearing. A preformed liposome dispersion may be dissolved successively with detergent at the desired preparation temperature until a clear solution is achieved [94].

Reserves Phase Evaporation Method

In this method first water in oil emulsion is formed by brief sonication of a two phase system containing phospholipids in organic solvent (diethylether or isopropylether or mixture of isopropyl ether and chloroform) and aqueous buffer. The organic solvents are removed under reduced pressure, resulting in the formation of a viscous gel. The liposomes are formed when residual solvent is removed by continued rotary evaporation under reduced pressure. High encapsulation efficiency up to 65% can be obtained in a medium of low ionic strength (0.01 M NaCl). This method has been used to encapsulate small, large and macromolecules. The main disadvantage of the method is the exposure of the materials to be encapsulated to organic solvents and to brief periods of sonication. These conditions may possibly result in the denaturation of some proteins or breakage of DNA strands [95].
Materials

Solid lipid Nanoparticles

Solid lipid Nanoparticles (SLN) are composed of a core solid lipid with bioactive material constituting a part of the lipid matrix. Such particles are stabilized by the surfactant layer. The term lipid indicates the use of triglycerides, partial glycerides and fatty acids. An advantage of SLN is that they can reduce the risk of acute and chronic poisoning [96].
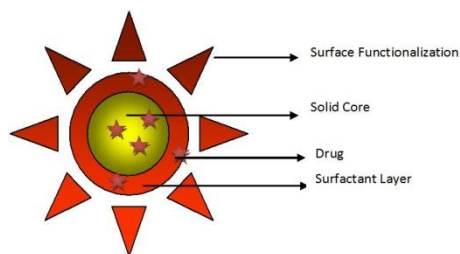
FIGURE 2.13
Solid lipid nanoparticles [97].

SLN permeation across blood brain barrier: Blood brain barrier penetration is one of the most difficult and crucial challenges in pharmaceutical research. Two anti cancer drugs namely camptothecin and doxorubicin when loaded with SLN resulted in drug accumulation into the brain after oral and IV route [98].
Transdermal application: The smallest particle size is observed with SLN, incorporation of SLN in gel like systems which is acceptable for direct application on the skin. SLN have also been to modulate the release of drug into the skin and to improve drug delivery to the particular skin layer [99].

Nanostructure Lipids

Solid nanostructure lipids had attracted attention as drug delivery system as an alternative carrier system to liposome, emulsion and polymeric nanoparticles due to exceptional stability, scaling up potential and biocompatible components. The application of NLC is enhanced by eliminating the use of organic solvents in the preparation stage and using high pressure homogenization technique [100]. Encapsulation of water soluble anticancer compounds: An approach to allow water soluble anticancer pharmaceuticals NLC have been very effective. These drugs can be encapsulated in the hydrophilic cavity of the NLC and outer coating of lipid gives good permeability for absorption.
NLC able to avoid reticuloendothelial scheme(RES): Number off cytotoxic drug which own undertaking to overcome the multi drug resistance phenotypes in units resistant to cytotoxic drug have been emerged. The use of NLC helps to overcome water solubility, drug release and clearing RES system [101].

Liposome

Physico-chemical properties: It readily disperse in aqueous media to reform the original colloidal dispersion. The typical range for lipid based formulation includes a particle size less than 1micro-meter. The solubility differs according to the type of the surfactant used and type of acidic or basic drug.
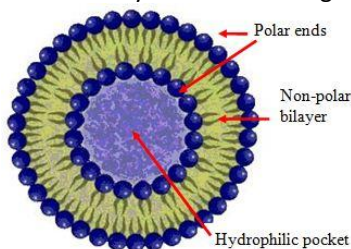
FIGURE 2.14
Liposomes [102].

Applications

- Delivery of nucleic acid and DNA: Liposome could be effective delivery system of Nucleic acid and DNA. Liposomal system with low surface area and small size using detergent dialysis procedure could exhibit the long term circulation of active ingredient. A recent advancement for manufacture of siRNA systems has been the application of microfluidic mixing and encapsulating siRNA with the control over the size has been achieved [103].
- Liposomal delivery as a mechanism to enhance synergism between anticancer drugs: Liposome can serve as a controlled release carrier these include clearance from reticuloendothelial system, longer systemic circulation, hepatic and spleen distribution. Drugs entrapped under liposome are not biologically active and must be released to gain access to the intracellular target [104].
- Breast cancer involving the chest wall: In a multimodality strategy, hyperthermia has been used to modulate delivery of liposomal drugs. Long circulation of liposomal accumulation with tumor tissue to be heated induces vascular permeability and microcirculatory dynamics which further facilitates liposome extraversion from tumor vessels [105].

- Application in ophthalmic drug delivery: Liposome can deliver ophthalmic drugs due to biodegradable and biocompatible in nature. Verteporfin is being clinically used in photodynamic therapy for treatment of subfoveal chorodial neovascularization, ocular histoplamosis or pathological myopia [106].
- Liposomes can be used to entrap anti-asthma drugs (salbutamol, beclometason) and in gastric ulceration [107, 108]

Nanogels

Nanogels are nanoscalar polymer network, with the tendency to imbibe water when placed in an aqueous environment. The advantage of nanogels over nanoparticles is the high degree of encapsulation [109]. Nanogels uses burst release system. They distinguish themselves from the bulk delivery system in that, they can be enter cells to delivers the drug. This property can be very helpful in cancer therapy, where the size of the delivery system is the key to target cancer through enhanced permeability and retention [110]. Nanogels can also be used for encapsulating cytoxic drug, due to the presence of polymeric network. The flexibility in the polymeric network has application in oligonucleotide binding [111].

Synthesis

Different Nanogels uses different methods for synthesis. Carboxymethyl chitosan nanogel was prepared by carboxymethylation in which the hydroxyl groups are substituted with alkyacid groups, the acid and amino groups help in chelation [112]. Similarly nanogels of pullulan was synthesized in which hydroxyethyl methyacrylate and vinyl methylacrylate is grafted on the glucose residue [113].

Noval pullulan chemistry modification

Synthesis of cholesterol based pullulan nanogel was done by reacting mixture of cholesterol isocynate in dimethyl sulfoxide and pyridine. Pullulan was substituted with 1.4 cholesterol moieties per 100 anhydrous glucoside units. The preparation was freeze dried and in aqueous phase it formed nanogel. It further modified with acrylate group and their thiol group was modified with polyethylene glycol by adopting Michael addition reaction, this allowed reduction in mesh size to 40 nm encapsulating 96% interleukin-12. These nanosystems have also been investigated by modifying cholesterol units by 1.1 units of cholesteryl group per 100 glucose units of parent pullulan, shown significant interaction with Aβ oligomer and monomer for alzhiemer's disease treatment by enhancing microglia and cortical cell viability.

Novel photochemical approach

Photochemical approach have been developed to produce ferric oxide nanoparticles nanogel for MRI application by coating oxide with N-(2-aminoethyl)methyiacrylamide and N,N'-methylene bis acrylamide treared with UV radiation at 388 nm for 10 minutes recovering the product after washing with water. Likewise, diacrylated pluronic and glycidyl methyacrylated chitooligosacchride were loaded with plasmid DNA at different ratios and were photo irradiated with long wave length UV light at 365 nm, the photo initiator was igracure added to the mixture for cross linking offering advantage to gene delivery.

Emulsion photopolymerisation process

Emulsion photopolymerisation using UV was utilized for preparing cationic dextran nanogel in which the dextran hydroxyethyl methacrylate was emulsified with ABIL EM 90 as emulgent in mineral oil, the product was obtained in acetone:hexane(1:1), the precipitate was centrifuged, lyophilized and dessicated. The photosensitizer meso-tetraphenylporphine disulfonate was introduced in the preparation to cause breakage of endosomal membranes in cell and release of genes in cytoplasm and nuclease [114].

Applications

Nanogels have been shown to promising result for drug delivery of cancer drugs, other drugs that can be delivered includes delivery of anti-inflammatory drug for the treatment of rheumatoid arthritis. Chitosan based nanogels can be used to target macrophages [110].
Pullulan nanogels crosslinked with poly ethylene glycol were used to prepare biodegradable hydrogel. Galation with pullulan nanogels were used for preparing homogenized hydrogel. This hydrogel can be efficiently used for the delivery of anabolic agents in bone and cytokines [115].

Dendrimers

Dendrimers are synthetic nanostructures ranging from 10 to 200 Angstroms in diameter. They are hyper branched and monodisperse three-dimensional molecules with defined molecular weights, large numbers of functional groups on the surface and well-established host-guest entrapment properties. The surface of a dendrimer is characterized by the presence of functional groups that together can be utilized as a backbone for the attachment of several types of biological materials [116,117].
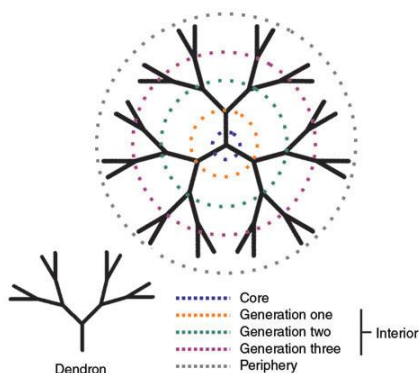
FIGURE 2.15
Anatomy of a dendrimers [118].

Synthesis

Divergent dendrimer synthesis

In the divergent approach, the construction of the dendrimer takes place in a stepwise manner starting from the core and building up the molecule towards the periphery using two basic operations (1) coupling of the monomer and (2) deprotection or transformation of the monomer end-group to create a new reactive surface functionality and then coupling of a new monomer *etc*., in a manner, somewhat similar to that known from solid-phase synthesis of peptides or oligonucleotides

For the poly (propyleneimine) dendrimers, which are based on a skeleton of poly alkylamines, where each nitrogen atom serves as a branching point, the synthetic basic operations consist of repeated double alkylation of the amines with acrylonitrile by "Michael addition" results in a branched alkyl chain structure. Subsequent reduction yields a new set of primary amines, which may then be double alkylated to provide further branching *etc* [119].

Polyamidoamine (PAMAM) dendrimers being based on a dendritic mixed structure of tertiary alkylamines as branching points and secondary amides as chain extension points was synthesised by Michael alkylation of the amine with acrylic acid methyl ester to yield a tertiary amine as the branching point followed by aminolysis of the resulting methyl ester by ethylene diamine.

The divergent synthesis was initially applied extensively in the synthesis of PPI and PAMAM dendrimers, but has also found wide use in the synthesis of dendrimers having other structural designs, *e.g*. dendrimers containing third period heteroatoms such as silicium and phosphorous [120].

Convergent Method

The second method developed by Hawker and Fréchet follows a "convergent growth process" In which several dendrons are reacted with a multifunctional core to obtain a product [121]. The convergent approach was developed as a response to the weakness of divergent synthesis. Convergent growth begins at what will end up being the surface of the dendrimer, and works inwards by gradually linking surface units together with more [122]. The advantage of convergent growth over divergent growth stem is that, only two simultaneous reactions are required for any generation adding step. Recently a breakthrough in the practice of dendrimer synthesis has come with the concept of double exponential growth. This approach allows the preparation of monomers of both convergent and divergent growth from a single starting material [123, 124].

Materials

Polyamidoamine (PAMAM)

PAMAM dendrimers are biocompatible, non-immunogenic, water soluble and possess terminal modifiable amine functional groups for binding various targeting or guest molecules [125]. The high density of amino groups and internal cavities in PAMAM dendrimers is expected to have potential applications in enhancing the aqueous solubility of low solubility drugs [126, 127] Caminade et al investigated that the water solubility of phosphorus-containing dendrimers was mainly due to the presence of hydrophilic end groups, which bear either positive or negative charges. These dendrimers can be used as in vitro DNA transfecting agents or in vivo anti-prion agents [128].

Dendrimers provide unique solutions to minimize delivery problems for ocular drug delivery. Recent research efforts for improving residence time of pilocarpine in the eye was increased by using PAMAM

dendrimers with carboxylic or hydroxyl surface groups. These surface-modified dendrimers were predicted to enhance pilocarpine bioavailability [129-130]. Many surface modified PAMAM dendrimers are non-immunogenic, water-soluble and possess terminal-modifiable amine functional groups for binding various targeting or guest molecules. PAMAM dendrimers are hydrolytically degradable only under harsh conditions because of their amide backbones, and hydrolysis proceeds slowly at physiological temperatures.

Polypropylenimine (PPI)

Cationic dendrimers (Polypropylenimine (PPI) dendrimers) deliver genetic materials into cells by forming complexes with negatively charged genetic materials through electrostatic interaction. Cationic dendrimers lend themselves as non-viral vectors for gene delivery because of their ability to form compact complexes with DNA

Applications

- Dendrimers have narrow polydispersity; nanometer size range of dendrimers can allow easier passage across biological barriers. All these properties make dendrimers suitable as host either binding guest molecules in the interior of dendrimers or on the periphery of the dendrimers.
- The family of dendrimers most investigated in drug delivery is the poly (amido amine) dendrimers (PAMAM). PAMAM dendrimers are biocompatible, non-immunogenic, water soluble and possess terminal modifiable amine functional groups for binding various targeting or guest molecules [125].
- For the in vivo pharmacokinetic and pharmacodynamic studies, indomethacin and dendrimer formulations were applied to the abdominal skin of the Wistar rats and blood collected from the tail vein at the scheduled time. The indomethacin concentration was significantly higher with PAMAM dendrimers when compared to the pure drug suspension. The results showed that effective concentration could be maintained for 24 h in the blood with the G4 dendrimer–indomethacin formulation. Therefore, data suggested that the dendrimer–indomethacin based transdermal delivery system was effective and might be a safe and efficacious method for treating various diseases [131].
- The anticancer drug paclitaxel (PTX) is a mitotic inhibitor used in chemotherapy to treat patients with lung, ovarian, breast, and head and neck cancers as well as advanced forms of Kaposis sarcoma. The drug works by interfering with normal microtubule growth during cell division, which especially affects fast growing cancer cells. In order to enhance its poor water solubility, paclitaxel has been encapsulated mainly into micelle-based formulations [132-135].
- The encapsulation of silver salts within PAMAM dendrimers produced conjugates exhibiting slow silver release rates and antimicrobial activity against various Gram-positive bacteria [136].
- Dendrimers can act as carriers, called vectors, in gene therapy. PAMAM dendrimers have also been tested as genetic material carriers. Cationic dendrimers (Polypropylenimine (PPI) dendrimer) deliver genetic materials into cells by forming complexes with negatively charged genetic materials through electrostatic interaction. Cationic dendrimers lend themselves as non-viral vectors for gene delivery because of their ability to form compact complexes with DNA. PAMAM dendrimers functionalized with α-cyclodextrin showed luciferase gene

expression about 100 times higher than for unfunctionalized PAMAM or for non-covalent mixtures of PAMAM and α-cyclodextrin [137].

Gold Nanoparticles

Gold has been one of the most coveted and prized metals since the very ancient times. In 1857, Faraday first reported that gold was pink when its size was extremely small [138]. Gold nanostructures have attracted considerable scientific interest in recent years for their potential to enhance both the diagnosis and treatment of cancer through their advantageous chemical and physical properties. The key feature of Au nanostructures for enabling this diverse array of biomedical applications is their attractive optical properties [139].

Types of Gold Nanoparticles

Gold nanoshells
Gold nanocages
Gold nanorods
Gold nanosphere
SERS nanoparticles [140].
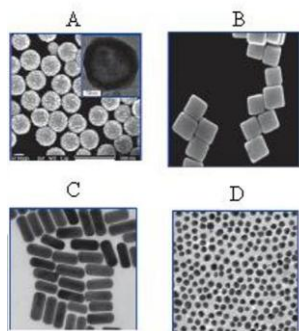
FIGURE 2.16
a) Gold nanoshells b) Gold nanocages c) Gold nanorods d) Gold nanosphere [141].

Gold Nanoshells

Gold nanoshells are spherical particles with diameters typically ranging in size from 10 to 200 nm composed of a dielectric core covered by a thin gold shell. They possess a remarkable set of optical, chemical and physical properties, which make them ideal candidates for enhancing cancer detection, cancer treatment, cellular imaging and medical biosensing [142].

Synthesis

Gold nanoshells with SPR peaks in the NIR region can be prepared by coating silica or polymer beads with gold shells of variable thickness. Silica cores are grown using the Stöber process, the basic

reduction of tetraethyl orthosilicate in ethanol. To coat the silica nanoparticles with gold in an aqueous environment, a seeded growth technique is typically used. Small gold nanospheres (2–4 nm in diameter) can be attached to the silica core using an amine-terminated silane as a liner molecule, allowing additional gold to be reduced until the seed particles coalesced into a complete shell. The diameter of the gold nanoshell is largely determined by the diameter of the silica core, and the shell thickness can be controlled through the amount of gold deposited on the surface of the core.

Gold nanoshells have also been synthesized via in situ gold nanoparticle formation using thermosensitive core-shell particles as the template. The use of microgel as the core offers signifi cantly reduced particle aggregation, as well as thickness control of the gold nanoshells using electroless gold plating. In one study, a virus scaffold has been used to assemble gold nanoshells. This approach may potentially provide cores with a narrower size distribution and smaller diameters (80 nm) than those of silica [143].

Properties

The properties of metallic nanoshells include optical, magnetic, photothermal, and catalytic. Gold nanoshells have been used for biomedical imaging and therapeutic applications because they offer highly favourable optical and chemical properties.

Gold nanoshells particles conjugated with enzymes and antibodies can be embedded in a matrix of the polymer. These polymers, such as Nisopropylacrylamide (NIPAAm), and acrylamide (AAm), have a melting temperature which is slightly above body temperature. When such a nanoshell and polymer matrix is illuminated with resonant wavelength, nanoshells absorb heat and transfer to the local environment.

Nanoshells function as useful and versatile imaging agents because of their large extinction cross - sections, immunity to photobleaching, spectral tunability, absorption/scattering ratio tunability, electromagnetic near – field enhancement, and enhanced luminescence. These optical phenomena are in large part due to a resonance phenomenon, known as surface plasmon resonance [144-146]

Applications

Gold Shells are used for drug delivery of Tumor necrosis factor-alpha (TNF-α), Methotrexate, methylene blue, insulin, and lysozyme [143].

Gold Nanocages

Noble-metal nanocages represent a novel class of nanostructures with hollow interiors and porous walls. They are prepared using the remarkably simple galvanic replacement reaction between solutions containing metal precursor salts and Ag nanostructures prepared by polyol reduction [147].

Synthesis

Gold nanocages with controllable pores on the surface have been synthesized via galvanic replacement reaction between truncated silver nanocubes and aqueous $HAuCl_4$. Silver nanostructures with controlled morphologies can be generated through polyol reduction, where $AgNO_3$ is reduced by ethylene glycol to generate silver atoms and then nanocrystals or seeds. Subsequent addition of silver atoms to the seeds produces the desired nanostructures through controlling the silver seed crystalline

structures in the presence of poly(vinylpyrrolidone), a polymer that is capable of selectively binding to the surface. The silver nanostructures, used as a sacrificial template, can then be transformed into gold nanostructures with hollow interiors via the galvanic replacement. The dimension and wall thickness of the resultant gold nanocages could be readily controlled, to very high precision, by adjusting the molar ratio of silver to HAuCl [143].

Properties

AuNCs have a range of hidden qualities that make them unique for theranostic applications.

- They are single crystals with good mechanical flexibility and stability, as well as atomically flat surfaces.
- They can be routinely produced in large quantities with wall thicknesses tunable in the range of 2–10 nm with an accuracy of 0.5 nm.
- LSPR peaks can be easily and precisely tuned to any wavelength of interest in the range of 600–1200 nm by simply controlling the amount of HAuCl4 added to the reaction.
- The hollow interiors can be used for encapsulation.
- Their porous walls can be used for drug delivery, with the release being controlled by various stimuli.
- Their sizes can be readily varied from 20 to 500 nm to optimize biodistribution, facilitate particle permeation through epithelial tissues, or increasing drug loading.
- Their LSPR peaks can be dominated by absorption or scattering to adapt to different imaging modalities.
- Other noble metals such as Pd and Pt can be incorporated into the walls during a synthesis to maneuver their optical properties [139].

Applications

The using of Ag nanocubes as a template for galvanic replacement with HAuCl4 offers an elegant way to make complementary hollow gold nanocages with controllable void size, wall thickness, and wall porosity [148-150]. Nanocages are used in cancer targeting, photothermal cancer treatment, controlled release of a drug such as doxorubicin [139].

Future Perspective

A desirable situation in drug delivery is to have smart drug delivery systems that can be integrated into the human body. This area of nanotechnology will play an extremely important role. Time-release tablets, which have a relatively simple coating that dissolves in specific locations, also involve the use of nanoparticles. Pharmaceutical companies are using nanotechnology to create intelligent drug-release devices. For example, the control of the interface between the drug/particle and the human body can be programmed so that when the drug reaches its target, it can then become active. The use of nanotechnology for drug-release devices requires autonomous device operation. For example, in contrast to converting a biochemical signal into a mechanical signal and being able to control and communicate with the device, autonomous device operation would require biochemical recognition to

generate forces to stimulate various valves and channels in the drug delivery systems, so that it does not require any external control.

It is now appears that we are on the verge of bioengineering molecular motors for specialized applications on nanoscale. These systems might be the key to yet unsolved biomedical applications that include nonviral gene therapy and interneuron drug delivery [151]

Conclusions

Numerous fields of science are converging to study science at a very fundamental level or building block level, namely nanoscience. The majority of studies have focused on materials sciences with some applications emerging in the biomedical field. Very few fundamental studies have been performed in the pharmaceutical field discussing the fundamentally different properties of materials at the nanolevel. The application is clear and promising; however, the basics of nanoscience in drug delivery are poorly understood.   With sound investigation of these basic properties, the scope of pharmaceutical sciences within the invisible nanoworld seems poised to result in a revolution in medical world.

References

1. Ghenadii Korotcenkov, editor. Chemical Sensors Fundamentals of Sensing Materials: Volume 2 Nanostructured Materials. Momentum Press; 2010.
2. Lifeng Dong, Michael M. Craig, Dongwoo Khang, and Chunying Chen. Applications of Nanomaterials in Biology and Medicine. Journal of Nanotechnology. Volume 2012, Article ID 816184, 2 pages, doi:10.1155/2012/816184.
3. H. AI, J. GAO. Size-controlled polyelectrolyte nanocapsules via layer-by-layer self-assembly. Journal of Materials Science 2004; 39: 1429 – 1432.
4. P. Couvreur. Nanoparticles in drug delivery: Past, present and future. Advanced Drug Delivery Reviews 2013; 65: 21–23.
5. Deepak Thassu, editor. Nanoparticulate Drug Delivery Systems. Informa Healthcare. USA Inc; 2007.
6. Quintanar-GD, Allémann E and Fessi H. Preparation Techniques and Mechanisms of Formation of Biodegradable Nanoparticles from Preformed Polymers. Drug Development and Industrial Pharmacy 1998; 24(12): 1113-1128.
7. PrasadRao J., Kurt E. Geckeler. Polymer nanoparticles: Preparation techniques and size control parameters. Progress in Polymer Science 2011; 36: 887-913.
8. Catarina Pinto Reis, Ronald J. Neufeld, Antonio J. Ribeiro and Francisco Veiga. Nanoencapsulation Methods for preparation of drug-loaded polymeric nanoparticles. Nanomedicine: Nanotechnology, Biology, and Medicine 2006; 2: 8–21.
9. Vargas A, Pegaz B, Debefve E, Konan-Kouakou Y, Lange N and Ballini JP. Improved photodynamic activity of porphyrin loaded into nanoparticles: an in vivo evaluation using chick embryos. International Journal of Pharmaceutics 2004; 286: 131- 45.

10. Konan YN, Gurny R and Allemann E. State of the art in the delivery of photosensibilizers for photodynamic therapy. *Photochem Photobiol B* 2002; 66: 89 - 106.
11. Yoo HS, Oh JE, Lee KH and Park TG. Biodegradable nanoparticles containing PLGA conjugate for sustained release. *Pharm Res* 1999; 16: 1114- 8.
12. Perez C, Sanchez A, Putnam D, Ting D, Langer R and Alonso MJ. Poly (lactic acid)-poly (ethylene glycol) nanoparticles as new carriers for the delivery of plasmid DNA. *J Control Release* 2001; 75: 211- 24.
13. Lu W, Zhang Y, Tan Y-Z, Hu K-L, Jiang X-G and Fu S-K. Cationic albumin conjugated pegylated nanoparticles as novel drug carrier for brain delivery. *J Control Release* 2005; 107: 428- 48.
14. Saxena V, Sadoqi M and Shao J. Indocyanine green-loaded biodegradable nanoparticles: preparation, physicochemical characterization and in vitro release. *Int J Pharm* 2004; 278: 293-301.
15. El-Shabouri MH. Positively charged nanoparticles for improving the oral bioavailability of cyclosporin-A. *Int J Pharm* 2002; 249: 101- 8.
16. Fessi H, Puisieux F, Devissaguet JP, Ammoury N and Benita S. Nanocapsule formation by interfacial deposition following solvent displacement. *Int J Pharm* 1989, 55: R1- R4.
17. Barichello JM, Morishita M, Takayama K and Nagai T. Encapsulation of hydrophilic and lipophilic drugs in PLGA nanoparticles by the nanoprecipitation method. *Drug Dev Ind Pharm* 1999; 25: 471- 6.
18. Galindo-Rodriguez S, Allemann E, Fessi H and Doelker E. Physicochemical parameters associated with nanoparticle formation in the salting-out, emulsification-diffusion, and nanoprecipitation methods. *Pharm Res* 2004; 21: 1428- 39.
19. Ganachaud F and Katz JL. Nanoparticles and nanocapsules created using the ouzo effect: Spontaneous emulsification as an alternative to ultrasonic and high-shear devices. *Chem Phys Chem* 2005; 6: 209- 16.
20. Wehrle P, Magenheim B and Benita S. Influence of process parameters on the PLA nanoparticle size distribution, evaluated by means of factorial design. *Eur J Pharm Biopharm* 1995; 41: 19-26.
21. Nemati F, Dubernet C, Fessi H, Verdiere AC, Poupon MF, Puisieux F. Reversion of multidrug resistance using nanoparticles in vitro: influence of the nature of the polymer. Int J Pharm 1996; 138: 237- 46.
22. Molpeceres J, Guzman M, Aberturas MR, Chacon M, Berges L. Application of central composite designs to the preparation of polycaprolactone nanoparticles by solvent displacement. J Pharm Sci 1996; 85:206 - 13.
23. Irache JM, Huici M, Konecny M, Espuelas S, Campanero MA, Arbos P. Bioadhesive properties of gantrez nanoparticles. Molecules 2005; 10:126 - 45.
24. Arbos P, Wirth M, Arangoa MA, Gabor F, Irache JM. Gantrez AN as a new polymer for the preparation of ligand nanoparticle conjugates. J Control Release 2002; 83:321- 30.
25. Allemann E, Leroux JC, Gurny R. Polymeric nano-microparticles for the oral delivery of peptides and peptidomimetics. Adv Drug Deliv 'Rev 1998; 34:171- 89.
26. Yamuna Reddy Charabudla. Process for Formation of Cationic Poly (Lactic-Co-Glycolic Acid) Nanoparticles Using Static Mixers. Master's Theses. University of Kentucky; 2008.
27. Feng-Qian Li, Cheng Yan and Juan Bi et al. A novel spray-dried nanoparticles-in-microparticles system for formulating scopolamine hydrobromide into orally disintegrating tablets, International Journal of Nanomedicine 2011:6 897–904.

28. Mu, L. Feng, S.S. Fabrication, Characterization and In-vitro Release of Paclitaxel (TaxolR) Loaded Poly (Lactic-co-Glycolic Acid) Microspheres Prepared by Spray Drying Technique with Lipid/Cholesterol Emulsifiers. J. Control. Release 2001; 76: 239–254.

29. Gavini, E. Chetoni, P. Cossu, M et al. PLGA Microspheres for the Ocular Delivery of a Peptide Drug, Vancomycin Using Emulsification/Spray-Drying as the Preparation Method: In Vitro/In Vivo Studies. Eur. J. Pharm. Biopharm. 2004; 57: 207–212.

30. Nie, H.; Lee, L.Y.; Tong, H. & Wang, C. PLGA/Chitosan Composites from a Combination of Spray Drying and Supercritical Fluid Foaming Techniques: New Carriers for DNA Delivery. J. Control. Release 2008; 129: 207–214.

31. R. Jain, N.H. Shah, A.W. Malick & C.T. Rhodes. Controlled Drug Delivery by Biodegradable Poly (ester) Devices: Different Preparative Approaches, Drug Dev. Ind. Pharm. 1998; 24: 703–727.

32. Hirenkumar K. Makadia and Steven J. Siegel. Poly Lactic-co-Glycolic Acid (PLGA) as Biodegradable Controlled Drug Delivery Carrier. Polymers 2011; 3: 1377-1397.

33. Uhrich K.E, Cannizzaro, S.M.; Langer, R.S.; Shakesheff, K.M. Polymeric systems for controlled drug release. Chem. Rev. 1999, 99, 3181–3198.

34. Wu X.S & Wang N. Synthesis, Characterization, Biodegradation and Drug Delivery Application of Biodegradable Lactic/Glycolic Acid Polymers. Part II: Biodegradation. J. Biomater. Sci. Polym. 2001; 12: 21–34.

35. Yang Y.Y, Chung T.S, Ng N.P. Morphology, Drug Distribution and in vitro Release Profiles of Biodegradable Polymeric Microspheres Containing Protein Fabricated by Double-Emulsion Solvent Extraction/Evaporation Method. Biomaterials 2001; 22: 231–241.

36. T. Niwa, H. Takeuchi, T. Hino et al. Preparations of Biodegradable Nanospheres of Water-Soluble and Insoluble Drugs with D,L-lactide / glycolide Copolymer by a Novel Spontaneous Emulsification Solvent Diffusion Method and the Drug Release Behavior. J. Control. Rel. 1993; 25: 89–98.

37. Stickler M & Rhein T. Polymethacrylates. In Elvers B, Hawkins S, Schultz G, eds. Ullmann's encyclopedia of industrial chemistry. VHS. Vol. 421: p. 473.

38. Ana Bettencourt and Anto´nio J. Almeida. Poly(methyl methacrylate) particulate carriers in drug delivery. Journal of Microencapsulation. 2012; 1–15.

39. Hall EW, Rouse MS, Jacofsky DJ et al. Release of Daptomycin from Polymethylmethacrylate Beads in a Continuous Flow Chamber. Diagn Microbiol Infect Dis. 2004; 50(4): 261–265.

40. Corry D & Moran J. Assessment of Acrylic Bone Cement as a Local Delivery Vehicle for the Application of Non-steroidal anti-inflammatory Drugs. Biomaterials. 1998; 19: 1295–1301.

41. Wang HM, Crank S, Oliver G and Galasko CS. The Effect of Methotrexateloaded\ Bone Cement on Local Destruction by the VX2 Tumour. J Bone Joint Surg [Br]. 1996; 78-B: 14–17.

42. Healey JH, Shannon F, Boland P and DiResta GR. PMMA to Stabilize Bone and Deliver Antineoplastic and Antiresorptive Agents. Clin Orthop Rel Res. 2003; 415(Suppl.): S263–275.

43. Sealy PI, Nguyen C, Tucci M et al. Delivery of Antifungal Agents Using Bioactive and Nonbioactive Bone Cements. Ann Pharmacother. 2009; 43(10): 1606–1615.

44. Gref R., Rodrigues J. & Couvreur P. Polysaccharides Grafted with Polyesters: Novel Amphiphilic Copolymers for Biomedical Applications. Macromolecules 2002; 35(27): 9861-9867.

45. Lemarchand C., Couvreur P., Besnard M., Costantini D. & Gref R. Novel Polyester-Polysaccharide Nanoparticles. Pharm Res 2003; 20(8): 1284-1292.

46. Jing X. B., Yu H. J., Wang W. S., Chen X. S. & Deng C. Synthesis and Characterization of the Biodegradable Polycaprolactone-Graft-chitosan Amphiphilic Copolymers. Biopolymers 2006; 83(3): 233-242.

47. Sinha VR, Bansal K, Kaushik R, Kumria R and Trehan A. Poly-Epsilon-Caprolactone Microspheres and Nanospheres: an overview. Int J Pharm 2004; 278: 1–23.

48. Rodrigues J. S., Santos-Magalhaes N. S., Coelho L. C. B. B., Couvreur P., Ponchel G. & Gref R. Novel Core (Polyester)-Shell(Polysaccharide) Nanoparticles: Protein Loading and Surface Modification with Lectins. Journal of Controlled Release 2003; 92: 103-112.

49. Vineet Singh and Meena Tiwari. Structure-Processing-Property Relationship of Poly(Glycolic Acid) for Drug Delivery Systems: Synthesis and Catalysis. International Journal of Polymer Science. Volume 2010.

50. Vero´nica Lassalle & Marı´a Luja´n Ferreira. PLA Nano- and Microparticles for Drug Delivery: An Overview of the Methods of Preparation. Macromol. Biosci. 2007; 7: 767–783.

51. Quynh T.M, Mitomo H, Nagasawa N, Wada Y, Yoshii F and Tamada M. Properties of Crosslinked Polylactides (PLLA & PDLA) by Radiation and Its Biodegradability. European Polymer Journal. 2007; 43 (5): 1779-1785.

52. Agnihotri SA, Mallikarjuna NN, Aminabhavi TM. Recent Advances on Chitosan-Based Micro- and Nanoparticles in Drug Delivery. J Control Release 2004; 100: 5–28.

53. Thanou M., Kean T. & Roth S. Trimethylated Chitosans as Non-Viral Gene Delivery Vectors: Cytotoxicity and Transfection Efficiency. Journal of Controlled Release 2005; 103(3): 643-653.

54. Tharanathan R. N. & Ramesh H. P. Carbohydrates - The Renewable Raw Materials of High Biotechnological Value. Critical Reviews in Biotechnology 2003; 23(2): 149-173.

55. Yuan & Zhuangdong. Study on the Synthesis and Catalyst Oxidation Properties of Chitosan Bound Nickel (II) Complexes. Journal of Agricultural and Food Chemistry 2007; 21(5): 22-24.

56. Vipin Bansal, Pramod Kumar Sharma, Nitin Sharma, Om Prakash Pal and Rishabha Malviya. Applications of Chitosan and Chitosan Derivatives in Drug Delivery. Advances in Biological Research 2011; 5 (1): 28-37.

57. Prabaharan M & Mano JF. Chitosan-Based Particles as Controlled Drug Delivery Systems. Drug Deliv 2005; 12: 41–57.

58. Ying Zhang, Hon Fai Chan and Kam W. Leong. Advanced Materials and Processing for Drug Delivery: The Past and the Future. Advanced Drug Delivery Reviews 2013; 65: 104–120.

59. George M & Abraham TE. Polyionic Hydrocolloids for the Intestinal Delivery of Protein Drugs: Alginate and Chitosan — A Review. J Control Release 2006; 114: 1-14

60. Jinchen Sun and Huaping Tan. Alginate-Based Biomaterials for Regenerative Medicine Applications. Materials 2013; *6*: 1285-1309

61. Coester CJ, Langer K, van Briesen H and Kreuter J. Gelatin Nanoparticles by Two Step Desolvation-A New Preparation Method, Surface Modifications and Cell Uptake. J Microencapsul 2000; 17:187–193.

62. Kaul G & Amiji M. Biodistribution and Targeting Potential of Poly(ethylene glycol)- Modified Gelatin Nanoparticles in Subcutaneous Murine Tumor Model. J Drug Target 2004; 12: 585–591.

63. Balthasar S, Michaelis K, Dinauer N, von Briesen H, Kreuter J and Langer K. Preparation and Characterisation of Antibody Modified Gelatin Nanoparticles as Drug Carrier system for Uptake in Lymphocytes. Biomaterials 2005; 26: 2723–2732.

64. C.E. Mora-Huertasa, H. Fessi and A. Elaissari. Polymer-Based Nanocapsules for Drug Delivery. International Journal of Pharmaceutics 2010; 385: 113–142.

65. Georgi Yordanov. Poly(alkyl cyanoacrylate) Nanoparticles as Drug Carriers: 33 Years Later, Bulgarian Journal of Chemistry 1(2): 61-73.

66. Julien Nicolas and Patrick Couvreur. Synthesis of Poly(alkyl cyanoacrylate) Based Colloidal Nanomedicines, Nanomed. Nanobiotechnol 2009; 1: 111–127

67. Satish Singh Kadian & S.L. Harikumar, Eudragit and its Pharmaceutical Significance, Roorkee, p.17 (2009). http://www.pharmainfo.net/satishsinghkadian/publications/eudragit-and-its-pharmaceutical-significance (accessed 27th oct 2013).

68. Meenakshi Joshi. Role of Eudragit in Targeted Drug Delivery. International Journal of Current Pharmaceutical Research 2013; 5(2): 58-62.

69. Kewal K. Jain, The Handbook of Nanomedicine, Humana Press, 2008, page 35.

70. http://eng.thesaurus.rusnano.com/wiki/article1931 (accesed 28th jan 2014)

71. Charles M. lieber, Chia-Chun chen, preparation of fullerenes and fullerene-based materials, Solid state physics, 48, 1994, 109-148.

72. www.saffron.pharmabiz.com/article/detnews.asp?articleid=40923&sectionid=50 (accessed 27-10-2013)

73. Melgardt M. de Villiers, Pornanong Aramwit, Glen S. Kwon, Nanotechnology in Drug Delivery, springer 2009.

74. J. C. Rathi et al. Formulation and Evaluation of Lamivudine Loaded Polymethacrylic Acid Nanoparticles. International Journal of PharmTech Research 2009; 1(3): 411-415.

75. Manouchehr Vossoughi et al. Conjugation of Amphotericin B to Carbon Nanotubes via Amide-Functionalization for Drug Delivery Applications. Engineering Letters 2009; 17: 4-12.

76. Smriti Khatri et al. Carbon Nanotubes in Pharmaceutical Nanotechnology: An Introduction to Future Drug Delivery System, Journal of Chemical and Pharmaceutical Research 2010; 2(1): 444-457.

77. Nadine Wong Shi Kam, Michael O'Connell et al. Carbon Nanotubes as Multifunctional Biological Transporters and Near Infrared Agents for Selective Cancer Cell Destruction. Proceedings of National Academy of Science of the United States of America. 2005; 102(33): 11600-11605.

78. http://www.intechopen.com/books/carbon-nanotubes-polymer-nanocomposites/polymer-carbon-nanotube-nanocomposites (accessed 29th jan 2014).

79. Michael O'Connell, Jeffrey A. Wisdom. Producers Association of Carbon Nanotubes in Europe (PACTE)- Code of Conduct for the Production and Use of Carbon Nanotubes, 2008; Version 1.0:1-3.

80. Andrea Szabó, Caterina Perri, Anita Csató et al. Synthesis Methods of Carbon Nanotubes and Related Materials, *Materials* 2010, *3*, 3092-3140.

81. T. Guo, P. Nikolaev, A. Thess, D.T. Colbert and R.E. Smalley, Catalytic growth of single-walled nanotubes by laser vaporization, *Chem. Phys. Lett*., 1995, 243, 49-54.

82. A. Thess, R. Lee, P. Nikolaev, H. Dai, P. Petit, J. Robert, C. Xu, Y.H. Lee, S.G. Kim, A.G. Rinzler, D.T. Colbert, G.E. Scuseria, D. Tománek, J.E. Fischer, and R.E. Smalley, Crystalline ropes of metallic carbon nanotubes, *Science*, 1996, 273, 483–487.

83. W. S. Mcbride, Synthesis of Carbon Nanotube by Chemical Vapor Deposition, Undergraduate Degree Thesis, College of William and Marry in Virginia, Wil-liamsburg, 2001.

84. Caroline L. Strasinger et al, Carbon Nanotube Membranes for use in the Transdermal Treatment of Nicotine Addiction and Opioid Withdrawal Symptoms, Substance Abuse: Research and Treatment 2009; 3: 31-39.

85. T. A. Hilder & J. M. Hilly. Encapsulation of the Anticancer Drug Cisplatin into Nanotubes International, Conference on Nanoscience and Nanotechnology, ICONN 2008, Melbourne, February 2008, 107-112.

86. Susana Martins, Bruno Sarmento, Domingos C Ferreira and Eliana B Souto. Lipid-based colloidal carriers for peptide and protein delivery – liposomes versus lipid nanoparticles. International Journal of Nanomedicine 2007:2(4) 595–607.

87. Joseph A Zasadzinki. Novel Approaches to Lipid Based Drug Delivery. Current Opinions in Solid state and Material Science. 1997; 2.

88. Assadjuman Md & Mishuk Ahmed Khan. Novel Approaches In Lipid Based Drug Delivery Systems. Journal of Drug Delivery and Therapeutics. 2013; 3: 124-130.

89. Dr Hassan Benameur. Lipid Based Dosage Forms- an Emerging Platform for Durg Delivery, Capsugel Inc.

90. Milan Stuchlik & Stansliv Zak. Lipid Based Vehicles for Oral Delivery. Biomed Papers, 2001; 145: 17-26.

91. Mohammed Mehanna et al. Pharmaceutical Particulate Carriers: Lipid-Based Carriers. National Journal of Physiology, Pharmacy and Pharmacology. 2012; 2: 10-22.

92. Manju Rawat, Depander Singh, S. Saraf and Sawarathna Saraf. Lipid Carriers: A Versatile Vehicle for Protein and Peptides. The Pharmaceutical Society of Japan. 2002; 129: 269-280.

93. Leeladhar prajapati & Sudhakar Rao Naik. Lipospheres: Recent Advances in Various Drug Delivery System. International Journal of Pharmacy and Technology, 2013; 5: 2446-2464

94. Rolf Schubert, Liposome Preparation by Detergent Removal. Methods in Enzymology, 2003, 367, 46–70.

95. Mohammad Riaz, liposomes preparation methods, pakistan journal of pharmaceutical sciences vol.19(1), january 1996, pp.65-77.

96. Elwira Lason & Jan Ogonowski, Solid liqid nanoparticles-Characteristic, application and obtaining, CHEMIK, 2011, 65.

97. http://www.intechopen.com/books/novel-gene-therapy-approaches/solid-lipid-nanoparticles-tuneable-anti-cancer-gene-drug-delivery-systems (accesd 28th jan 2014).

98. Vijay Kumar Sharma, Anupama Dhawan, Satish Sardhana and Vipan Dhall, Solid lipid nanoparticles System: An overview, International journal of research in pharmaceutical science, 2011; 3: 450-461

99. Wolfgang Mehnert & Karsten Madar. Solid lipid nanoparticles production, characterization and application. Advance Drug delivery reviews. 2001; 47: 165-196.

100. Chee Wun How, Rasedee Abdullah and Roghyayeh Abbasalipourkabir. Physicochemical properties of nanostructured lipid carriers as colloidal carrier system stabilized with polysorbate 20 and polysorbate 80, African Journal of Biotechnology, 2011; 10 (9): 1684-1689.

101. Subramanian Selvamuthukumar & Ramaiyan Velmurgan, Nanostructure lipid carriers: A potential drug carrier for cancer therapy, Lipids in Health and Disease 2012; 11.

102. http://www.horiba.com/scientific/products/particle-characterization/applications/pharmaceuticals/liposomes (accesd 28th jan 2014).

103. Theresa. M. Allen & Peter. R. Cullis, Liposomal drug delivery system: From concept to clinical application, Advanced Drug Delivery Reviews, 2013; 65: 36-48.

104. Robert. J. Lee, Liposomal delivery as a mechanism to enhance synergism between anticancer drugs, Molecular Cancer Therapeutics, 2006; 5: 1639-1640.

105. John. W. Park, Liposome based drug delivery in breast cancer treatment, Breast Cancer research, 2002; 4: 95-99.

106. Gyan. P. Mishra, Mahuya Bagui, Viral Tamboli, Ashim. K. Mitra, Recent application of liposome in ophthalmic drug delivery. Journal of Drug Delivery 2011; 4.

107. Abdelbary M.A. Elhissi, Joanna Giebultowicz, Anna A. Stec et al. Nebulization of ultradeformable liposomes: The influence of aerosolization mechanism and formulation excipients. International Journal of Pharmaceutics 436 (2012) 519– 526.

108. Abdelbary M. A. Elhissi, Waqar Ahmed, David McCarthy & Kevin M. G. Taylor, A Study of Size, Microscopic Morphology, and Dispersion Mechanism of Structures Generated on Hydration of Proliposomes. Journal of Dispersion Science and Technology, 33:1121–1126, 2012.
109. Salvatrice Rigoglioso, Maria A. Sabatino, Giorgia Adamo, Natascia Girmaldi, Clelia Dispenza, Giulio Ghersi. Polymeric Nanogels: Nanocarriers for drug delivery application. Chemical Enigeering transactions, 2012; 27.
110. Reuben T. Chacko, Judy Ventura, Jiaming Zhuang, S. Thayumanavan. Polymer nanogels: A versatile nanoscopic drug delivery platform, Advanced Drug Delivery Reviews, 2012; 64: 836-851.
111. Serguei V. Vinogradov, Arin D. Zeman, Elena V. Batrakova, Alexander V. Kabanov. Polyplex Nanogel formulation for drug delivery of cytotoxic nucleoside analogs. J Control Release 2005 Sep 20, 107(1), 143-157.
112. Reem K. Farag, Riham R. Mohamed. Synthesis and characterization of carboxymethyl chitosan nanogels for swelling studies and antimicrobial activity. Molecules, 18, 2013.
113. Silvia A. Ferreira, Paulo J.G Coutinho and Francisco M. Gama. Synthesis and Characterization of Self-Assembled nanogels made of pullulan. Materials 4, 2011.
114. Dhawal Dorwal. Nanogels as novel and versatile pharmaceuticals. International Journal of pharmacy and pharmaceutical sciences 2012; 4(3).
115. K. Akiyoshi. Nanogel based materials for drug delivery System. European Cells and Materials, 2007; 14(3).
116. Babu VR, Mallikarjun V, Nikhat S, Srikanth G. Dendrimers: A New Carrier System for Drug Delivery. Int J Pharma Applied Sci 2010; 1: 1-10.
117. Padilla O,Ihre H, Gagne L, Fréchet J, Szoka F. Polyester dendritic systems for drug delivery applications: in vitro and in vivo evaluation. Bioconjug Chem 2002; 13: 453–461.
118. Cameron C Lee, John A MacKay, Jean M J Fréchet & Francis C Szoka. Designing dendrimers for biological applications. Nature Biotechnology 2005, 23 (12), 1517-1526.
119. E.M.M. De Brander van den Berg and E.W. Meijer, *Angew. Chem.*, 1993, 105, 1370.
120. J.-P. Majoral and A.-M. Caminade, Dendrimers Containing Heteroatoms (Si, P, B, Ge, or Bi). *Chem. Rev.*, 1999, 99, 845.
121. Hawker CJ, Fréchet JM. Preparation of polymers with controlled molecular architecture. A new convergent approach to dendritic macromolecules. J Am Chem Soc 1990; 112: 7638–7647.
122. Nishiyama N, Kataoka K. Current state, achievements and future pros-pects of polymeric micelles as nanocarriers for drug and gene delivery. Pharmacol Ther 2006; 112: 630–648
123. Na C, YiyunX, Yang T, Xiaomin W, Zhenwei L, Dendrimers as potential drug carriers, Part II: Prolonged delivery of ketoprofen by in vitro and in vivo studies. Eur J Pharma Sci 2006; 41: 670–674.
124. Antoni P, Hed Y, Nordberg A, Nystrom D, Holst H, Hult A, Angew, M. Bifunctional Dendrimers: From Robust Synthesis and Accelerated One-Pot Post functionalization Strategy to Potential Applications. Int Ed 2006; 48: 2126-2130.
125. Esfand R, Tomalia D. A Polyamidoamine Dendrimer-Capped Mesoporous Silica Nanosphere-Based Gene Transfection Reagent. Drug Discov Today 2001; 6 : 427–436.
126. Svenson S, Chauhan AS. Dendrimers for enhanced drug solubilisation. Nanomedicine 2008; 3: 679–702.
127. Asthana A, Jain N. Dendritic systems in drug delivery applications. Expert Opin Drug Deliv 2007; 4 : 495–512.

128. Caminade A, Majoral J. Water-soluble phosphorus-containing dendrimers. Progress in Polymer Science. 2005; 30: 491-505.

129. Bhadra D. Bhadra, S, Jain N. PEGylated peptide-based dendritic nanoparticulate systems for delivery of artemether. J Drug Del Sci Tech 2005; 15: 65–73.

130. Yang H, Kao W. Dendrimers for pharmaceutical and biomedical applications. Journal of biomaterials science. Polymer edition 2006; 17: 3-19.

131. Chauhan A, Jain A. Dendrimer mediated transdermal delivery; enhanced bioavailability of indomethacin. . J Control Release 2003; 90 (3) 335–343.

132. Shuai X, Merdan T, Schaper A, Xi F, Kissel T. Core-cross-linked polymeric micelles as paclitaxel carriers. Bioconjug Chem 2004; 15: 441–448.

133. Shim W, Kim S, Choi E, Park H, Kim J, Lee D. Novel pH sensitive block copolymer micelles for solvent free drug loading. Macromol Biosci 2006; 6:179–186.

134. Lee H, Zeng F, Dunne M, Allen C. Methoxy poly(ethylene glycol)-blockpoly(d-valerolactone) copolymer micelles for formulation of hydrophobic drugs. Biomacromolecules 2005; 6: 3119–3128.

135. Yusa S, Fukuda K, Yamamoto T, Ishihara K, Morishima Y. Synthesis of well defined amphiphilic block copolymers having phospholipids polymer sequences as a novel biocompatible polymer micelle reagent. Biomacromolecules 2005; 6: 663–670.

136. Balogh L, Swanson DR, Tomalia DA, Hagnauer G, McManus A. Dendrimer–silver complexes and nanocomposites as antimicrobial agents. Nano Lett 2001; 1:18–21.

137. Arima H, Kihara F, Hirayama F, Uekama K. Enhancement of gene expression by polyamidoamine dendrimer conjugates with and_α-cyclodextrins. Bioconjug Chem 2001; 12: 76–484.

138. Faraday, M. Experimental Relations of Gold (and Other Metals) to Light. *Philos. Trans. R. Soc. London* 1857, *147*, 145-181.

139. Younan xia, weiyang li, claire m. Cobley, jingyi chen, xiaohu xia, qiang zhang, miaoxin yang, eun chul cho, and paige k. Brown, gold nanocages: from synthesis to theranostic applications, acc chem res. 2011 october 18; 44(10): 914–924.

140. Avnika Tomar and Garima Garg, Short Review on Application of Gold Nanoparticles, Global Journal of Pharmacology 2013; 7 (1): 34-38.

141. L. A. Dykman and N. G. Khlebtsov. Gold Nanoparticles in Biology and Medicine: Recent Advances and Prospects. Acta Naturae 201.

142. Tim A. Erickson and James W. Tunnell, Gold Nanoshells in Biomedical Applications, Nanomaterials for the Life Sciences Vol. 3: Mixed Metal Nanomaterials, WILEY-VCH Verlag GmbH & Co, 2009

143. Weibo Cai, Ting Gao, Hao Hong, Jiangtao Sun, Applications of gold nanoparticles in cancer nanotechnology, Nanotechnology, Science and Applications 2008:1 17–32.

144. Alisha D. Peterson, Synthesis and Characterization of Novel Nanomaterials: Gold Nanoshells with Organic- Inorganic Hybrid Cores, 2010. Graduate School Theses and Dissertations. University of South Florida.

145. Suchita Kalele, S. W. Gosavi, J. Urban and S. K. Kulkarni. Nanoshell particles: synthesis, properties and applications. Current Science, 2006. 91 (8). 1038-1052.

146. Challa S. S. R. Kumar, Nanomaterials for the Life Sciences Vol. 3: Mixed Metal Nanomaterials. WILEY-VCH Verlag GmbH & Co. KGaA, Weinheim. 2009.

147. Sara e. Skrabalak, jingyi chen, yugang sun, xianmao lu, leslie au, laire m. Cobley, and younan xia. Gold nanocges: synthesis, properties, and applications. acc chem res. 2008; 41(12): 1587–1595.

148. Sun Y & Xia Y. Alloying and Dealloying Processes Involved in the Preparation of Metal Nanoshells through a Galvanic Replacement Reaction. Nano Lett. 2003; 3: 1569-1572.
149. Sun Y & Xia Y. Mechanistic Study on the Replacement Reaction between Silver Nanostructures and Chloroauric Acid in Aqueous Medium. J. Am. Chem. Soc. 2004; 126: 3892-3901.
150. Chen J, McLellan J. M, Siekkinen A, Xiong Y, Li Z and Xia Y. Facile Synthesis of Gold-Silver Nanocages with Controllable Pores on the Surface. J. Am. Chem. Soc. 2006; 128: 14776-14777.
151. Vargas A, Pegaz B, Debefve E, Konan-Kouakou Y, Lange N, Ballini JP. Improved photodynamic activity of porphyrin loaded into nanoparticles: an in vivo evaluation using chick embryos. Int J Pharm 2004; 286:131- 45.

3

Advances in Nanosheet Technology Towards Nanomedical Engineering

Toshinori Fujie and Shinji Takeoka

Department of Life Science and Medical Bioscience, School of Advanced Science and Engineering, Waseda University, Tokyo, 162-8480, Japan,
Department of Life Science and Medical Bioscience, School of Advanced Science and Engineering, Faculty of Science and Engineering, Waseda University (TWIns), 2-2 Wakamatsu-cho, Shinjuku-ku, Tokyo 162-8480, Japan.

Outline:

Introduction

Nanobiotechnology plays an important role in the development of clinical therapeutics and diagnostics e.g., bioimaging/sensing,[1] drug delivery systems[2] and tissue engineering.[3] Tissue engineering contributes to regenerative medicine, which generates tailor-made transplantable biological tissues by employing an engineered cellular matrix. However, this innovative approach also has some drawbacks such as an elevated risk of infection during cell processing and extended periods of cell culture. Thus, there are ongoing efforts towards the development of so called smart biomaterials that enhance the healing process in wound tissue or assist in the integration of implanted cells by directing cellular organization. Nonetheless, the engineered materials should be stable at the wound site without eliciting an inflammatory response or post-surgical adhesion. Thus, reducing the side effects of the implanted materials is crucial for the improvement of conventional therapeutics.

Ultra-thin polymeric films (often called as nanosheets, nanofilms or nanomembranes) are a new class of polymeric nanomaterials, conventionally studied in the field of polymer physics.[4] These films are typically tens-of-nm in thickness and have unique interfacial and mechanical properties that are controlled in a thickness-dependent manner, resulting in non-covalent adhesiveness, tunable flexibility and molecular permeability (Fig. 3.1).[5,6,7] In addition, a quasi-two-dimensional feature of the nanosheet is an attractive structure for synthetic mimics of extracellular matrix (ECM) in native tissues, which has an ideal structure and function to direct the cellular organization and therefore to regenerate and maintain tissues and organs. These properties are beneficial for the development of advanced biomaterials, including wound dressings, drug release devices and tissue engineering materials. In this chapter, we introduce recent developments in nanosheet technology for biomedical applications, focusing on the fabrication, physical properties and practical applications of nanosheets, particularly in the area of surgical procedures (e.g., wound dressing materials) and tissue engineering (e.g., cellular scaffolds).
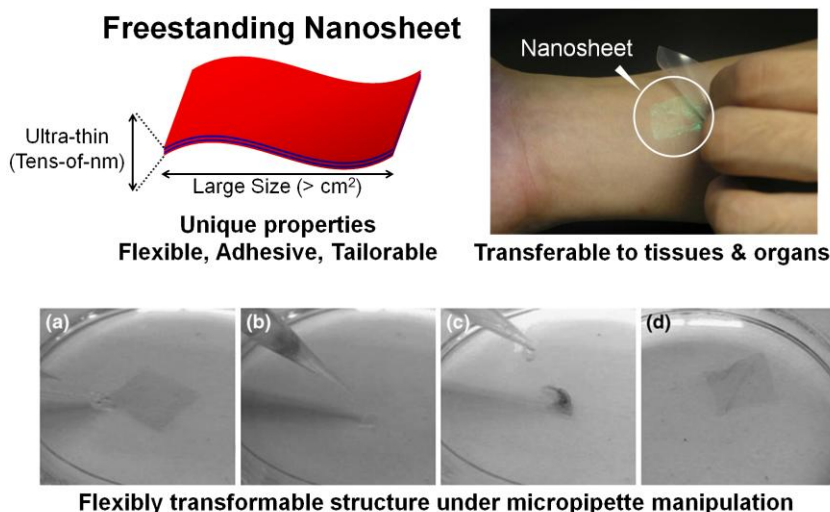
FIGURE 3.1
Biomedical application of polymer nanosheets utilizing their unique characteristics such as physical adhesiveness and high flexibility. Nanosheets with tens- to hundres-of-nm thickness (2 cm × 2 cm) were transferred to the human skin surface or manipulated by a micropipette, respectively (partially reproduced from references 7 and 34).

Fabrication and Fundamental Properties of Nanosheets

Preparation of freestanding nanosheets

There have been significant developments over the past five years in the fabrication of freestanding nanosheets. Typical characteristic features of the nanosheets are as follows: (i) a thickness of tens-of-nm, (ii) a huge size-aspect ratio ($>10^6$), (iii) unique interfacial and mechanical properties, such as tunable flexibility, non-covalent adhesiveness and high transparency. From a structural viewpoint, a quasi-two-dimensional arrangement of polymer nanosheets could represent an ideal interface to mimic extracellular matrix (ECM) in biological tissues, which comprise of a well-organized permeable membrane that controls nutrient flux in living systems.[8,9] Therefore, polymer nanosheets are regarded as a new category of quasi-two dimensional soft materials. Thus far, various techniques to fabricate the freestanding polymer nanosheets have been introduced, including a simple spincoating method, a Layer-by-Layer (LbL) method, a Langmuir–Blodgett method with crosslinkable amphiphilic copolymers and a sol–gel method with organic–inorganic interpenetrating networks.[10,11,12,13]

One novel methodology for the fabrication of nanosheets is an LbL technique. The LbL method involves alternative deposition of oppositely charged polyelectrolytes by non-covalent bonding such as electrostatic interactions, hydrogen-bonding or hydrophobic interactions.[14,15,16,17,18] Thus, a variety of functional electrolytes (including proteins, DNA or charged particles) can be integrated into the LbL structure. Applications of LbL-based nanomaterials have been explored in several fields such as electrochemical devices, chemical sensors, nano-mechanical sensors, nano-scale chemical/biological reactors and drug delivery systems.[19] In particular, a combination of the spin-coating procedure with LbL (spincoating assisted layer-by-layer: SA-LbL) is useful for the preparation of well-organized nanosheets. The resulting material has a controllable thickness with a flat and smooth surface due to the high-speed horizontal diffusion of polymers during the spincoating process.

Freestanding polymer nanosheets can be detached from the solid substrate by employing a "sacrificial layer method" (Fig. 3.2a) or "(water-soluble) supporting film method" (Fig. 3.2b). In the sacrificial layer method, the precoated sacrificial polymeric layer is dissolved by specific organic solvents such as acetone or ethanol that do not dissolve the upper film. In the supporting film method, the water-soluble supporting film, such as a PVA film, is prepared on the surface of the SA-LbL film, which allows convenient collection of the free-standing nanosheet by peeling the complex film from an SiO_2 substrate, followed by dissolution of the PVA film. It should be noted that in a complex film, interaction between the nanosheet and the PVA film is greater than that between the nanosheet and the SiO_2 substrate. This transfer method is an efficient means of transferring the nanosheet from one substrate to another surface, including human skin or organs.
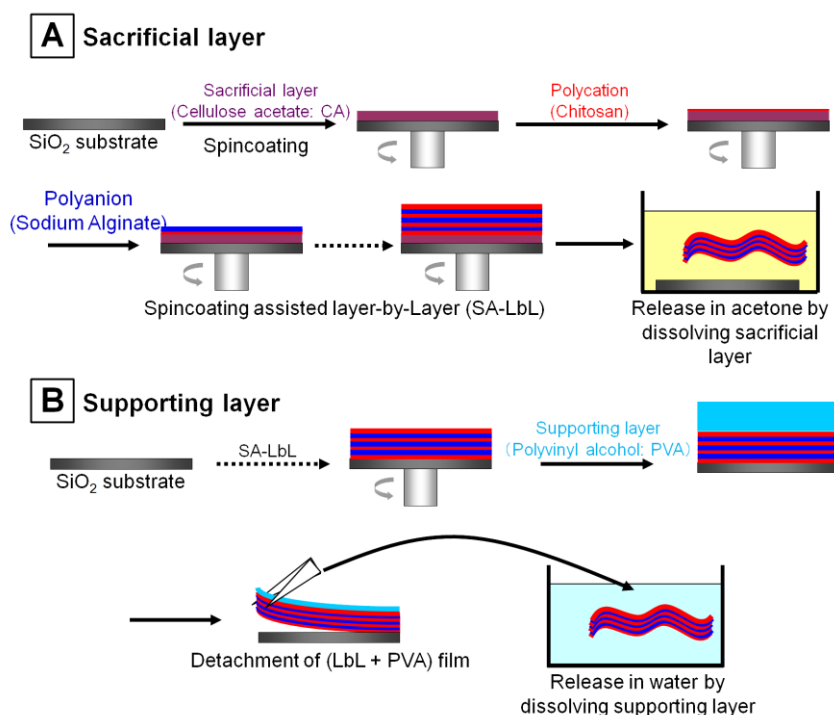
FIGURE 3.2
Preparation of freestanding polymer nanosheets by two different approaches: (a) sacrificial layer method and (b) supporting film method (partially reproduced from reference 6).

For example, we used polysaccharide electrolytes such as chitosan and sodium alginate, which have amino and carboxylic acid groups as cationic and anionic species at ambient pH (Fig. 3.3a). These polysaccharides are often used in biomedical fields, such as wound dressings or as artificial skin, because of their biocompatibility and bioabsorbability.[20,21] Therefore, we prepared freestanding polysaccharide nanosheets by using the sacrificial layer method. Each polysaccharide layer was assembled on the sacrificial layer (e.g., cellulose acetate) by the SA-LbL method. The thickness was proportional to the number of layer pairs, suggesting a well-organized structure of the nanosheet at the nanoscale (Fig. 3.3b). The polysaccharide nanosheet was then released in acetone by dissolution of the cellulose acetate; the freestanding structure maintained the original size and shape of the SiO_2 substrate (Fig. 3.3c). Large-scale (90 μm × 90 μm) topographic images by AFM revealed that the surface of the polysaccharide nanosheet was as smooth and flat as the silicon wafer without any corrugations or wrinkles. From the cross-sectional analysis of the edge of the nanosheet, the AFM thickness of the nanosheet was estimated to be 30.2 ± 4.3 nm (10.5 layer pairs of polysaccharide), corresponding to the ellipsometric thickness (30.7 ± 4.5 nm) of the nanosheet on the SiO_2 substrate. As a result, the smooth and flat surface was obtained with root-mean-square roughness (RMS) of 7.1 ± 2.4 nm owing to the spincoating effect in LbL. It is noteworthy the same polysaccharide nanosheet can also be detached from the SiO_2 substrate by using the supporting film method, which can be then be released into water by dissolution of the PVA film.
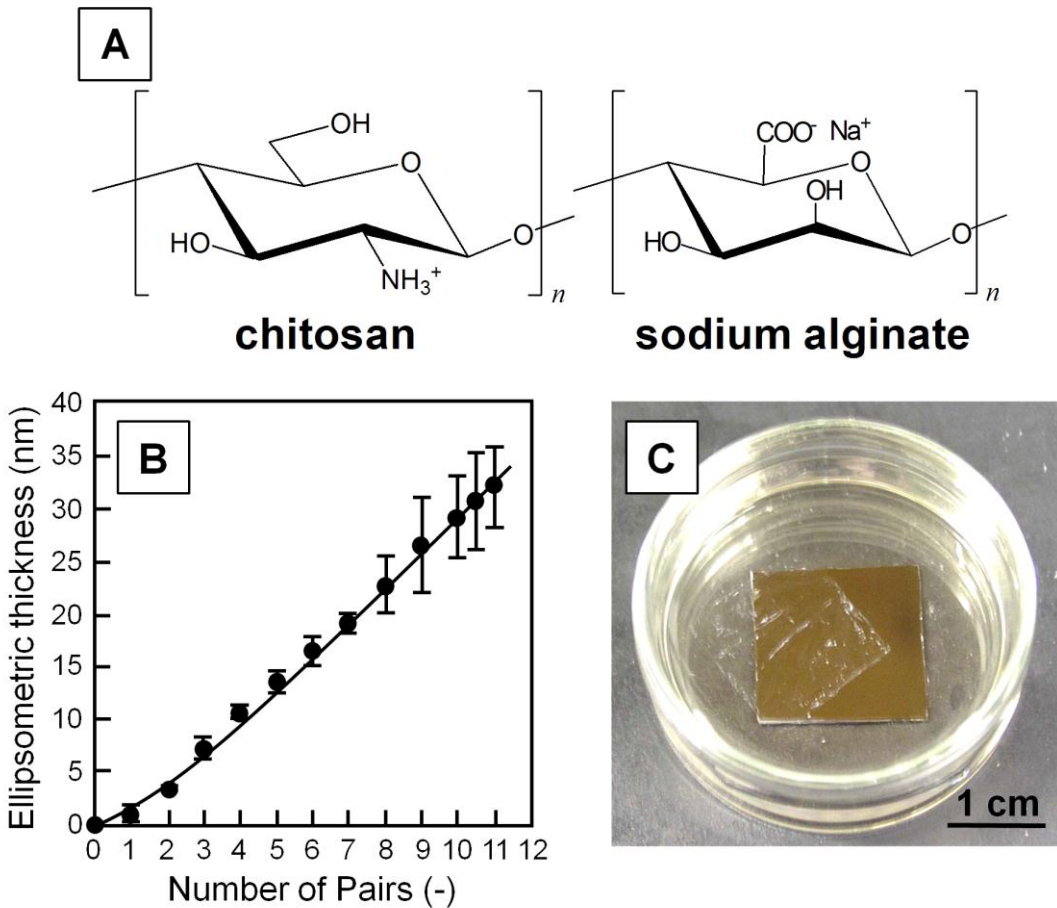
FIGURE 3.3
Polysaccharide nanosheets: (a) Molecular structure of chitosan and sodium alginate, (b) thickness profile as a function of layer pairs, and (c) a freestanding polysaccharide nanosheet in acetone (partially reproduced from reference 34).

Poly(lactic acid) (PLA) is an aliphatic polyester made up of lactic acid (2-hydroxy propionic acid) building blocks.[22] PLA has been widely studied not only because of its convenient production from lactic acid but also because of its biocompatibility and biodegradability, which make it a good candidate for biomedical applications.[23] In a similar manner to polysaccharide nanosheets, we also succeeded in fabrication of freestanding poly(L-lactic acid) (PLLA) nanosheets by both the sacrificial layer method and supporting film method. Unlike the LbL methods, these technique are applicable for various "hydrophobic" polymers, particularly biodegradable polyesters such as PLLA, poly(lactic-co-glycolic acid) (PLGA) and polycaprolactone (PCL). A PLLA solution was spincoated onto the PVA sacrificial layer on the SiO_2 substrate, or directly spincoated onto the SiO_2 substrate and subsequently detached using the PVA supporting film. The thickness of the nanosheet could be easily controlled because the thickness was proportional to the PLLA concentration used for spin-coating; the minimal thickness of the freestanding PLLA nanosheet was estimated to be 23 ± 5 nm when the concentration of the PLLA solution was 5 mg/mL. After dissolution of the PVA film, the freestanding PLLA nanosheet was obtained in water (Fig. 3.4a). The thickness was measured as 23 ± 5 nm and the RMS value was as low as 3.6 ±

0.5 nm. The PLLA nanosheet with an extremely high size-aspect ratio of greater than 10^6 maintained the same shape and size as the SiO_2 substrate (4×4 cm^2). The transparent PLLA nanosheet could be scooped and held in air with a supporting wire frame (Fig. 3.4b), which was stable without bursting for at least one year.
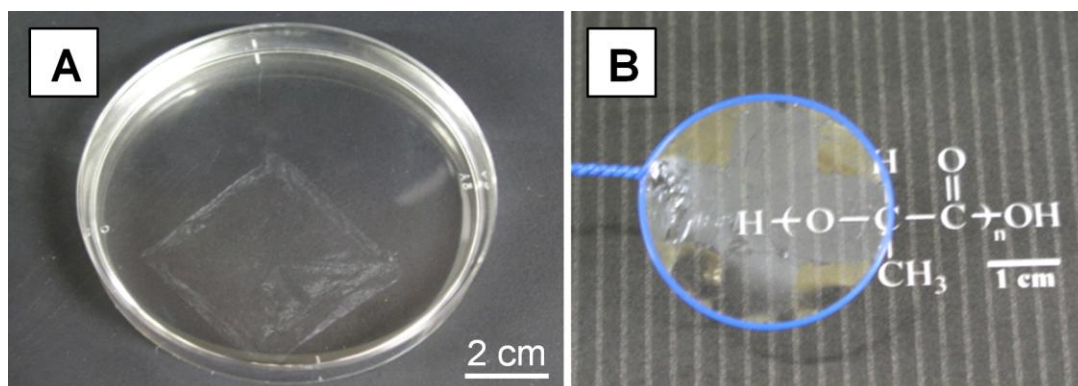
FIGURE 3.4
PLLA nanosheets: (a) a freestanding PLLA nanosheet in water, (b) suspended by a wire loop (partially reproduced from reference 36).

Adhesive properties of the nanosheets

A micro-scratch test can be used to evaluate the macroscopic adhesive properties of ultra-thin films such as nanosheets.[24] The micro-scratch tester employs a diamond stylus that oscillates parallel to the surface of the nanosheet on the SiO_2 substrate. The adhesive failure of the nanosheet with the stylus is detected as the 'critical load' of the nanosheet, relative to the adhesive force. Interestingly, the critical load of the polysaccharide nanosheets drastically increased as their thickness decreased below 200 nm; the critical load of a 39-nm thickness nanosheet (0.15×10^6 N m^{-1}) was approximately 7.5 times greater than that with a thickness of 1482-nm (0.02×10^6 N m^{-1}) (Fig. 3.5a). Moreover, microscopic observations revealed different trail marks after scratching depending on the thickness of the nanosheet, such as 'cut-off (1482 nm)' and 'drawn (77 nm)'-like trails (Fig. 3.5a, inset). This observation suggested that the elasticity of the nanosheet was critically reduced at a thickness of less than 200 nm. In contrast, the critical load of the PLLA nanosheet (thickness: 23 ± 5 nm) was calculated to be 0.17×10^6 N m^{-1}, and was equal to that of a nanosheet with a thickness of 60 ± 14 nm (0.18×10^6 N m^{-1}) (Fig. 3.5b). These values were also comparable to that of a copper film (thickness: 200 nm, approximately 0.40×10^6 N m^{-1}) on a glass substrate prepared by vacuum deposition under the same measurement conditions. However, when the thickness was over 100 nm, the critical load was significantly decreased. Furthermore, these values were the same as for the nanosheet fabricated directly on the SiO_2 substrate, indicating that the nanosheet with a large contact area could conform to the SiO_2 surface because of its exquisite flexibility and low roughness. Taking into account the results from the microscratching tests for both polysaccharide and PLLA, the adhesive properties generated by nanometeric thickness is of great potential in biomedical applications.
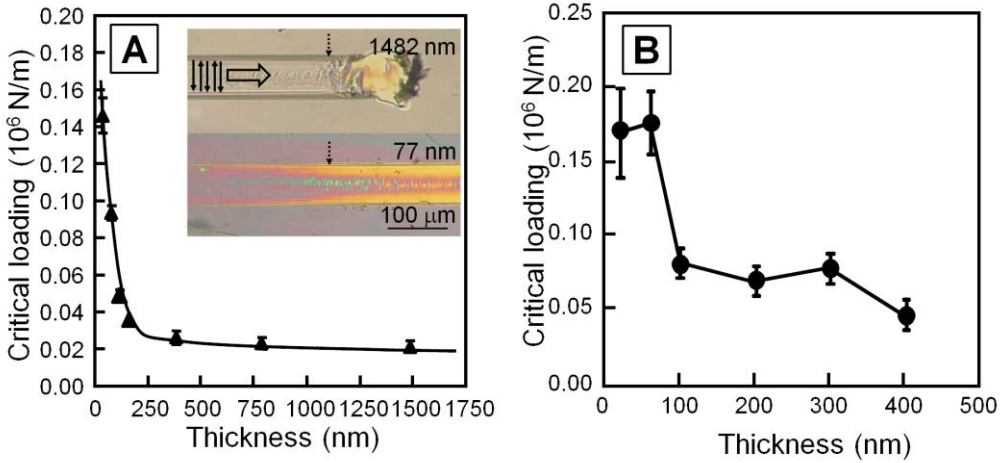
FIGURE 3.5
Adhesion properties of different nanosheets between (a) polysaccharide and (b) PLLA. Inset: microscopic morphologies of the polysaccharide nanosheets after performing the micro-scratch test for different thicknesses (1482 nm and 77 nm) (partially reproduced from references 35 and 36).

Mechanical properties of nanosheets

The bulge test, which vertically compresses a nanosheet placed on a plate with a circular hole (Fig. 3.6a), is frequently used for the evaluation of the mechanical strength of nanosheets.[25,26] For example, three kinds of polysaccharide nanosheets with different thicknesses (35, 75 and 114 nm), were fixed on the steel plates with a 1 mm diameter circular hole in the center and kept under ambient conditions (temperature: 25 ± 1°C, humidity: 37 ± 3%). It is noteworthy that the nanosheet adhered readily to the steel plate without using chemical adhesion. As pressure was applied to the polysaccharide nanosheet through the circular hole, deflection of the nanosheet was monitored from a side-view of the plates until distortion occurred (Fig. 3.6b). The relationship between pressure and deflection was non-linear, suggesting that the elasticity of the polysaccharide nanosheet was dependent on the total film thickness (Fig. 3.6c). The ultimate tensile strength (σ_{max}), elongation (ε_{max}) and elastic modulus (E) were calculated for nanosheets of different thickness from the initial elasticity of the stress-strain curve. The elastic modulus of the 35 nm polysaccharide nanosheet was 1.1 ± 0.4 GPa, which is considerably less than that of a cellulose film (E = 15 GPa) with a thickness of over 1 μm. This result suggested that the nanosheet with a thickness of tens-of-nm is quite flexible due to its low elastic modulus. As the thickness of the polysaccharide nanosheet was increased, the elastic modulus increased to approach that of the bulk value (75 nm: 8.1 ± 2.5 GPa, 114 nm: 11.0 ± 1.6 GPa).
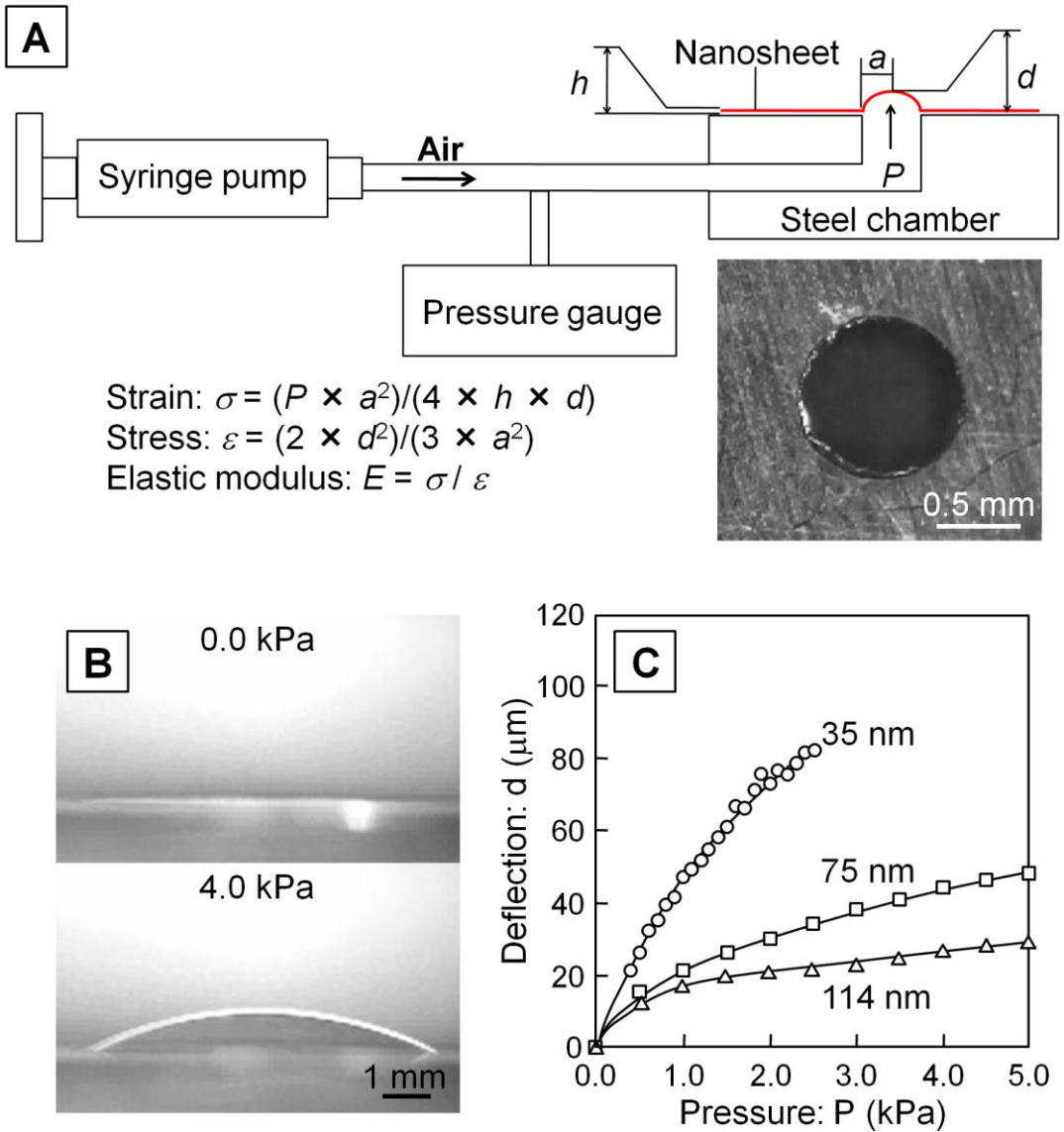
FIGURE 3.6
Mechanical properties of polysaccharide nanosheets: (a) bulge test apparatus, (b) nanosheets deflected by compressed air, and (c) pressure-deflection curve for different thicknesses of nanosheets (partially reproduced from reference 35).

Mechanical property of the PLLA nanosheet also shows similar trends. The PLLA nanosheet with thicknesses of 23 ± 5 nm deflected gradually and gave an almost semicircular deflection until a pressure of approximately 4 kPa was reached. The elastic modulus of the nanosheets was calculated to be 1.7 ± 0.1 GPa, which was quite low compared to the bulk PLLA (7-10 GPa).[27] Moreover, the mechanical properties of PLLA nanosheets were evaluated by means of "strain induced elastic buckling instability for mechanical measurement (SIEBIMM)".[28] The SIEBIMM test is based on the buckling metrology

between an elastic substrate (such as polydimethylsiloxane: PDMS) and the nanosheet under compression or stretching, which allowed calculation of Young's modulus of the nanosheet. The modulus is calculated by measuring the buckling wavelength of the nanosheet on a mechanically forced matrix. A continuous buckling pattern was clearly observed on the surface of the PLLA nanosheets after compression by PDMS strain relaxation (Fig. 3.7a). It is noteworthy that the wrinkle formation is no longer observed when the thickness was 703 nm due to the fact that the PLLA nanosheet was partially detached from the PDMS slab during the buckling process. This weak adhesiveness in higher thickness nanosheets could be explained by the thickness-related adhesion property of the polymeric nanosheets; increment of the nanosheet thickness reduced material flexibility as well as van der Waals force to the underlying materials. We previously evaluated the elastic modulus of PLLA nanosheets using the bulge test, although these measurements were only possible in the tens-of-nm thickness range due to low adhesion of nanosheets thicker than 100 nm. Considering the broader range of analyzed thicknesses, the SIEBIMM test was more suitable for evaluating Young's modulus of PLLA nanosheets. In fact, mean wavelength was proportional to the thickness of the PLLA nanosheets up to 318 nm (R^2 = 0.998) (Fig. 3.7b). The calculated Young's modulus of the PLLA nanosheet gradually increased as the thickness of the nanosheet increased (Fig. 3.7c). The Young's modulus of a 29-nm PLLA nanosheet is 3.5±1.3 GPa, while that of a 318-nm PLLA nanosheet is 6.6±1.7 GPa. Hence, we found that the mechanical modulus of both polysaccharide and PLLA nanosheets can be controlled by changing the thickness from tens to hundreds of nanometers.

Permeable properties of nanosheets

In general, PLA (T_g~58°C) are classified as copolymers of poly(L-lactic acid) (PLLA) and poly(D,L-lactic acid) (PDLLA), which are produced from L-lactides and D,L-lactides, respectively. PLLA is known as a semi-crystalline polymer, which is rubbery above T_g and becomes a glass below T_g. By constrast, PDLLA is an amorphous polymer without crystallinity. In this regard, we focused on the crystalline domains of PLLA nanosheets by applying an annealing treatment above the T_g (referred as PLLA(+)), and envisaged using the resulting crystalline domains as a molecular sieve for a filtration membrane.[29] Atomic force microscope (AFM) images showed a remarkably morphological difference between PLLA (-) (Fig. 3.8a) and PLLA (+) (Fig. 3.8b), in which homogeneous distribution of grains attributed to PLLA crystals (~100 nm in diameter) as well as microscopic apertures between crystals (~100 nm in space) were clearly observed in PLLA (+) (Fig. 3.8c).
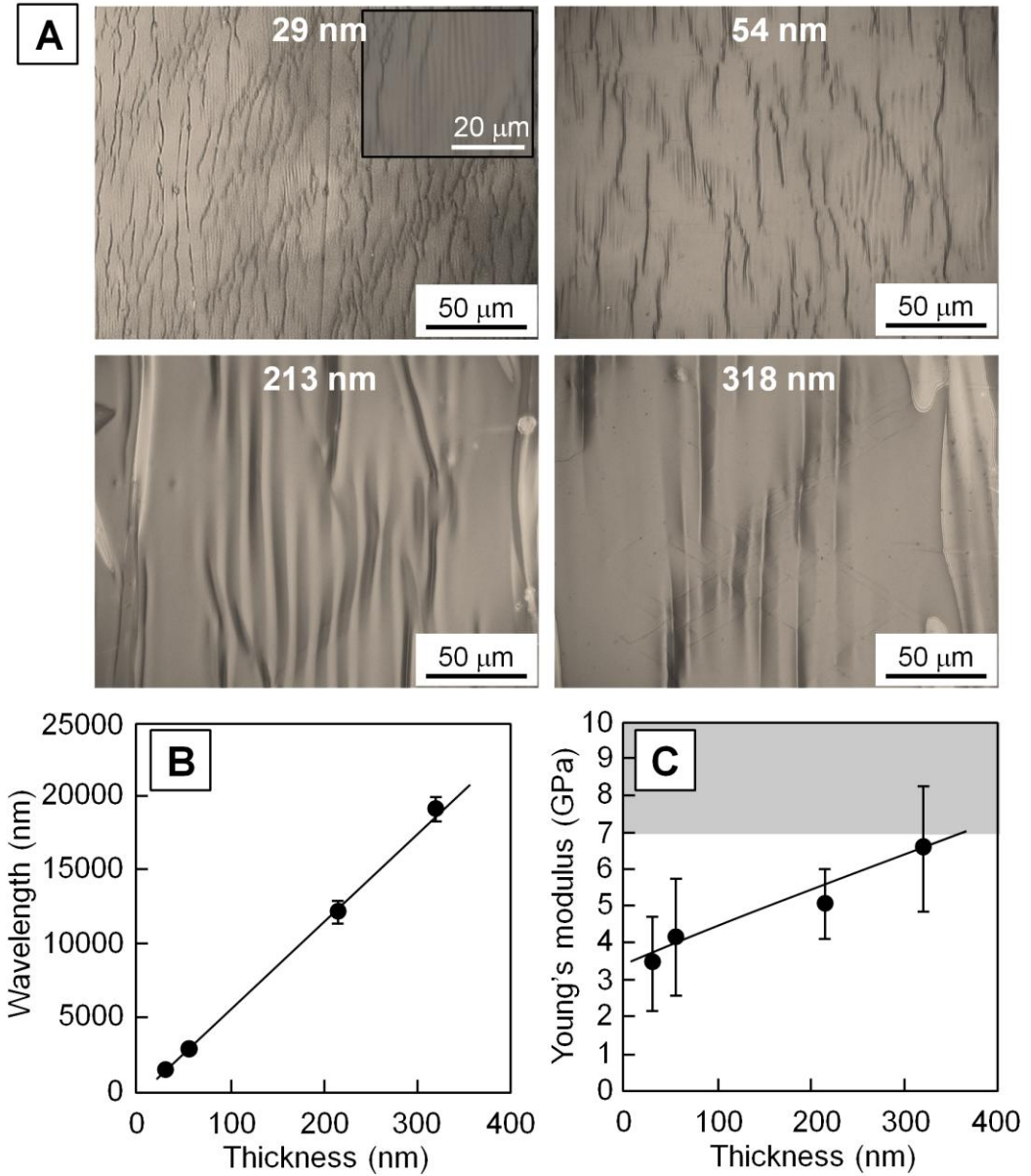
FIGURE 3.7
Mechanical properties of PLLA nanosheets with different thickness. (a) Optical images of buckled PLLA nanosheets by SIEBIMM test. (b) Measured wavelength. (c) Calculated Young's modulus as a function of film thickness. The shaded region in (c) shows the Young's modulus of a bulk PLLA film (partially reproduced from reference 9).
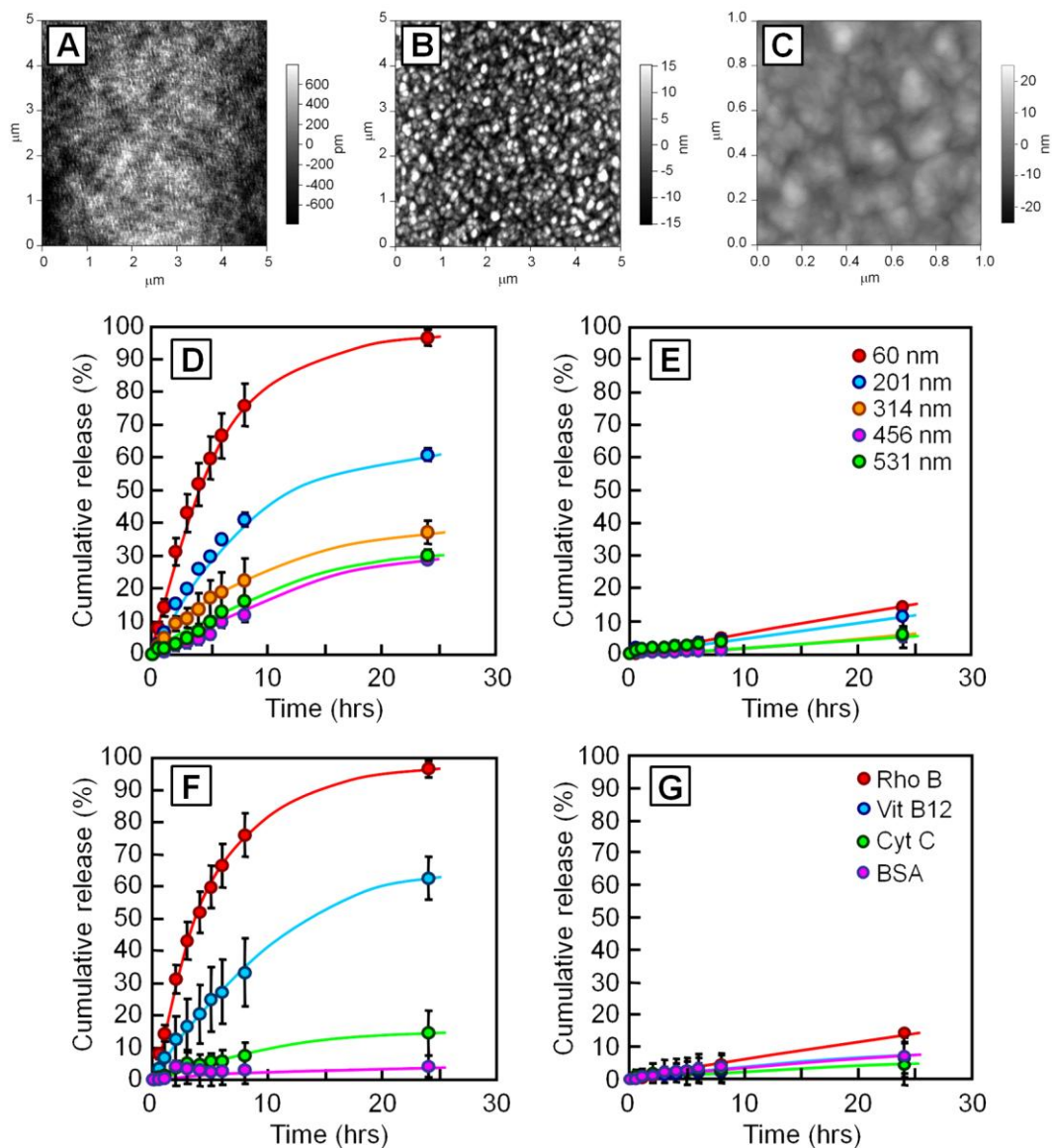
FIGURE 3.8
AFM images of 60 nm thick PLLA nanosheets before (a) and after (b) the annealing process (80°C, 2 h), and (c) a magnified image of (b). Comparison of cumulative release of analytes through PLLA (+) (d and f) and PLLA (−) (e and g) as a function of different thicknesses (d and e, symbols in e) and different molecular weights (f and g, symbols in g). For (d) and (f), the thickness of the PLLA nanosheets was 60 nm (partially reproduced from reference 29).

The molecular permeability of the PLLA nanosheet was also evaluated as a function of the cumulative relase profile of analytes with respect to the film thickness and solution molecular mass of the analyte. The transfer of analytes through the nanosheet was continually monitored for up to 24 hrs using a UV-Vis spectrophotometer. A series of experiments were performed using model analytes of different

molecular weights. These model analytes included rhodamine B (RhoB: 479 Da / ~1.0 nm in size), vitamin B12 (VB12: 1,355 Da / ~2.4 nm), cytochrome C (Cyt C: 13.4 kDa / ~3.8 nm) and bovine serum albumin (BSA: 66.5 kDa / ~6.4 nm).[30] First, molecular permeability of RhoB was compared between PLLA (+) and PLLA (-) as a function of film thickness (60, 201, 314, 456 and 531 nm). PLLA (+) showed thickness-dependent permeability (Fig. 3.8d), while PLLA (-) displayed only a modest level of permeability (<10% after 12 hrs) for all thicknesses of PLLA (-) (Fig. 3.8e). Next, the molecular permeability through the 60-nm thick PLLA nanosheets was analyzed for different molecular weights of analytes; PLLA (+) displayed size-dependent permeability (Fig. 3.8f), while PLLA (-) showed slight permeability (<10% after 12 hrs) for all of the analytes (Fig. 3.8g).

Moreover, flux analysis indicated that the mass transport of PLLA (+) was controlled by the film thickness. Thus, modulation of the film thickness would give a critical threshold of molecular weight cut-off (MWCO) value for the filtration process. For example, MWCO of 60-nm PLLA (+) can be determined as ca. 10 kDa (less than 0.1 mmol h^{-1}m^{-2} below MWCO). It is noteworthy that the selective permeability displayed by PLLA (+) was not evident in amorphous PDLLA. Therefore, the presence of PLLA derived crystalline domains in the nanosheet is crucially important for facilitating selective permeability. This technique is useful for the direct conversion of thermodynamic properties of semi-crystalline polymers to that of a nano-structured material e.g., selective molecular permeability.

Fabrication and Fundamental Properties of Nanosheets

Nano-adhesive plasters

Surgical repair for tissue defects is generally achieved by three fundamental methods; suture, plication and overlapping. Despite their high reliabilities for wound repair, the conventional repair of a tissue defect by suture and plication usually reduces the volume of the original tissue. For example, pulmonary air leakage due to visceral pleural injury is one of the most common postoperative complications after thoracic surgery. Plication of a pleural defect sometimes decreases respiratory function. Such complications might be caused by prolonged placement of a drainage tube and/or an extended period of hospitalization, which may even lead to thoracic empyema. Therefore, tight and firm repair of a pleural injury/defect is critically important in order to prevent air leakage.[31,32] Nevertheless, it is sometimes difficult to suture or plicate a large defect or fragile tissue of the emphysematous lung. Overlapping is therefore seen as an ideal means of repairing a pleural defect, because it simply seals the injured surface without reducing the tissue volume of the injured lung. As a conventional sealant, fibrin glue (sheet) composed of fibrin-glue-coated collagen fleece, a typical adhesive material, is effective for the repair of a visceral pleural defect.[33] However, this material sometimes causes severe pleural adhesion. For high-risk patients with respiratory failure, such a severe pleural adhesion might further deteriorate pulmonary dysfunction, leading to serious complications. Therefore, a novel tissue sealant that does not cause tissue adhesion is required. Herein, we focused on the high flexibility and physical adhesiveness of the nanosheet. The flexible nanosheet can densely overlap and adhere to the biological surface like an adhesive plaster (e.g., human skin) (Fig. 3.1).[34] We envisage developing this concept further to generate a ''nano-adhesive plaster'' as a new class of wound dressing material. Such a material will overlap and treat the tissue defect in a minimally invasive way without an associated major inflammatory response or post-surgical adhesion.

Sealing operation using nanosheets

We employed a surgical procedure that involved using polysaccharide nanosheets to repair a visceral pleural defect in beagle dogs.[35] The polysaccharide nanosheet, or a fibrin sheet used as a positive control, was placed onto a pleural defect area prepared by a 3.2 cm^2 aorta punch on the right anterior, middle and posterior lobes. The 75 nm polysaccharide nanosheet was placed on a supporting PVA film (70 μm in thickness) for handling. By dissolving the PVA film with a PBS solution, the underlying nanosheet fitted on the curvature of the remaining tissue fully overlapping the pleural defect without any chemical adhesive reagents (Fig. 3.9a). After drying for a few minutes, the nanosheet was completely assimilated to the tissue surface. The airway pressure at which air leakage occurred, termed 'bursting pressure', was measured after repair using a manometer. The maximum airway pressure applied was 60 cmH$_2$O because air leakage could occur from the intact pulmonary hilum at higher pressures. At 5 min after repair, the nanosheet showed a bursting pressure (31.7 ± 10.3 cmH$_2$O) lower than that of the fibrin sheet (45.0 ± 5.5 cmH$_2$O). The bursting pressure of the nanosheet was slightly lower than that found in the bulge test (ca. 45 cmH$_2$O for the 6 mm diameter hole prepared on the steel substrate). At 3 hrs after repair, the outline of the square shaped nanosheet assimilating to the tissue surface could be faintly seen, and the bursting pressure of the nanosheet reached 56.7 ± 6.1 cmH$_2$O, which is the same level as that of the fibrin sheet.

From histological examination, it is noteworthy that the wound healing after treatment with the nanosheet was quite distinct from that with the fibrin sheet (Fig. 3.9b). Although it was difficult to observe the nanosheet overlap on the pleural defect, the formation of flat-shaped blood clots localized along the nanosheet was clearly observed in the region of the defect at 3 hrs after repair without significant inflammatory response. This finding suggested that blood cells initially deposited under the nanosheet were subsequently transformed to stable blood clots. At 3 days after repair, fibroblasts had grown around the blood clots, replacing the preformed clots. At 7 days after repair, angiogenesis was observed where the blood clots had originally formed under the nanosheet. Importantly, the sequence of the wound healing process never occurred on the outside of the polysaccharide nanosheet. Hence, no incidence of post-surgical adhesive lesion in the thoracic cavity was observed. At 30 days after repair, the original tissue-defect site was no longer discernible. In contrast to the polysaccharide nanosheet, repair of the pleural defect by the fibrin sheet exhibited large vacant air spaces at 3 hrs because the thick fibrin sheet was too firm to densely overlap the defect site. This lack of flexibility results in haphazard retention of blood components in the overlapped area. At 3 days, the random growth of fibroblasts was observed as well as the induction of an inflammatory tissue reaction, such as the emergence of macrophages. Furthermore, it is a critically important clinical issue that the fibrin sheet also strongly adheres to the chest wall. Severe pleural adhesions could reduce respiratory function and may cause a reoccurrence of pneumothorax.
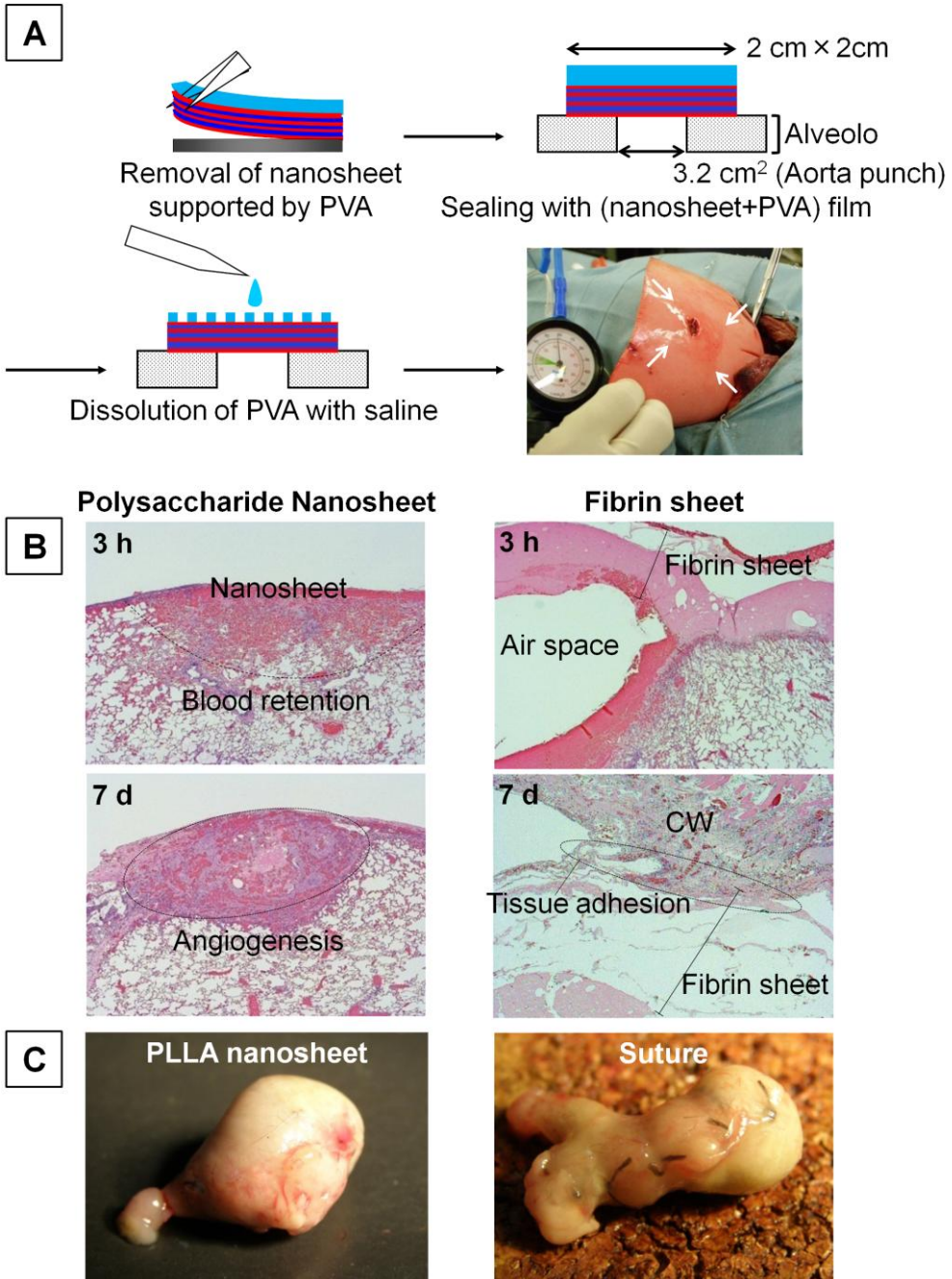
FIGURE 3.9
(a) Schematic representation of visceral pleural defect repair using polysaccharide nanosheets, and (b) histological findings at different time points after treatment with polysaccharide nanosheets and fibrin sheet. (c) Macroscopic images of stomachs treated with PLLA nanosheet and conventional suture/ligation (partially reproduced from references 35 and 36).

PLLA nanosheets may be useful as dressing materials for acidic environments such as the stomach.[36] For example, an incision of approximately 1 cm in length was made in the anterior wall of the stomach in mice using a surgical knife. A supporting suture was stitched (without ligation) at the middle of incision line to invert the reflected mucosa. Thereafter, the PLLA nanosheet supported with the PVA supporting film (typically 1.5 × 1.0 cm) was placed over the incision site. Immediately after covering, the supporting suture (no ligation) was pulled out. The PVA supporting film was then dissolved in saline. At 7 days after surgical intervention (PLLA nanosheet- and suture-treated), the stomachs were removed from the mice. Sealing treatment with the nanosheet did not cause tissue adhesion, and surprisingly, few postoperative cicatrices remained on the surface of the stomach (Fig. 3.9c). In contrast, tissue adhesion was observed in several examples of suture-treated mice with apparent cicatrization in the stomach, causing severe deformity and shrinkage.

Histological observations also highlighted remarkable differences in wound healing between wounds sealed with a nanosheet or suture/ligation. In the nanosheet-sealed mice, the gastric mucosa at the incision site was loosely bent because the PLLA nanosheet just sealed the surface of the gastric serosa. Fibroblasts regenerating in response to wound healing grew normally and smoothly sealed the incision site; the thickness of fibroblasts was equal to that of serosa around the incision site. However, in the conventional suture/ligation-treated mice, gastric mucosa was tightly stitched by suturing. The number of regenerating fibroblasts markedly increased at the incision site, which is typical of the normal wound healing process following conventional suturing treatment. Our results suggest that the PLLA nanosheet directs the balance between conflicting phenomena involved in tissue repair and resistance to tissue adhesion. Specifically, when the surface of the PLLA nanosheet adheres directly to the stomach (obverse surface) it is exposed to blood and tissue fluid containing various growth factors. Fibroblasts grow normally on the surface of the PLLA nanosheet in the presence of growth factors. However, it is intrinsically difficult for cells to adhere to the outer surface of the PLLA nanosheet (reverse surface).

Overall, the nanosheets have desirable properties for acting as sealants in medical applications: high flexibility and physical adhesiveness without the requirement for chemical and biological adhesives used in conventional dressing materials. Thus, repair by overlapping a tissue defect with the polysaccharide nanosheet has significant advantages in maintaining the function of the remaining lung against sustained ventilation and the pressure from respiration and bleeding. Moreover, the PLLA nanosheet displays a sealing effect for a gastric incision procedure, which is restricted in conventional suturing surgery. It is also noteworthy that careful selection of polymers and related physical properties would be important for the application of nanosheets, depending on the types of tissue and organs.

Advanced therapeutics using drug loaded nanosheets

Bacterial infection is a major cause of peritonitis leading to severe sepsis. Postoperative anastomotic breakdown, which is one of the major complications after gastrointestinal surgery, also causes bacterial peritonitis.[37,38] Therefore, therapeutic treatment by suture repair of a perforated/leaked lesion is crucial. Such procedures, however, are often technically challenging because the tissues in the area of the perforated/leaked lesion are usually inflamed and friable. A therapeutic approach for gastrointestinal perforation or high-risk/difficult anastomoses to replace conventional intervention is urgently needed. We reasoned that the polysaccharide nanosheet constitutes a stable platform for loading drugs such as antibiotics, which are an effective therapeutic tool against bacterial infection.
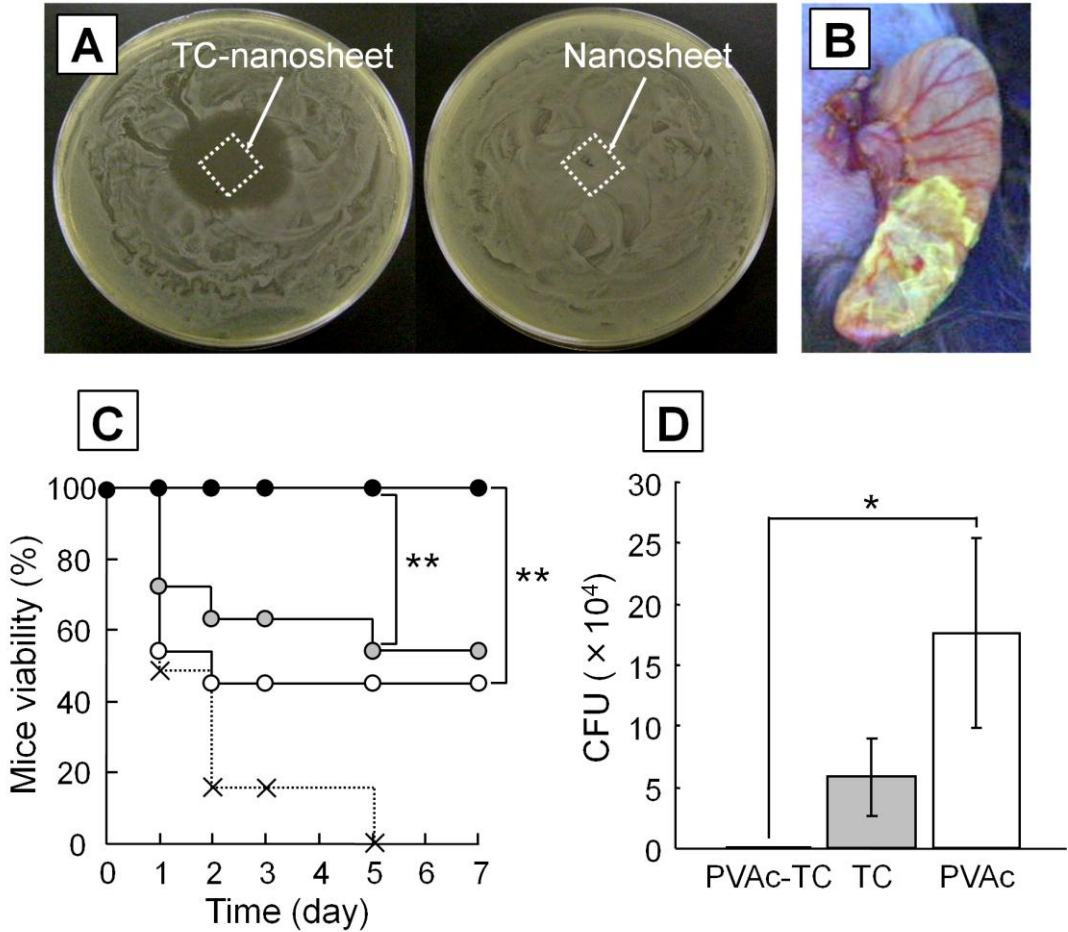
FIGURE 3.10

(a) Antimicrobial effect of polysaccharide nanosheets with (left) and without (right) tetracycline (TC) using the Kirby-Bauer assay. A clear zone of inhibition is seen around the nanosheet loaded with TC (left). (b) Macroscopic image of murine cecum treated with a PVAc-TC-nanosheet illuminated under black light. (c and d) Anti-inflammatory effects of PVAc-TC-nanosheets for a period of 7 days after the operation for PVAc-TC-nanosheets (black circle), TC-nanosheets (gray circle) and PVAc-nanosheets (white circle). (c) Murine sviability and (d) number of bacteria in the intraperitoneal lavage. The dashed line in (c) represents murine viability for the sham (partially reproduced from reference 39).

We have developed an antibiotic-loaded nanosheet to inhibit bacterial penetration and investigated its therapeutic efficacy using a model of a murine cecal puncture. [39] Tetracycline (TC) was sandwiched between a poly(vinylacetate) (PVAc) layer and the polysaccharide nanosheet (named "PVAc-TC-nanosheet"). Under physiological conditions TC was released from the nanosheet for 6 hours. The antimicrobial effect of the PVAc-TC-nanosheet was evaluated by a Kirby-Bauer (KB) test.[40] Growth of *Escherichia coli* on the agar medium was inhibited by TC released from the PVAc-TC-nanosheet, but not by the PVAc-nanosheet (Fig. 3.10a). Hence, incorporation of TC in the nanosheet should show an antimicrobial effect. We optimized the amount of TC loaded on the nanosheet by varying the level of

antibiotic on a 1 x 1 cm^2 sized nanosheet. The size of the zone of inhibition (ZOI) plateaued above 8 μg/cm^2 due to a saturating amount of TC diffusing into the medium. In general, a clinically recommended dose of TC determined by the KB test is 94 μg/cm^2 (ZOI: 3.5-7.0 mm), which was calculated from the datasheet approved by the Clinical and Laboratory Standards Institute (CLSI). [41] Hence, we determined the minimum loading amount of TC on the PVAc-TC-nanosheet as 6.2 ± 0.5 μg/cm^2 (ZOI: 7.0 ± 1.7 mm). Thus, the dose of TC can be reduced by over 15 fold compared with the conventionally required dose. Such a reduction in the dosage of antibiotic should significantly reduce the incidence of adverse side effects in clinical practice.

A PVAc-TC-nanosheet, TC-nanosheet (without the PVAc layer) or PVAc-nanosheet (without the TC layer), each with the cut size of 1 cm × 1 cm ([TC] = 6.2 μg/cm^2), was placed onto a cecal punctured lesion (0.8 mm^2) contaminated with enterobacteria. All of the nanosheets were supported by the PVA film because the freestanding nanosheet itself shrank in air spontaneously. Thereafter, the supporting PVA film was dissolved by dropwise addition of a PBS solution, where the punctured lesion was sealed with a nanosheet in the absence of any adhesive agents. The punctured lesion covered with the PVAc-TC-nanosheet was observed upon illumination with black light. The results suggested a flexible and effective adhesion of the nanosheet on the murine cecum (Fig. 3.10b). In the sham group (without sealing), no mice survived longer than 5 days owing to lethal bacterial peritonitis (data not shown). It is noteworthy that the overlapping treatment with the PVAc-TC-nanosheet showed 100% survival in mice at 7 days, while the control TC-nanosheet and PVAc-nanosheet showed a survival rate of 55% and 45%, respectively (Fig. 3.10c, **p<0.01). Next, we examined the number of viable bacteria in murine peritoneal lavage one day after cecal puncture. Overlapping treatment with the PVAc-TC-nanosheet decreased the viable cell count by 15×10^4-fold compared with the PVAc-nanosheet in the peritoneal lavage of the mice (Fig. 3.10d, *p<0.05). Our results strongly suggest that a PVAc-TC-nanosheet overlapping the punctured lesion affords significant protection against bacterial peritonitis by two distinct barrier effects. Firstly, a physical barrier caused by the nanosheet structure itself and secondly a pharmacological barrier due to the loaded antibiotic (TC). Thus, overlapping treatment with the PVAc-TC-nanosheet reduced the number of intraperitoneal bacteria as well as increasing mouse survival rate after cecal puncture. Taken together, these results suggest loading antibiotics on the nanosheet is an effective means of sealing the punctured lesion. Moreover, capping the surface of the nanosheet with a hydrophobic barrier, comprising a PVAc layer, is also important for the stable maintenance of the TC layer under physiological conditions. Hence, the PVAc-TC-nanosheet almost completely suppressed bacterial growth in the peritoneal cavity of mice with a cecal puncture, suggesting a complete inhibition of bacterial penetration through the PVAc-TC-nanosheet.

Various other drugs, including anticancer agents or growth factors, may be used in place of antibiotics in the drug layer of the nanosheet. For example, it is possible to embed anti-glaucoma drug (i.e., latanoprost) on the polysaccharide nanosheet. Indeed, the latanoprost-loaded nanosheet successfully down regulated intraocular pressure (IOP) reduction of rat cornea for 1 week. [42] Therefore, integration of pharmaceutics will further enhance the applicability of nanosheets for advanced therapeutics; the nanosheet being an ideal platform to manage the controlled release of loaded drugs.

Patchwork coating by fragmented nanosheets

A burn wound is a complex and evolving injury. Extensive burn injuries produce, in addition to local tissue damage, systemic consequences. [43] In the management of burn wounds, much attention should be paid to minimize the risk of burn wound infection during wound healing. Otherwise, superficial and partial thickness wounds often deteriorate into deeper tissue damage. Severe sepsis resulting from burn wound infection is considered to be one of the most critical complications because of its

associated high mortality rate. A wide variety of wound dressings is currently available for the treatment of partial thickness burn wounds.[44] Although such conventional dressings appear to be suitable for wrapping relatively flat interfaces, it is often difficult to efficiently wrap burn wounds with an irregular (non-flat) shape such as those associated with fingers, toes and the perineum.

To this end, we fragmented numbers of PLLA nanosheets into the suspended state, and performed a simple patchwork technique using the fragmented nanosheets to effectively wrap different shaped materials (Fig. 3.11a).[45] We investigated the coating properties of the nanosheet by first labeling it with octadecylrhodamine. Using a vertical dipping and lifting method, we were able to demonstrate that the labeled fragmented nanosheets efficiently coat several different interfaces, such as a lower half of the mouse body, including the perineum that constitutes an irregular shape, by fluorescence stereomicroscopy. The nanosheets were barely detectable under visible light, indicating that the ultra-thin and flexible fragmented nanosheets could be adhered along the roughness of the interfaces at the nanometer scale. This is a noteworthy characteristic of nanosheets generated using the patchwork technique when adhered to an irregular surface.

We also studied an *in vivo* therapeutic barrier effect of the fragmented PLLA nanosheets using a mouse model of superficial dermal burn injury (SDB). Histological observations showed that the epidermis of the SDB-induced dorsal skin was defective by comparison with normal dorsal skin. Next, the suspension of the fragmented nanosheets was simply dropped onto the region of the SDB and then dried for 5 min. SEM observations clarified that the fragmented nanosheets could perfectly wrap the site of burn injury (Fig. 3.11b). This finding indicates that the flexible fragmented nanosheets adhere not only onto flat interfaces, such as SiO_2 substrate and membranes, but also onto uneven interfaces such as skin, resulting in a perfect patchwork. Next, we tested the effectiveness of the seal by carefully dropping a suspension of *Pseudomonas aeruginosa* onto the region of nanosheet-patchwork. We proposed the repeated patchwork treatment of the fragmented nanosheets as follows: SDB-induced skin was sealed with the fragmented nanosheets (1st patchwork). On day 3 after treatment of fragmented nanosheets, the region of nanosheet-patchwork was sealed or not with the nanosheets again (2nd patchwork), and then a suspension of *P. aeruginosa* was applied onto the same region. The repeated patchwork treatment of fragmented nanosheets was found to prevent the infection caused by degradation of the 1st patchwork. These findings suggest that the repeated patchwork treatment has the potential to prevent infection for longer periods of time (i.e., over 3 days). The patchwork technique using fragmented nanosheets shows immense potential as a novel burn wound therapy for both relatively flat dermal skin and skin with an irregular surface shape.
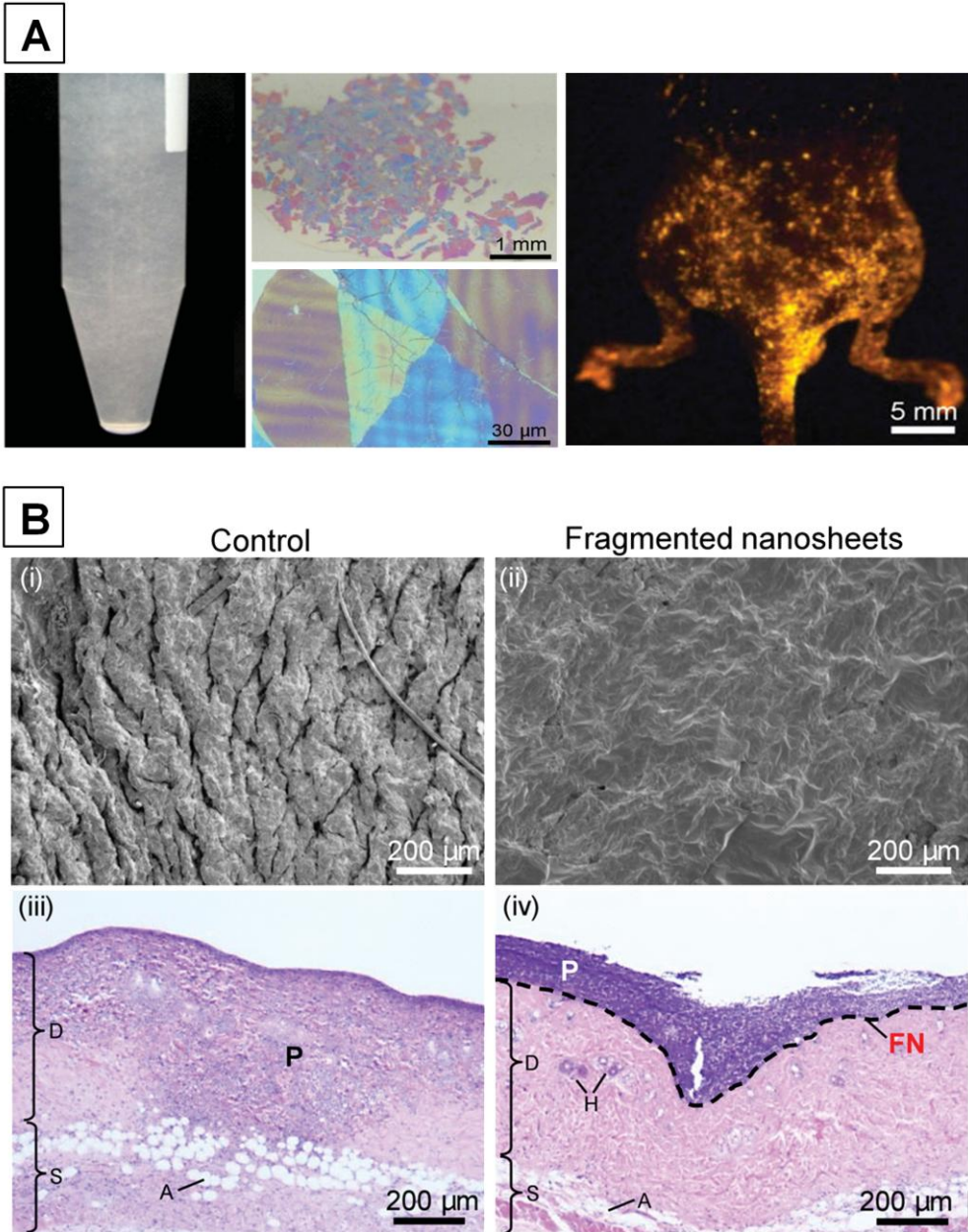
FIGURE 3.11

(a) A macroscopic image of fragmented PLLA nanosheets in water (left), on a SiO$_2$ substrate (center), and on murine skin (right, colored by rhodamine). (b) *In vivo* therapeutic barrier assay. (i) and (ii) SEM images of SDB-induced skin injury before (i) and after (ii) patchwork treatment with the fragmented nanosheets. (iii), iv) Histological images stained with H&E, showing the skin with SDB-induced injury without (iii) or with (iv) the nanosheet-patchwork. The letters A, D, FN, H, P, and S in the histological images indicate adipose tissue, dermis, fragmented nanosheets, hair root, P. aeruginosa and subcutaneous layer, respectively (partially reproduced from reference 45).

Tissue Engineering Applications of Nanosheets

Engineered interface for directing cellular organization

Directing cellular organization is important for the development of various synthetic tissues in biosensing, biorobotics and regenerative medicine. To this end, there have been significant efforts in recreating tissue structure by combining materials with nano- or microscale technologies.[46] ECM is made from nanofibrous structures (e.g., structural proteins and polysaccharides) containing numerous types of cell adhesive domains (e.g., collagen, laminin, fibronectin, vitronectin, and elastin). As such, ECM has an ideal structure and function to direct the cellular organization and therefore to regenerate and maintain tissues and organs (Fig. 3.12a). To mimic the ECM, topographically and mechanically tailored structures have been created by using polymeric materials, microfabrication techniques and functional nanomaterials (e.g., nanofibers, nanowires or nanotubes), which direct cellular organization and induce tissue formation.[47] Though materials, such as hydrogels and elastomers have been employed as cellular scaffolds owing to their tailorable structures and tunable mechanical properties, these materials display size and polymer components that sometimes hinder the hierarchical assembly of the cells into complex tissue structures. Thus, it is technically challenging to recreate the natural complexity of ECM in miniaturized engineered structures that aim to build functional tissue structures.

Microfabrication techniques to generate functional nanosheets

To engineer functional tissues *in vitro*, various novel approaches have been reported using micro- and nanostructured materials or cell manipulation techniques, such as porous polymeric scaffolds,[48] self-organized microwrinkles,[49] electrospun nanofibers,[50] bioprinting,[51] and others.[52] One such microfabrication technique (also known as "soft lithography"), which includes replica molding and microcontact printing, is a highly promising approach towards the creation of defined structures, shapes and arrangements at the micrometer scale. This technique employs microstructured elastomeric molds, consisting of poly(dimethyl siloxane) (PDMS), which allow for precise positioning of proteins and cells, control of shape and function of the cells, and even recapitulation of 3D culture microenvironments for highly structured cells and tissues.[53] One of the important achievements of soft lithography was microcontact printing (μCP); micropatterning of ECM molecules in a 2D configuration can display similar levels of tissue-specific differentiation in a 3D culture system. If ECM molecules are distributed as small, flat adhesive islands, such a configuration can control cell adhesion morphology in order to mimic characteristic cell shapes observed in native tissues. In this regard, we hypothesized that a quasi two-dimensional structure of free-standing nanosheets may be useful as synthetic mimics of the natural basement membrane in ECM, which has an amorphous, dense, sheet-like structure of 50-100 nm in thickness.[54] We attempted to recapitulate the ECM properties (such as flexibility, cell adhesiveness and nanostructure) on the nanosheets towards the development of functional nanosheets for use as flexible biodevices.
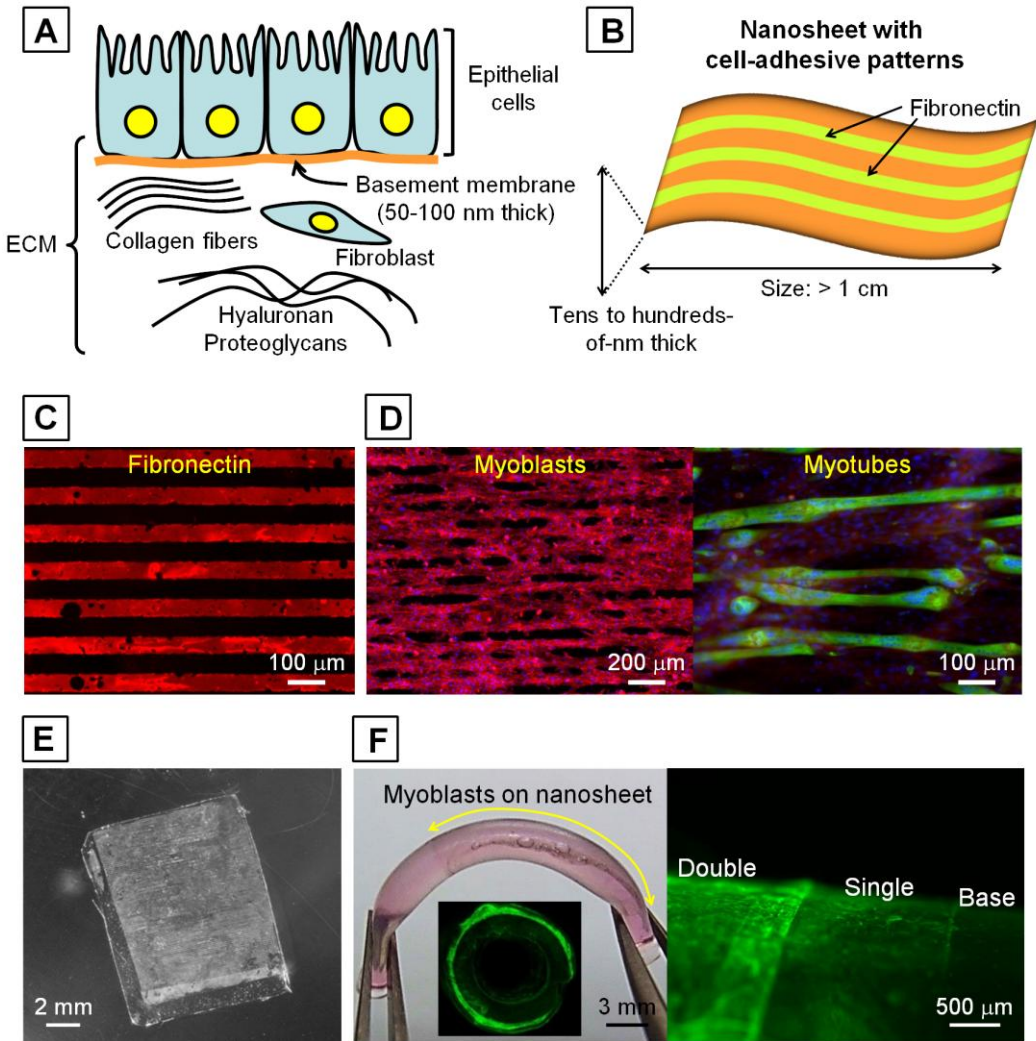
FIGURE 3.12
Biomimetic cellular organization directed by functional nanosheets: (a) Schematic representation of the ECM microstructure and (b) a functionalized nanosheet with cell-adhesive micropatterns. (c) A fluorescent image of fibronectin micropatterns. (d) Alignment of skeletal myoblasts (left) and myotubes (right) on PS nanosheets. (d) a macroscopic image of a freestanding nanosheet with micropatterned C2C12 myoblasts (1×1 cm^2). (e) A macroscopic image of rolled myoblasts on the nanosheet around a silicone tube (3 mmϕ) (Inset: a cross-sectional image stained by calcein AM) (left), and a fluorescent image of the layered structure wrapped approximately twice around the tube (stained by CellTracker Green CMFDA) (right) (partially reproduced from reference 54).

We made freestanding nanosheets, and functionalized them with cell adhesive proteins by μCP for the anisotropic alignment of skeletal muscle cells (Fig. 3.12b). The alignment of the muscle cells is crucially important for their organization in muscle tissues. We employed polystyrene (PS) to generate the nanosheet, due to its manufacturability, well-known physical properties, ease of surface modification as well as its long history of use in cell culture applications. Prior to the spincoating of PS, we prepared

thermo-responsive sacrificial layer consisting of poly(N-isopropylacrylamide) (pNIPAM). The water-solubility of pNIPAM layer is drastically changed among lower critical solution temperature at 32°C. Thus, the PS nanosheet is stable at 37°C (pNIPAM: hydrophobic) during cell culture, and can be released at 4°C (pNIPAM: hydrophilic). Next, we prepared fibronectin (Fn) micropatterns on the nanosheet using µCP to functionalize the film surface for organizing the cells. The µCP process was performed by using poly(dimethyl siloxane) (PDMS) molds with microscopic groove-ridge features of 50 µm in width and 50 µm separation. These dimensions were chosen because it was shown that myotube alignment is enhanced on cell-adhesive micropatterns that are less than 100 µm wide.[55] The unpatterned regions were rendered cytophobic by application of Pluronic F-127 to promote the initial cell alignment. The µCP process resulted in the preparation of spatially controlled micropatterns on the nanosheet (Fig. 3.12c).

We also exploited the large surface of the nanosheet, and evaluated the effect of the Fn micropatterns on cellular morphology using murine skeletal myoblasts (C2C12). Surface structure is an important factor in directing the morphogenesis of myoblasts and myotubes. After 24 hrs of cell seeding, we observed the anisotropic alignment of C2C12 myoblasts on the Fn micropatterned surfaces (Fig. 3.12d). We also investigated myotube formation on the nanosheet because myotube alignment is crucial for maximizing the contractility of muscle tissue. After 8 days in differentiation medium, the formation of C2C12 myotubes was confirmed by immunostaining of myosin heavy chain. We observed aligned C2C12 myotubes on the Fn micropatterned surface. These findings suggested that the improved alignment of the myoblasts promoted end-to-end connection with each other, which favored the assembly of myotubes during the differentiation process.

Functional nanosheets towards flexible biodevices

Tissues with tubular structures, such as blood vessels and intestinal tracts, have a function that originates from their overall structure (e.g., controlled flux of blood or nutrients). In particular, the blood vessel has a specific structure consisting of multilayered smooth muscle cells with anisotropic alignment around the endothelialized layer. Thus, the recapitulated muscular structure may be a good model of the artery wall to study physiology and dysfunction of the blood vessels.[56] In this regard, the tubular structure mediated by the flexible nanosheet could be used for mimicking the natural tissue arrangement, which may facilitate the engineering of drug-screening devices. Thus, we utilized the freestanding nanosheets as an ultra-thin flexible substrate for building biomimetic cellular constructs. Specifically, we demonstrated how to generate an artificial tubular structure consisting of myoblasts cultured on the micropatterned nanosheet. These structures can be fabricated by simply rolling the cell/nanosheet construct around the template whilst maintaining cellular alignment. After one day of culture, we released the nanosheet bearing micropatterned myoblasts by dissolution of the pNIPAM layer at 4°C (Fig. 3.12e). Myoblasts subsequently aligned anisotropically along the CNT-Fn micropattern and remained viable. The freestanding cell/nanosheet construct was used to produce a tubular structure by wrapping it around a template (e.g., silicone tube, 3 mm diameter) (Fig. 3.12f). Although such a wrapping process to engineer multilayered tissue structures has been recently proposed,[57] they employed PDMS thin films that were more than 10 µm in thickness. As a consequence, there is always a thick barrier between the cells on the neighboring sheets. By contrast, the cross-sectional image of the rolled myoblasts on the nanosheet (2×2 cm^2) showed a tightly wrapped structure surrounding the outer wall of the silicone tube (Fig. 3.12f, inset). From the lateral image, we also confirmed fluorescent signals of layered myoblasts due to the esterase activity of the myoblasts. The results suggest that the freestanding nanosheet can serve as a synthetic basement membrane to engineer hierarchical cellular

organization. Moreover, the flexible nanosheet is such a spatially pliable structure that it can be shaped and integrated into a microfluidic system to study the functional properties of synthetic tissues.

Micropatterned nanosheets towards advanced cell delivery systems

There have been ongoing efforts towards the development of cell delivery systems to overcome several intractable diseases. Age-related macular degeneration (AMD) is the leading cause of visual impairment and blindness in the elderly population, whose main complication is the development of subretinal choroidal neovascularization and degeneration of retinal pigment epithelial (RPE) cells.[58] In this regard, subretinal transplantation of the RPE cells to the degenerated site has attracted a great deal of attention as an innovative therapeutic approach for the treatment of AMD.[59] However, poor viability, distribution and integration of the transplanted cells in suspension to the narrow subretinal space have limited this strategy. Therefore, the development of effective cell delivery devices would bring significant benefits for the treatment of AMD.

To this end, we focused on the high degree of flexibility of the nanosheets. Specifically, we designed micropatterned nanosheets consisting of biodegradable PLGA.[60] Next, the RPE monolayer was selectively engineered onto the micropatterned nanosheet to facilitate local delivery of the cellular organization to the narrow subretinal space in a minimally invasive way (Fig. 3.13a). Micropatterned nanosheets were prepared by a combination of spincoating and the μCP technique. A PDMS stamp with columnar convex portions (diameter: 300-1000 μm) was fabricated by conventional photolithography using SU-8 molds. A PLGA solution was mixed with magnetic nanoparticles (MNPs) (10 nmφ) in order to visualize the nanosheet, and the mixture was then spincoated onto the PDMS stamp. The resulting PLGA/MNPs layer was transferred onto a PVA coated glass substrate, on which collagen was spincoated to promote cell adhesion. Then, the sample surface was covered with RPE cell suspension, and the freestanding cell/nanosheet construct was obtained by dissolving the PVA layer in phosphate buffered saline (PBS). The PLGA/MNPs nanosheets with circular shapes were fabricated on the substrate, and dissolution of the PVA layer allowed for the release of brown colored nanosheets with 170 nm thickness (Fig. 3.13b, 500 μmφ). Due to the high degree of flexibility, the freestanding nanosheet (e.g., 1000 μmφ) was easily aspirated inside the intravenous catheter (24 G, 470 μm in inner diameter) (Fig. 3.13c). Next, the RPE cells were selectively cultured on the micropatterned nanosheets. The cellular organization on the nanosheet was then characterized using a confocal laser scanning microscope (CLSM) because monolayer formation is an important structural aspect of epithelial cells. CLSM imaging clearly showed the RPE monolayer on the nanosheet (colored by Rhodamine B) (Fig. 3.13d).

Despite the mechanical share stress induced by aspiration and injection through the syringe needle, the RPE monolayer on the nanosheet retained its original shape without any fracture, and maintained >80% viability regardless of the sheet diameter. Moreover, we evaluated the thickness effect on cell viability after syringe injection. Finally, we demonstrated the injection of the micropatterned nanosheet to the subretinal space using a swine ocular globe, in which the freestanding micropatterned nanosheet (1000 μmφ) was injected via an intravenous catheter. The injected nanosheet was successfully released and spread into the subretinal region where it subsequently fixed without structural distortion to the macula after removing the pre-filled saline (Fig. 3.13e). The flexible structure of the micropatterned nanosheet is beneficial not only for allowing deformation of the shape inside the needle, but also reducing the mechanical stress on the cell monolayer. This injectable micropatterned nanosheet that is delivered using a conventional syringe holds great promise for transplanting engineered cell monolayers in a minimally invasive fashion.

Conclusions and Future Outlook

In this chapter, we have described recent developments of nanosheet technology including the fabrication process, physical properties of the nanosheets themselves (structural, adhesive, mechanical and permeability) as well as their practical applications. The use of nanosheets as nano-adhesive plasters highlight the unique characteristics of these materials that make them ideally suited to surgical applications; in particular their high degree of flexibility and physical adhesiveness to tissue defects. Our *in vivo* results demonstrate that treatment involving the nanosheets is a minimally invasive procedure that does not elicit a significant inflammatory response. These benefits are crucial for designing implantable biomaterials. Further investigation of cell-material interaction involving the nanosheet is required in order to further analyze the surface properties of the nanosheet. In this regard, integration of advanced microfabrication techniques is an important approach to the understanding of the cell-material interface. Moreover, this methodology will be crucial for investigating how to direct cellular organization in tissue engineering applications. Nanosheets are an ideal platform for integrating various functions as exemplified by drug administration, development of new nanomaterials and even living organisms. We believe this research will open up new avenues for generating innovative biomaterials in the field of nanobiotechnology.

Acknowledgements
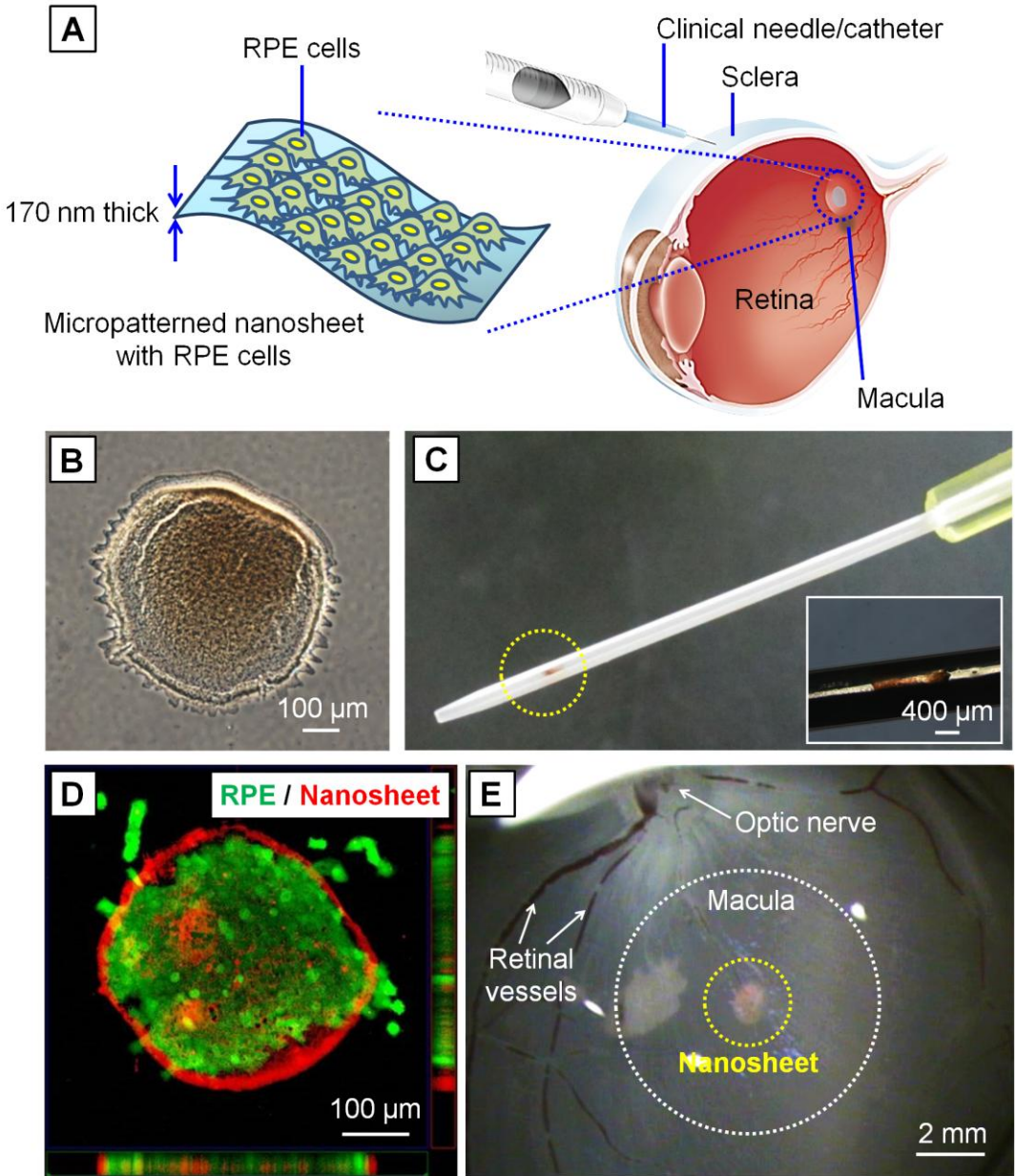
FIGURE 3.13
Local delivery of retinal pigment epithelial (RPE) cells by micropatterned nanosheets: (a) schematic image, (b) a microscopic image of a micropatterned PLGA nanosheet (500 μmϕ), and (c) folded structure inside a 24 G intravenous catheter (470 μm inner diameter). (d) A CLSM image showing monolayer formation by the RPE cells on the nanosheet (stained with rhodamine B), and (e) a microscopic image of the injected nanosheet, fixed onto swine macula (partially reproduced from reference 60).

References

1. Chan, J., Dodani, S. C., Chang, C. J. *Nat. Chem.* **2012**, *4*, 973-84.
2. Miyata, K., Nishiyama, N., Kataoka, K. *Chem. Soc. Rev.* **2012**, *41*, 2562-74.
3. Khademhosseini, A., Vacanti, J. P., Langer, R. *Sci. Am.* **2009**, *300*, 64-71.
4. Forrest, J. A., Dalnoki-Veress, K. *Adv. Colloid Interface Sci.* **2001**, *94*, 167-96.
5. Takeoka, S., Okamura, Y., Fujie, T., Fukui, Y. *Pure Appl. Chem.* **2008**, *80*, 2259-71.
6. Fujie, T., Okamura, Y., Takeoka, S. In *Functional Polymer Films.*; Knoll, W., Advincula, R. C., Eds.; Wiley-VCH, Weinheim, Germany, **2011**, Vol. 2, pp. 907-931.
7. Ricotti, L., Taccola, S., Pensabene, V., Mattoli, V., Fujie, T., Takeoka, S., Menciassi, A., Dario, P. *Biomed. Microdevices* **2010**, *12*, 809-19.
8. Fernandes, H., Moroni, L., van Blitterswijk, C., de Boer, J. *J. Mater. Chem.* **2009**, *19*, 5474-84.
9. Fujie, T., Ricotti, L., Desii, A., Menciassi, A., Dario, P., Mattoli, V. *Langmuir*, **2011**, *27*, 13173-82.
10. Forrest, J. A., Dalnoki-Veress, K., Stevens, J. R., Dutcher, J. R. *Phys. Rev. Lett.* **1996**, *77*, 2002-5.
11. Jiang, C., Tsukruk, V. V. *Adv. Mater.* **2006**, *18*, 829-40.
12. Endo, H., Kado, Y., Mitsuishi, M., Miyashita, T. *Macromolecules* **2006**, *39*, 5559-63.
13. Vendamme, R., Onoue, S., Nakao, A., Kunitake, T. *Nature Mater.* **2006**, *5*, 494-501.
14. Lvov, Y., Decher, G., Möhwald, H. *Langmuir* **1993**, *9*, 481-6.
15. Lvov, Y., Ariga, K., Ichinose, I., Kunitake, T. *J. Am. Chem. Soc.* **1995**, *117*, 6117-23.
16. Decher, G., Lvov, Y., Schmitt. J. *Thin Solid Films* **1994**, *244*, 772-7.
17. Tsukruk, V. V., Bliznyuk, V. N., Visser, D., Campbell, A. L., Buning, T. J., Adams. W. W. *Macromolecules* **1997**, *30*, 6615-25.
18. Decher, G. *Science* **1997**, *277*, 1232-7.
19. Decher, G. In *Multilayer Thin Films.*; Decher, G., Schlenoff, J. B., Eds.; Wiley-VCH, Weinheim, Germany, **2003**, pp. 1-46.
20. Liao, I., Wan, A. C. A., Yim, E. K. F., Leong, K. W. *J. of Controlled Release.* **2005**, *104*, 347-58.
21. Kumar, M. N. V. R., Muzzarelli, R. A. A., Muzzarelli, C., Sashiwa, H., Domb, A. J. *Chem. Rev.* **2004**, *104*, 6017-84.
22. Lim, L.-T., Auras, R., Rubino, M. *Prog. Polym. Sci.* **2008**, *33*, 820-52.
23. Gross, R. A., Kalra, B. *Science* **2002**, *297*, 803-7.
24. Baba, S., Midorikawa, T., Nakano, T. *Appl. Surf. Sci.* **1999**, *144*, 344-9.
25. Vlassak, J. J., Nix. W. D. *J. Mater. Res.* **1992**, *7*, 3242-9.
26. Markutsya, S., Jiang, C., Pikus, Y., Tsukruk. V. V. *Adv. Funct. Mater.* **2005**, *15*, 771-80.
27. Eling, B., Gogolewski, S., Pennings, A. J. *Polymer* **1982**, *23*, 1587-93.
28. Stafford, C. M., Harrison, C., Beers, K. L., Karim, A., Amis, E. J., Vanlandingham, M. R., Kim, H., Volksen, W., Miller, R. D., Simonyi, E. E. *Nature Mater.* **2004**, *3*, 545-50.
29. Fujie, T., Kawamoto, Y., Haniuda, H., Saito, A., Kabata, K., Honda, Y., Ohmori, E., Asahi, T., Takeoka, S. *Macromolecules*, **2013**, *46*, 395-402.
30. Yamaguchi, A., Fumiaki, U., Takashi, Y., Tatsuya, U., Tanamura, Y., Yamashita, T., Teramae, N. *Nature Mater.* **2004**, *3*, 337-41.
31. Porte, H. L., Jany, T., Akkad, R., Conti, M., Gillet, P. A., Guidat, A., Wurtz, A. J. *Ann. Thorac. Surg.* **2001**, *71*, 1618-22.
32. Kawamura, M., Gika, M., Izumi, Y., Horinouchi, H., Shinya, N., Mukai, M., Kobayashi, K. *Eur. J. Cardiothorac. Surg.*, **2005**, *28*, 39-42.
33. Gika, M., Kawamura, M., Izumi, Y., Kobayashi, K. *Interact. Cardiovasc. Thorac. Surg.*, **2007**, *6*, 12-5.

34. Fujie, T., Okamura, Y., Takeoka, S. *Adv. Mater.* **2007**, *19*, 3549-53.
35. Fujie, T., Matsutani, N., Kinoshita, M., Okamura, Y., Saito, A., Takeoka, S. *Adv. Funct. Mater.*, **2009**, *19*, 2560-8.
36. Okamura, Y., Kabata, K., Kinoshita, M., Saitoh, D., Takeoka, S. *Adv. Mater.* **2009**, *21*, 4388-92.
37. Malangoni, M. A. *Am. J. Surg.*, **2005**, *190*, 255-9.
38. Brook, I. *Dig. Dis. Sci.*, **2008**, *53*, 2585-91.
39. Fujie, T., Saito, A., Kinoshita, M., Miyazaki, H., Ohtsubo, S., Saitoh, D., Takeoka, S. *Biomaterials*, **2010**, *31*, 6269-78.
40. Grunlan, J. C., Choi, J. K., Lin, A. *Biomacromolecules*, **2005**, *6*, 1149-53.
41. Clinical and Laboratory Standards Institute. Performance standard for antimicrobial susceptibility testing. Document M100-S15. Wayne (PA): CLSI, **2005**.
42. Kashiwagi, K., Ito, K., Haniuda, H., Ohtsubo, S. Takeoka, S. *Invest Ophthalmol Vis Sci.* **2013**, *54*, 5629-37.
43. Saito, A., Miyazaki, H., Fujie, T., Ohtsubo, S., Kinoshita, M., Saitoh, D. Takeoka, S. *Acta Biomater.*, **2012**, *8*, 2932-40.
44. Wasiak, J., Cleland, H., Campbell, F. *Cochrane Database Syst. Rev.* **2008**, CD002106.
45. Okamura, Y., Kabata, K., Kinoshita, M., Miyazaki, H., Saito, A., Fujie, T., Ohtsubo, S., Saitoh, D., Takeoka, S. *Adv. Mater.*, **2013**, *25*, 545-51.
46. Khademhosseini, A., Langer, R., Borenstein, J. T., Vacanti, J.P. *Proc. Natl. Acad. Sci. USA*, **2006**, *103*, 2480-7.
47. Bettinger, C. J., Langer, R., Borenstein, J. T. *Angew. Chem. Int. Ed.*, **2009**, *48*, 5406-15.
48. Hollister, S. J. *Nature Mater.*, **2005**, *4*, 518-24.
49. Fu, C., Grimes, A., Long, M., Ferri, C. G. L., Rich, B. D., Ghosh, S., Ghosh, S., Lee, L. P., Gopinathan, A., Khine, M. *Adv. Mater.*, **2009**, *21*, 4472-6.
50. Liang, D., Hsiao, B. S., Chu, B. *Adv. Drug Deliv. Rev.*, **2007**, *59*, 1392-412.
51. Schuurman, W., Khristov, V., Pot, M. W., van Weeren, P. R., Dhert, W. J .A., Malda, J. *Biofabrication*, **2011**, *3*, 021001.
52. Tawfick, S., De Volder, M., Copic, D., Park, S.-J., Oliver, C. R., Polsen, E. S., Roberts, M. J., Hart, A. J. *Adv. Mater.*, **2012**, *24*, 1628-74.
53. Huh, D., Hamilton, G. A., Ingber, D. E. *Trends Cell Biol.*, **2011**, *21*, 745-54.
54. Fujie, T., Ahadian, S., Liu, H., Chang, H., Ostrovidov, S., Wu, H., Bae, H., Nakajima, K., Kaji, H., Khademhosseini, A. *Nano Lett.*, **2013**, *13*, 3185-92.
55. Hosseini, V., Ahadian, S., Ostrovidov, S., Camci-Unal, G., Chen, S., Kaji, H., Ramalingam, M., Khademhosseini, A. *Tissue Eng., Part A* **2012**, *18*, 2453-65.
56. Günther, A., Yasotharan, S., Vagaon, A., Lochovsky, C., Pinto, S., Yang, J., Lau, C., Voigtlaender-Bolz, J., Bolz, S-S. *Lab Chip* **2010**, *10*, 2341-9.
57. Yuan, B., Jin, Y., Sun, Y., Wang, D., Sun, J., Wang, Z., Zhang, W., Jiang, X. *Adv. Mater.* **2012**, *24*, 890-6.
58. Hynes, S. R., Lavik, E. B. *Graefes. Arch. Clin. Exp. Ophthalmol.* **2010**, *248*, 763-78.
59. Binder, S., Stanzel, B. V., Krebs, I., Glittenberg, C. *Prog. Retin. Eye Res.* **2007**, *26*, 516-54.
60. Fujie, T., Mori, Y., Ito, S., Nishizawa, M., Bae, H., Nagai, N., Onami, H., Abe, T., Khademhosseini, A., Kaji, H. *Adv. Mater. 2014, 26, 1699-705*.

4

Effectiveness of an alkaloid fraction on carbon steel corrosion inhibition evaluated by green chemistry biotechnological approach

Maria Aparecida M. Maciel[a,b*], Cássia Carvalho de Almeida[b], Maria Beatriz Mesquita Cansanção Felipe[c]; Luan Silveira Alves de Moura[b], Melyssa Lima de Medeiros[a], Silva Regina Batistuzzo de Medeiros[d], Djalma Ribeiro da Silva[c]

[a]Post Graduate Program in Biotechnology, University Potiguar Laureate International Universities, Campus Salgado Filho, 59075-000, Natal, RN (Brazil)
[b]Institute of Chemistry, Center of Exact Sciences and Earth, Federal University of Rio Grande do Norte, 59072-970, Natal, RN (Brazil)
[c]Center for Research in Oil and Renewable Energy, Federal University of Rio Grande do Norte, 59072-970, Natal, RN (Brazil)
[d]Department of Cellular Biology and Genetics, Federal University of Rio Grande do Norte, Campus, Lagoa Nova, 59072-970, Natal, RN, Brazil.

Outline:

Introduction

Corrosion phenomena is a natural process that results in considerable waste of industrial investment. Corrosion inhibitors are common for protecting steel structures and their alloys in industry. This phenomenon can easily be found in different types of surfaces causing major economic losses in the industrial sector. Chemicals used as corrosion inhibitors are very toxic even in small concentrations, leading to environmental agencies requesting prohibition. Corrosion control involves different aspects such as environmental, economical and technical resulting in major advances of science and biotechnology. Considerable attention has been focused on corrosion inhibitor handling and its chemical residue aimed health and environmental safety. Hence, there is a growing demand for environmentally appropriate inhibitors such as vegetal inhibitors. It is estimated that more than 30 % of the steel produced worldwide is used for spare parts, pieces of equipment and facilities damaged by corrosion. The chemical, electrochemical or electrolytic corrosion processes are spontaneous, leading to modifications in the physicochemical characteristics of materials (Figure 4.1). Corrosion is costly due to any operational downtime necessary for parts replacement. There is also concern about damage to the environment for example the breaking of oil pipelines in the petroleum industry. Corrosion resistant products are in great demand and have been increasing in technological advances.

Recent studies have estimated that annual costs worldwide related to corrosion damage are around 4 % of the Gross Domestic Product (GDP) of an industrialized country [1]. Management practices and corrosion control can reduce 20 % of direct costs [maintenance (protection processes) and/or replacement of parts or equipment] or indirect, such as downtime due to equipment failure, product contamination, production losses and personal and also environmental safety [1,2].

We have been developing studies in green chemistry applied to corrosion phenomena using microemulsions as vehicles of plant extract or synthetic organic compounds aiming to lower the inhibitors concentrations without loss of effectiveness. Saponified coconut oil is a green chemistry surfactant as part of the microemulsion system applied on corrosion inhibition of carbon steel AISI 1020, in saline medium [3-6]. Microemulsions optimize solubilization of water insoluble organic compounds and plant extracts, increasing its adsorption potential due the presence of surfactant, and subsequent expansion of the surface area covered. The microemulsified saponified coconut oil MES-SCO (reported as OCS-ME) effectiveness on carbon steel corrosion inhibition process was evaluated using an electrochemical method of polarization resistance. This microemulsion system showed inhibitors effect 77 % at lower concentrations of the surfactant (0.5 %). Meanwhile, the free surfactant saponified coconut oil (SCO solubilized in H_2O) showed lower efficacy (63 % at 0.20-0.25 % of SCO concentration). The greatest inhibitory effect of MES-SCO was correlated with the rich o/w microemultion system which is very important for adsorption phenomena [3].

In this study, an alkaloid fraction (AF) obtained from the stem bark of the plant species *Croton cajucara* Benth (Euphorbiaceae) was evaluated as a green chemistry corrosion inhibitor. AF loaded in the green MES-SCO system was analyzed in corrosion inhibition of carbon steel AISI 1020, in saline medium. This was followed by a description of phytochemical aspects of AF and its antioxidant and bactericidal influences into MES-AF aiming to finding a more suitable inhibitor effective in both spontaneous corrosion processes and biocorrosion phenomena.
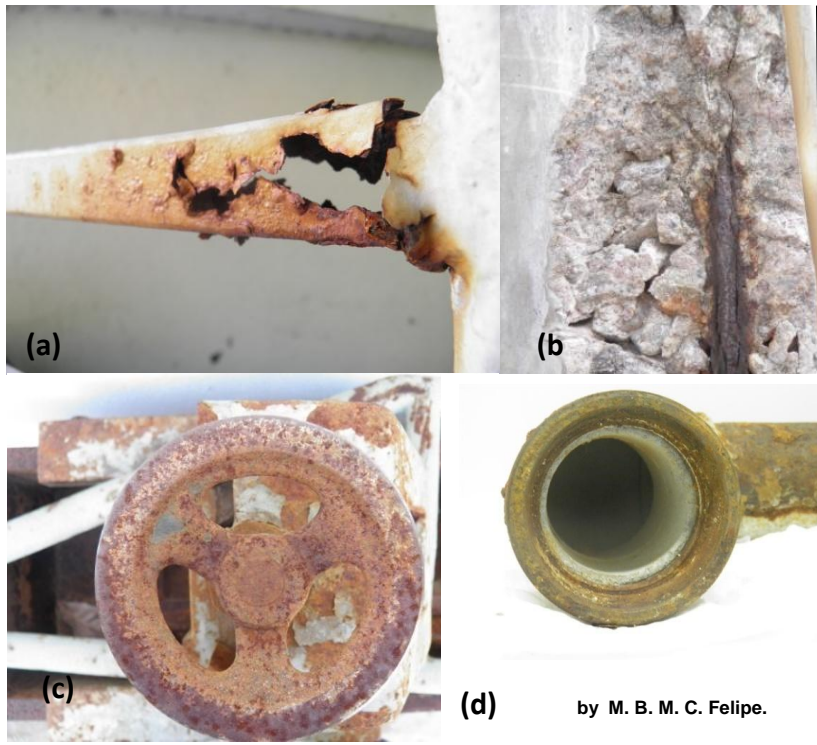
FIGURE 4.1
Metallic structures damaged by corrosion: (a) handrail; (b) metal structure inside a concrete block; (c) tap; (d) tube from an oil pipeline.

General

Great scientific interest has focused on the natural inhibitors from plant sources due to the significant microbiological control and inhibitive property on electrochemical corrosion. Academic researchers need studies using plant extracts as natural effective corrosion bioinhibitors, including biocorrosion process which is influenced by microorganisms. Behpour *et al.* [7] studied the effect of *Punica granatum* in acidic solution (HCl 2 M and H_2SO_4 1 M) through electrochemical impedance spectroscopy and potentiodynamic polarization technique, indicating that this extract could be used as excellent corrosion inhibitor. *Phyllanthus amarus* leaf extract has also demonstrated to protect carbon steel of corrosion deterioration [8]. Anticorrosive properties was also documented for other types of natural compounds *Zanthoxylum alatum, Lawsonia, Occimum viridis, Telfer occidentalis*, *Azadirachta indica* and *Hibiscus sabdariffa* extracts, in acid solution [9]. The methanol extract of *Artemisia pallens* showed 96.5 % of corrosion inhibition efficiency on steel exposed to a 4 N HCl solution [10], among other [12-13].

Atmospheric corrosion is a phenomena derived from condensation of moisture on the metal surface, similar characteristics such as varying of pH, temperature, medium chemical composition, aeration aspects and also the deterioration of a material due to microbiological activity commonly known as biocorrosion or as corrosion influenced by microorganisms (CIM), should all be considered [14]. Since

MIC phenomenon results from interactions between the metal surface with abiotic products in the presence of microbial cells and their metabolites, various environments are advantageous to microbial growth, thus many equipment are subject to biocorrosion [14]. The main types of bacteria associated with metals in aquatic or terrestrial habitat are sulphate reducing bacteria (SRB), sulfur-oxidizing bacteria, manganese-oxidizing bacteria, iron-oxidizing/reducing bacteria, bacteria secreting acids and organic sludge, and algae and fungi [15]. Examples of environments susceptible to microorganism attack include: seawater, rivers and cooling systems, wetlands, and soils containing salts or organic waste.

To assess the prospect of exploiting biomass extracts for the simultaneous control of chemical and microbiologically influenced corrosion, studies have shown that vegetal extracts acting as bifunctional inhibitors on MIC and electrochemical corrosion. The effect of the aqueous extracts of *Piper guineense* (PG) was appraised on low-carbon steel corrosion in acidic medium using gravimetric and electrochemical techniques. The agar disc diffusion method was employed to determine the biocidal effect of the extract on corrosion-associated sulfate-reducing bacteria (SRB), *Desulfotomaculum* species. PG was found to be an excellent inhibitor for both corrosion and SRB growth. The corrosion process was inhibited by adsorption of the extract organic matter on the steel surface, whereas the antimicrobial effect results from disruption of the growth and essential metabolic functions of the SRB [16].

An aqueous methanolic extract of the whole plant of *Artemisia pallens* has shown good antibacterial activity against *Pseudomonas aeruginosa* and *Shigella flexneri*. The crude extract also showed significant anticorrosive efficiency against mild steel, in acidic solution [17].

Hence, the investigation of antibacterial activity and antioxidant property of *Croton cajucara* Benth and its inhibiting action on corrosion aiming development of a green chemistry inhibitor are presented.

Material and Methods

Plant material

The stem bark of *Croton cajucara* Benth was purchased in the Amazon region of Brazil at the free market called Ver-o-peso (Belém, state of Pará) and was chemically identified by phytochemical experimental procedures using standard material [18]. Previously, Nelson A. Rosa performed a botanic identification of this specimen, in which a voucher specimen (no. 247) has been deposited in Herbarium of the Paraense Emílio Goeldi Museum (Belém, Brazil).

Hydroalcoholic extract of Croton cajucara Benth and its phenolic acids and alkaloid fraction

Extraction of the powdered bark (1 kg) of *Croton cajucara* was carried out with aqueous methanol in a Soxhlet apparatus for 48 hr. This hydroalcoholic extract was obtained after solvent removal. Phytochemistry approach was worked out according to previously procedures aiming the plant chemical authenticity and also isolation of phenolic acid compounds and its semi-synthetic derivatives as previously described [18,19]. To obtain the alkaloidal fraction (AF) the extract obtained with a yield of 9.2 % (92 g) was subjected to an open column chromatography on silica gel (230-80 mesh) and 64 fractions were obtained which were eluted with gradient polarity of the mixed solvent. The more polar fraction [eluted with methanol/water (9:1 to 8:2)] after work out in Sephadex and spectroscopic characterization, proved to be a rich source of isoquinoline alkaloids compounds. The total characterization of the natural compounds were performed by spectroscopic methods such as IR, UV,

MS, 1D and 2D-NMR (300 MHz), in which part of that such as alkaloidal fraction chemical identity and its characterization are first reported herein.

Determination of total antioxidant capacity by phosphomolybdenum method

The total antioxidant activity of AF in a water solution (AF-WS) was determined by green phosphomolybdenum complex formation. Triplicates of 100 µL of AF-WS (1 mg/mL of solvent) and standard (ascorbic acid) were added to 3 mL of reagent solution (0.6 M sulfuric acid, 28 mM sodium phosphate and 4 mM ammonium molybdate). The reaction mixture was incubated at 95 ºC for 90 min [20]. The absorbance of the solution was measured at 695 nm using a spectrophotometer (Shimadzu, UV-1650Pc) against blank after cooling to room temperature. Total antioxidant activity was expressed as the number of equivalents of ascorbic acid in milligram per gram of solution.

Antimicrobial assay

Minimal inhibitory concentration (MIC) of *C. cajucara* Benth hydroalcoholic extract (CC-HE) was determined by broth microdilution method [21] using 96-well microtitre plates. The pre-inoculum culture consisted of a bacterial colony cultivated in 15 mL LB medium, for 16-18h at 37 °C at 180 rpm. After this period, 150 µL of pre-inoculum was transferred to 150 mL of LB and incubated at 37 °C at 180 rpm until optical density of 0.8 at 600 nm measured by UV-VIS (Quant, Biotek) was achieved. Concentrations of CC-HE extract were tested in the range of 0.06-1.0 mg/mL against gram-negative bacteria, *Escherichia coli* ATCC25822, *Chromobacterium violaceum*, *Pseudomonas aeruginosa* ATCC27853, and gram-positives, *Bacillus cereus* ATCC11778, *Enterococcus faecium* and *Staphylococcus aureus* ATCC25923 cultures. Ampicilin (2.0 µg/mL) e chloramphenicol (12.5 µg/mL) were used as positive controls and appropriate controls with no extracts and only solvent were done. The experiments were done in triplicate.

Microemulsion system approach

The microemulsion system MES-SCO was used as vehicle to dissolve the plant extract resulting in the MES-AF formulation. MES-SCO containing saponified coconut oil in lower concentration as surfactant and butan-1-ol as cosurfactant, was performed with large microemulsion region. Specifically, the MES-SCO was obtained from the titration methodology and mass fractions in pseudoternary phase diagram containing a mixture of 40 % C/S (cosurfactant/surfactant), 5 % of kerosene as the oily phase and 55 % of double-distilled water as the aqueous phase [3-6].

Efficiency of corrosion inhibition

The MES-AF formulation efficiency was evaluated in saline medium (3.5 % NaCl) by polarization resistance methodology using PGSTAT 300 potentiostat coupled with GPES version 4.9 software aiming calculate corrosion parameters. An electrochemical cell consisted of a reference electrode (Ag/AgCl), a graphite auxiliary electrode, and a working electrode was used. The working electrode was constructed using a cylindrical piece of carbon steel AISI 1020 with exhibition area of 1.77 cm^2. The concentrations of the tested alkaloidal fraction ranged from 50 to 400 ppm. The polarization curves were recorded at a scanning rate of 0.05 V/min with varying potential from the observed open circuit potential after one hour of immersion. The corrosion parameters were obtained by extrapolating the Tafel curves and

used to calculate corrosion inhibition efficiency (IE) according to the following equation:

$$IE(\%) = \frac{Ecorr - Ecorr(inh)}{Ecorr}$$

where Ecorr and Ecorr(inh) are the corrosion potentials of the steel coupons in the absence and presence of MES-AF, respectively.

To evaluate the adsorption process of MES-AF on the metal surface, Langmuir and Frumkin adsorption isotherms were obtained by the equations presented in Table 4.1 [22].

TABLE 4.1
Equations for the isotherms of Langmuir and Frumkin.

Isotherm	Equation
Langmuir	$\theta/(1-\theta) = KC$
Frumkin	$\text{Log}(\theta/(1-\theta).C) = \log K + g\,\theta$

The surface coverage (θ) was calculated from the rates of corrosion inhibition obtained by polarization resistance data at 25 °C, in which "C" represents the inhibitor concentration in ppm and "K" is the adsorption equilibrium constant. Finally "g" is the degree of lateral interaction among the adsorbed molecules.

Results and Discussion

The species *Croton cajucara* Benth (Figure 4.2) commonly known as *sacaca* (which means spell in a specific indigenous language) is a native tree (4 to 6 m tall) from Amazon region of Brazil. Studies point out that the stem bark (Figure 4.3) of this plant is largely used as tea or pills to combat diabetes, diarrhea, stomach upset and to control high levels of cholesterol [23]. Despite the enormous potential of plants around the world only a minor fraction of globe's living species has ever been tested for any bioactivity. This is not the case of *Croton cajucara* Benth with has a large historic of multidisciplinary researches, confirming its medicinal properties on a progressive biotechnological development. There is a number of *Croton cajucara* Benth devoted to its chemical, biochemical, pharmacological and potential advantages of molecular incorporation into drug delivery systems [23-26]. Phytochemical studies carried out with this specie had involved plants ageing from 1 ½ to 6 years old (native and cultivated plants) showing stem barks as a rich source of clerodane-type diterpenes. Among them, the biocompound *trans*-dehydrocrotonin (DCTN) detected in trees ageing up to 3 years old, which have shown pharmacological results that lead to the phytotherapy validation of *Croton cajucara* Benth. The encapsulation of DCTN in liposomes enhanced its antitumor activity [26].

FIGURE 4.2
Croton cajucara Benth.

Source: http://www.maniadeamazonia.com.br

FIGURE 4.3
Stem bark of *Croton cajucara* Benth.

Ongoing studies with *Croton cajucara* Benth using classical column chromatography were performed with an aqueous methanol extract. *Croton* fractions eluted with a mixture of hexane/EtOAc (6:4 to 1:1) affording a mixture of phenolic acids (vanillic acid and 4-hydroxy-benzoic acid) and an aminoacid (Figure 4.4) identified as N-methyltyrosine [white powder; mp 240-241 °C; crystallization from MeOH/H_2O/HCl (8:1.5:0.5); its TLC analysis were performed using n-BuOH/Me_2CO/AcOH/H_2O (2.0:3.5:3.5:1.0), detection performed with ninhydrin reagent, R_f 0.4]. The phenolic acids mixture was subjected to preparative TLC using hexane/EtOAc (6:4) as eluted solvent (it was eluted five times, R_f 0.5) to yield vanillic acid (white needles, mp 209-210 °C) and 4-hydroxy-benzoic acid (white needles, mp 214-215 °C).

The polar alkaloid fraction (AF) also obtained from this aqueous methanol extract of *Croton cajucara* was eluted with methanol/water (9:1 to 8:2). In that, alkaloid-type compounds were detected by Dragendorff reagent applied in TLC and also by ^{1}H NMR spectrum analysis. Structure elucidation of those compounds was achieved by spectroscopic measurements including NMR experiments revealing in the AF fraction the presence of isoquinoline alkaloids mixture such as magnoflorine (Figure 4.5) and N,N-dimethyl-lindicarpine (Figure 4.6). This isoquinoline alkaloids mixture presented in the AF fraction, showed b.p. over 280 °C; TLC-analysis eluted with $CHCl_3$:MeOH:H_2O (6.5:5.0:1.0) Rf=0.5; IR absorptions at 3451, 2922, 1655, 1154 cm^{-1}. ^{1}H NMR spectrum of AF fraction, recorded at 300MHz (CD_3OD/D_2O) allowed hydrogen attribution of magnoflorine: H8 [6.94 d (*J* = 8.0 Hz)]; H9 [6.83 d (*J* = 9.0 Hz)]; H3 [6.58 s]; H6a [3.77 broad t (*J* = 9.8 Hz)], H5 (2.29 – 3.33 m); H7e (2.82 m); H4e (2.55 broad d); H7a (2.41 broad t); OH (9.34 s); OCH_3 - C2 (3.90 s); OCH_3 - C10 (3.89 s); N[+]-CH_3B (3.44 s); N[+]- CH_3A (3.08 s) and for N,N-dimethyl-lindicarpine: H8 (7.31 d); H9 (7.24 d); H3 (6.83 s); H5e (4.10 m); H7 (3.66 m); H6a (3.68 m); H5a (2.85-2.83 m); H4 (2.85-2.83 m); OH (9.51 s); OCH_3 (3.90 s); OCH_3 (3.89 s); N[+]-CH_3 A (3.26 s); N[+]-CH_3B (3.44 s).

The structures of the phenolic acids (vanillic acid, 4-hydroxy-benzoic acid and N-methyltyrosine) were identified as previously described [19] using 300 MHz NMR and MS experiments and for the vanillic acid its chemical transformation with diazomethane give the two methylated derivative esters I and II (Figure 4.4). ^{1}H and ^{13}C NMR (DMSO/DCl) data of N-methyltyrosine were in accordance with the authentic sample of 2-amino-3-(4-hydroxyphenyl) propanoic acid (known as tyrosine) obtained from commercial material. The different observed peaks were assigned to the N-Me group of N-methyltyrosine [19].

vanillic acid (R_1, R_2 = H)

R_1 = H R_2 = Me **(derivative I)**

R_1, R_2 = Me **(derivative II)**

N-methyltyrosine
(R = CH_3)

tyrosine
(R = H)

4-hydroxy-benzoic acid
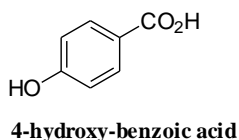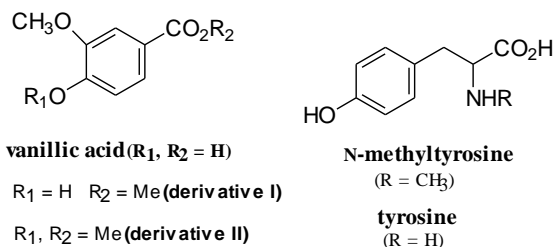
FIGURE 4.4
Chemical structure of phenolic acids from the aqueous methanol extract of *Croton cajucara* Benth.
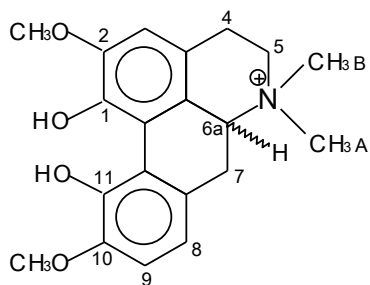
FIGURE 4.5
Chemical structure of the alkaloid magnoflorine obtained from AF fraction.
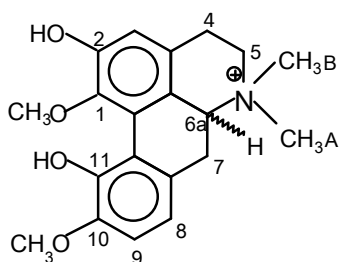
FIGURE 4.6
Chemical structure of the alkaloid N,N-dimethyl-lindicarpine obtained from AF fraction.

The microemulsion system MES-SCO was obtained from the titration methodology and mass fractions in pseudoternary phase diagram containing saponified coconut oil (SCO) in lower concentration as surfactant and butan-1-ol as cosurfactant (C/S=1) showed a large microemulsion region (Figure 4.7). The quinoline alkaloid fraction AF loaded in MES-SCO resulted in a MES-AF formulation which was evaluated in the presence of carbon steel AISI 1020, in saline medium.
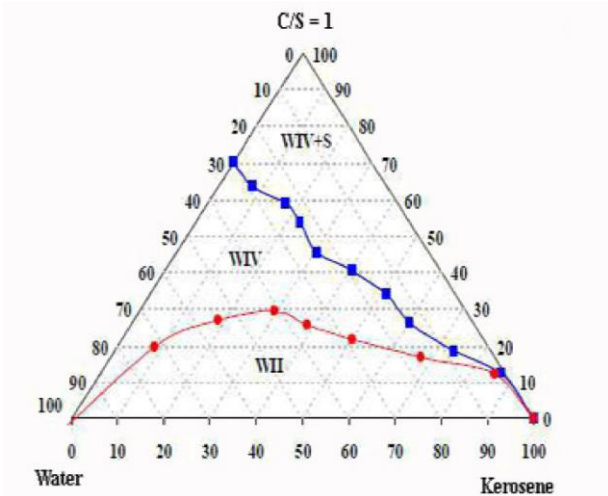
FIGURE 4.7
Schematically representation of MES-SCO system.

The effective solubilization of the alkaloidal fraction (AF) in the microemulsion system (MES-SCO) was evaluated by measurement of absorbance in ultraviolet region, being observed that volume of 1 mL of MES-SCO dissolved 10.50 mg of AF fraction. Surface tension measurements of MES-AF were taken at constant temperature of 25 °C varying the concentration of the system in two different medium such as distilled water and saline solution (3.5 % NaCl). The Critical Micellar Concentration (CMC) was estimated in the region where the curve changed abruptly, corresponding to saturation of the surface. The CMC value calculated was 0.0148 mol/L in pure distilled water and 0.0084 mol/L in saline solution. Scattering coefficients remained constant with approximate values of 38.60 (pure water) and 38.00 mN/m (saline solution) and surface tensions were plotted against small concentrations of surfactant (Figure 4.8). The observed results suggested satisfactory stability of the micellar system since the surface tension decreases with increasing concentration of MES-AF without abrupt changes in the structure of micelles after reaching the CMC.
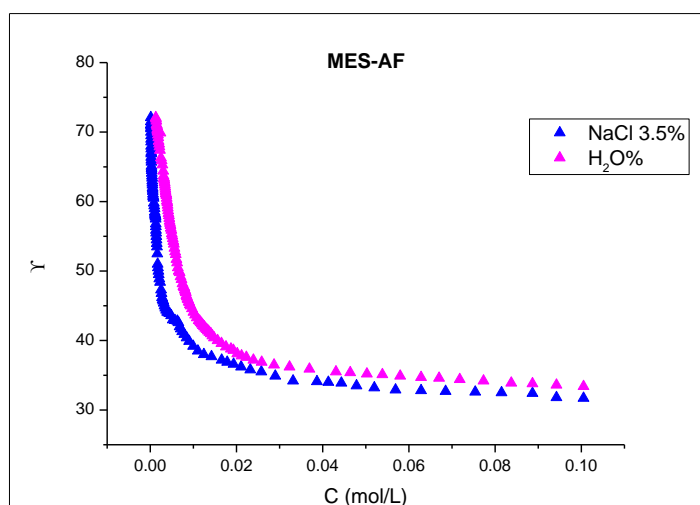
FIGURE 4.8
Surface tension of saponified coconut oil in the micellar system MES-AF in pure distilled water and saline solution.

The total antioxidant activity is a spectroscopic method for the quantitative determination of antioxidant capacity, through the formation of phosphomolybdenum complex. The assay is based on the reduction of Mo (VI) to Mo (V) by the sample analyte and subsequent formation of a green phosphate Mo (V) complex at acidic pH. Total antioxidant capacity can be calculated by the method described by Prieto *et al.* [20]. In the ranking of the antioxidant activity obtained by this method, the isoquinoline alkaloid fraction in a water solution (AF-WS) showed higher phosphomolybdenum reduction, followed by MES-AF and MES-SCO as shown in Figure 4.9. This study reveals that the antioxidant activity of the alkaloid mixture presented in the AF fraction, increase with the increasing concentration of AF regardless of the type of solution, which is 0.2 mg/mL (200 µg/mL) for AF-WS. Therefore, AF solubility evaluation on MES-SCO was of limited solubility 10 mg of AF/1 mL of MES-SCO affording the tested MES-AF formulation applied in the corrosion experiments. Water dilution of MES-AF resulted in 2.06 µg/mL of the load AF. For the antioxidant analysis MES-AF showed poor efficiency as evidenced in Figure 4.9.
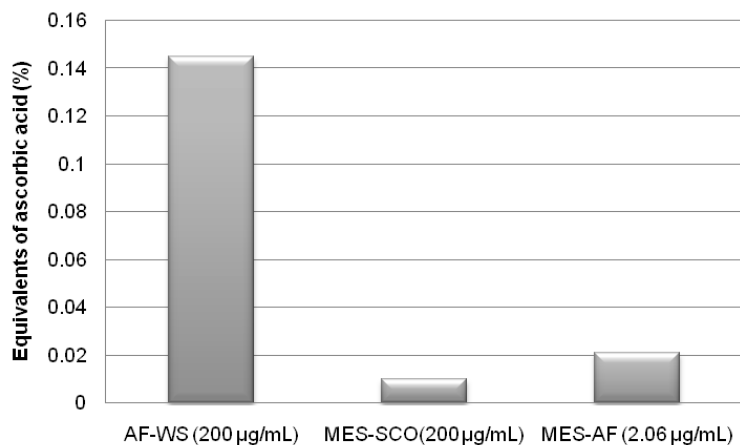
FIGURE 4.9
Antioxidant activity of AF expressed as the number of equivalents of ascorbic acid.

Previously, we investigated the effectiveness of the hydroalcoholic extract of the plant species *Croton cajucara* (CC) dissolved in the microemulsion system MES-SCO (reported as MES-CC) as well as dissolved in DMSO, as corrosion inhibitor on carbon steel AISI 1020 in saline medium. Comparatively, in that study, according to the obtained results using a potentiodynamic technique and Tafel extrapolation, the maximum inhibition efficiencies were observed for plant extract loaded in MES-SCO (93.84 %) with predominant control of cathodic reaction [4].

Generally, a specific inhibitor is classified as effective when electric current that flows in a given specific system is significantly reduced [1-5,9]. In the present work, Figure 4.10 shows the polarization curves for carbon steel in NaCl 3.5 % in the absence or in the presence of AF loaded in the microemulsion formulation MES-SCO (named MES-AF). The observed results showed that MES-AF systems (AF loaded in different concentrations) presented displacement of the corrosion potential for positive values which is correlated with concentration increases of AF dissolved in the microemulsion system MES-SCO.

The corrosion inhibition efficiency (IE%) was obtained from extrapolation of Tafel region (Table 4.2). The increase in concentration for the system evaluated (MES-AF) caused a reduction in current densities, indicating that the inhibitor are acting on the steel surface, slowing down the corrosion process. Conclusively, corrosion rates calculated proved MES-AF as effective in inhibiting corrosion of mild steel in brine (maximum efficiency 92.20 %).

Generally, the application of organic and inorganic corrosion inhibitors is one of the most common practices for the protection of steel structures and their alloys in industry. Inhibitors are mostly organic compounds rich in nitrogen, sulfur and oxygen atoms, and aromatic type-compounds [1-5,9]. Plant extracts rich in alkaloids, phenolic substance, terpenoids, or biomolecules (carbohydrates, lipids and proteins) also act as corrosion inhibitors [11]. Considering the chemical structures of these components, the effect of MES-AF in corrosion inhibition may result from AF as well as a synergistic effect of the MES-SCO.
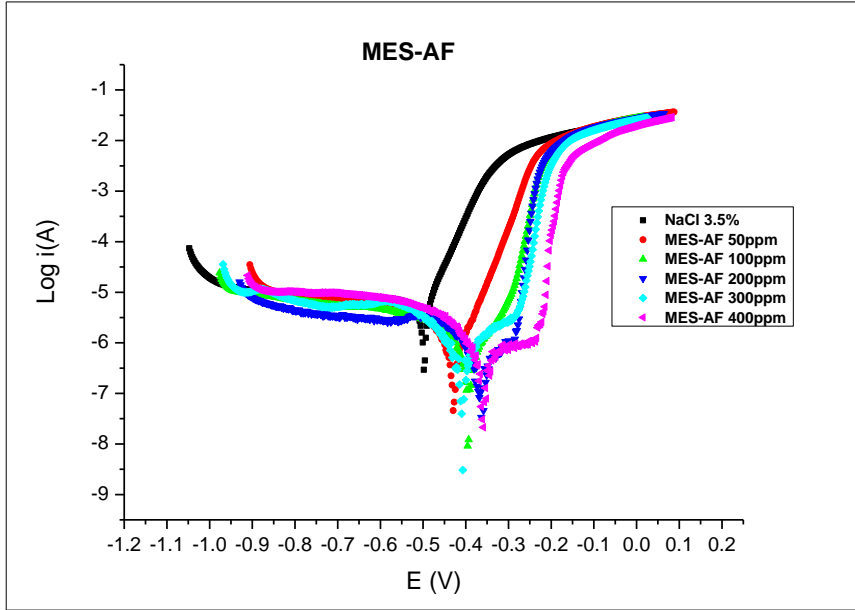
FIGURE 4.10
Tafel plots for carbon steel AISI 1020 in 3.5 % NaCl solution, ranging concentrations MES-AF.

Concentration (ppm)	I_{corr} (A/cm)	IE (%)
0	2.40×10^{-5}	0
MES-AF		
50	4.18×10^{-6}	82.60
100	3.14×10^{-6}	86.92
200	3.27×10^{-6}	90.12
300	2.02×10^{-6}	91.58
400	1.87×10^{-6}	92.20

FIGURE 4.2
Parameters obtained from polarization curves for carbon steel AISI 1020 in saline solution containing MES-AF.

Concerning to the adsorption phenomena, isotherms were plotted in order to evaluate the adsorption behavior of the microemulsion MES-AF to the metallic surface. From isotherm equations it was possible to estimate the value of adsorption equilibrium constant (K), which leads to the calculation of the standard free energy of adsorption (ΔGads), using the equation,

$$K = \frac{1}{55.5} \times e^{-\Delta G_{ads}/RT}$$

The value of 55.5 refers to the concentration of water in mol / L, and the equilibrium constant adopted for the calculation of the ΔGads was Langmuir isotherm, since it is more consistent with the usual equilibrium constant [22]. For MES-AF, two adsorption isotherms were tested: Langmuir and Frumkin. The best fit was obtained for the Langmuir isotherm ($R^2 = 0.9993$) (Figure 4.11a), suggesting a model for the adsorption of the inhibitor adsorption phenomena on the metal surface occurs with monolayer. The heat of adsorption (ΔGads) calculated was -6.14 kJ/Mol (MES-AF), the negative value indicates that the process is exothermic and spontaneous, as well as considered a physical process since is under 20 kJ/Mol. As suggested above, inhibitor probably promotes the formation of a protective film on the metal surface acting as a barrier to the transfer of mass and charge.
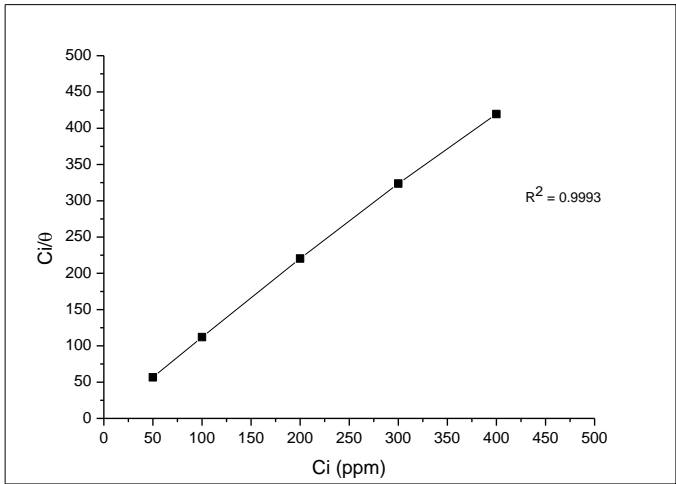
(a) Langmuir
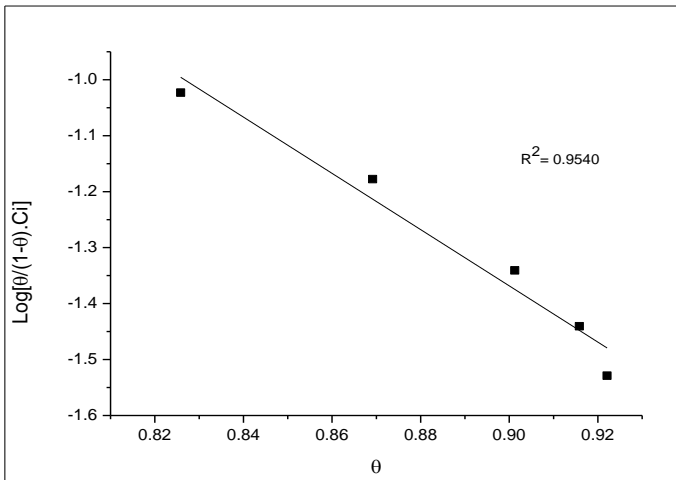
(b) Frumkin

FIGURE 4.11

Isotherms (a) Langmuir e (b) Frumkin for carbon steel at 25 ° C exposed to 3.5 % NaCl solution and MES-AF.

Concerning to the tested microorganisms, the results of the bioassays showed that the *C. cajucara* hydroalcoholic extract exhibited positive antimicrobial activity against all of the tested microorganisms, except *E. faecium* and *P. aeruginosa* cells. The Gram-negative *Chromobacterium violaceum*, and gram-positives, *Bacillus cereus* ATCC11778, and *Staphylococcus aureus* ATCC25923 were inhibited only in higher concentrations of the extract (MIC value 2.0 mg/mL) while gram-negative *E. coli* showed to be more affected when treated with lower concentration of *C. cajucara* (MIC values 0.06-0.25 mg/mL) (Table 4.3). Solvent controls results are shown on Table 4.4.

The mechanism of action of *C. cajucara* hydroalcoholic extract as an antimicrobial agent is not known. Antimicrobial agents can act by different manners, such as interfering in cell membrane wall, protein synthesis inhibition, nucleic acid synthesis blockage, metabolic pathway inhibition and others [27]. The inhibitor effect observed for CC-HE can be attributed to the presence of alkaloids and/or terpenoids in the hydroalcoholic extract mainly due to their cytotoxicity generated by interaction with cell membrane [28,29].

TABLE 4.3
Bacteria inhibition rate (%) by *C. cajucara* hydroalcoholic extract (CC-HE).

CC-HE (mg/mL)	Gram-Negative			Gram-positive		
	Ec	*Cv*	*Pa*	*Bc*	*Ef*	*Sa*
NC	0.00±0.0	0.00±0.00	0.00±0.00	0.00±0.0	0.00±0.0	0.00±0.00
0.06	67.32±3.70	6.20±2.93	n.i.	n.i.	n.i.	n.i.
0.12	51.35±9.17	7.01±0.90	n.i.	n.i.	n.i.	n.i.
0.25	55.84±2.55	12.81±2.14	n.i.	n.i.	n.i.	n.i.
0.50	48.08±6,14	12.14±3.25	n.i.	n.i.	n.i.	n.i.
1.00	49.04±3.54	24.72±2.89	n.i.	n.i.	n.i.	n.i.
2.00	50.47±2.26	72.31±6.31	n.i.	76.55±15.28	n.i.	61.32±2.04
PC	98.18±0.16	95.76±0.23	96.43±2.19	90.18±0.03	94.74±1,70	87.16±1.10

Ec, Escherichia coli, Cv, Chromobacterium violaceum, Pa, Pseudomonas aeruginosa, Bc, Bacillus cereus, Ef, Enterococcus faecium, Sa, Staphylococcus aureu.s. NC: Negative Control, PC: Positive Control , n.i.: No inhibition.

TABLE 4.4
Bacteria inhibition rate (%) by DMSO.

DMSO (mg/mL)	Gram-negative			Gram-positive		
	Ec	*Cv*	*Pa*	*Bc*	*Ef*	*Sa*
NC	0.00±0.00	0.00±0.00	0.00±0.00	0.00±0.00	0.00±0.00	0.00±0.00
0.30	n.i	7.40±2.16	n.i	n.i	8.13±2.88	4.83±4.79
0.60	n.i	9.91±1.99	n.i	n.i	13.99±3.96	3.33±0.25
1.25	n.i.	6.09±2.66	n.i.	n.i.	11.38±3.46	5.39±0.91
2.50	n.i	14.98±1.90	n.i	n.i	21.71±4.88	6.29±1.82
5.00	11.11±5.16	41.75±3.67	23.68±8.69	n.i	25.02±1.78	23.77±2.02
10.00	63.04±1.80	84.95±0.23	88.76±4.21	n.i	94.14±2.13	40.37±2.26
PC	96.93±0.18	96.31±0.34	92.97±7.01	90.73±2.83	99.52±0.20	89.36±2.52

Ec, Escherichia coli, Cv, Chromobacterium violaceum, Pa, Pseudomonas aeruginosa, Bc, Bacillus cereus, Ef, Enterococcus faecium, Sa, Staphylococcus aureu.s. NC: Negative Control, PC: Positive Control , n.i.: No inhibition.

Conclusions

The microemulsion system MES-SCO containing saponified coconut oil (SCO) as surfactant dissolved effectively the alkaloid fraction (AF) which was obtained from the stem bark of *C. cajucara* Benth, affording the load system MES-AF. The critical micelle concentration (CMC) of MES-AF occurs at low surfactant concentrations in pure distilled water, and brine (3.5 % NaCl). MES-AF showed good inhibition efficiency of 92.20 % with AF load at low concentration (0,4 mg/mL of MES-SCO). Comparatively, AF missing system (MES-SCO) showed lower efficacy (77 %). The higher efficiency observed for MES-AF may be explained by the presence of the aromatic rings and heteroatoms of the alkaloidal components with conjugated double bonds extended to methoxyl and hydroxyl groups in these organic structures, enhancing the adsorption of MES-AF. In fact, it is known that organic inhibitor molecules with N, O and S atoms as well with carge and π-electrons increases the adsorption in metal surface.

The *Croton cajucara* hydroalcoholic extract was shown to be rich in compounds containing functional eletronegative groups, aromatic rings and π-electrons in conjugated double bonds exhibited both antibacterial activity and quantitative corrosion inhibition (93.84 % with predominant control of cathodic reaction [4]).

To develop green and eco-friendly corrosion inhibitors with low cost, the green microemulsion system MES-AF containing the very cheap saponified coconut oil as surfactant and the polar fraction AF from

Croton cajucara hydroalcoholic extract, represent a promising bifunctional bioproduct against electrochemical corrosion and biocorrosion.

Reinforcing this suggestion, the polar fraction AF is a rich source alkaloid compounds (magnoflorine and N,N-dimethyl-lindicarpine) and the whole hydroalcoholic extract from the stem bark of *Croton cajucara* (from which AF was obtained) present remarkable antioxidant aromatic acids (vanillic acid, 4-hydroxy-benzoic acid and N-methyltyrosine) [23].

These results show the *Croton cajucara* polar extract load into MES-SCO to be a great biotechnological product of strong ecological importance, because the main components of MES-AF are obtained from renewable, biodegradable, easily obtainable and low cost components.

Acknowledgements

References

1. Bardal E. Corrosion and Protection. London:Springer-Verlag; 2003.
2. Gentil A. Corrosão. Rio de Janeiro: LTC Livros Técnicos e Científicos S.A; 2011.
3. Rossi CGFT, Scatena H, Maciel MAM, Dantas TNC. Comparative Effectiveness Microemulsions of Diphenylcarbazide and Saponified Coconut Oil in the Carbon Steel Corrosion Inhibition Process. Química Nova 2007; 30(5) 1128-132.
4. Felipe MBMC, Silva DR, Martinez-Huitle CA, Medeiros SRB, Maciel MAM. Effectiveness of *Croton cajucara* Benth on Corrosion Inhibition of Carbon Steel in Saline Medium. Materials and Corrosion 2013; 63 530-534.
5. Moura ECM, Souza ADN, Rossi CGFT, Silva DR, Maciel MAM. Avaliação do Potencial Anticorrosivo de Tiossemicarbazonas Solubilizadas em Microemulsão. Química Nova 2013; 36(1) 59-62.
6. Anjos GC, Almeida CC, Melo DMA, Martinez-Huitle CA, Rossi CGFT, Maciel MAM. Eficiência de *Anacardium occidentale* Linn em um Sistema Microemulsionado na Inibição a Corrosão de Aço Carbono. Revista Virtual de Química 2013; 5(4) 760-769.
7. Behpour M, Ghoreishi SM, Khayatkashani M, Soltani N. Green Approach to Corrosion Inhibition of Mild Steel in Two Acidic Solutions by the Extract of *Punica granatum* Peel and Main Constituents. Materials Chemistry and Physics 2012; 131 621-633.
8. Okafor PC, Ikpi ME, Uwah IE, Ebenso EE, Ekpe UJ, Umoren SA. Inhibitory Action of *Phyllanthus amarus* Extracts on the Corrosion of Mild Steel in Acidic Media. Corrosion Science 2008; 50(8) 2310-2317.
9. Oguzie EF. Evaluation of the Inhibitive Effect of Some Plant Extracts on the Acid Corrosion of Mild Steel. Corrosion Science 2008; 50 2993-2998. [9a] El-etre AY, Abdallah M, El-tantawy ZE. Corrosion Inhibition of Some Metals Using *Lawsonia* Extract. Corrosion Science 2005; 47 385-395. [9b] Li X, Deng S, Fu H. Adsorption and Inhibition Effect of Vanillin on Cold Rolled Steel in 3.0 M H_3PO_4. Progress in Organic Coatings 2009; 67(4) 420-426.

10. Kalaiselvi P, Chellammal S, Palanichamy S, Subramanian G. *Artemisia pallens* As Corrosion Inhibitor for Mild Steel in Hcl Medium. Materials Chemistry and Physics 2010; 120(2-3) 643-648.

11. Raja PB, Sethuraman MG. Natural Products as Corrosion Inhibition for Metals in Corrosive Media - A Review. Materials Letters 2008; 62 113-116.

12. Chen G, Zhang M, Zhao J, Zhou R, Meng Z, Zhang J. Investigation of Leave Extracts *Ginkgo biloba* as Corrosion and Oil Field Microorganism Inhibitors. Chemistry Central Journal 2013; 7(83) 1-7.

13. Felipe MBMC, Maciel MAM, Medeiros SRB, Silva DR. Aspectos Gerais Sobre Corrosão e Inibidores Vegetais. Revista Virtual de Química 2013; 5(4) 746-758.

14. Videla H; Herrera LK. Microbiologically Influenced Corrosion: Looking to the Future. International Microbiology 2005; 8 169-180.

15. Beech IB, Sunner J. Biocorrosion: Towards Understanding Interactions Between Biofilms and Metals. Current Opinion in Biotechnology 2004; 15 181-186.

16. Oguzie EE, Ogukwe CE, Ogbulie JN, Nwanebu FC, Adindu CB, Udeze IO, Oguzie KL, Eze FC. Broad Spectrum Corrosion Inhibition: Corrosion and Microbial (SRB) Growth Inhibiting Effects of *Piper guineense* Extract. Journal of Materials Science 2011; 47 3592-3601.

17. Elango A, Nandi D, Vinayagam JM, Arumugam P, Churala DS, Giri VS, Mukherjee J, Garai S, Jaisankar P. Antibacterial Activity and Anticorrosive Efficiency of Aqueous Methanolic Extract of *Artemisia pallens* (Asteraceae) and Its Major Constituent. Journal of Complementary & Integrative Medicine 2009. DOI:10.2202/1553-3840.1208.

18. Maciel MAM, Pinto AC, Brabo SN, Silva MN. Terpenoids from *Cronton cajucara*. Phytochemistry 1998; 49(3) 823-828.

19. Maciel MAM, Martins JR, Pinto AC, Kaiser CR, Esteves-Souza A, Echevarria A. Natural and Semi-Synthetic Clerodanes of *Croton cajucara* and Their Cytotoxic Effects Against Ehrlich Carcinoma And Human K562 Leukemia Cells. Journal of Brazilian Chemical Society 2007; 18(2) 391-396.

20. Prieto P, Pineda M, Aguilar M. Spectrophotometric Quantitation of Antioxidant Capacity Through the Formation of A Phosphomolybdenum Complex: Specific Application to the Determination of Vitamin E. Analytical Biochemistry 1999; 269(2) 337-341.

21. Kloucek P, Svobodova B, Polesny Z, Langrova I, Smrcek S, Kokoska L. Antimicrobial Activity of Some Medicinal Barks Used in Peruvian Amazon. Journal of Ethnopharmacology 2007; 111 427-429.

22. Cardoso SP, Reis FA, Massapust FC, Costa JD, Tebaldi LS, Araujo LFL, Silva MVA, Oliveira TS, Gomes JADP, Hollauer E. Evaluation of Common-Use Indicators as Corrosion Inhibitors. Química Nova 2005; 28(5) 756-760.

23. Maciel MAM, Pinto AC, Arruda AC, Pamplona SGSR, Vanderline FA, Lapa AJ, Echevarria A, Grynberg NF, Côlus IMS, Farias RAF, Luna Costa AM, Rao VSN. Ethnopharmacology, Phytochemistry and Pharmacology: A Successful Combination in the Study of *Croton cajucara*. Journal of Ethnopharmacology 2000; 70(1) 41-55.

24. Maciel MAM, Pinto AC, Veiga JR. VF, Echevarria A, Grynberg NF. Plantas Medicinais: A Necessidade de Estudos Multidisciplinares. Quimica Nova 2002; 25(3) 429-438.

25. Maciel MAM, Dantas TNC, Câmara JKP, Pinto AC, Veiga Junior VF, Kaiser CR, Pereira NA, Carneiro CMTS, Vanderlinde FA, Lapa AJ, Agner AR, Cólus IMS, Lima JE, Grynberg NF, Souza AE, Pissinate K, Echevarria A. Pharmacological and Biochemical Profiling of Lead Compounds From Traditional Remedies: The Case of *Croton Cajucara*, In: Mahmud Tareq Hassan Khan; Arjumand Ather. (Org.). Lead Molecules from Natural Products, Discovery and New Trends.

Lead Molecules from Natural Products, Discovery and New Trends. 2ed. Amstredan: Elsevier Sciences; 2006; 225-253.

26. Lapenda TLS, Morais WA, Almeida FJF, Ferraz MS, Lira MCB, Santos NPS, Maciel MAM, Santos-Magalhães NS. Encapsulation of *Trans*-dehydrocrotonin in Liposomes: An Enhancement of The Antitumor Activity. Journal of Biomedical Nanotechnology 2013; 9(3) 499-510.

27. Cavalieri SJ, Harbeck RJ, McCarter YS, Ortez JH, Rankin ID, Sautter RL, Sharp SE, Spiegel CA. Manual of antimicrobial susceptibility testing. American Society for Microbiology; 2005; 3-7.

28. Cowan MM. Plant Products as Antimicrobial Agents. Clinical Microbiology Reviews 1999; 12(4) 564-582.

29. González-Lamothe R, Mitchell G, Gattuso M, Diarra MS, Malouin F, Bouarab K. Plant Antimicrobial Agents and Their Effects on Plant and Human Pathogens. Internattional Journal of Molecular Science 2009; 10(8) 3400-3419.

5

Carbon nanotubes: A new biotechnological tool on the diagnosis and treatment of cancer

Benjamín Pineda[1], Norma Y. Hernández-Pedro[1], Roxana Magaña Maldonado[1], Verónica Pérez-De la Cruz[2], Julio Sotelo[1]

[1]Neuroimmunology and Neuro-Oncology Unit, Instituto Nacional de Neurología y Neurocirugía.
[2]Neurochemistry Unit, Instituto Nacional de Neurología y Neurocirugía.

Outline:

Introduction

Cancer is one of the leading causes of death worldwide. Treatment of cancer requires a careful selection of one or more intervention, such as surgery, radiotherapy, and chemotherapy. However, these standard treatments do not improve the prognosis and quality of life of patients. Nanotechnology allows highly personalized and safer medicines with the potential of improve cancer diagnosis and therapy. A wide variety of nanomaterials are under investigation, including polymeric/non-polymeric nanoparticles, dendrimers, quantum dots, carbon nanotubes, lipid- and micelle-based nanoparticles. These nanomaterials reduce toxicity associated with cancer therapy, their ability to carry and controlled deliver site-specific cytotoxic drugs as paclitaxel, docetaxel, cisplatin and multivalent-ligand targeting.

Carbon nanotubes (CNTs) have received considerable interest for diagnosis and treatment of cancer due to their minimum toxicity and biocompatibility, although CNTs are safety, they present some cytotoxic effects [1]. They represent an important group of nanomaterials with attractive geometrical, electronic and chemical properties. There are two main kinds of carbon nanotubes (CNT), single-walled nanotubes (SWNTs) consisting of a single graphite sheet seamlessly wrapped into a cylindrical tube and multiwalled nanotubes (MWNTs) comprise an array of such nanotubes that are concentrically nested like rings of a tree trunk. CNTs have been studied for intracellular delivery of proteins, peptides, drugs and fluorescence contrast agents to MRI. They are often functionalized with cationic molecules or polymers in order to interact electrostatically with negatively charged siRNAs or plasmid DNAs and also for vaccine development. The CNTs may become attached to the surfaces of biological membranes by adsorption or electro-static effects, causing damage to cells by generating reactive oxygen species, resulting in lipid peroxidation, protein denaturation, DNA damage, and ultimately cell death.

Recently, CNTs has been coupled to diverse quantum dots (QDs) and they have been used for localization of cancer cells due to their nano size and ability to penetrate individual cancer cells and high-resolution imaging derived from their narrow emission bands compared with organic dyes. The conjugation of QDs to CNTs offers the opportunity for simultaneous diagnosis and treatment of cancer. Initially they allow localization of the cancer cells by imaging with QDs, and subsequent cell killing, via drug release or thermal treatment, due to their ability to deliver drugs to a site of action or convert optical energy into thermal energy. Likewise, CNTs release substantial vibrational energy after exposure to near-infrared radiation; this produces heating localized within a tissue, which could be used as potentially phototherapy in the treatment of cancer.

In the same way, CNTs provide a versatile, biodegradable, and non-immunogenic delivery alternative to viral vectors for molecular therapy or immunotherapy and direct delivery of antigens to antigen presenting cells (APCs). Once of CNTs are delivered, they were connected to tumor proteins by formation of a covalent bond with polypeptides or formation of complexes between CNTs and tumor proteins. The CNT-tumor protein complex promotes phagocytosis of dendritic cells in the tumor tissue, the enhancing of immunogenicity is through to augment the ability of lymphocytes to attack and destroy the tumor.

CNTs have been diversely modified to improve or increase their effect under cancer cells. The preparation and attractive performance of carbon-nanotube modified glassy-carbon (CNT/GC) electrodes for improved detection of purines, nucleic acids, and DNA hybridization are described. The surface-confined MWCNT facilitates the adsorptive accumulation of the guanine nucleobase and greatly enhances its oxidation signal.

Even though CNTs have emerged as important in the treatment of cancer, their cytotoxicity has limited their use. *In vitro* studies have shown that CNT have many toxic effects, including decreased cell viability, induction of apoptosis, disruption of the cell cycle, generation of oxidative stress and inflammatory responses. CNT can damage the respiratory system of mice by entering the alveolar space, causing a chronic inflammatory reaction characterized by intermittent granulomatous lung tissue and finally pulmonary fibrosis, with significantly greater toxicity than ordinary carbon black. CNT distribute throughout the body via the circulatory and lymphatic systems in mice; therefore, their toxicity is not limited to the site of administration. It is possible that CNT have toxic effects in several organ systems. Moreover, it has been confirmed that CNT pass through the blood-brain barrier into the central nervous system in mice, and neuronal apoptosis due to peroxide-induced inflammation and oxidative stress in stimulated neurons and glial cells has been observed.

This chapter is focus on the application of carbon nanotubes in diagnosis and therapy that are under preclinical and clinical trials and the new possibilities to use them on the diagnostics and prognosis of cancer patients. We also discuss the possible challenges that have to be resolved before the establishment of used nanomedicine in cancer.

Carbon nanotubes characteristics

Nanotubes have the simplest chemical composition and atomic bonding configuration but exhibit perhaps the most extreme diversity and richness among nanomaterials in structures and structure-property relations. Carbon nanotubes (CNT) consist of graphene sheets rolled up into a cylindrical shape with a high aspect ratio and a diameter in the nano-scale range. CNT are classified by their structure into two main types: single-walled carbon nano-tubes (SWNT) and multiwalled carbon nanotubes (MWNT) [2].

The SWNTs are characterized by strong covalent bonding, a unique one dimensional structure, and nanometer size of 0.4–2 nm; which impart unusual properties to the nanotubes including exceptionally high tensile strength, high resilience, electronic properties ranging from metallic to semiconducting, high current carrying capacity, and high thermal conductivity [2]. MWNT comprise multiple layers of concentric cylinders with the space from 2–100 nm (Meziani and Sun 2003). Nonetheless, MWNTs exhibit advantages over SWNTs, such as ease of mass production, low product cost per unit, and enhanced thermal and chemical stability. In general, the electrical and mechanical properties of SWNTs can change when functionalized, due to the structural defects occurred by C=C bond breakages during chemical processes. However, intrinsic properties of carbon nanotubes can be preserved by the surface modification of MWNTs, where the outer wall of MWNTs is exposed to chemical modifiers.

CNT can be differentiated in two zones: the tips and the sidewalls. The tips are reminiscent of the structure of a fullerene hemisphere and are relatively reactive [3]. The sidewalls can be approximately considered as curved graphite, the degree of curvature, of course, depending on the diameter of the tube [2]. The length of MWCNTs varies greatly depending on their application. The concentric nanotube layers are held together by secondary Van der Waals forces. The walls of each layer of MWCNTs lie parallel to their central axis [4] CNTs are available in diverse structural designs and various electron arrangements; due to these structural differences, SWCNT and MWCNT tend to exhibit different physical properties.

Functionalization
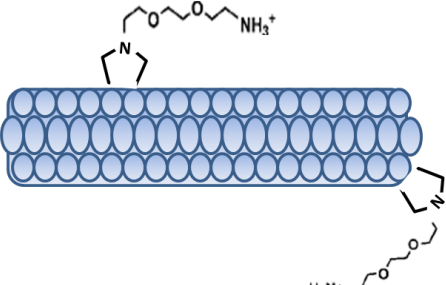
Functionalized CNT are highly promising as novel delivery systems especially based on their ability to cross biological barriers independently of the cell type. Generally, the functionalization require organic solvent or water-solubilization, enhancement of functionality, dispersion and compatibility or lowering the toxicity of CNT also, the process involves functional groups to carry simultaneously several moieties for targeting, imaging, and therapy.
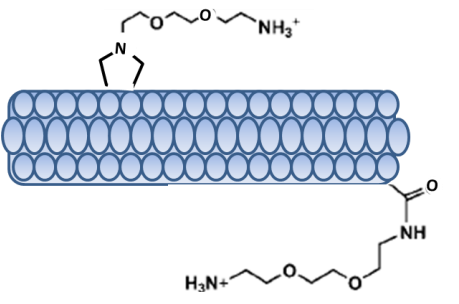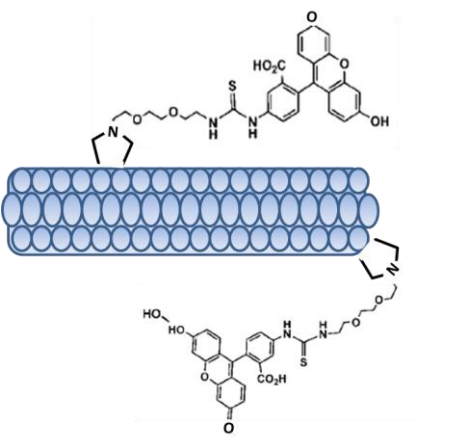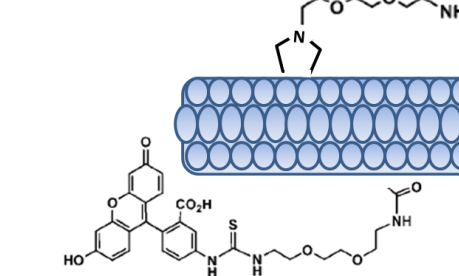
The attachment may be achieved via covalent or non-covalent bonding. Non-covalent functionalization has the advantage that it results in the preservation of the electronic structure of the nanotube atomic and it not cause noticeable toxicity when animals were treated [5, 6]. Poly ethylene glycol (PEG) is the most adopted species for functionalization, which increases the dispersity in aqueous solution and biocompatibility of CNTs. Adding PEG also allows for modification of the CNT with different functional groups such as terminal amine (PEG-NH2) and carboxyl (PEGCOOH) groups that offer further new functionalization sites for biomolecules [7, 8].
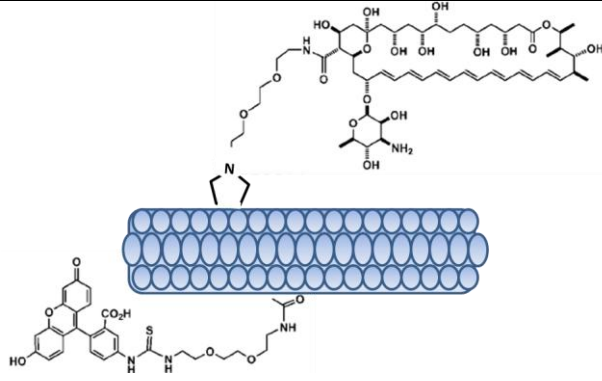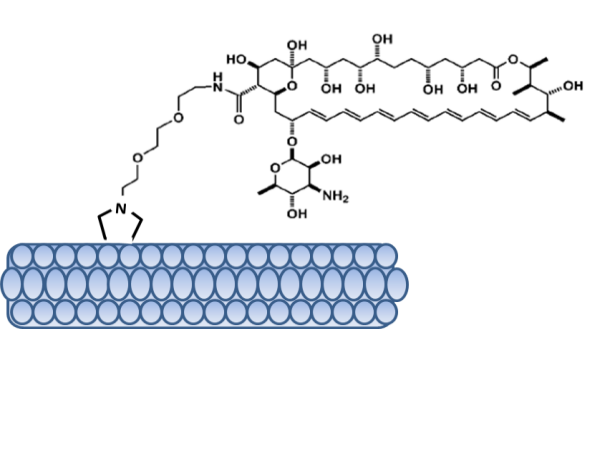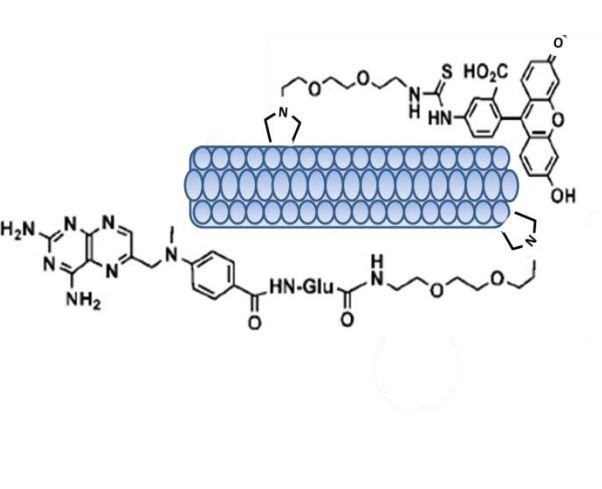
Functionalized SWNTs are attracting increasing attention as new vectors for the delivery of therapeutic molecules. Oxidized SWNTs can be functionalized at their carboxylic groups with proteins [9] peptide [10], nucleic acid [11], oligonucleotide [12], sugar moieties [13] and poly oxide derivatives [14].

Some studies show that ammonium-functionalized CNTs (f-CNTs) are able to associate with plasmid DNA through electrostatic interactions. Upon interaction with mammalian cells, these f-CNTs penetrate the cell membranes and are taken up into the cells. The nanotubes exhibit low cytotoxicity and f-CNT-associated plasmid DNA is delivered to cells efficiently; gene expression levels up to 10 times higher than those achieved with DNA alone were observed [10]. Although some of them are under *in vivo* and *in vitro* investigations, it could be a standard nano-treatment.

Carbon nanotubes were covalently modified by using a method based on the 1,3-dipolar cycloaddition of azomethine ylides. Both single-walled and multi-walled carbon nanotubes (SWNTs and MWNTs) were functionalized with a pyrrolidine ring bearing a free amino-terminal oligoethylene glycol moiety attached to the nitrogen atom. This modifications allow that the CNT are capable of traversing the plasma membrane and promoting the cellular uptake of small molecules and macromolecules (e.g. nucleic acids and peptides) [15].

Compounds	Bioassays
	Cell internalization [68-70]
	Intracelular trafficking([68-70]
	Cell viability [68]
	Plasmid DNA delivery [70, 71]

	Precursor for the praparation of CNT (4) and (5)
	Cell internalization [15, 69, 72] Intracellullar trafficking [15, 69, 72] Cell viability [15, 69, 72]
	Cell internalization [69].

	Cell internalization [69, 73] Cell viability [73]
	Antibiotic delivery [73]
	Cell internalization [74] Cell viability [74] Anticancer delivery [74]

	Immunogenic activity [75, 76]
	Immunogenic activity[76]
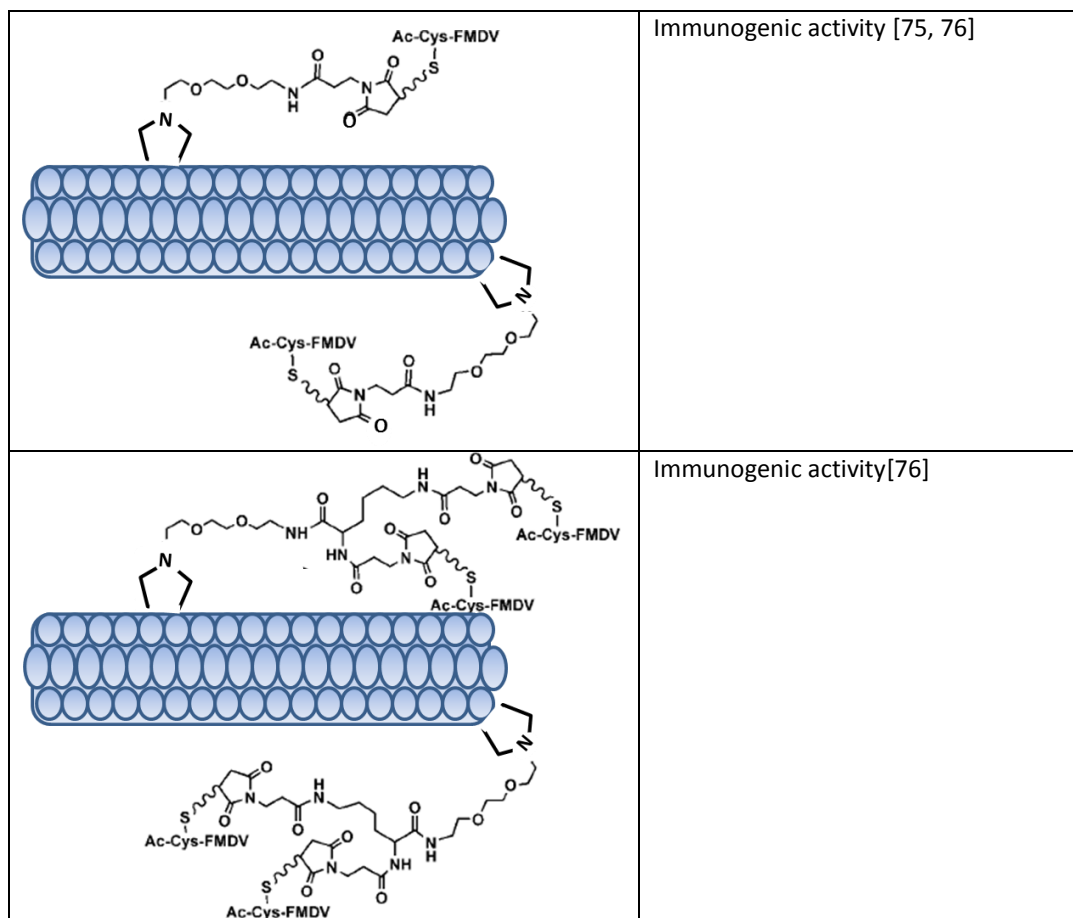
FIGURE 5.1
Molecular structures of the carbon nanotubes conjugated with different therapeutic agents. The different components that can be used during the synthesis and the diverse biological assays according to their structural properties are show. The table was taken and modified by [67].

Other modification to functionalized CNT has been developed, such as novel *in situ* atom transfer radical polymerization (ATRP) to functionalize multiwalled MWNT. The living ATRP approach displays at least three merits: (1) both styrene and acrylate/acrylamide monomers can be directly used as the raw materials; (2) the initiating sites in the reaction system remain constant after the graft polymerization and purification of the products, so it is convenient to further perform block copolymerization and chain extension; and (3) it presents an access to prepare the polymers with a functional group in each repeating unit such as poly-(hydroxyethyl methacrylate)[16]

Carbon nanotubes on diagnosis

In the imaging field, the development of nanoparticles as contrast agents has enabled detailed cellular and molecular imaging, monitoring drug delivery specifically to tumoral areas to be carried out, and providing data for efficient surgical removal of solid tumors [17]. CNTs as emerging drug and imaging carrier systems show significant versatility. One of the extraordinary characteristics of CNTs as Magnetic Resonance Imaging (MRI) contrasting agent is the extremely large proton relaxivities when loaded with gadolinium ion (Gdn3+) clusters. MRI is a widely accepted modality for providing anatomical information and high spatial-resolution anatomic images primarily based on contrast derived from the tissue-relaxation parameters T(1)- and T(2)∗-weighted sequences[18]. Sitharaman et al. developed the first CNT-based contrast agent. They demonstrated that Gd@Ultra-short single-walled carbon nanotubes (gadonanotubes) drastically increase MRI efficacy compared to the traditional CAs [19]. However, the most challenging part of using CNTs in biological system is lack of solubility and hence its toxicity. Even though oxidation of CNTs improve their dispersibility, but it`s still not enough to call them as a suitable carriers. To overcome these disadvantages the gadonanotubes have been modified on their surface; addition of polyethylene glycol to this complex could improve its solubility, stability and more over MRI contrasting ability [20].

Clinically their main application is for imaging cancer cells,[21] they can be used for localization of cancer cells due to their nano size and ability to penetrate individual cancer cells and high-resolution imaging derived from their narrow emission bands compared with organic dyes.

Immunosensors

Immunosensors are a novel amplification strategy for SWNT and applications to the detection of a cancer biomarker in real biomedical samples. SWNT immunosensors can be adapted easily for the detection of other relevant biomarkers and have the potential for fabrication into arrays to facilitate multiplexed detection with very high sensitivity and selectivity [22].
Xin Yu et col. in 2006 reported the combination of electrochemical immunosensors using SWNT forest platforms with multi-label secondary antibody-nanotube bioconjugates for highly sensitive detection of a cancer biomarker in serum and tissue lysates. They used bioconjugates featuring horseradish peroxidase (HRP) labels and secondary antibodies (Ab2) linked to CNT at high HRP/Ab2 ratio. SWNT immunosensors were capable of sensitive quantitative measurement and it has an excellent correlation results obtained in two different ways for prostate specific antigen (PSA) in human serum samples with standard ELISA results[22].
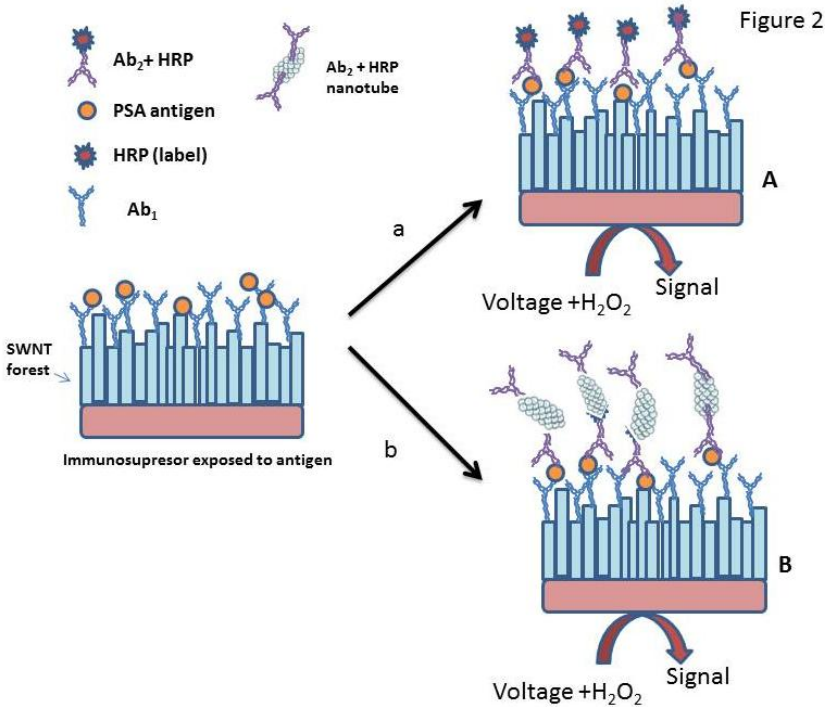
FIGURE 5.2
The components of Immunosensors. The SWNT forest serves as the immunosensor platform that it has been equilibrated with an antigen along with the biomaterials used for fabrication (HRP is the enzyme label). Primary antibody on the SWNT sensor binds antigen in the sample, which in turn, binds a peroxidase-labeled antibody (Scheme 1A), shows the imunosensor after treating with a conventional HRP-Ab2 providing one label per binding event, while section B shows the immunosensor after treating with HRP-CNT-Ab2 to obtain amplification by providing numerous enzyme labels per binding event. The final detection involves immersing the immunosensor after secondary antibody attachment into a buffer containing mediator in an electrochemical cell, applying voltage, and injecting a small amount of hydrogen peroxide. Amperometric signals are developed by adding small amounts of hydrogen peroxide to a solution bathing the sensor to activate the peroxidase electrochemical cycle, and measuring the current for catalytic peroxide reduction while the sensor is under a constant voltage. Taken and modified by [22].

Carbon nanotubes acopled to quantum dots

CNTs offer the potential for drug delivery and thermal treatment of tumors whilst QDs offer the potential for tumor imaging. QDs are semiconductor nanocrystals constituted by inorganic nanomaterials in range from 1–10 nm. They contain elements found in groups II–IV (eg, CdSe, CdTe, CdS, and ZnSe) or III–V (eg, InP and InAs) of the periodic table [23]. They have fluorescent properties which offer superior features to conventional organic dyes including high quantum yield,[24] broad absorption, narrow emission spectra, photostability of coated QDs against photobleaching and tolerance to changes in the pH of biological electrolytes [25].
QDs consist of an inorganic core, an inorganic shell and aqueous organic coating. The size of the inorganic core determines the wavelength (color) of light emitted following excitation. An inorganic core consisting of group III–V elements is preferable for clinical work in comparison to group II–IV

elements. This is mainly due to the higher stability and lower toxicity of the group III–V elements, the stability of these is known to be due to the presence of covalent rather than ionic bonding [26], but one of the main disadvantages of group III–V is its low quantum yield in comparison to group II–VI [27]. These nanomaterial properties offer the opportunity for QDs to be engineered allowing particle size, shape, and chemical composition to be used simultaneously in diagnosis and treatment of cancer. Two properties that are often manipulated are the size and composition of QDs; this will determine whether the QD is chemically excited in ultraviolet (UV) or NIR light. For example, nanocrystals of 2-nm size, comprising CdSe, emit light in the range 495–515 nm, whereas larger CdSe nanocrystals of 5-nm size emit light in the range 605–630 nm. The inorganic shell is responsible for increasing the photostability and luminescent properties of the QDs and the aqueous organic coating is used for conjugation of biomolecules to the QD surface [28] The photo stability of the inorganic shell has allowed QDs to be used as probes for imaging cells and tissues over long time periods.
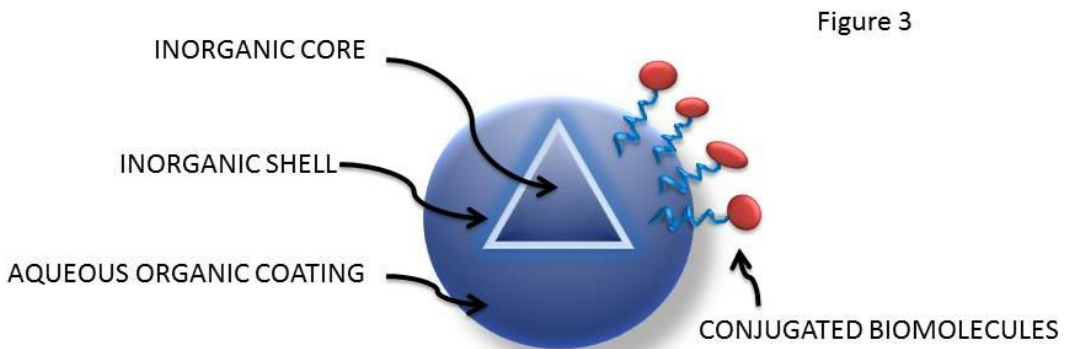
FIGURE 5.3.
Schematic diagram of quantum dots (QD) structure, QD consist in an inorganic core, and inorganic shell and aqueous organic coating.

Bimolecular coatings such as the attachment of antibodies enable the delivery of QDs to a specific organ or another site of action. The choice of antibody is important as antibody size may increase the overall size of the quantum dot to between 5–30 nm [29]

QDs have been shown to accumulate at disease sites and appear as bright and easily detected stains after illumination, which allows the location of diseased tissue to be identified [26, 30].
CNTs can destroy cancer cells via thermal ablation and functions as a tool for drug-delivery platforms [31]. Labeling CNTs with fluorescence materials such as QDs enables researchers to track the movement of CNTs [32].
The QDs may be linked to the CNT surface by either direct attachment or an intermediate molecule such as a polymer that has previously been conjugated to either the CNT or the QD. In covalent bonding, a linker between the functional group of the CNTs and QDs is needed [33]. Pre-functionalization of the surface of the CNTs with a polymer-wrapping technique may prove helpful. In this approach, the QDs form bonds with a polymer that coats the CNT side wall. Such a method may also prevent the CNT side wall from invasive damage and defects and also ensures stability of the QDs on the CNT.
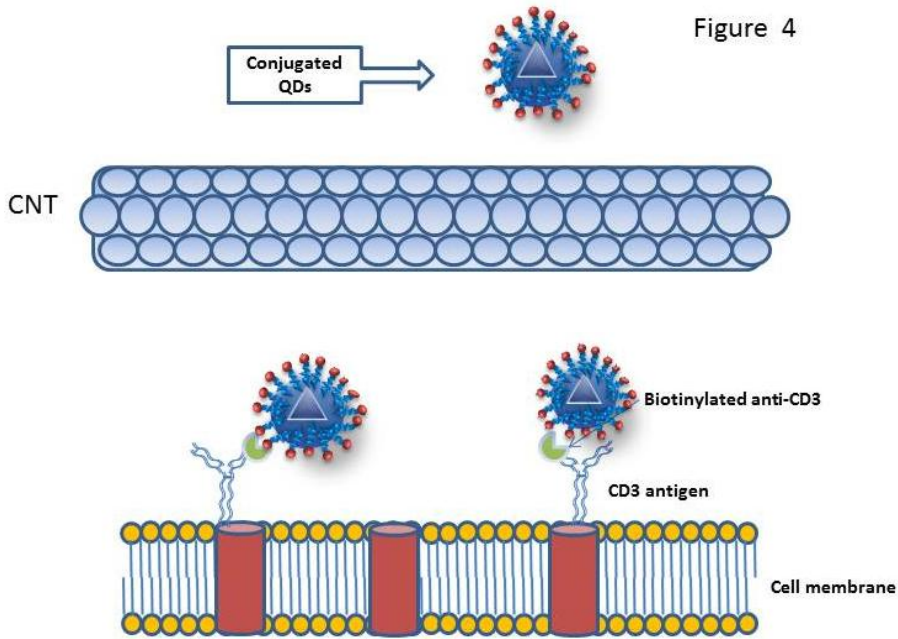
FIGURE 5.4
CNTs coupled with QDs. Bimolecular coatings such as the attachment of antibodies enable the delivery of QDs to a specific organ or another site of action. The choice of antibody is important as antibody size may increase the overall size of the quantum dot to between 5–30 nm. The image shows an example of the interaction between CD3 receptors on the Jurkat T leukemia cell membranes and a CNT-QD nanoassembly. A biotinylated anti-CD3 monoclonal antibody was used to link CD3 to the nanoassembly Taken and modified by[32]**.**

The QD-CNT complex has applications in biomedical sciences, they been used in the optoelectronic and biosensor fields. These complexes due to the electrochemical luminescent properties have one of the major applications on intracellular fluorescent imaging. Furthermore, QD-CNT complexes can also function as biosensors and biological nanoprobes as well as tools for drug delivery into cells [34]. Combining QDs to CNTs may enable the CNT to be located to particular cell types and has been shown not to be a barrier to penetration into inaccessible tumor sites. By attaching different QDs to CNTs containing different drugs, the delivery of drugs to cancer cells could be monitored, which allows the efficacy of treatments to be evaluated [32, 35].

Drugs released

To improve the target of the drug-loaded CNTs to the site of action, the surface of these materials need to be modified, preferably with an antibody or a peptide.
Studies about biodistribution of the lipid-polymer polyethylene glycol (PL-PEG) functionalized CNT showed that CNT is safe because it can be excreted via the biliary and renal pathways after intravenous injection and it does not cause noticeable toxicity in the treated animals [39]. More importantly, a high tumor accumulation of PL-PEG functionalized SWNT could be achieved by conjugation of targeting ligands to SWNT. In recent years, SWNT have been encapsulating such as drug-loaded CNT into artificial cells for targeted delivery [40]. The polymeric membrane of artificial cells could prevent drug degradation from the harsh gastrointestinal environment in the route of oral delivery, and the surface

of artificial cells could be engineered for the targeted delivery. Also it has been incorporated pro-angiogenic genes functionalized CNT into stents for efficient gene therapy [41].

On the other hand, since the number of folic acid receptors on the surface of the cancer cells increases, the presence of folic acid on CNT allows the tubes to be used to target cancer cells and enhance drug delivery [35]. CNTs loaded with the anticancer drugs are injected into the circulation so that the antibody on the surface of the CNTs would direct these materials to the site of action. The drugs contained within the CNT are delivered to the cells depending on stimulation factors such as a change in the pH or by an enzyme produced by the tumor that may cleave the drug molecule and release them from the nanotube [32].

Wu et al. research about to delivery an anticancer drug, 10- hydroxyl camptothecin (HCPT), by covalent attachment on the outer surface of the MWCNT. Carbon nanotubes coated with HCPT and amino group were functionalized by carboxylic group. This enhances the cell uptake of MWCNTs-HCPT and increased blood circulation with high drug accumulation to the tumor [42]. Liu et al. had conjugated paclitaxel (PTV) to branched polyethylene glycol chain on SWNTs. SWNTs-PTV conjugate exhibited higher drug accumulation, higher bioavailability, and little toxicity. Murine 4T1 breast cancer model shows suppression in tumor growth, enhanced permeation and retention. SWNTs-PTV delivery is the promising treatment for cancer therapy in the future, with higher efficacy and minimum cytotoxic effect [43].

Carbon nanotubes are capable of penetrating the cell membrane and are widely considered as potential carriers for gene or drug delivery. Since the C-C and C=C bonds in carbon nanotubes are nonpolar, functionalization is required for carbon nanotubes to interact with genes or drugs as well as to improve their biocompatibility. Huang y col. (2013) produced polyethylenimine (PEI)-functionalized single-wall (PEI-NH-SWNTs) and multiwall carbon nanotubes (PEI-NH-MWNTs) to be used as nonviral gene delivery reagents. This complex has modified such as carriers for nonviral gene delivery, as opposed to viral transfection which applies viral vectors to achieve high transfection efficiency, carbon nanotubes are often functionalized with cationic molecules or polymers in order to interact electrostatically with negatively charged siRNAs or plasmid. The chemically modified with amino groups were capable of delivering plasmid DNAs into A549, HeLa, and CHO cell lines and induced cell deaths in a dose-dependent manner but were less cytotoxic compared to pure polyethylenimine (PEI)-functionalized single-wall[44].

Recently, it has been developed conjugates bounded to small interfering RNA (SiRNA) was targeting towards breast cancer. The SWNTs facilitate the coupling of siRNA specifically targeting Murine Double Minute Clone 2 (MDM2) to form MDM2 siRNA–f-SWNTs complexes and the efficiency of siRNA carried by f-SWNTs. The results showed an increase in the uptake of SWNTs-SiRNA into the breast carcinoma Bcap-37. The siRNA-MDM2 released silence MDM2 gene, which inhibited the functions of p53, and resulted in inhibiting cell proliferation and promoting apoptosis. This novel strategy of chemical functionalization is effective carrier system and is a very advanced or significant therapy for breast cancer in the future [45].

Thermal treatment

Hyperthermia is a therapeutic procedure used to raise the temperature of a region of the body that was affected by cancer. It is administered together with other cancer treatment modalities. A synergistic interaction between heat and radiation dose as well as CNT treatments has been validated in preclinical studies. The ability of CNTs to convert near-infrared (NIR) light into heat provides an opportunity to create a new generation of immunoconjugates for cancer photo-therapy with high

performance and efficacy [46]. Hyperthermia also preferentially increases the permeability of tumor vasculature compared with normal vasculature, which can enhance the delivery of drugs into tumors. Therefore, the thermal effects generated by targeted CNTs may have important advantages.

The ability of CNTs to NIR light into heat provides an opportunity to create a new generation of immunoconjugates for cancer photo-therapy with high performance and efficacy. The use of NIR light in the 700- to 1,100-nm range for the induction of hyperthermia is particularly attractive because living tissues do not strongly absorb in this range [47]. Hence, an external NIR light source should effectively and safely penetrate normal tissue and ablate any cells to which the CNTs are attached. The generation of targeting moieties consisting of mAb-NAs attached to dispersed biotinylated CNTs. The use of biotinylated CNTs (B-CNTs) and mAb-NAs gives the flexibility to ''assemble'' the targeted CNTs by using any cell binding mAb. The one-step strategy of generating dispersed CNTs by using biotinylated polar lipids has the advantage of preventing subsequent chemical treatments that remove the polar lipids and/or destroy their optical properties. Previously studies have demonstrated that folic acid-coated CNTs could be targeted to folate receptor (FR)-positive cells and that NIR light killed the cells [48]. These CNTs were also evaluated for *in vivo* biodistribution [49], but control peptide-CNTs were not used to demonstrate specificity. Another approach for targeting CNTs to cells is to non-covalently attach monoclonal antibodies (mAbs) that can be used in photothermal therapy or imaging [50]. However, attachment of mAbs by direct adsorption on CNTs involves a potential loss of the targeting function of the mAbs [50].

CNTs are well-ordered, all carbon, hollow graphitic nanomaterials with a high aspect ratio, high surface area and ultralight weight, in addition they contain unique physical and chemical properties [51, 52] CNTs also absorb near-infrared (NIR) light, generating heat. These unique properties facilitate the use of CNTs in drug delivery and thermal treatment of cancer [53].

Antibodies conjugated to nanoparticles

Tumor-specific targeting using nanotechnology is a mainstay of increasing efficacy of antitumor drugs. One of the most significant advances in tumor targeted therapy is the surface modification of nanoparticles with monoclonal antibodies (mAbs) alone or in combination with antineoplastic drugs in cancer therapy [54]. Another important advantage of this technology is the possibility of masking the unfavorable physicochemical characteristics of the incorporated molecule. In particular, the treatment of brain tumors takes advantage of these characteristics due to efficient and specific brain delivery of the anticancer drugs [55].These different strategies can be exploited for a variety of biomedical applications such as cancer immunotherapy that manipulate the immune system for therapeutic benefits and minimize adverse effects[56].

Single-walled carbon nanotubes attached to antibodies or peptides represent another approach to targeting cancer cells. Previously studies demonstrated that neutravidin (NA)-conjugated MAbs attached to a biotinylated (B) polymer that non-covalently coated to CNTs can specifically target and kill cells *in vitro* [57]. Subsequently the MAbs were stably attached to the CNTs modifications added to mouse IgG1 anti-human CD22. The tested on human Burkitt's lymphoma cell line shown that the conjugates bound specifically to target cells and the binding remained specific even after the MAb-CNTs were incubated in mouse serum. Both results showed not significant differences in the selectivity

and killing efficiencies between non-covalently and covalently conjugates, using identical targeting MAbs, MAb-CNTs of similar dimensions[58].

Immune response

As nanovectors, CNTs have the advantage of providing a versatile, biodegradable, and nonimmunogenic delivery alternative to viral vectors for molecular therapy or immunotherapy as direct delivery of antigens to antigen presenting cells (APCs) or microglia in the central nervous system [59]. Kateb et al. evaluated the efficacy of multiwalled carbon nanotubes (MWCNTs) as potential nanovectors for delivery of macromolecules into microglia (MG) using the cell line BV2 (a microglia cell line) to determine the capacity to uptake MWCNTs by BV2 cells *in vitro*, demonstrating the ability of BV2 cells to more efficiently internalize MWCNTs as compared to glioma cells without any significant signs of cytotoxicity. They were able to visualize ingestion of MWCNTs into MG, cytotoxicity, and loading capacity of MWCNTs under normal culture conditions, suggesting that MWCNTs could be used as a novel, nontoxic, and biodegradable nanovehicles for targeted therapy in brain tumors. On the other hand, this group also analyzed the internalization of these nanotubes in an intracranial glioma model and characterized some changes in tumor cytokine production following intratumoral injection of MWCNTs in GL261 murine glioma model. Authors demonstrated that MWCNTs were preferentially detected in tumor macrophages (MPs), and to a lesser extent in MG. In addition to MG and MP, a small fraction of glioma cells, which are not typically capable of phagocytosis, also became positive for MWCNTs; FACS and quantitative RT-PCR were performed to analyze the inflammatory response and cytokine profile. A transient influx of MP was seen in both normal brain and GL261 gliomas in response to MWCNTs; whereas no significant change in cytokine expression was noted in normal group [60].They concluded that CNTs can potentially be used as a nanovector delivery system to modulate MP function in tumors.

Toxicity

Toxicity of CNTs has been evaluated in a variety of cell or animal models. The CNT attributes contribute the most to pulmonary toxicity according to metallic impurities, aggregate size and both CNT length and diameter. Some studies have evaluated toxicity induced by CNT. Subcutaneous injection of the nanotubes induced paw edema; also elicited hyperalgesic response, seen by the increase of animal paw withdrawal. The oxidized multiwalled carbon nanotubes elicit inflammatory and hyperalgesic effects associated to severe tissue damage in rats [61]. In other hand, CNT are capable to induce inflammatory fibrosis in the peritoneal cavity, as the same manner to long asbestos fibers. Besides the accumulation of CNT induce macrophages attempt to phagocytosis which can result in frustrated phagocytosis and stimulated recruitment of inflammatory cells and mesothelial cell damage, leading to chronic inflammation and granuloma development [62, 63]

Studies have shown that CNT have many toxic effects, including decreased cell viability, induction of apoptosis, disruption of the cell cycle, generation of oxidative stress, inflammatory responses, also PEG-SWCNTs may cause occasional teratogenic effects in mice beyond a threshold dose[64]. Although CNT has shown a promissory field in the area or drug delivery, and imaging, some aspect need

improved to be possible applied clinically.

Conclusions

Studies on the biological composition, administrations and adverse events of new nanomaterials suited for biomedical applications, are important for therapeutic drug delivery and the development of innovative and better treatments [65]. Furthermore, the engineering of the particle backbone structure, size, shape of the nanoparticle surface and the core itself provides yet another dimension of physical control that can be directed toward an increased strength, increased chemical specificity or heat resistance. Most polymeric nanoparticles are biodegradable and biocompatible, and have been adopted as a preferred method for drug delivery. Since nanoparticles come into direct contact with cellular membranes, their surface properties may determine the mechanism of internalization and intracellular localization [66]. They also exhibit a good potential for surface modification via chemical transformations, provide excellent pharmacokinetic control, and are suitable for the entrapment and delivery of a wide range of therapeutic agents.

The use of nanoparticles could be a good option in diagnosis and treatment of gliomas. Studies suggest that a variety of NP's can be engineered to become part of the next generation of agents delivery and specific treatment on gliomas. The use of a biocompatible system of NP's conjugates should highly reduce the toxicity and side effects of systemic drugs administration, and therefore improve the quality of life in cancer patients. However, several studies conducted largely in mice; have shown undesired side effects such as inflammatory response including substantial lung neutrophil influx and mortality at high doses. In addition, NP's may feasibly represent a useful imaging tool to diagnosis and follow-up; also, it to be used to assess/monitor efficacy of anti-angiogenic or other anti-tumour treatments, and thus improving the clinical management of brain tumours. Nevertheless, additional research is required in multifunctional NP's based drug delivery systems to overcome the problems and understand how nanoparticles interact with biological systems and the environment for effective therapy.

References

1. Muller, J., et al., *Respiratory toxicity of multi-wall carbon nanotubes.* Toxicol Appl Pharmacol, 2005. **207**(3): p. 221-31.
2. Niyogi, S., et al., *Chemistry of single-walled carbon nanotubes.* Acc Chem Res, 2002. **35**(12): p. 1105-13.
3. Tasis, D., et al., *Chemistry of carbon nanotubes.* Chem Rev, 2006. **106**(3): p. 1105-36.
4. Smart, S.K., et al., *The biocompatibility of carbon nanotubes.* Carbon, 2006. **44**(6): p. 1034-1047.
5. Chen, R.J., et al., *Noncovalent sidewall functionalization of single-walled carbon nanotubes for protein immobilization.* J Am Chem Soc, 2001. **123**(16): p. 3838-9.
6. Liu, Z., et al., *Preparation of carbon nanotube bioconjugates for biomedical applications.* Nat Protoc, 2009. **4**(9): p. 1372-82.
7. Lay, C.L., J. Liu, and Y. Liu, *Functionalized carbon nanotubes for anticancer drug delivery.* Expert Rev Med Devices, 2011. **8**(5): p. 561-6.

8.   Kidane, A.G., et al., *A novel nanocomposite polymer for development of synthetic heart valve leaflets.* Acta Biomater, 2009. **5**(7): p. 2409-17.

9.   Huang, W.J., et al., *Attaching proteins to carbon nanotubes via diimide-activated amidation.* Nano Letters, 2002. **2**(4): p. 311-314.

10. Pantarotto, D., et al., *Translocation of bioactive peptides across cell membranes by carbon nanotubes.* Chemical Communications, 2004(1): p. 16-17.

11. Williams, K.A., et al., *Nanotechnology: carbon nanotubes with DNA recognition.* Nature, 2002. **420**(6917): p. 761.

12. Nguyen, C.V., et al., *Preparation of Nucleic Acid Functionalized Carbon Nanotube Arrays.* Nano Letters, 2002. **2**(10): p. 1079-1081.

13. Pompeo, F. and D.E. Resasco, *Water Solubilization of Single-Walled Carbon Nanotubes by Functionalization with Glucosamine.* Nano Letters, 2002. **2**(4): p. 369-373.

14. Sano, M., et al., *Self-Organization of PEO-graft-Single-Walled Carbon Nanotubes in Solutions and Langmuir–Blodgett Films.* Langmuir, 2001. **17**(17): p. 5125-5128.

15. Pantarotto, D., et al., *Translocation of bioactive peptides across cell membranes by carbon nanotubes.* Chem Commun (Camb), 2004(1): p. 16-7.

16. Kong, H., C. Gao, and D. Yan, *Controlled functionalization of multiwalled carbon nanotubes by in situ atom transfer radical polymerization.* J Am Chem Soc, 2004. **126**(2): p. 412-3.

17. McCarthy, J.R. and R. Weissleder, *Multifunctional magnetic nanoparticles for targeted imaging and therapy.* Adv Drug Deliv Rev, 2008. **60**(11): p. 1241-51.

18. Liu, L., et al., *Silver nanocrystals sensitize magnetic-nanoparticle-mediated thermo-induced killing of cancer cells.* Acta Biochim Biophys Sin (Shanghai), 2011. **43**(4): p. 316-23.

19. Sitharaman, B., et al., *Superparamagnetic gadonanotubes are high-performance MRI contrast agents.* Chem Commun (Camb), 2005(31): p. 3915-7.

20. Jahanbakhsh, R., et al., *Modified Gadonanotubes as a promising novel MRI contrasting agent.* Daru, 2013. **21**(1): p. 53.

21. Ghasemi, Y., P. Peymani, and S. Afifi, *Quantum dot: magic nanoparticle for imaging, detection and targeting.* Acta Biomed, 2009. **80**(2): p. 156-65.

22. Yu, X., et al., *Carbon nanotube amplification strategies for highly sensitive immunodetection of cancer biomarkers.* J Am Chem Soc, 2006. **128**(34): p. 11199-205.

23. Mansur, H.S., *Quantum dots and nanocomposites.* Wiley Interdiscip Rev Nanomed Nanobiotechnol, 2010. **2**(2): p. 113-29.

24. Iverson, C., *Project 2000. Who's it all for?* Nurs Stand, 1991. **5**(28): p. 48.

25. Chan, W.C. and S. Nie, *Quantum dot bioconjugates for ultrasensitive nonisotopic detection.* Science, 1998. **281**(5385): p. 2016-8.

26. Bharali, D.J., et al., *Folate-receptor-mediated delivery of InP quantum dots for bioimaging using confocal and two-photon microscopy.* J Am Chem Soc, 2005. **127**(32): p. 11364-71.

27. Manna, L., et al., *Epitaxial growth and photochemical annealing of graded CdS/ZnS shells on colloidal CdSe nanorods.* J Am Chem Soc, 2002. **124**(24): p. 7136-45.

28. Tan, A., et al., *Quantum dots and carbon nanotubes in oncology: a review on emerging theranostic applications in nanomedicine.* Nanomedicine (Lond), 2011. **6**(6): p. 1101-14.

29. Jiang, W., et al., *Semiconductor quantum dots as contrast agents for whole animal imaging.* Trends Biotechnol, 2004. **22**(12): p. 607-9.

30. Dubertret, B., et al., *In vivo imaging of quantum dots encapsulated in phospholipid micelles.* Science, 2002. **298**(5599): p. 1759-62.

31. Klingeler, R., S. Hampel, and B. Buchner, *Carbon nanotube based biomedical agents for heating, temperature sensing and drug delivery.* Int J Hyperthermia, 2008. **24**(6): p. 496-505.

32. Madani, S.Y., et al., *Conjugation of quantum dots on carbon nanotubes for medical diagnosis and treatment.* Int J Nanomedicine, 2013. **8**: p. 941-50.

33. Pan, B., et al., *Covalent attachment of quantum dot on carbon nanotubes.* Chemical Physics Letters, 2006. **417**(4–6): p. 419-424.

34. Gao, X., et al., *In vivo cancer targeting and imaging with semiconductor quantum dots.* Nat Biotechnol, 2004. **22**(8): p. 969-76.

35. Xiao, Y., et al., *Anti-HER2 IgY antibody-functionalized single-walled carbon nanotubes for detection and selective destruction of breast cancer cells.* BMC Cancer, 2009. **9**: p. 351.

36. Klippstein, R. and D. Pozo, *Nanotechnology-based manipulation of dendritic cells for enhanced immunotherapy strategies.* Nanomedicine, 2010. **6**(4): p. 523-9.

37. Adams, G.P. and L.M. Weiner, *Monoclonal antibody therapy of cancer.* Nat Biotechnol, 2005. **23**(9): p. 1147-57.

38. Schrama, D., R.A. Reisfeld, and J.C. Becker, *Antibody targeted drugs as cancer therapeutics.* Nat Rev Drug Discov, 2006. **5**(2): p. 147-59.

39. Schipper, M.L., et al., *A pilot toxicology study of single-walled carbon nanotubes in a small sample of mice.* Nat Nanotechnol, 2008. **3**(4): p. 216-21.

40. Koizumi, F., et al., *Novel SN-38–Incorporating Polymeric Micelles, NK012, Eradicate Vascular Endothelial Growth Factor–Secreting Bulky Tumors.* Cancer Research, 2006. **66**(20): p. 10048-10056.

41. Lee, P.C., et al., *Targeting colorectal cancer cells with single-walled carbon nanotubes conjugated to anticancer agent SN-38 and EGFR antibody.* Biomaterials, 2013. **34**(34): p. 8756-65.

42. Wu, W., et al., *Covalently combining carbon nanotubes with anticancer agent: preparation and antitumor activity.* ACS Nano, 2009. **3**(9): p. 2740-50.

43. Liu, Z., et al., *Drug Delivery with Carbon Nanotubes for In vivo Cancer Treatment.* Cancer Research, 2008. **68**(16): p. 6652-6660.

44. Huang, Y.P., et al., *Delivery of small interfering RNAs in human cervical cancer cells by polyethylenimine-functionalized carbon nanotubes.* Nanoscale Res Lett, 2013. **8**(1): p. 267.

45. Chen, H., et al., *Functionalization of single-walled carbon nanotubes enables efficient intracellular delivery of siRNA targeting MDM2 to inhibit breast cancer cells growth.* Biomed Pharmacother, 2012. **66**(5): p. 334-8.

46. Falk, M.H. and R.D. Issels, *Hyperthermia in oncology.* Int J Hyperthermia, 2001. **17**(1): p. 1-18.

47. Weissleder, R., *A clearer vision for in vivo imaging.* Nat Biotechnol, 2001. **19**(4): p. 316-7.

48. Ning, S., et al., *Integrated molecular targeting of IGF1R and HER2 surface receptors and destruction of breast cancer cells using single wall carbon nanotubes.* Nanotechnology, 2007. **18**(31): p. 315101.

49. Liu, Z., et al., *In vivo biodistribution and highly efficient tumour targeting of carbon nanotubes in mice.* Nat Nanotechnol, 2007. **2**(1): p. 47-52.

50. Welsher, K., et al., *Selective probing and imaging of cells with single walled carbon nanotubes as near-infrared fluorescent molecules.* Nano Lett, 2008. **8**(2): p. 586-90.

51. Lay, C.L., et al., *Delivery of paclitaxel by physically loading onto poly(ethylene glycol) (PEG)-graft-carbon nanotubes for potent cancer therapeutics.* Nanotechnology, 2010. **21**(6): p. 065101.

52. Jamieson, T., et al., *Biological applications of quantum dots.* Biomaterials, 2007. **28**(31): p. 4717-32.

53. Madani, S.Y., et al., *Functionalization of single-walled carbon nanotubes and their binding to cancer cells.* Int J Nanomedicine, 2012. **7**: p. 905-14.

54. Zhang, T. and D. Herlyn, *Combination of active specific immunotherapy or adoptive antibody or lymphocyte immunotherapy with chemotherapy in the treatment of cancer.* Cancer Immunol Immunother, 2009. **58**(4): p. 475-92.

55. Kreuter, J. and S. Gelperina, *Use of nanoparticles for cerebral cancer.* Tumori, 2008. **94**(2): p. 271-7.

56. Pozo, D., *Immune-based disorders: the challenges for translational immunology.* J Cell Mol Med, 2008. **12**(4): p. 1085-6.

57. Chakravarty, P., et al., *Thermal ablation of tumor cells with antibody-functionalized single-walled carbon nanotubes.* Proc Natl Acad Sci U S A, 2008. **105**(25): p. 8697-702.

58. Marches, R., et al., *Specific thermal ablation of tumor cells using single-walled carbon nanotubes targeted by covalently-coupled monoclonal antibodies.* International Journal of Cancer, 2009. **125**(12): p. 2970-2977.

59. Salvador-Morales, C., et al., *Complement activation and protein adsorption by carbon nanotubes.* Mol Immunol, 2006. **43**(3): p. 193-201.

60. Klumpp, C., et al., *Functionalized carbon nanotubes as emerging nanovectors for the delivery of therapeutics.* Biochim Biophys Acta, 2006. **1758**(3): p. 404-12.

61. Pinto, N.V., et al., *Inflammatory and hyperalgesic effects of oxidized multi-walled carbon nanotubes in rats.* J Nanosci Nanotechnol, 2013. **13**(8): p. 5276-82.

62. Donaldson, K., et al., *Pulmonary toxicity of carbon nanotubes and asbestos - Similarities and differences.* Adv Drug Deliv Rev, 2013.

63. Snyder-Talkington, B.N., et al., *Multi-walled carbon nanotubes induce human microvascular endothelial cellular effects in an alveolar-capillary co-culture with small airway epithelial cells.* Part Fibre Toxicol, 2013. **10**: p. 35.

64. Campagnolo, L., et al., *Biodistribution and toxicity of pegylated single wall carbon nanotubes in pregnant mice.* Part Fibre Toxicol, 2013. **10**(1): p. 21.

65. Faraji, A.H. and P. Wipf, *Nanoparticles in cellular drug delivery.* Bioorg Med Chem, 2009. **17**(8): p. 2950-62.

66. Murakami, H., et al., *Preparation of poly(DL-lactide-co-glycolide) nanoparticles by modified spontaneous emulsification solvent diffusion method.* Int J Pharm, 1999. **187**(2): p. 143-52.

67. Prato, M., K. Kostarelos, and A. Bianco, *Functionalized carbon nanotubes in drug design and discovery.* Acc Chem Res, 2008. **41**(1): p. 60-8.

68. Pantarotto, D., et al., *Functionalized carbon nanotubes for plasmid DNA gene delivery.* Angew Chem Int Ed Engl, 2004. **43**(39): p. 5242-6.

69. Kostarelos, K., et al., *Cellular uptake of functionalized carbon nanotubes is independent of functional group and cell type.* Nat Nanotechnol, 2007. **2**(2): p. 108-13.

70. Lacerda, L., et al., *Intracellular Trafficking of Carbon Nanotubes by Confocal Laser Scanning Microscopy.* Advanced Materials, 2007. **19**(11): p. 1480-1484.

71. Singh, R., et al., *Binding and condensation of plasmid DNA onto functionalized carbon nanotubes: toward the construction of nanotube-based gene delivery vectors.* J Am Chem Soc, 2005. **127**(12): p. 4388-96.

72. Dumortier, H., et al., *Functionalized carbon nanotubes are non-cytotoxic and preserve the functionality of primary immune cells.* Nano Lett, 2006. **6**(7): p. 1522-8.

73. Wu, W., et al., *Targeted delivery of amphotericin B to cells by using functionalized carbon nanotubes.* Angew Chem Int Ed Engl, 2005. **44**(39): p. 6358-62.

74. Pastorin, G., et al., *Double functionalization of carbon nanotubes for multimodal drug delivery.* Chem Commun (Camb), 2006(11): p. 1182-4.

75. Pantarotto, D., et al., *Synthesis, structural characterization, and immunological properties of carbon nanotubes functionalized with peptides.* J Am Chem Soc, 2003. **125**(20): p. 6160-4.
76. Pantarotto, D., et al., *Immunization with peptide-functionalized carbon nanotubes enhances virus-specific neutralizing antibody responses.* Chem Biol, 2003. **10**(10): p. 961-6.

6

Cell chip composed of nanostructured layers for diagnosis and sensing environmental toxicity

Md. Abdul Kafi[a,b] and Jeong-Woo Choi[b, c *]

[a]Department of Microbiology and Hygiene, Bangladesh Agricultural University, Mymensigh-2202, Bangladesh
[b]Interdisciplinary Program of Integrated Biotechnology, and [c]Department of Chemical and Biomolecular Engineering, Sogang University, Seoul, 121-742, Republic of Korea
Corresponding author

Outline:

Introduction

Cell-based research has been applied in a wide variety of fields, such as pharmacology, medicine, cell biology, toxicology, basic neuroscience, and environmental monitoring. In vitro assays are popular methods for drug screening or assessment of chemical toxicity because they can monitor effects of chemicals more easily and readily than any other method, including animal-based research. It is well known that cell is a basic building block of all kinds of living organisms. Therefore, useful informations obtained from a living cell reflects information of the respective tissue, organ or even whole living organism. Hence, using cells, effects of drugs, toxins, or functional particles can be easily and accurately monitored. This is not possible in protein/DNA analysis or in animal-based tests. Many techniques incorporate optical or fluorescence methods, which may cause unwanted signal errors or variations due to light interference or photo-bleaching effects. They can cause critical errors in determining the cellular responses, whereas, the cell chip consisting of a conducting surface with a chamber for cell immobilization has been developed to improve accuracy and compatibility by detecting redox or electrical reactions via electron generation and transfer on the cell-electrode interface [1]. A variety of electrochemical sensing techniques have been developed to detect the cellular signal, such as open circuit potential at the cell/sensor interface, electric cell-substrate impedance sensing (ECIS), and electrochemical impedance spectroscopy (EIS) [2]. These electrochemical tools have been used to assess the effects of anticancer drugs, histamine toxicity, cell viability, and cell proliferation [3,4,5,6]. Each of these methods detected cellular behavior sensitively; however, they also detect voltammetric signals, which are strongly dependent on cell adhesion to electrode surfaces. These findings are very important to the field of electrical detection of cellular response because most cells anchor weakly on the artificial electrode surface due to insufficient amounts of positively charged extracellular matrix (ECM) proteins [3]. Hence, modifications of chip surfaces using cell adhesion motifs are of great interest in the fabrication of a cell-based chip.

Cellular behaviors (e.g., adhesion, migration, proliferation, and differentiation) are known to be sensitive to the bioactivity, interspacing, and density of surface RGD ligands on artificial ECM materials. Cell surface receptors play a major role in establishing links between cell and artificial surface. Several ECM proteins, such as fibronectin, collagen, laminin, and their components (RGD, PLL, etc.), possess excellent ability to immobilize cells on metal surfaces via integrin receptor-based linking [7,8]. The cell adhesion process involves complex mechanisms; however, most are related to integrin-mediated cell adhesion because integrin connects cytoskeleton to the ECM components that provide strong attachments [1,8]. Consequently, homogenously structured $C(RGD)_4$, RGD-MAP-C, and collagen produced by self-assembly techniques have been used to attach living cells to chip surfaces. The RGD motifs successfully linked the $\alpha_v\beta_3$ domain of integrin to the Au surface, but the large portion of the motif not used for cell attachment blocked electron transfer around the cell surface and decreased the sensitivity of electrochemical signals [1,3]. Therefore, the spatial organization of the integrin-specific domain of ECM components on artificial substrates has been investigated as an approach to improve cell adhesion and maintain high electrical sensitivity; the nano-scale RGD ligand patterns increased cell adhesion more effectively than monolayer peptides [1,9].

Cell-artificial surface interactions have attracted considerable attention due to the difficulty of cell immobilization on artificial surfaces whilst maintaining *in vivo*-like conditions, which is the most important factor in *in vitro* research. In this chapter the details of cell based chip fabrication for electrochemical analysis of living cell based on electrochemical dynamics at cell-electrode interface have been discussed. Cysteine terminated $C(RGD)_4$ peptide film was fabricated on a gold electrode for improving the attachment of cells [1,3,9]. The comparative efficacy of several biomaterials, such as synthetic $C(RGD)_4$, RGD-MAP-C peptide, and poly-L-lysine on cell adhesion, proliferation and

electrochemical signal transmission were studied. RGD-MAP-C provided the strongest voltammetric signals when the chip was subjected to cyclic voltammetry and differential pulse voltammetry [1]. It was also observed that nanopatterned peptides are more suitable than nonpatterned monolayers. Amongst the nanopatterned peptides three dimensional RGD nanopillars arrays were found to be more suitable than RGD nanodots and RGD nanorods [9]. Recently, a newly fabricated RGD nanopillar array was applied as a novel platform for the electrochemical determination of cell-cycle-arrest, where a cell-based chip has been employed for the assay of electrochemical redox property from cell at different phases of growth cycle [10]. In addition, phase specific cytotoxicity of BPA and PCB were analyzed using the cell-chips completely synchronized at G1/S and G2/M phase, respectively [11]. This newly developed chip-based living cell detection system can be a useful tool for diagnostic applications. The current disease diagnosis methods commonly based on conventional cell culturing process are costly, laborious and susceptible to contamination. Cell chip based methods may overcome above limitations due to their simple fabrication process and rapid detection techniques. Moreover, the accuracy and high sensitivity prove the potential of cell based chip for biological and clinical testing and disease diagnosis in the near future.

Cell-based Chip design and fabrication

Cell chip chamber design and fabrication is the first step of the cell chip based research. Size and shape of a chip chamber greatly influences the cumulative signal intensity arise from the numbers of cells cultured on it. The cell numbers vary from single to millions depending on exposure arrears of the chip. The chip designed with micro scale exposure area for cell attachment is known as microchip [12-18]. Integration of several microchips on a single silicon support has been used for obtaining cumulative signal intensities since the last decade [1,3,9-11]. Recently single chip with centimeter scale exposure area has been simply fabricated on silicon support [1,3,9-11]. According to Choi's group cell chip chamber (Lab-Tek®, Thermo fisher scientific, USA) of 2 cm × 2 cm × 0.5 cm (width × length × height) dimensions created on freshly prepared Au working electrodes with an area of 3 cm^2 is the most suitable design for appropriate electrode positioning to achieve maximum signal intensities [1,3,9-11]. In most cases chip chamber are established on a silicon based Au working electrode [3, 19]. A 50-nm thick titanium (Ti) layer is established on the silicon substrate and then a 150-nm thick gold (Au) layer patterned by DC magnetron sputtering [3,19]. The Au surface is cleaned with piranha solution previously described elsewhere [1,3-6,9]. It is then polished carefully by sonication in absolute alcohol and double-distilled water for 5 min, respectively. Finally, the electrode is electrochemically cleaned in 0.5 M H_2SO_4 until a stable cyclic voltammogram is obtained and dried with purified nitrogen [10]. To develop an adhesion molecule (AM) layer on the Au surface, a freshly cleaned Au substrate is incubated in desired concentrations of AM solution diluted in distilled water at 37^{0}C for 24 h. for the formation of cell immobilization platform [1,3, 9-11]. Finally, the substrate is washed with deionized distilled water and dried under N_2 gas. Schematic of the fabricated cell based chip is shown in figure 6.1.
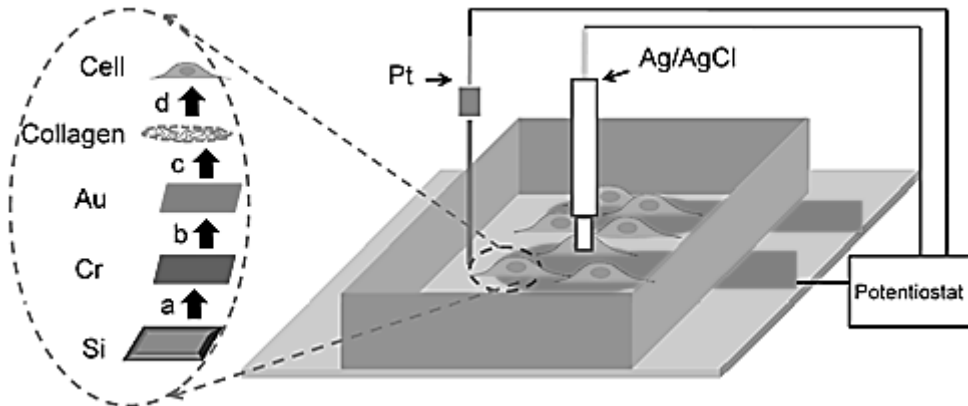
FIGURE 6.1
Schematic of a cell-chip: the dotted circle shows the steps of fabrication, (a) sputtering of 50nm titanium on silicon, (b) establishment of 150nm Au, (c) collagen coating and (d) cell seeding. Figure reproduced with permission from: ref. 42, © 2011ASP.

Establishment of Nanostructured bio-ligand molecule on chip surface

Surface engineering of a bio-platform creates materials which elicit controlled cellular adhesion and plays an important role in the transmission of intracellular signals to extracellular surfaces [2]. Some extracellular matrix (ECM) components, such as laminin, fibronectin, collagen, and their functional domains (Arg-Gly-Asp (RGD) motif) actively promote cellular adhesion via interactions with integrin receptors [20]. The specific conformation of the RGD amino acid sequence in the ECM proteins determines its specificity for different integrin subtypes [21]. Following the discovery of this RGD small active domain, numerous other adhesion peptide sequences have been isolated [22]. Some are specific to particular cell types or functions through binding to distinct integrin subtypes [23]. The RGD sequence is one of the most effective cell recognition motifs. The RGD sequence stimulates cell adhesion on artificial surfaces, involves a cascade of four overlapped reactions such as cell attachment, cell spreading, actin-skeleton formation, and focal-adhesion formation, and is important for transmitting cell signals related to cell behavior and cell cycle [24-25]. RGD peptides do not only trigger cell adhesion effectively, but can also be used to address selectively certain cell lines and elicit specific cell responses [26]. So, RGD peptides immobilized on a substrate enables cell adhesion and mimics the cellular signals [27]. Therefore, Choi`s group designed Cystein (Cys) terminated RGD tripeptide sequence for specially immobilizing on Au surface via thiol-gold (S-Au) coupling method (Figure 6.2). The designed peptides (C(RGD)$_4$ and RGD-MAP-C) were synthesized from Peptron (Korea).
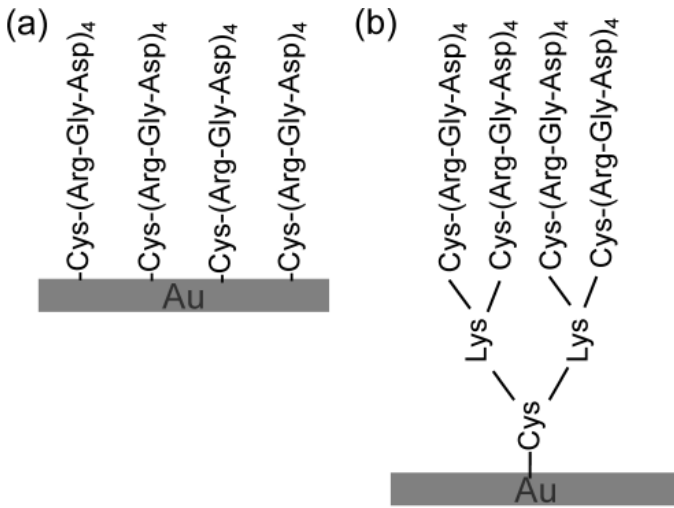
FIGURE 6.2
Schematics of the C(RGD)$_4$ (a) and RGD-MAP-C (b) peptide immobilized on Au surface. Figure reproduced with permission from: ref. 3, © 2007 Springer.

In addition to natural biomolecules and peptides, some non-native proteins/peptides have been shown to promote cell adhesion. Poly-L-lysine modulates cell adhesion via a non-receptor- mediated cell binding mechanism [11]. Positive charges on poly-L-lysine attract the negatively charged cell membrane resulting in electrostatic bond formation [11]. Prior to the PLL immobilization the Au surface is functionalized with MUA-11 self-assembled monolayer (Figure 6.3).
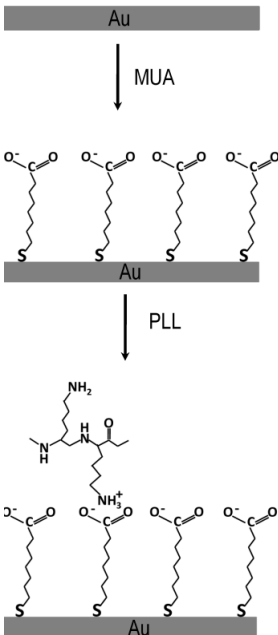
FIGURE 6.3
Immobilization of PLL on MUA functionalized Au surface. (Reproduced with permission from: ref. 11, © 2013 Elsevier).

In vitro nanoscale assembling of molecular building blocks such as nucleic acids, proteins and phospholipids, biological organisms have been used as a versatile tool in nanotechnology. In a recent study, thiol self-assembly was achieved by reacting thiol containing compounds with clean gold surfaces (Figure 6.4). Sulfhydryl groups on molecules will covalently bind to gold, thus allowing molecules to be arranged two dimensionally over a gold surface [3,19]. This is very useful since gold conducts electricity and makes for excellent electrical contacts, thus electrochemical measurements can be made on such samples. Therefore, cell adhesion molecules were mutagenically modified with cysteine residues (an amino acid containing a thiol group) [1,3,19]. Exposing a gold surface to such engineered molecules results in self-assembled monolayer's of cell adhesion molecules.

RGD peptide

Au elctrode
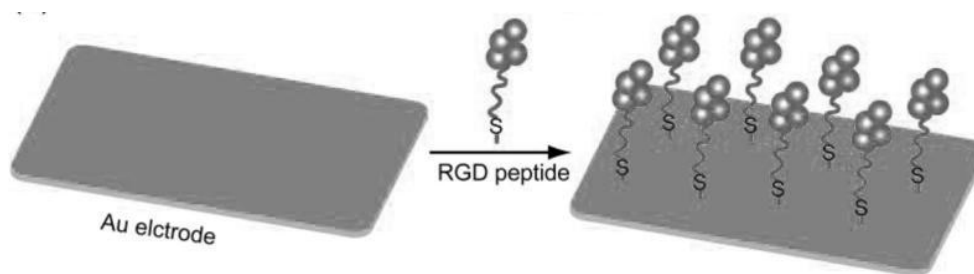
FIGURE 6.4
Self assembly of Cysteine terminated RGD peptide on Au surface. (Reproduced with permission from: ref. 43, © 2011ASP).

To develop an oligopeptide layer on the Au surface, the Au substrate was incubated in the C(RGD)$_4$ solution diluted in distilled water at 37°C for 10 hours [1,3,9,19]. Different concentrations of the C(RGD)$_4$ peptide varying from 0.05 mg/ml to 0.1 mg/ml can be applied for the formation of cell immobilization platform [6]. The optimum cell adhesion efficiency is achieved using a peptide concentration of 0.1 mg/ml [1].

In surface engineering, nano-patterned biomaterials are of great significance to enhance receptor specific coupling or trapping target molecules. In the patterned surface biomolecules are aliened according to the receptors specificity with a desired spacing. On a cell chip the adhesion molecules are nano structured according to the receptor availability on the cell surface. Therefore, cells are firmly attached to the chip surface that can withstand several washing steps during the electro analysis process. In the past decade several top down (Externally directed nanopatterning: Nanoimprint lithography, Scanning probe lithography, Atomic manipulation) and bottom up (Self-assembly) processes are employed for patterning biomolecules in a desired pattern. Self-assembly of biomaterials has become a popular method due to its simple and ease of fabrication process. Recently, Choi`s group introduced a new modification of self-assembly method, termed as Mask Guided Self Assembly Method (MGSAM) [1] (Figure 6.5). For this, a porous alumina (AAO) membrane was fabricated by a two-step anodization method, as previously described [1,9-10]. In brief, nanoporous AAO was obtained from aluminum anodized at a constant voltage of 40 V in oxalic acid solution. The alumina layer formed during the first long period of the anodization process was removed by wet etching [28]. This treatment revealed the periodic nano-concave patterned surface of the aluminum. The nano porous alumina membrane was placed on the freshly cleaned, smooth Au surface and fixed by adding a drop of acetone. Subsequently, a treatment consisting of 0.01 mg/ml of various peptides diluted with DI water was added separately on the porous AAO membrane and was maintained at 12 hours at 4^{0}C. The electrode was placed in a 2 M NaOH solution for 3 min to remove the AAO membrane form the Au

surface, followed by washing with DI water and drying under nitrogen steam (the peptide-modified electrodes are denoted as Au/C(RGD)$_4$, Au/RGD-MAP-C, and Au/PLL, respectively) [1,9].
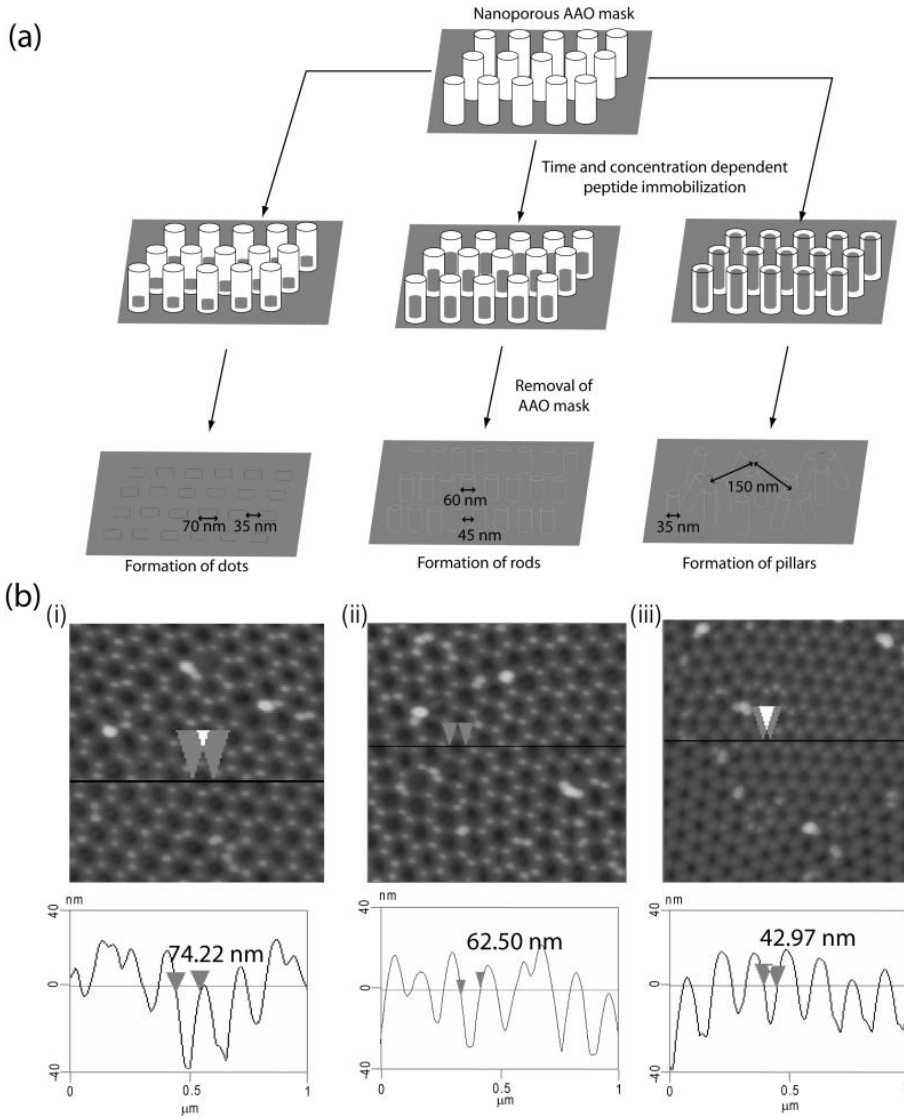
FIGURE 6.5
(a) Schematic of fabrication of various topographic RGD nanopattern, (b) AFM images of mask with varying pore size with their respective cross section analysis. (Reproduced with permission from: ref. 9, © 2012 Elsevier).

Cell immobilizations

In vitro immobilization of living cells is an important process in the fabrication of a cell-based chip [29]. The interaction between cell-cell and the adhesion of cells onto the chip surface can be a reliable candidate for cellular attachment without loss of viability. The cell adhesion process involves complex mechanisms; however, most are related to integrin-mediated cell adhesion because integrin connects cell cytoskeleton to the ECM components that provides strong attachment [30-31]. At the development of a neuronal cell chip with PC12 cells established from a rat pheochromocytoma cells, a major drawback is that the cells anchor to the chip surface weakly because of insufficient amounts of positively charged ECM proteins [32]. Modification of the chip surface with ECM proteins such as collagen was reported to enhance the attachment of the cell types [33]. However, the surface modification with the ECM proteins is not effective for measuring electrochemical signals due to the protein natures [34-35]. Choi`s group immobilized newly designed different architectures of cysteine modified RGD tri-peptide sequence (C(RGD)4, RGD-MAP-C) on gold (Au) surface using the self-assembled monolayer (SAM) technique to promote the binding of PC12 cells because the strong integrin affinity of RGD influences the binding capacity of cell immobilization.

The RGD motifs successfully linked the $\alpha v \beta 3$ domain of integrin to the Au surface [2], but the large portion of the motif that was not used for cell attachment blocked electron transfer around the cell surface and decreased the sensitivity of electrochemical signals [3]. It is well known that cellular behaviors (e.g., adhesion, migration, proliferation, and differentiation) are quite sensitive to the bioactivity, interspacing, and density of surface RGD ligands on artificial ECM materials [36-37]. Therefore, the spatial organization of the integrin-specific domain of ECM components on artificial substrates has been investigated to improve cell adhesion and maintain high electrical sensitivity; the nano-scale RGD ligand patterns increased cell adhesion more effectively than monolayer peptides [1,3,9].

Besides studies related to investigation of ECM materials to facilitate cell adhesion on the artificial surface, research regarding the fabrication of nanopatterned surfaces has been conducted to determine the influence of surface topology on cell adhesion. The spacing and height of Au nanoparticles deposited on a surface, which is subsequently coated with ECM protein, influences cell adhesion, motility, and spreading [38-39]. We recently observed that RGD peptides containing cysteine residue can be fabricated easily on Au surface (e.g., as a homogeneous nanodot array using the self-assembly technique), and promote cell adhesion without decreasing the sensitivity of electrochemical detection. Our group fabricated two types of cysteine-modified peptides, C(RGD)$_4$ and RGD-MAP-C, and PLL peptide nanodots, rods and pillars on Au surfaces via the self-assembly technique through an AAO mask [1,9]. The performance of the fabricated nanostructure was intensively evaluated with respect to the cell adhesion speed, attachment strength, spreading, cofilin phosphorylation, and mitochondrial activity. Cell functions significantly increased on the 3D-RGD-MAP-C nanopatterned surface compared to the RGD-MAP-C monolayer and nanodot surface, regardless of the cell line. Among the peptide nanostructures, nanopillar array was more suitable for cell adhesion and spreading than nanorod array due to the increased binding sites for integrin receptor on the cell surface that contribute to the formation of a strong link between the cells and Au.

FIGURE 6.5
(a) Schematic of fabrication of various topographic RGD nanopattern, (b) AFM images of mask with varying pore

Electrochemical measurements

Cell-based chips are special devices that employ living cells immobilized on a metal surface as sensing elements, combined with sensors to perform real-time bioassays dynamically and rapidly, and have numerous applications ranging from biomedicine to environmental detection [40]. It is used for detecting the cellular responses to intracellular and extracellular stimuli. Interaction between stimulus and cell recorded as electro-physiological parameters produce responses using simple electrochemical detection system [2].

The electrochemical measurements carried out with a CHI660C Potentiostat (CH Instruments). The commonly used three-electrode configuration is employed for the electrochemical measurements, while standard silver (Ag/AgCl) served as the reference and a platinum wire as the counter electrode (Figure 6.1). Prior to the electrochemical measurement cell chip electrode with living cells needs to be washed twice with a 10 mM PBS buffer (pH 7.4) containing NaCl- 0.138M and KCl -0.0027M. Finally, electrochemical measurements performed using 2 ml of same PBS as the electrolyte. Before the measurement, the buffer solution should be first bubbled thoroughly with high-purity nitrogen for 30 min. A stream of nitrogen is then blown gently across the surface of the solution in order to prevent aerobic oxygen throughout the measurement.

Voltammetric Behavior of Different Cell Lines

Cell is the basic structural and functional unit of a tissue and obviously possesses a unique functional response, which varies with the tissues from which cell line was derived. Therefore, electrochemical response from cells immobilized on chip obviously should show cell line specificity.

The rat pheochromocytoma (PC12) cells on a collagen immobilized chip showed quasi-reversible redox behavior when subjected to cyclic voltammetry analysis using a potential window -0.2V to 0.8 V at a 100 mVs^{-1} scan rate, with a anodic current peak at +75 mV and cathodic peak at + 350 mV, whereas HeLa cells originated from human endothelium gave anodic peak at -75 mV and cathodic peak at + 150 mV [Figure 6.7]. This indicates distinguishable differences in redox behavior of two kinds of cells due to the differences of their origin that agreed with our hypothesis. The difference between the potential peaks $|E_{pc}-E_{pa}|$ exceeded 100 mV and the peak current ratio $I_{pa}/I_{pc} \geq 1$, which indicated the distinct quasi-reversible characteristics of the both cell [1]. These results demonstrated the advantage of the gold electrode over low conductive metal, semiconductor or non-metal based electrodes by offering faster electron transfer kinetics.
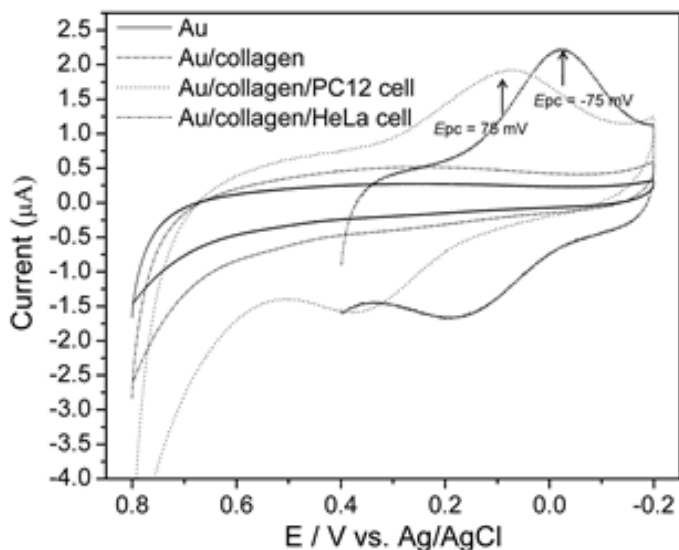
FIGURE 6.7

Redox behavior of PC12 and HeLa cell on collagen modified Au surface. CV was measured using PBS (0.01 M, pH 7.4) as electrolyte at a scan rate of 100 mVs−1 and the whole experiment was conducted at 27 ± 1°C. The experiment was repeated thrice maintaining identical condition. (Reproduced with permission from: ref. 41, © IARIA, 2011. ISBN: 978-1-61208-145-8).

The cell line specific CV signal was further confirmed by another sensitive amperometric method, differential pulse voltammetry. Considering anodic peak potential that was obtained from CV technique a potential window of -0.2 to 0.4 V was applied to measure DPV from both the cell lines at a scan rate of 100 mVs^{-1}, with 50mV pulse amplitude and 50 ms pulse width. The well distinguished DPV signal was measures from PC12 and HeLa cell. Figure 6.8 shows PC12 cell gave peaks at + 75 mV and HeLa cell at -75 mV, whereas no peaks were observed from bare Au surface indicating that peaks are certainly appears from the cells when they were immobilized on the Au electrode surfaces. Therefore, the cell line specific electrochemical signals were proved by the both of the amperometric method.
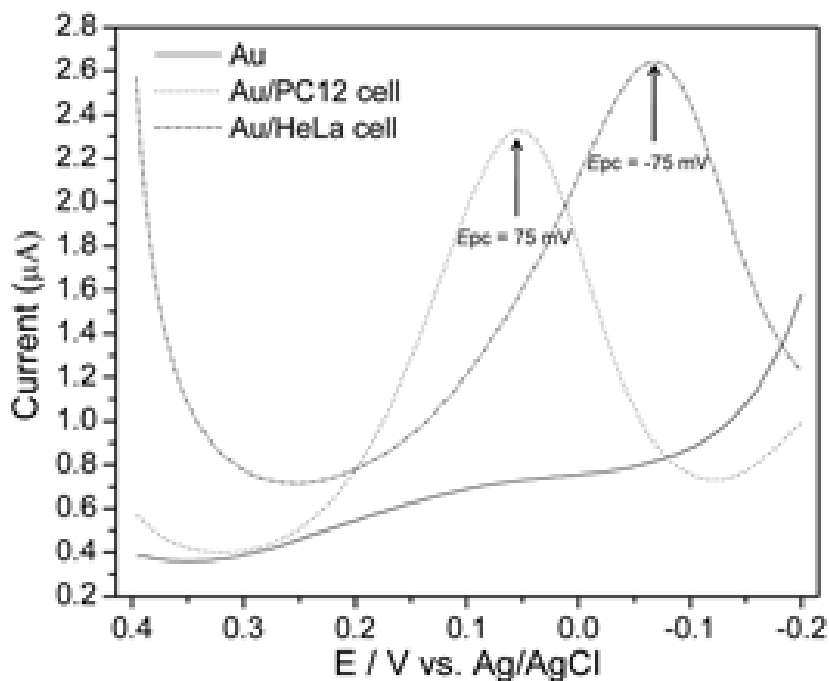
FIGURE 6.8
Differential Pulse voltammogram of PC12 and HeLa cell on collagen modified Au surface. DPV was measured using PBS (0.01 M, pH 7.4) as an electrolyte at a scan rate of 100 mVs−1. Pulse amplitude and pulse width were 50 mV and 50 ms, respectively. (Reproduced with permission from: ref. 41, © IARIA, 2011. ISBN: 978-1-61208-145-8).

Voltammetric Behavior of Different Phases of Same Cell Line

The cell immobilized electrode was treated with 2 mM thymidine in a culture medium (RPMI 1640) for 18 h, followed by a 8 h release (replaced by fresh medium) and again 2 mM thymidine for another 18 h to block cell at synthesis phase. Similarly, another cell immobilized electrode was treated initially with 2 mM thymidine as mentioned before for 18 h, followed by a 4 h release in fresh medium and then, 100 ng/ml Nocodazole was treated for another 10 h to block cell at mitosis phase. Thus, the cell chip was prepared for the measurement of electrochemical signal of the cells at the different phases of the growth cycle. A cell chip with the same number of non-treated cells served as control in parallel.
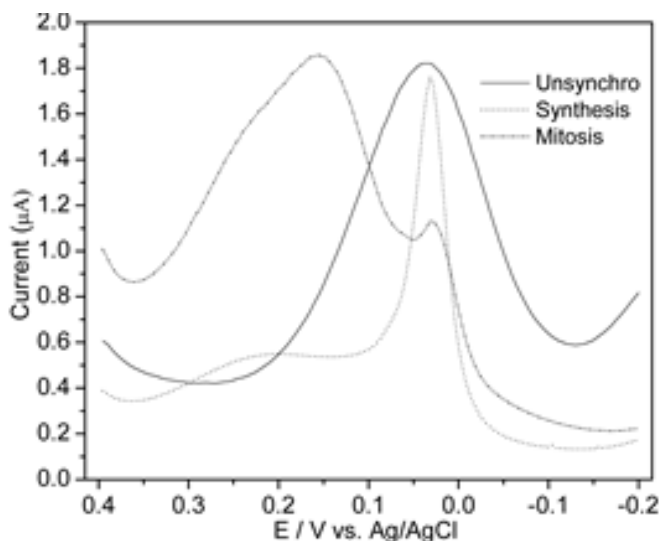
FIGURE 6.9
Differential Pulse voltammogram of PC12 cell synchronized at synthesis and mitosis phase as compared with unsynchronized (control). All the experimental condition was maintained as mentioned before. (Reproduced with permission from: ref. 41, © IARIA, 2011. ISBN: 978-1-61208-145-8).

Considering the cell line specificity of electrochemical signal we assume that same cell at different stages of its growth cycle might have different redox. During cell growth, cells pass through a number of complex processes, including prophase, prometaphase, metaphase, anaphase, and telophase, leads to several changes in the cell physiology and morphology. These cytological changes might be responsible for alterations in the electrochemical behavior of the cell. To prove this hypothesis PC12 cells synchronized at synthesis and mitotic phase of its cycle were subjected to DPV analysis. When the cells immobilized on the Au electrode were synchronized at synthesis stage, a sharp electrochemical signal appeared at +50 mV, whereas peak was observed at +150 mV when the cells were synchronized at mitotic stage during DPV measurement (Figure 6.9). Both the peaks from synchronized cells showed remarkable differences with unsynchronized cells. These differences in DPV signaling from identical cells in different phases (synthesis, mitosis) may have been due to changes in the redox properties of morphologically-altered cells [10]. Therefore, the specific DPV signals from cells in synthesis and mitosis phase which is completely different from unsynchronized cells might be useful for detection of metastatic cells of unknown origin.

Applications of cell chip for sensing environmental toxicant

Integration of living cells with metal-electrode is a novel approach that has significant advantages in tissue engineering and for studying cellular electro-physiologic states [2]. Potential uses for cell-based electrochemical systems have a wide range of applications in the field of pharmacology, medicine, cell biology, toxicology, basic neuroscience, and environmental monitoring [40]. Alteration in the cellular electro-dynamic systems gives information about the effect of a stimulus on living systems. Establishment of strong cell-substrate interaction is essential for obtaining proper functional rather than analytical information. We recently introduced cell chip technology capable of effectively

measuring changes in cell viability upon exposure to different kinds of environmental toxins [5,11] or anticancer drugs [4] based on simple and rapid electrochemical techniques. These electrical or electrochemical methods also have been incorporated into cell-based sensor arrays and electrical sensing devices for the detection of signal-frequency patterns produced by cells in growth media [40]. These whole cell-sensing systems employ sensor cells whose electro physiologic state varies upon exposure to toxic substances. The toxin treated cells produce readily measurable differences in signal intensities that used as new tools for cell viability assay [5]. These whole-cell sensing systems can be visualized as an environmental switch that is turned on in the presence of toxins or stressful conditions. In a recent study, HEK-293 cells seeded on a peptide coated Au surface and allowed culture medium containing different concentrations of bisphenol-A (BPA) and dichlorodiphenyltrichloroethane (DDT) were subjected to electrochemical measurement [6]. Figure 6.10a shows reduction peak current (I_{pc}) were decreased linearly at the concentration of BPA from 0 to 7.5 µM (Fig. 10b). The effect of DDT on CV response of HEK-293 cells also showed similar results to (Figure 6.10c). Figure 6.10d showed a significant negative linear correlation between DDT concentration and I_{pc}, indicating decreasing viability and proliferation of the HEK-293 cells.
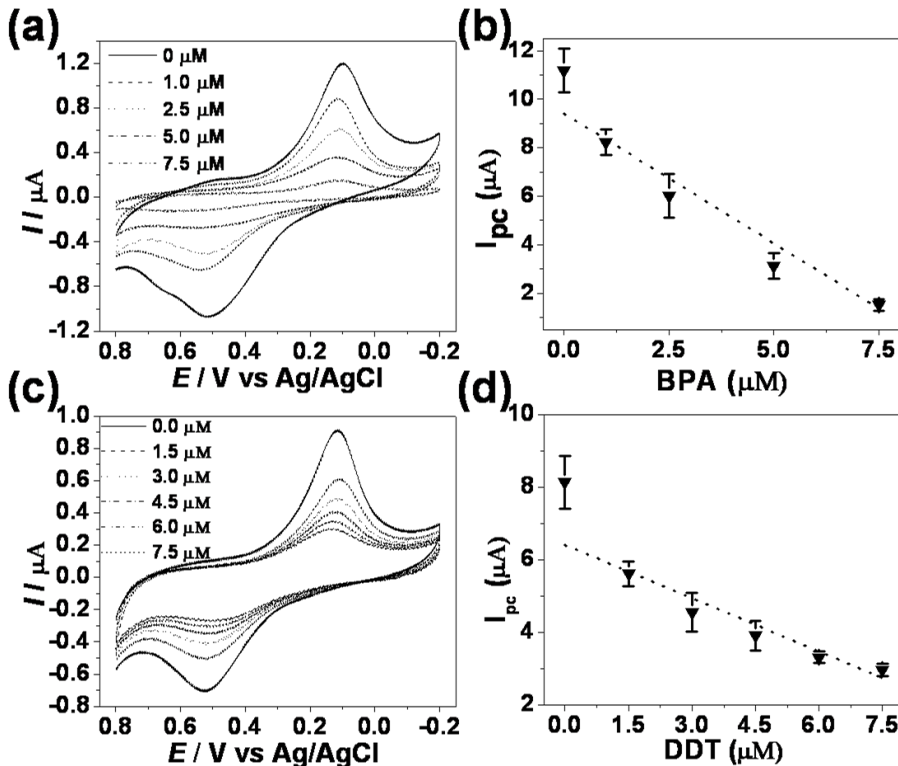
FIGURE 6.10

Cyclic voltammogram of (a) 0–7.5 µM bisphenol-A (BPA) and (c) 0–7.5 µM dichlorodiphenyltrichloroethane (DDT) treated cells; arrow indicates I_{pc} decreased 1.12–0.15 µA and 0.84–0.29 µA respectively, with the increasing concentration of toxicant. Linear plots obtained from various concentrations of (b) BPA and (d) DDT treated cells, every point corresponds to the average value of three independent measurements (error bars indicate the standard deviation). CV was measured using PBS (0.01 M, pH 7.4) at 100 mVs−1. (Reproduced with permission from: ref. 6, © 2010 Springer).

In addition, we found that the redox phenomenon at the cell-electrode interface is critical for detecting the electrochemical characteristics of target cells, which vary depending on the cell line [41]. Recently, we also observed that the electrochemical properties of each cell depend on the cell cycle stage, which is used as a potential label-free technology for cell cycle monitoring [10]. It is well known that cells tend to show cycle-dependent characteristics, which are defined by a sequence of events (G1, G2, M and S-phase) in which several specific nuclear changes occur. Among these numerous cytological changes M-phase and S-phase are most vulnerable to environmental or endogenous stimulations which is used as an environmental switch for sensing systems that is turned on in the presence of toxins or stressful conditions [11]. Therefore, controlling the cell cycle on a chip at S and M phases' specific electrochemical signal has been achieved by electrochemical readout [10] (Figure 6.11). Recently, these phase specific signals were employed in sensing phase specific effect of environmental toxin.
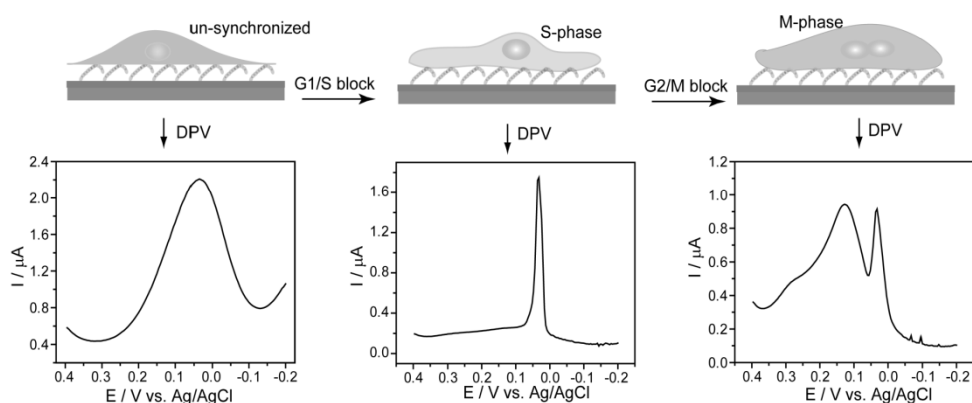
FIGURE 6.11
Figure shows synchronized S-phase (middle), M-phase (right), and unsynchronized (left) cells with their respective DPV signals (down arrows indicate respective signals). (Reproduced with permission from: ref. 10, © 2011ACS).

In a study, a chip containing both G1/S and G2/M-phase, subjected to PCB and/or BPA toxicity and electrochemical measurements were performed. The result shows that G1/S peaks sharply decreased due to 500 nM BPA treatment remaining the intact G2/M peaks (Figure 6.12a). But, peaks for G2/M decreased when 50 nM PCB was treated without affecting G1/S peak (Figure 6.12b). These results suggested that BPA toxicity affect the cells of G1/S and PCB affects G2/M phase. Whereas both the peaks decreased when a mixture of low concentrations (200 nM BPA and 20 nM PCB) of both toxin added. Moreover, no peak was detected when high concentration of mixed toxin (600 nM BPA and 60 nM PCB) added which indicates complete death and washout of cells from the electrode (Figure 6.12c). The neurotoxic doses of BPA and PCB are in agreement with a previous study [1,5] that reported 150 nM BPA and 20 nM PCB are toxic for PC12 cells. Therefore, the decreased phase specific electrochemical signal is certainly responsible for the effect of toxin used in this study. So, analysis and quantification of the current peak obtained from DPV signal intensities can be useful indirectly but accurately for determining the dose effect of the respective toxicant on completely synchronized cells.
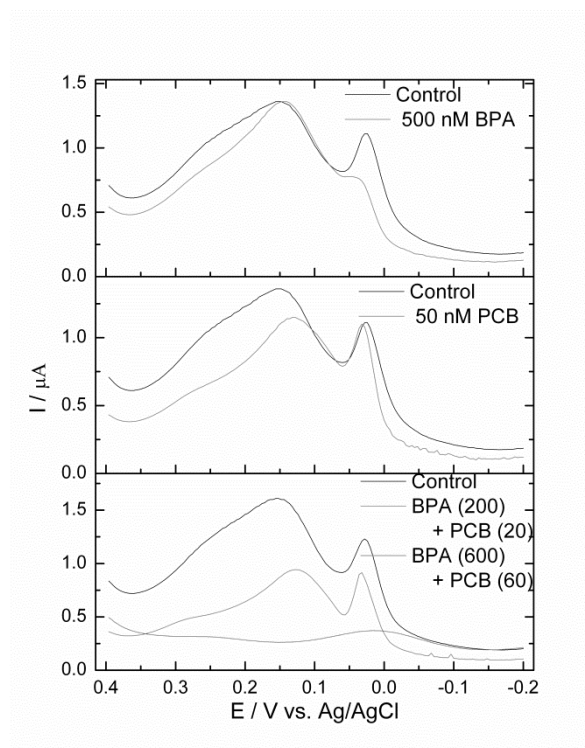
FIGURE 6.12
Phase specific toxicity of BPA and PCB are analyzed based on the two peaks obtained from cells 6 h released from G1/S,(top) image shows BPA toxicity affects mostly on G1/S peak whereas (middle) PCB affect G2/M peak, but, both the peak decreased when mixture of both the toxin treated (bottom) and no peak found when high concentration of toxin used. (Reproduced with permission from: ref. 11, © 2013Elsevier).

After confirming the complete synchronization cells at G1/S and G2/M phases, a varying concentration of PCB and BPA was exposed for sensitive electrochemical detection of cell viability. For the effective toxicity measurement 3.5×10^5 cells/ml of cells were synchronized on each chip because high density are not suitable for proper synchronization as well as for electrochemical measurements [10]. Prior to recording DPV current responses G2/M phase synchronized cells were exposed to several concentrations of PCB and G2/M phase synchronized cells to BPA. Figure 6.13a shows that the current responses from G2/M cells exposing various PCB concentrations from 20 nM to 120 nM. A dose dependent decreased in DPV current signals were recorded as functions of treated PCB concentrations (Figure 6.13c). Where, the current peaks from initial concentration (20 nM) remained unchanged comparing with non-treated control, indicating the sub-toxic dose. But, the reduction peak showed a negative linear correlation when cells were exposed to 40 nM to 120 nM concentrations of PCB (Figure 6.13b inset) which indicates cytotoxicity of PCB. Several previous study reported that electrochemical signals have positive linear correlations with the concentration of viable cells; therefore, signal decrease observed from toxin-treated cells certainly attributed to the loss of cell viability [4,5,6,11].
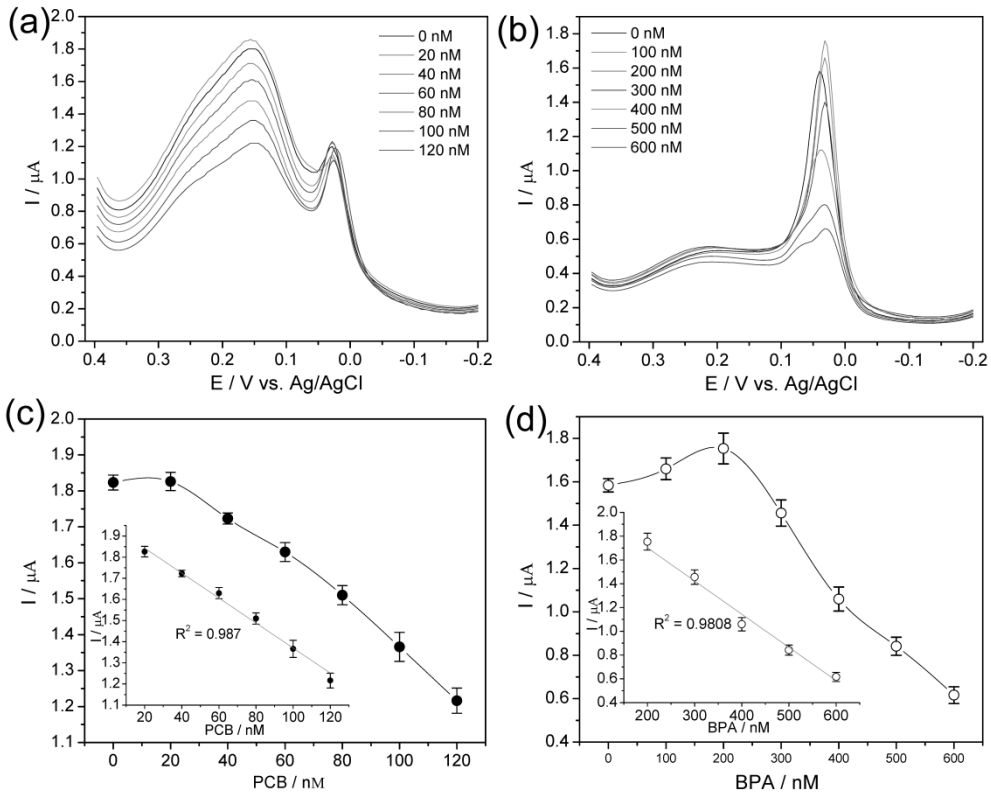
FIGURE 6.13
Concentration dependent cyto-toxicity assay; (a) effect of PCB on cell synchronized at G2/M phase and (b) effect of BPA on cell synchronized at G1/S phase. Dose response curve obtained from PCB treatment on G2/M synchronized chip (c) and BPA treatment on G1/S synchronized chip (d). (Reproduced with permission from: ref. 11, © 2013Elsevier).

Perhaps, the current responses from BPA exposed G1/S cells are plotted in Figure 6.13b, where unlikely to the other toxicants, BPA shows dose dependent dual effect [5]. The current peaks increase for 100 nM to 200 nM BPA treatments; whereas, decreased with further increasing concentrations (Figure 6.13d). The reduction peak showed a negative linear correlation when cells were exposed to 400 nM to 600 nM concentrations of BPA (Figure 6.13d inset). This finding is completely coincided with our previous report where BPA toxicity was analyzed on unsynchronized cells [5]. Therefore, it is depicted that cells at different phases of it's cycle can be susceptible for different environmental toxin which can be useful for monitoring the effect of mixed toxicity from environmental sources accurately using the developed synchronized cell based chip.

 Based on the above discussions, it is suggested that whole cell either in unsynchronized or synchronized state are able to monitor single or multiple toxins from bulk environmental sample. However, technical challenges still remain before the devices will become widely used for toxicity testing. Particularly, the lack of compatibility of the miniaturized cell chip platform with bulk environmental sample is the main drawback of this rapid detection method. However, incorporation a micro method that can filter the sample before exposed to the chip chamber can overcome this limitation.

Applications of cell chip for diagnosis

Cell-chip based sensor devices are now becoming practical tools for the rapid screening of chemicals and drugs, and several have been developed specifically as toxicity screening assays. Besides these numerous environmental monitoring, the distinct cell line specific redox behavior of the cell based chip has explored the opportunity of its diagnostic application. In the recent past, activity of several extracellular biochemical parameters such as effect of glucose and potassium on neurotransmitter release [42] were monitored efficiently using the cell based chip. We observed dopaminergic behavior of PC12 cells using cell immobilized chip [42]. Glucose and potassium activated dopamine release from neuronal cell were also confirmed voltammerically using the cell based chip. In Figure 6.14, the increased current peaks due to the glucose and potassium treatment for PC12 cells were contributed by increased exocytosis of intracellular dopamine [43].
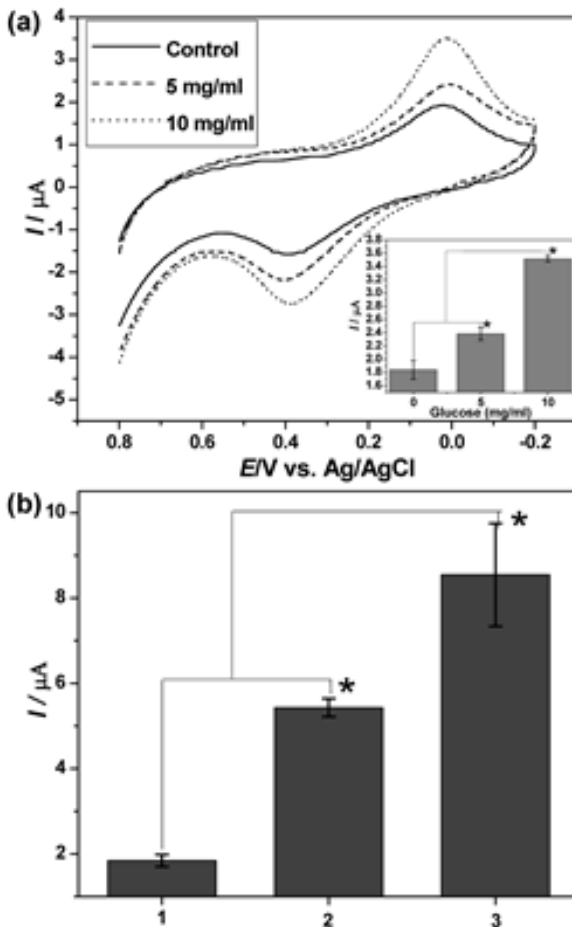
FIGURE 6.14
a) CV of glucose treated PC12 cell, inset shows current increase significantly with doses. b) Current peak from cells treated with 30 μM KCl combined with (1) 0 mg/ml, (2) 5 mg/ml and (3) 10 mg/ml glucose. (Reproduced with permission from: ref. 41, © 2011ASP).

Therefore cell chip based voltammetric monitoring of clinical specimens derived from different system of a patient can provide clear clinical information. For this cell from each system of the body should be used to achieve respective information of the system. This system specific clinical information can be achieved by analyzing and quantifying the voltammetric information of the cell chip. Finally, doctor can easily depict the clinical state of a patient from the system specifics clinical information of the chip. This quick response and analysis makes it possible for one to use as portable and disposable cell chip based assay and as early warning systems of the clinical state of a patient. However, technical challenges still remain before the use of the clinical samples such as urine, sputum, stool and other discharged specimens because of the biocompatibility concern. The external samples need to be processed before exposed to the chip chamber. Therefore, researchers are looking for the new cell based chip by combining micro fabrication and microfluidic technologies that can processed the clinical specimens to ensure biocompatibility to miniaturized cell chip platform in real-time. This chip can also be integrated with other medical equipment for automation and real-time monitoring.

Conclusions

This chapter focused on establishing strategies to develop a living cell chip based on electrochemical detection. As a model system; neural cell such as rat pheochromocytoma cells and human fibro-blastoma cells were chosen as the main analytic candidates, whereas human fibro-blastoma cells, human embryonic kidney cells and human epithelial carcinoma cells were also subject to electrochemical investigation by several researchers. The electrochemical measurements such as cyclic voltammetry and differential pulse voltammetry were conducted to examine the redox behavior of the model cell immobilized on electrode. Based on this redox behavior cell viability was determined electrochemically. However, in order to improve cell adhesion and enhance electrochemical signal cell adhesion molecules were organized on the electrode in a nanoscale array. The performance of the nanoscale peptide modified electrodes were checked and found to have positive effect on cell adhesion, spreading, proliferation and electrochemical signal transmission. Nanopatterend peptide modified cell chip proved to be potent for determination of environmental toxicity sensitively. Furthermore, fabricated nano-bio-platform was applied for artificial regulation of cell cycle on chip based electrochemical detection method. Finally, the synchronized cell chip at a definite phase of a cycle was applied for sensitive phase specific electrochemical determination of cyto-toxicity of environmental toxicant. This system works well in terms of synchronization of cells into the specific phase of its growth cycle and its electrochemical readout. It can be used as a future nano-biochip in developing sensitive cell based diagnostic devices.

Acknowledgements

References

1. Kafi, M. A., Kim, T. –H, Yea, C. -H., Kim, H. and J. -W. Choi, Biosens. Bioelectron. 2010, 26, 1359.
2. Bery, M. N. and Grivrll, M. B. "Bioelectrochemistry of Cells and Tissues", Birkhauser, Basel, Verlag, pp. 134, 1995.
3. Yea, C. H., Min, J. and Choi, J. W. Biochip J. 2007, 1, 219.
4. El-Said, W. A., Yea, C. -H., Kwon, I. -K. and Choi, J. -W. Biochip J. 2009, 3, 105.
5. Kafi, M. A., Kim, T.-H., An, J. H. and Choi, J.-W. Biosens. Bioelectron. 2011, 26, 3371.
6. Kafi, M. A., Kim, T. -H., Yagati, A. K., Kim, H. and Choi, J. -W. Biotechnol. Lett. 2010, 32, 1797.
7. Dwyer, D.S., Liu, Y. and Bradley, R.J. J. Cell. Physiol. 1999, 178, 93.
8. Pierschbacher, M. D. and Ruoslahti, E. Nature 1984, 309, 30.
9. Kafi, M. A., El-Said, W. A., Kim, T. –H and Choi, J. -W. Biomaterials 2012, 33, 731-739.
10. Kafi, M. A., Kim, T.-H., An, J. H. and Choi, J.-W. Analchem 2011, 83, 2104-2111.
11. Kafi, M. A., Yea, C. H., Kim, T. -H., Yagati, A. K., and Choi, J. -W. Biosens. Bioelectron. 2013, 41, 192.
12. Sundberg, S.A. Curr. Opin. Biotechnol. 2000, 11, 47.
13. Kuang, Y., Biran, I. and Walt, D.R. Anal. Chem. 2004, 76, 2902.
14. Flaim, C.J., Chien, S. and Bhatia, S.N. Nat. Meth. 2005, 2, 119.
15. Ben-Yoav, H., Biran, A., Pedahzur, R., Belkin, S., Buchinger, S., Reifferscheid, G. and Shacham-Diamand, Y. Electrochem. Acta. 2009, 54, 6113.
16. Cagnin, S., Caraballo, M., Guiducci, C., Martini, P., Ross, M., SantaAna, M., Danley, D., West, T. and Lanfranchi, G. Sensors 2009, 9, 3122.
17. Biran, A., Yagur-Kroll, S., Pedahzur, R., Buchinger, S., Reifferscheid, G., Ben-Yoav, H., Shacham-Diamand, Y., and Belkin, S. Microb. Biotechnol. 2010, 3, 412.
18. Scarano, S., Mascini, M., Turner, A.P.F. and Minunni, M. Biosens. Bioelectron. 2010, 25, 957.
19. Choi. J.-W. Biotechnol. Bioprocess. Eng. 2005, 9, 12-20.
20. Ruoslahti, E. Annu. Rev. Cell Dev. Biol. 1996, 12, 697.
21. Pfaff, M., Tangemann, K., Müller, B., Gurrath, M., Müller, G., Kessler, H., Timp, R. and Engel, J. J. Biol. Chem. 1994, 269, 20233
22. Hubbell, J. A. Bio/technol. 1995, 13, 565.
23. Robin, A. Q., Weng, C. C., Martyn, C. D., Saul, J. B. T. and Kevin, M. S. Biomaterials 2001, 22, 865.
24. Pierschbacher, M. D. and Ruoslahti, E. Nature 1984, 309, 30.
25. Chen, C. S., Alonso, J. L., Ostuni, E., Whitesides, G. M. and Ingber, D. E. Biochem. Biophys. Res. Co. 2003, 307, 355.
26. Hersel, U., Dahmen, C. and Kessler, H. Biomaterials 2003, 24, 4385.
27. Yamada, K. M. and Kennedy, D. W. J. Cell. Biol. 1984, 24, 99.
28. Jung, M., Lee, S., Tae, B.Y., Min, J.Y., Ho, K. S., Woo, D. -H. and Mho, S. -iL., Microelectron. J. 2008, 39, 526.
29. Choi, J. W., Nam, Y. S. and Fujihira, M. Biotechnol. Bioprocess. Eng. 2004, 9, 76.
30. Gallant, N.D., Michael, K.E. and Garcia, A.J. Mol. Biol. Cell, 2005, 16, 4329.
31. Huang, J., Grater, S.V., Corbellini, F., Rinck, S., Bock, E., Kemkemer, R., Kessler, H., Ding, J. and Spartz, J.P. Nano Lett. 2009, 9, 1111.
32. Donard, S. D., liu, Y. E. and Ronald, J. B. J. Cell. Physiol. 1999, 178, 93.
33. Hynda, K., Klebe, J. R. and George, R. J. Cell Biol. 1981, 88, 473.
34. Bershadsky, A., Chausovsky, A., Becker, E., Lyubimova, A. and Geiger, B. Curr. Biol. 1996, 6, 1279.

35. Hersel, U., Dahmen, C. and Kessler, H. Biomaterials 2003, 24, 4385.
36. Au, A., Boehm, C.A., Mayes, A.M., Muschler, G.F., and Griffith, L.G. Biomaterials 2007, 28, 1847.
37. Kalinina, S., Gliemann, H., Lopez-Garcia, M., Petershans, A., Auernheimer, J., Schimmel, T., Bruns, M., Schambony, A., Kessler, H. and Wedlich, D. Biomaterials 2008, 29, 3004.
38. Gallant, N.D., Michael, K.E. and Garcia, A.J. Mol. Biol. Cell, 2005, 16, 4329.
39. Huang, J., Grater, S.V., Corbellini, F., Rinck, S., Bock, E., Kemkemer, R., Kessler, H., Ding, J. and Spartz, J.P. Nano Lett. 2009, 9, 1111.
40. May, K. M., Wang, Y., Bachas, L. G. and Anderson, K. W. Anal. Chem. 2004, 76, 4156.
41. Kafi, M. A., Kim, T.-H. and Choi, J.-W., SENSORDEVICES 2011 : The Second International Conference on Sensor Device Technologies and Applications, Copyright (c) IARIA, 2011. ISBN: 978-1-61208-145-8
42. Kafi, M. A.. Kim, T. –H, An, J. H., Kim, H. and J. -W. Choi, Sens.Lett. 2011, 9, 147.
43. Kafi, M. A., Kim, T. H., Lee, T. and Choi J. -W. J. Nanosci. Nanotechnol. 2011, 11, 7086.

7

Cat-anionic vesicle-based systems as potential carriers in Nano-technologies

Aurelio Barbetta[1], Camillo La Mesa[1], Laura Muzi[2], Carlotta Pucci[1], Gianfranco Risuleo[2], Franco Tardani[1]

[1]Dept. of Chemistry, and [2]Dept. of Biology and Biotechnologies , "Sapienza University of Rome", P.le A. Moro 5, I-00185 Rome, Italy.

Outline:

Introduction

Vesicular systems offer great potentialities in delivering biological macromolecules, drugs, and cosmetics across the cell membrane [1-5]. The evaluation of their bio-compatibility is important in the application of these supra-molecular structures in biotechnology. This is of fundamental relevance when treating cells, or tissues, with vesicular or other carriers [6-16]. Undoubtedly, the physico-chemical properties of these vesicular aggregates must be properly tuned for the application. They play a crucial role in the interactions between vesicles and biopolymers, and of the resulting complexes with cells. The bio-oriented aspects must be combined with biophysical and physico-chemical strategies we report on, and be supported by synthetic work.

The preparation and characterisation of lipido-mimetic systems, LMSs, promising platforms for an efficient biopolymer binding and transfection are discussed. The matrices considered take the form of vesicles capable of significant exchange of matter with cells or tissues. LMS are vesicles and/or lipo-plexes (biopolymer-vesicle complexes) with sizes in the range 100-500 nm size. Hence, are suitable for bio-oriented applications. A plausible uptake mechanism of the above adducts involves the adhesion of lipo-plexes onto cells and subsequent pynocitosis, or fagocytosis. When the biopolymer is finally transfected in the cell matrix, it will activate the required biochemical reactions. Vesicles are chaperons for biopolymer(s) transfer into cells. To ensure a real bio-compatibility, they must be excreted or recycled at the end of the process.

The unique properties of cat-anionic vesicular carriers make applications extremely promising, potentially ensure a more efficient transfection compared to micelles, inorganic solid particles, co-acervates, and so forth. They operate in a controlled way and presumably, with no (or low) toxic effects. The rationale suggesting the use of vesicular carriers with respect to other matrices [6, 13-15] is due to the combination of different factors:

- high bio-compatibility towards cells and, eventually, tissues;
- significant adsorption onto vesicles of the species to be transferred;
- tunable physical state (gel, liquid- or liquid crystalline) of the composites, very similar to that of the cells;
- substantial and efficient binding onto cells.

Cat-anionic vesicles are supra-molecular aggregates formed by mixing in non-stoichiometric ratios cationic and anionic surfactant species [17-19]. Surfactants of opposite charge tend to aggregate in polar solvents, such as water. The electrostatic interactions between the polar heads and the hydrophobic tails favor the formation of self-assembled and organized supra-molecular structures. This phenomenon depends upon the so-called "Critical Micellar Concentration" (CMC), which represents the limit above which the surfactants in solution aggregate to form spontaneously micelles with different morphologies [20]. The diverse shapes depend on the geometry of the individual surfactant molecules. The relationship between molecular geometry of the surfactant and the morphology of the self-organized structures can be determined by the packing parameter (P) [21], i.e. the ratio between the volume of the hydrophobic tract (V) and the area of the polar head (A) times the length of the chain (L) being part of the same surfactant (P=V/AL). The modulus of P suggests the type of structure/shape that surfactants tend to assume upon aggregation. Vesicles form when the packing parameter reaches an optimal value leading to the formation of a close double layer.

The preparation of stable cat-anionic vesicular systems is not fully understood as to whether their stability is of thermodynamic, or kinetic, origin. The best strategies to control their size and charge density, and conditions for an efficient biopolymer binding are also described. Data relative to a few

selected systems, recently proposed and utilized on the purposes indicated above are discussed along with details of the preparation of cat-anionic vesicles based on lipid and/or surfactants. Optimization is necessary, since tuning the related physico-chemical properties is a prerequisite.

Preliminary physico-chemical aspects to be clarified concern vesicle size, charge density, bi-layer fluidity, as well as the charge and conformational state of the biopolymer(s) to be eventually transferred to cultured cells. The focus of this work is on biopolymer adsorption, biological assessment of the resulting vesicles and/or lipoplexes, and transfection methods. For the evaluation of biological effects, the protocols required for an effective cytotoxicity screening and uptake of exogenous bio-macromolecules are described.

The interaction of vesicles with bio-macromolecules, such as DNA, RNA or proteins, results in the formation of the cited lipoplexes. Hence, the potential tool to deliver genetic material across the cell membrane upon the formation of complexes between bio-macromolecules exposing a net negative charge such is the case for DNA and RNA, and vesicles having a positive surface charge. These complexes could be potentially delivered within the cell [6, 13]. However, cell cultures exposed to the action of vesicles or lipoplexes may suffer cytotoxic dose/response effects and are sensitive to the exposure time. There is little reported work on this specific aspect [22, 23] but recent work showed that tumor cells exhibit a higher sensitivity to treatment with SDS-CTAB vesicles as compared to normal mouse fibroblasts [24]. The experimental conditions can be adjusted to obtain an efficient vesicle-mediated transfection leading to the expression of exogenous genetic material [25 - 27]. Pilot-studies suggest that cat-anionic vesicles may find a use in anticancer therapy. The cytotoxic action of both the individual surfactants and vesicles formed by such compounds on HEK-293 cultured cells are reviewed. The transfection of an exogenous RNA mediated by SDS-CTAB vesicles and the level of translation of the reporter-protein are also reported. The data presented show that the nucleic acid is translated into protein with the correct configuration since it immuno-precipitates in the presence of the specific antibody. The novelty is that naked RNA, a biomacromolecule vulnerable by the resident RNases, is protected when it is vesicle-bound. Therefore, the above systems may find a use in biotechnology and gene therapy.

Physico-chemical background

Cat-anionic systems

The first attempt to obtain cat-anionic systems date back to the eighties of last century when Wennerström suggested that stoichimetric mixtures of two oppositely charged surfactants could give rise to lamellar order similar to phospholipids [28]. Lamellar, smectic, solids were experimentally observed. The definition of cat-anionic systems took place and it should be noted that the term "cat-anionic" was originally proposed by Ali Khan [29]. It was commonly accepted that non stoichiometric mixtures were far more appealing than stoichiometric ones. Balanced microemulsions, liquid crystals, and/or vesicles made of cat-anionic species occurred depending on the components [29-31]. Whether the stability of the latter is of thermodynamic or kinetic nature is debatable: in some instances the former definition applies [32].

Cat-anionic vesicles form in mixtures made of alkyl- or dialkylammonium salts (such as cetyltrimethylammoniun bromide, CTAB [18,33-35], tetradecyltrimethylammoniun bromide, TTAB [36], didodecyldimethylammoniun bromide, DDAB [37-39], dioctyldimethylammoniun bromide, DODAB [40,41]), and alkyl sulfates, (sodium dodecylsulfate, SDS, sodium octylsulfate, SOS), sulfonates (sodium bis-2-ethylhexylsulfosuccinate, AOT, [41,42], tetraethylammonium perfluorooctansulfonate, TEAPFOS,

[36]), carboxylates (sodium perfluorohexanoate, SPFH, [43,44]). Hydrocarbon-fluorocarbon mixtures were used, but are not stable, mostly when the fluoroalkyl chain is relatively long. Also mixtures made of DDAB and bile acid salts were considered [45]. Other systems have been reported in recent literature findings [17, 46]. In particular, mixtures of amino-acid based surfactants, AABS, and oppositely charged surfactants, or phospholipids, such as DPPA, exhibit the same phase behavior as the classical cat-anionic ones reported above. Because of their very low cyto-toxicity and high bio-compatibility AABS are sensitive to the medium pH, and their polar head groups are easily hydrolyzed. In addition, size modulation is induced by titration of acid or basic groups lying on the vesicle surface. The mixtures of lipids or of single chain surfactants are in the same category. A tentative list of the species considered to date is reported in Table 7.1.

TABLE 7.1
Acronyms and symbols indicating the species used to date to prepare cat-anionic vesicles.

Cationic

Acronym	Chemical name	Ref.
CTAB	Cetyltrimethylammonium bromide	[30-32]
TTAB	Tetradecyltrimethylammonium bromide	[33]
DTAB	Dodecyltrimethylammonium bromide	[34]
DDAB	Didodecildimethylammonium bromide	[35-37]
DODAB	Dioctyldimethylammonium bromide	[38,39]
AABS14	1,2-dimyristoyl-rac-glycero-3-O-(NR-acetyl-L-arginine) HCl	[40]
AABS12	1,2-dilauroyl-rac-glycero-3-O-(NR-acetyl-L-arginine) HCl	[40]

Anionic

Acronym	Chemical name	Ref.
SDS	Sodium dodecylsulfate	[19]
SOS	Sodium octylsulfate	[30,31]
AOT	Sodium bis-2-ethylhexylsulfosuccinate	[38,39,44,45]
SL	Sodium laurate	[41]
KPFH	Potassium perfluorohexanoate	[42]
TEAPFOS	Tetraethylammonium perfluorooctansulfonate	[33]
DPPA	Sodium 1,2-dipalmitoyl-sn-glycero-3-phosphate	[40]
STDC	Sodium taurodeoxycholate	[43]

The sequence leading from spherical micelles to vesicles implies a series of intermediate steps. On increasing the concentration of the minor surfactant ion up to charge neutralization, cat-anionic mixtures follow the sequence:

spherical micelles → swollen micelles → cylindrical micelles → vesicles → precipitates

The above sequence is controlled by the [C/A] charge (and mole) ratio, where C indicates the cationic and A the anionic species.

The surfactant ions used to prepare such mixtures can be single or multiple chain ones. Mixing oppositely charged single chain surfactant ions gives pseudo-double-chain cat-anionic surfactants, that is an analogue of single lipids. Literature also deals with single-double chain surfactants, forming pseudo-triple-chain cat-anionic mixtures. Phase behavior and the characterization of the more exotic pseudo-tetra-chain cat-anionic surfactants (DDAB/AOT) systems have been reported by Caria and Khan [48], and Karukstis et al. [49], respectively.

General considerations on surfactants or lipids

Due to their molecular ambivalence [50], due to the presence of polar and strongly non-polar moieties, surfactants and lipids self-organize to minimize the respective Gibbs energy contributions to the system stability. The non polar regions assemble in a fluid state, very similar to liquid hydrocarbons. Conversely, the polar groups face toward the aqueous solvent and stabilize the resulting aggregates and micelles, vesicles and bi-layers are formed. The two parts of these molecules are located in regions of different polarity. This is a prerequisite getting organized surfactant assemblies. The process is controlled by the "hydrophobic effect". Water is released from the alkyl chain surroundings, and the process is entropy driven [51]. Compartmentalization in regions of different polarity, therefore, is a prerequisite to attain organized surfactant assemblies.

The size of the aggregates formed is controlled by an additional constraint ensuring a preferred supra-molecular arrangement [52, 53]. The three-dimensional geometry of surface active molecules is characterized by the polar surface area, A, the volume of hydrocarbon chain(s), V, and the length of hydrophobic moieties, L, equal to the alkyl chain in extended conformation, Figure 7.1. The resulting a-dimensional V/AL ratio pertinent to a given amphiphilic molecule implies that spherical micelles (V/AL $\leq$ 1/3), cylindrical micelles (1/3 $\leq$ V/AL $\leq$ 1/2), vesicles (1/2 $\leq$ V/AL $\leq$ 1), or planar bi-layers (V/AL $\approx$ 1) may be formed. Modulating the geometry of the resulting aggregates is achieved by adding salts, long chain alkanols, fatty acids, sterols, and or by mixing two surface active species [54-58]. Hence, the molecules preferentially forming spherical micelles are forced from composition and other physico-chemical constraints to assume the form of disks, rods, or vesicular entities. Particularly appealing is the possibility to get by-layer vesicles. In all cases we report here, vesicle size and charge can be modulated by the mole ratio between anionic and cationic amphiphiles.
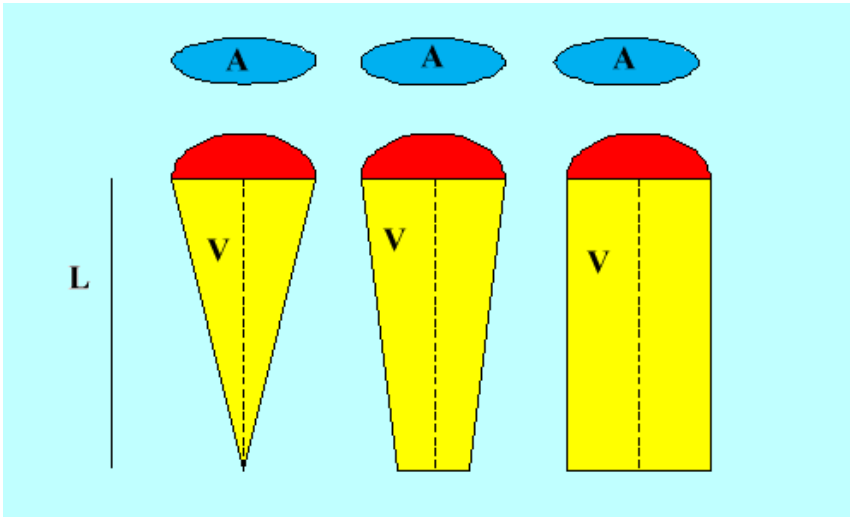
FIGURE 7.1

Two-dimensional view of surfactant molecules. The symbol A indicates the planar projection of the area per polar head group, L the alkyl chain length in extended conformation, and V the alkyl chain volume. The a-dimensional V/AL ratio pertinent to a given species implies that spherical micelles (V/AL $\leq$ 1/3), cylindrical micelles (1/3 $\leq$ V/AL $\leq$ 1/2), vesicles (1/2 $\leq$ V/AL $\leq$ 1), or planar bi-layers (V/AL $\approx$ 1) may be formed, in sequence. In proper conditions, the theory can be extended to surfactant mixtures, as well.

Electrostatic effects play a relevant role in the stability of such aggregates. Similarly charged groups facing outward the aggregates repel each other. To reduce such destabilizing effect counter-ions are firmly bound in the Stern layer of the aggregates [59] because of the fluid nature of such interfaces and it is also possible inserting in the aggregates oppositely charged amphiphilic species. Thus, mixing oppositely surfactants is the route to attain size and charge modulation. Hence, it is easy to tune the average interfacial curvature of the aggregates, i.e. their size.

Vesicles are characterized by sizes ranging from 10 nm to 1 μm. At fixed surfactant content, their surface charge density, σ, scales with the mole ratio and is in inverse proportion to the curvature radius, R_H [60] due to the semi-fluid nature of the bi-layers dictated by surface energy. At equilibrium, vesicle stability is controlled by the action of different forces acting on the bi-layers. Accordingly, the optimal R_H value will be tuned by the overlapping of several terms. In the case of spherical entities, in particular:

a)   the surface charges increase vesicle size;

b)   surface tension terms minimize its area;

c)   the bi-layer curvature elasticity tends to restore the original conditions after application of deformations;

d)   the optimal molecular packing, controlled by vdW forces and electrostatics, dictates the preferred vesicle size (at a given surfactant concentration);

e)   the osmotic gradients active across the vesicle bi-layer may decrease, or increase, vesicle size.

The combined action of the above contributions compels the vesicle to a preferred average curvature radius, $<R_H>$. In this context, entropy contributions always play an effective role in vesicle stability. These contributions arise from an un-favored odd-even distribution of the surfactant species in the bi-layers and from other entropy of mixing terms. It is conceivable, that the composition in the inner and outer part of the bi-layer may be different, due to packing and/or curvature constraints.

At a given composition, vesicles put in contact with the solvent partition their components in such a way that the respective chemical potentials in the aggregate and in the bulk, indicated as μ_i, are the same [61, 62]. Due to the thermodynamic equilibrium, the surface active components move to/from the vesicle, in proportion to their affinity with the solvent and/or the aggregate. Surfactants characterized by short alkyl chains are preferentially distributed in the bulk with respect to long chain ones. The same applies to lipids, although the partition occurs at much lower rates.

The partition is sensitive to the working temperature, because $(\partial\mu_i/\partial T) \neq 0$ and the related entropy term become significant, leading to relevant changes in vesicle size. Hence, cat-anionic vesicles made by short alkyl chain surfactants show a moderate thermal stability. Heating implies a vesicle size rearrangement, with subsequent changes in their dimensions. Thereafter, vesicular dispersions change their appearance from turbid to milky and, then, to opalescent or bluish color. At the end of the process, vesicles retain sizes in the 300 nm range for long times, even at room temperature (Figure 7.2).
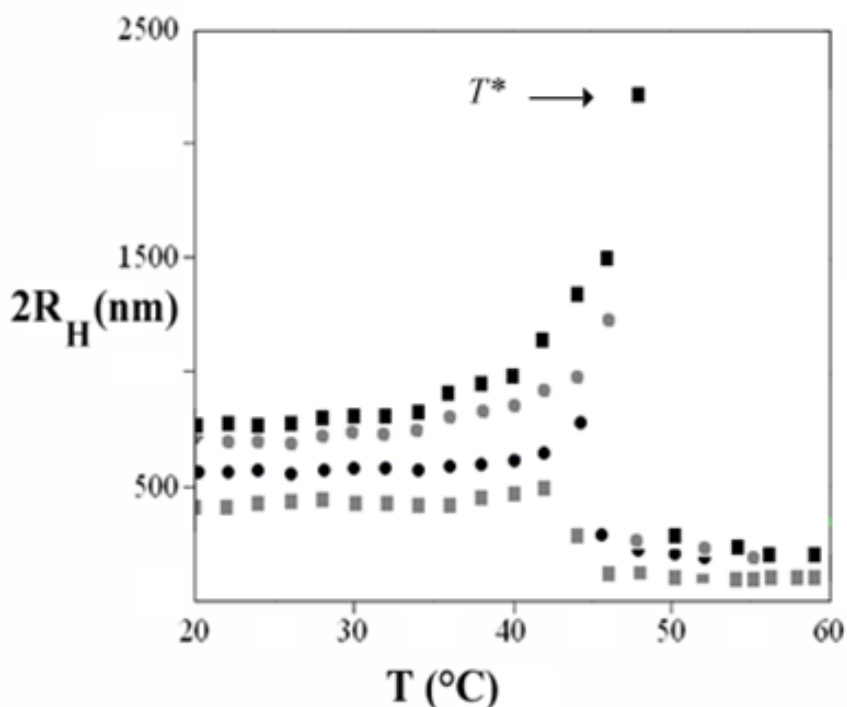
FIGURE 7.2
Average vesicle size, $2R_H$ (in nm), vs. T, in °C, for CTAB/SDS mole ratios equal to 0.286, light grey squares, 0.323, black circles, 0.379, grey circles, and 0.459, black squares. The overall mixture contains 6.0 mmol Kg^{-1} of SDS + CTAB. Note the significant increase in vesicle size on increasing T. The transition threshold depends on the CTAB/SDS mole ratios. It is considered in analogy to a second-order phase transition.

It has been demonstrated that such drastic changes in size and macroscopic appearance are concomitant to multi- to bi-layer thermal transitions [63]. The latter state is by far preferred for biomedical purposes, mainly when the internalization of a given component is required.

Vesicle preparation and characterization

As a rule, cat-anionic mixtures are formed by mixing dilute solutions (up to 10-15 mmol kg^{-1}) of oppositely charged surfactants in non-stoichiometric ratios. Mixing is rapid on an time scale (seconds) and leads to entities having sizes in the range of 10^2-10^3 nm, Figure 7.3.
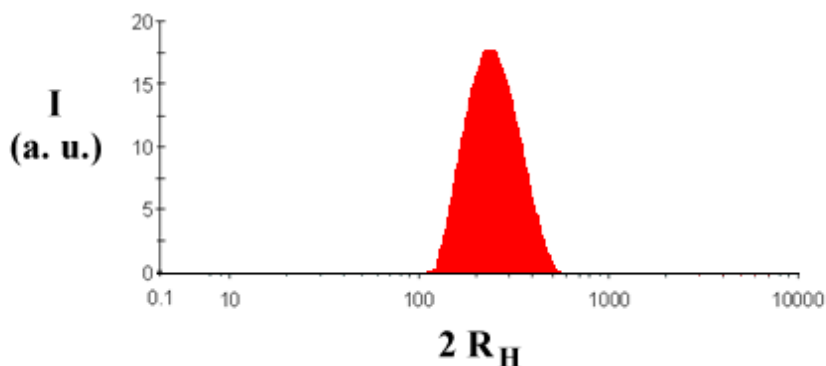
FIGURE 7.3
DLS intensity plot, showing the size distribution of a 4.05 mmol kg^{-1} DDAB/SDS vesicular system, having 3.82 as DDAB/SDS mass ratio, at 25.0°C. Note the uni-modal size distribution function.

Other approaches such as mixing the two solids and subsequent dissolving in water, or dispersing one solid surfactant into a solution of the other have also been used. Mixing of the two solutions is the fastest and more reliable route to get stable vesicles. Complete titration leads to a poorly soluble smectic (lamellar) phase, which precipitates out, leaving the respective counter-ions free in the bulk. This is a sort of metathesis. As a rule, the smectic phases obtained in this way show thermotropic, rather than lyotropic, liquid crystalline behavior [64].

Characterization by visual inspection, turbidity, DLS, ζ-potential, dielectric relaxation, TEM, surface tension, and SAXS is required. SAXS and DLS give information on vesicle size; the former also indicates the formation of bi- or multi-layer states. Cat-anionic vesicles made of SDS-CTAB are smaller than those observed in SDS-DDAB, which possibly makes them a good tool for transfection purposes. It is also worth noting that, in comparison to lipid-based vesicles, they are stable for long times.

TEM, mostly in cryo-mode, gives realistic estimates of vesicle size, bi- or multi-layer state, vesicle fusion, eventual biopolymer adsorption, formation of faceted entities and so forth [65, 66]. Atomic force microscopy, AFM, has also been used. The results are unsatisfactorily since vesicles tend to adhere, are transformed into lenses, and spread onto the surface of the substrates onto which they are deposited [67].

Zeta-potential gives information on the surface charge density, and is related to σ. Dielectric relaxation, finally, gives information on the double layer thickness surrounding the vesicles. Electro-phoretic mobility, related to ζ-potential, and interface polarization, detected by dielectric methods, jointly allow characterizing in detail the role of electrostatic contributions to vesicle stability. The results of these

measurements can be properly combined to determine the electric moment(s) active on the vesicle surface. As it is intuitive, the lower is the charge density the thicker is the double layer.
^{1}H NMR proton chemical shift measurements were also used [68]. The information is poor since the band-shapes are large and poorly resolved, Figure 7.4.
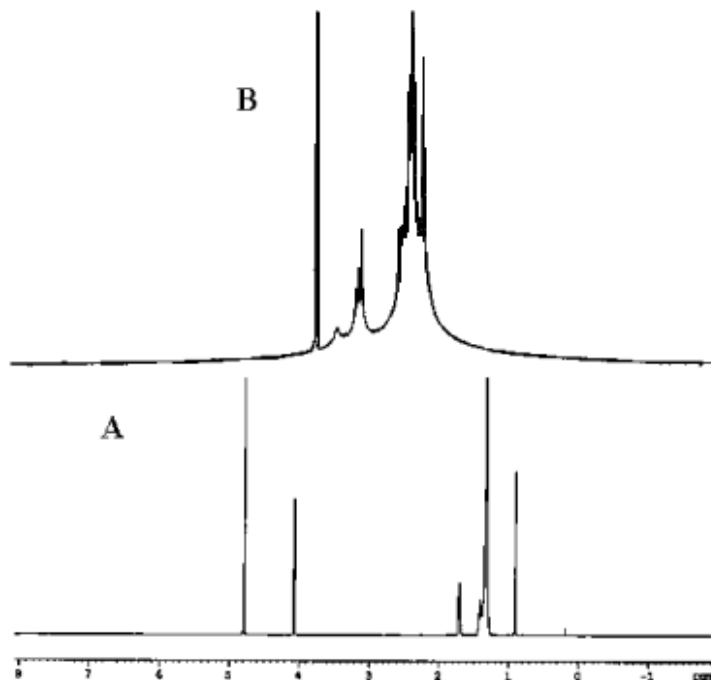
FIGURE 7.4
^{1}H NMR spectra of 20.0 mmol Kg^{-1} SDS, A, and 25.0 mmol Kg^{-1} SDS/CTAB mixture, having mole ratios 2.5/1.0. Data refer to 25.0° C. The spectra are redrawn from Ref. 74.

Conversely, NMR self-diffusion gives estimates of vesicle sizes because the decay of ^{1}H signals after the application and subsequent decay of gradient pulses is controlled by the diffusivity of the entities in which the protons are located [69, 70]. From the resulting self-diffusion values it is possible obtaining the vesicle average size, according to the Stokes-Einstein equation.
According to DLS and ζ-potential measurements there is direct proportionality between size, or charge, and the [A/C] mole ratio. When the latter is close to unity, vesicle size diverges (with eventual precipitation) and ζ-potential approaches zero, Figure 7.5.
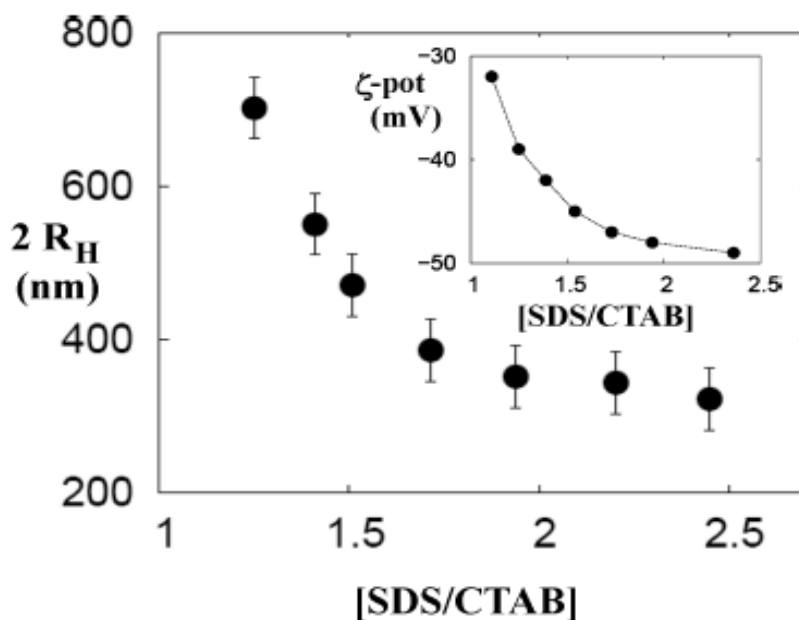
FIGURE 7.5
The average hydrodynamic radius, $2R_H$ in nm, of cat-anionic SDS/CTAB vesicles as a function of the mole (and charge) ratio, at 25.0°C. Data refer to mixtures containing 6.0 mmol Kg^{-1} as an overall surfactant content. In the inset is reported the composition dependence of ζ-potentials.

The same holds for its derivative with respect to the amount of added material. In proximity of an inflection point, derivation of the $(\partial\zeta/\partial c)$ function, where c is the concentration of the titrant, corresponds to $(\partial\tau/\partial c) + (\partial\sigma/\partial c) = 0$, since ζ is directly proportional to στ. Therefore, the double layer thickness, τ (the Debye's screening length), diverges as the surface charge density, σ, on the shear plane of the lipo-plexes approaches zero.

The two-phase system obtained by complete titration contains a poorly soluble inner CA smectic salt, when the solution contains essentially free counter-ions. From an applied viewpoint, more interesting are the results obtained when the [C/A] mole (or charge, more precisely) ratio is ≠ 1. In such cases vesicles are formed and shown by drawing ternary or pseudo-binary phase diagrams, Figure 7.6.
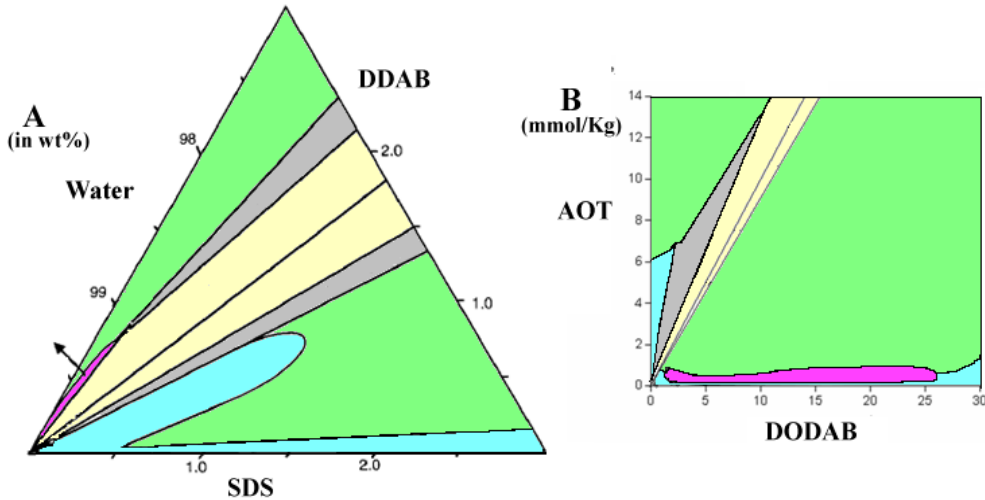
FIGURE 7.6
A. Phase map of the system water/DDAB/SDS, at 25.0° C. (A) Concentrations are in wt%. The figure has been redrawn according to Ref.s [36,37]. (B) Pseudo-binary phase diagram of the system wate/AOT/DODAB, at 25.0°C. Concentrations are in mmol Kg^{-1}. In both diagrams, the solution regions are indicated in light blue, the vesicular ones in cyan, the two phase lamellar + solution regions in green, the three phase solution + lamellar + solid in grey, the two-phase solution + crystal in yellow color. The black line dividing the yellow area in two is the equi-molar line.

Use of the latter approximation is made possible by the fact that water is always in large excess compared to all other components. The vesicular area occupies tiny regions in the phase diagram, and is usually located between the solution and the lamellar phase and/or the precipitate area. It can be readily recognized from the solutions and from the optically birefringent lamellar phase. Visual inspection, for instance, indicates the bluish, or slightly opalescent, appearance of most vesicular dispersions. The above behavior is related to the size of the disperse objects.

The region of existence is finely modulated by the overall amount of surfactant and, mostly, by their mole/charge ratios. This is a rather common feature met when preparing cat-anionic vesicles. Were the alkyl chain length the same, as in the DTAB-SDS system, the phase map would be symmetrical with respect to mole ratios, and cationic- or anionic-rich vesicles would be observed. Mixing double chain species having similar hydrophilic-lipophilic balance, such as DODAB and AOT or DDAB and AOT gives results consistent with the above statements.

Biopolymer adsorption

Small globular proteins, semi-synthetic poly-electrolytes derived from polysaccharides and/or DNA have been used as adsorbing species. As it is expected from considerations based on the molecular architecture of the species to be bound, the underlying mechanisms are quite different in the reported cases. The binding of small globular proteins, such as lysozyme and/or albumins, can be modeled in terms of the adsorption of small charged spheres onto large ones. The binding efficiency is governed by the number density of the protein with respect to vesicles and scales in proportion to the respective charges. For this to occur, it is possible to use proteins in spontaneous pH conditions. At values in the 5-

7 pH range, for instance, lysozyme has 8 positive charges in excess [68]. In such state, it promptly interacts with negatively charged vesicles by electrostatic interactions. This is the behavior observed when lysozyme is added to a dilute CTAB/SDS vesicular dispersion, in which the anionic species is in excess. Upon interaction, a sort of charge titration takes place and the size of vesicles increases. In the same time, the ζ-potential changes until surface saturation is approached. Thereafter, it remains essentially the same as the free protein. This is a clear indication that most surface sites available on the vesicle have been titrated. Therefore, it is necessary to estimate the binding efficiency. An adsorption isotherm can be drawn from electro-phoretic measurements.

Two more points still need to be considered. Saturation is not complete, due to repulsive, excluded volume, interactions between surface adsorbed protein molecules. Adsorbed lysozyme, in addition, may bridge different vesicles: such hypothesis finds support from the substantial increase in lipo-plexes size at the saturation threshold. The situation is more interesting in case of pH-dependent bovine serum albumin binding onto positively charged DDAB/SDS vesicles. The latter protein has its iso-electric point in the pH range close to 5.0-6.0. When the pH of the solution is low, no binding is observed; above pH 6.0, on the contrary, the efficiency in binding increases in proportion to the protein net charge [71], Figure 7.7.
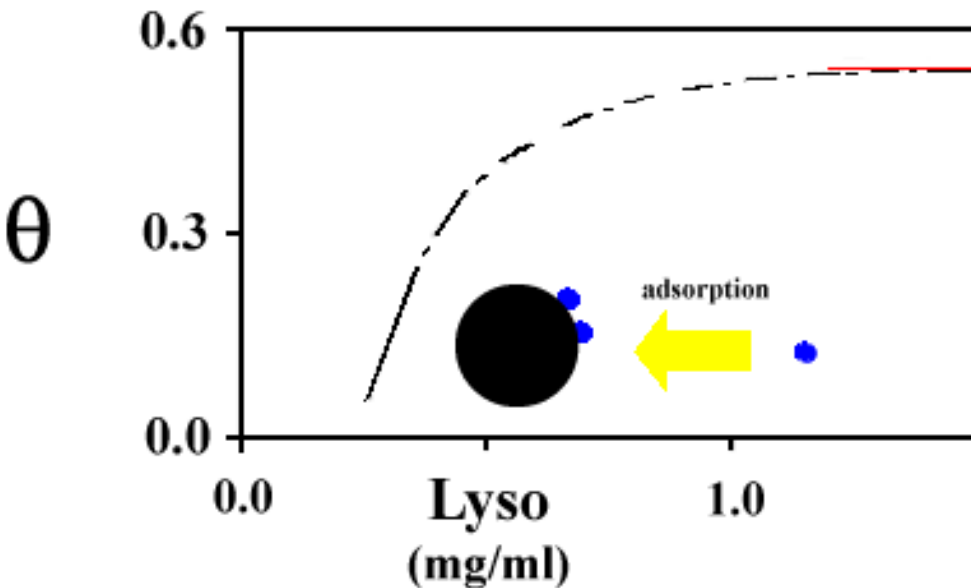
FIGURE 7.7
Surface adsorption isotherm and the related surface coverage, θ, calculated by proper rearrangement of ζ-potential values, as a function of added lysozyme, in mg/ml, to vesicular solution. Data refer to a 6.0 mmol Kg^{-1} SDS/CTAB vesicular mixture of mole ratio 2/1, at 25.0°C. Note that surface saturation occurs at high protein content, as indicated by the red line in the upper right side of the figure. Redrawn from Ref. [74].

Surface coverage changes with pH, although the number of charges neutralized upon binding remains essentially the same because more negative charges on the protein titrate a high number of surface binding sites. In addition, the interactions with vesicles is consistent with an increase in the amount of

β-sheet and random coil conformation of albumin. In such conditions, perhaps, albumin retains a significant part of its biological activity.

DNA binding, finally, has been utilized in the case of CTAB/SOS and DDAB/SDS vesicles [72, 73]. The latter bio-macromolecule is a long relatively rigid rod, which rolls around the vesicle surface. When adsorbed it does not interact with ethidium bromide. Conversely, when completely released from vesicles it has significant interactions with that dye and also retains its classical B conformation. In words, vesicle-bound DNA is substantially not accessible to the fluorophore, when is accessible to it when released. The same holds, very presumably, for all other molecules involved in stacking interactions. Released DNA reacts promptly with the products with which it is expected to interact, when it is internalized into cells.

Biomolecular and cellular evaluation of Cat-Anionic vesicles in Nano-technology

Before embarking in a study of the potential use of vesicles and similar supra-molecular aggregates in nano-biotechnology, an evaluation of their impact upon living cells is mandatory. The simplest way to investigate the effects of the exposure to vesicles is using cultured cell systems. The first effect that should be examined is the level of cytotoxic action exerted by vesicular suspensions. It should noted that the cytotoxicity is a unique feature for each vesicle type and depends upon on their chemical composition. Furthermore, the cellular/molecular phenomena underlying the toxic effect and subsequent cell death should also be highlighted. We report on cell death, on the possible mechanisms of DNA damage at the basis of this phenomenon and on the nature of the cell death. It is known that a cell dies following essentially the pathways of apoptosis and/or necrosis, even though phenomena such as necroptosis and autophagy are raising increasing interest. All the facets of these modes of cell death have been extensively reviewed in literature [74-78]. The possibilities of specific mRNA, a fundamental nucleic acid in the process of gene expression and protein bio-synthesis, once incorporated into vesicles can be successfully and efficiently transfected into recipient cells are discussed.

Evaluation of vesicle cytotoxicity and their individual components: involvement of DNA damage

The cytotoxic action of the individual surfactants SDS, CTAB and DDAB is exerted at differential extent on HEK293. The CTAB component is more toxic than SDS (Fig. 7.8, Left panel). The mortality rate is directly proportional to the concentration for both surfactants. Unpublished data from our laboratory showed that DDAB is *per se* dramatically more toxic than CTAB. Analysis of the cyto-toxicity of two different vesicles species: SDS-CTAB and SDS-DDAB, (Fig. 7.8, Center panel) shows that the latter ones are far more toxic than the SDS-CTAB ones. It is plausible to ascribe this higher toxicity to the intrinsic noxious action of DDA, although it cannot be ruled out that the association of the two chemical species may play a synergistic role. In any case, SDS-CTAB vesicles, due to their lower toxicity as compared to SDS-DDAB, are better candidates for the delivery of biological macromolecules and/or small molecules of industrial and biomedical interest. The cytotoxicity of SDA-CTAB vesicles with bound RNA results in a slight increase in cell mortality (Figure 7.8, Right panel): this may be ascribed to the commonly accepted toxic effect of free, non-vesicle associated, RNA present in the mixture.
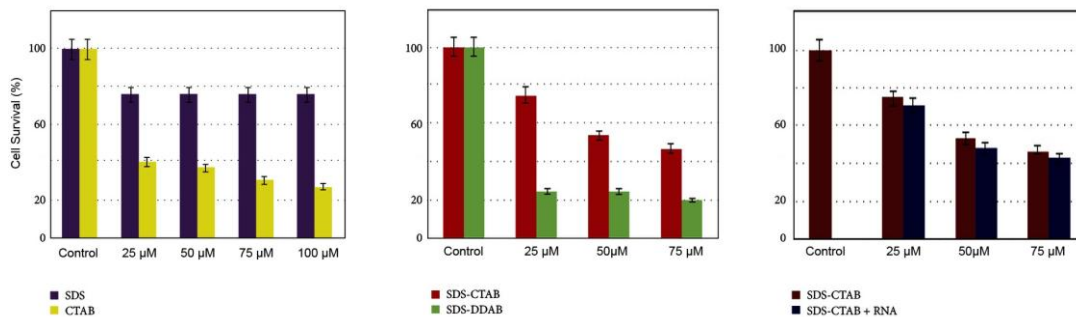
FIGURE 7.8

Effect of the separate surfactants and vesicles on the viability of HEK-293 cells. Left panel: Purple bars show the toxic effects of SDS and, CTAB (yellow bars). Center panel: Compared cytotoxicity of vesicles formed with SDS-CTAB (red bars) and SDS-DDAB (green bars). (Right panel) Cytotoxicity of vesicle/RNA lipoplexes. In all cases: Cell viability was assessed by the colorimetric Mossman assay [79]. The error bars indicate the Standard Error of the Mean.

The toxic effect of cat-anionic vesicles is dose and time-dependent as evidenced by the time course of the exposure time (Figure 7.9, Upper and Center Panel, respectively). Shorter treatment times with the vesicles do not significantly affect the cell survival. Interestingly, human tumor cells lines, such as HL60 and HeLa, are in general more sensitive as compared to the normal murine fibroblast line 3T6 (Figure 7.9 of the bottom panel). This phenomenon can be rationalized on the basis of the different structure membrane of tumor cells as compared to the normal one. Permeability may also play a crucial role since the virtual intracellular concentration of vesicles, in the case of tumor cells, could be higher than in normal ones (See also the following section for a detailed discussion of the possible role of the plasma membrane fluidity) [24]. Finally, at low concentration tumor cells do not respond significantly to the treatment thus suggesting that this population is not homogeneous but includes an intrinsically more resistant sub-population.

It is interesting to acsertain whether cytotoxicity is directly involved in a possible damage at DNA level. As shown by TUNEL assay [24], DNA undergoes a severe fragmentation in vesicle-treated cells thus suggesting a significant DNA damage which is visualized by fluorescent labelling both at single strand and double helix level (Figure 7.10, Center panel).
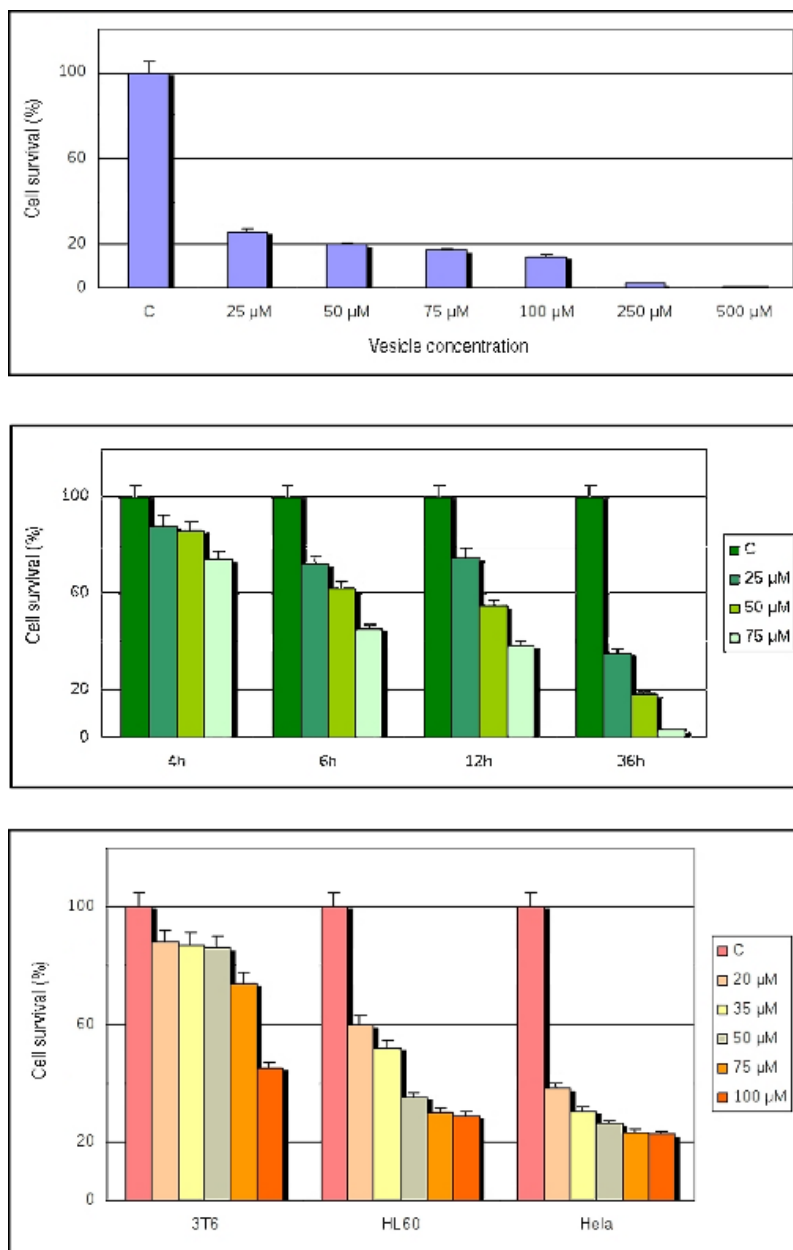
FIGURE 7.9

Dose, Time, and Differential Sensititvity to SDS-CTAB vesicles. (Upper Panel) Cytotoxity of vesicles at 24 hours of treatment. SDS-CTAB vesicles show a pronounced cytotoxicity eve at a concentration as low as 25 μM. (Center Panel) Effect of concentration and time dependence of vesicles ctyotoxicity. Murine fibroblasts 3T6 were grown in the presence of vesicles at the indicated concentration and time. (Bottom Panel) Cytoxicity of cat-anionic vesicle on different cell lines. Cells were treated with vesicles for 4 hours. After this treatment the cytotoxic effect of vesicles is minimal (see results of the previous figure). The cell types and vesicle concentrations are indicated in the figure. In all cases: Cell viability was assessed by the colorimetric Mossman assay [79]. The error bars indicate the Standard Error of the Mean.
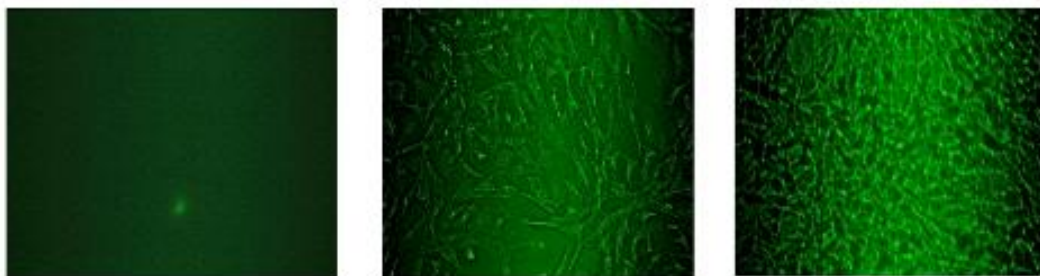
FIGURE 7.10

TUNEL assay for the evaluation of dell death. (Left panel) Untreated cells. (Center Panel) Cells (3T6) exposed to 35 µM vesicles for 24 hours. (Right Panel) Cells treated with H_2O_2 (positive control). In panel B an evident DNA fragmentation indicated by the specific fluorescent reaction, which is a sign of cell death, is present with respect to the untreated cells.

This is consistent with the cytotoxicity data discussed above: as matter of fact a heavy DNA damage may become not compatible with cell survival. However, the combined data of the toxicity tests, measured by the MTT assay [79] and the TUNEL results [24, 80], do not rule out the possibility that a defective proliferation, rather than actual cell death, is being observed or a combination of both events. A second good candidate to ascertain the mode of cell death is represented by measuring the level of membrane lipoperoxidation which is a good diagnostic of the response to an oxidative stress damage at membrane level. The role of the plasma membrane as a target for cat-anionic vesicles emerges from studies on the biochemical alterations of the lipid bi-layer as discussed in following section.

Cell death after exposure to vesicles: role of the plasma membrane alterations and level of apoptotic markers

Malonal dihaldehyde (MDA) is a compound not present in "healthy" cells but derives from the peroxidation of the poly-unsaturated fatty acids [79 - 81]. This molecule reacts with the free amino-groups of proteins, of phospholipids and/or with nucleic acids forming stable covalent bonds that eventually determine a loss of membrane fluidity, which is the basis of its functional *deficit* [82, 83]. Incidentally, alterations of the membrane fluidity have been also observed after interaction with liposomes formed with DMPC and DMPC/gemini [84] and after treatment with a non-cytotoxic natural compound [85] as well as after viral infection [86]. As shown in figure 7.11, the intracellular concentration of MDA in vesicle-treated cells is about two-fold higher as compared to controls, therefore the treatment with vesicles causes a serious oxidative stress with consequent damage at membrane level.

Combined data of the cytotoxic effect of SDS-CTAB vesicles, of the damage at the DNA level observed by TUNEL reaction and of the membrane lipoperoxidation, imply that the cell death observed after exposure to SDS-CTAB vesicles is essentially attributable to a membrane insult. A good tool to evaluate the role of this damage in the activation of the cell death process is provided by the assessment of three main phenomena*: i.e*. the activation of the enzyme poly-ADP-ribose polymerase (PARP), the mitochondrial release of cytochrome c and the expression of genes involved in the apoptotic process.
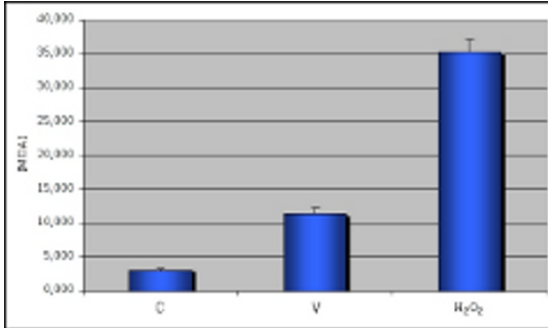
FIGURE 7.11

Lipo-peroxidation assay performed of vesicle-treated cells. Cells (3T6) were treated with vesicles for 4 hours at 75 µM. Non-treated cells were the negative control while H_2O treated cells represented the positive control. The comparison between the effect of H_2O_2 and vesicles is purely qualitative and no quantitative information can be inferred. The errors bars indicate the Standard Error of the Mean.

In particular PARP constitutes an important hallmark of apoptosis. This nuclear enzyme is activated following DNA damage and is commonly utilized as diagnostic of an on-going apoptotic process. PARP is a target of the proteolytic cleavage operated by caspases, a class of cysteine-aspartic acid proteases, which play an essential role in the apoptotic process [24, 86, 87]. In untreated cells, PARP is not cleaved by caspases (thus it appears as a single band appears after immuno-blotting (Fig 7.12). In contrast, in vesicle-treated cells the immuno-reaction evidences two different bands (with molecular weight of 116 and 85 kDa, respectively), and the amount of the cleaved fragment increases with concentration of vesicles. Hence, the treatment of cells with SDS-CTAB vesicles stimulates the expression of the caspases which cleave and inactivate PARP: the end of the biochemical story is failure to repair DNA resulting in the progression of the apoptotic process.
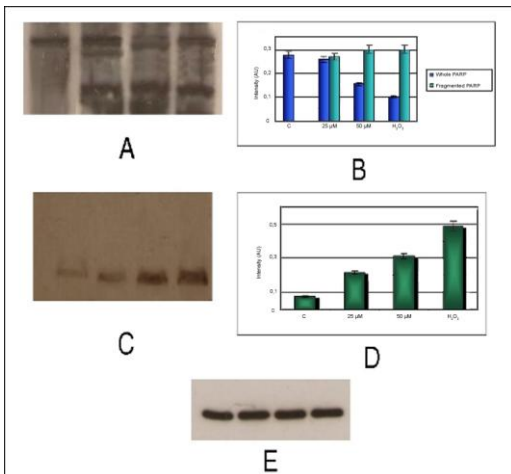
FIGURE 7.12

Evaluation of apoptotic markers. Poly (ADP-Ribose) Polymerase (PARP). Western blot pattern (Panel A) and quantitative analysis of full-length and cleaved PARP in control cells and vesicles treated cells (Panel B). Mitochondrial release of cytochrome c Western blot pattern (Panel C) and quantitative analysis of cytochrome c (Panel D). The errors bars indicate the Standard Error of the Mean. Panel E: Actin control gene.

The release of cytochrome c from mitochondria signals unleashes apoptotic progression. Our laboratory suggests that the treatment of cells with SDS-CTAB vesicles results in a higher permeability of the mitochondrial membrane, thus causing the release of cytochrome c in the cytoplasmic matrix. In any case, a further support to the idea that exposure to SDS-CTAB vesicles activates the apoptotic pathway is shown by PCR amplification of specific DNA markers. In particular the expression of Bcl-2 gene is drastically reduced in cells exposed to cat-anionic vesicles. This gene codes for a protein located at the membrane level where it prevents the cytoplasmic release of death factors. In conclusion, these data strongly suggest that exposure to SDS-CTAB vesicles is a primary cause of membrane damage thus causing cell death via activation of the apoptotic pathway.
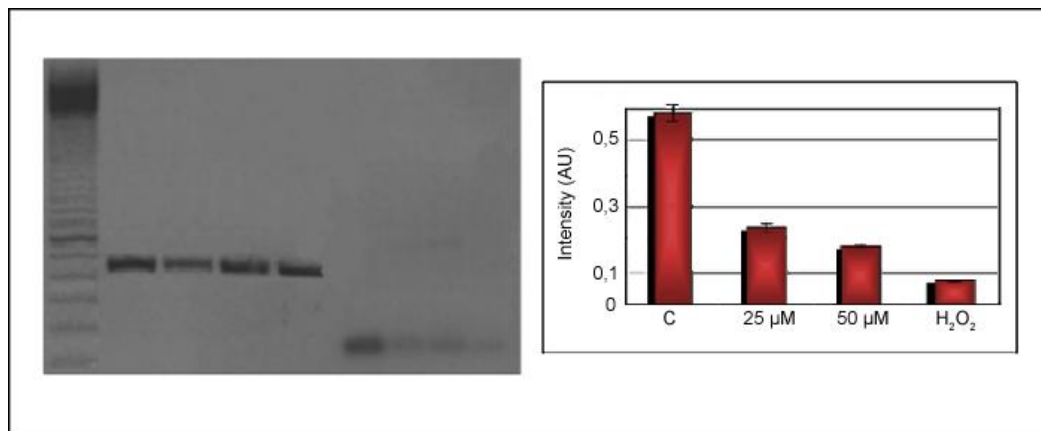
FIGURE 7.13
Amplification of the bcl-2 gene RNA by RT-PCR. (Left panel) Lanes 1 – 4: Actin control gene. Lane 5. Untreated control cells. Lanes 6 and 7: Cells treated with 25 and 50 μM vesicles, respectively. Lane 8: Cells treated with H_2O_2. (Right panel) Quantification of the Westrn blot data shown in the Left panel.

Cat-anionic vesicles do show cytotoxic action at relatively high concentrations and interestingly, they are more toxic towards human tumor cells than normal stabilized murine fibroblasts. This effect, as mentioned above, may be explained by an intrinsic different membrane permeability of tumor cells with respect to normal ones as also discussed in the "classical" works by Van Blitterswijk and Shinitzki [89 - 91]. The data discussed allows us to conclude that the cell membrane is possibly the main target of the SDS-CTAB vesicles. This emerges from the membrane lipoperoxidation assays in which the main product of oxidative stress, MDA, is significantly increased in vesicle-treated cells. The level of DNA damage, the levels of death markers and the higher permeability of the mitochondrial membrane lead to the conclusion that cell death occurs via the activation of the apoptotic pathway. However, the cytotoxic effects of SDS-CTAB are monitored at relatively high concentrations, possibly above the ones normally used in pharmacological application. The possibility of using supra-molecular aggregates in nano-biotechnology for the delivery of molecules as diverse as nuclear acids, proteins and small molecules of pharmaceutical interest remains.

RNase protection assay: Transfection of Chloramphenicol-Acetyl-Transferase reporter mRNA

A powerful tool to measure the expression of nucleic acid after transfection into recipient cells is measuring the level of Chloramphenicol-Acetyl-Transferase (CAT). This is a bacterial enzyme whose

cognate mRNA can be translated into active protein in eukaryotic cells. The rationale of these experiments is that CAT is not normally present in higher cells. The detection of this enzyme is the diagnostic sign that the CAT-mRNA has been successfully transferred across the plasma membrane by the vesicles and, subsequently, translated into protein within the cytoplasm matrix. Experiments where CAT mRNA was transfected into HEK 293 cells, using SDS-CTAB vesicles as molecular vehicles allow the quantification of the intracellular concentration of the enzyme by the immuno-enzymatic assay ELISA. The efficiency of RNA intracellular delivery of our vesicles is apparently lower as compared to Lipofectamine, a commercially available liposome transfection system. This occurs when the CAT mRNA is added to pre-formed vesicle and one can reasonably expect that the CAT mRNA is anchored via electrostatic interactions to the surface of the vesicles and the cargo molecule becomes an easy target for hydrolysis by RNases. This observation is validated by the transfection of naked CAT mRNA is almost totally hydrolyzed by the RNases normally present in the cytoplasm. Messenger RNA exists in a quasi-linear molecular configuration, which is easily hydrolyzed by the resident RNases. Figure 7.14 shows that the immuno-reaction between the CAT-protein and anti-CAT antibody is, as expected, almost absent in the case of the transfection with naked CAT-mRNA (bar to the right); this is consistent with the idea that the RNA is demolished by the RNases present in the cytoplasm and therefore becomes unavailable to be translated into protein. The transfection efficiency at the indicated concentrations of SDS-CTAB, is indeed lower that the one exhibited by Lipofectamine (Bar to the left) but, in any case is quite satisfactory.
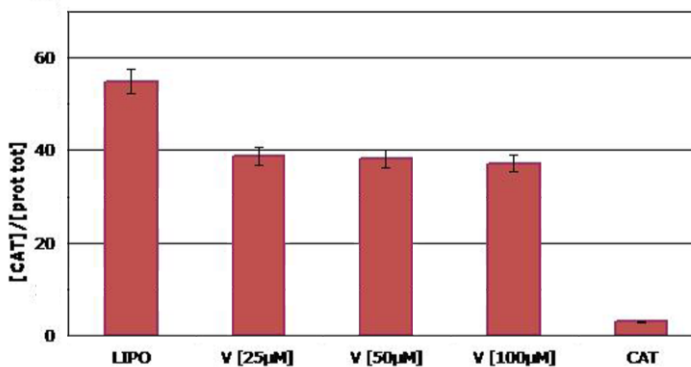
FIGURE 7.14
Transfection efficiency of mRNA-CAT. In this experiment, the RNA was added to pre-formed vesicles. The intracellular level of CAT is lower in the case of SDS-CTAB vesicles as compared to a commercial transfection system (Lipofectamine™). See text for further details. LIPO (Lipofectamine) ; V[25μM] (25 μM vesicle concentration) ; V[50μM] (50μM vesicle concentration) ; V[100μM] (100μM vesicle concentration) ; CAT (naked CAT mRNA).(Figura 5 Paper Laura).

The situation changes dramatically when the vesicles are formed in the presence of CAT-mRNA. In this case the RNA would be hosted in the aqueous *lumen* internal to the vesicles. If the lipoplexes thus obtained are transfected into the cells, the RNA is protected by the nucleolytic attack and this results in an improved delivery of the cargo molecule. Therefore a significant increase of the transfecting performance of the vesicles is monitored (Figure 7.15).
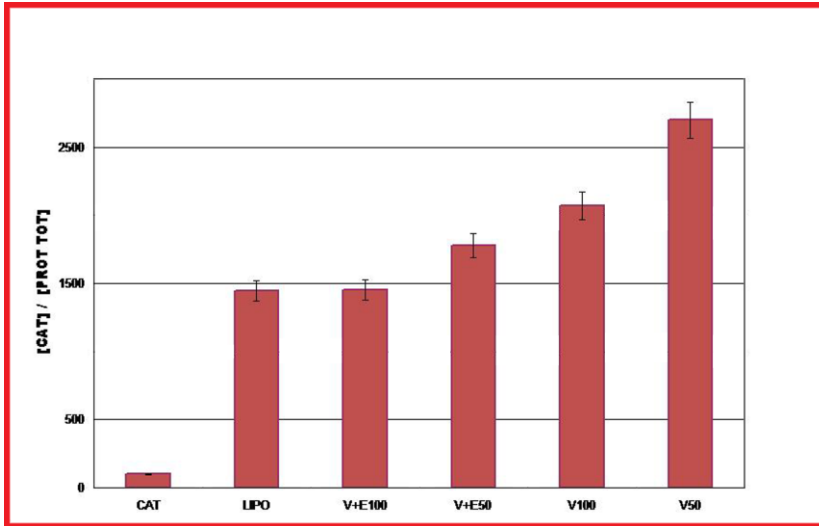
FIGURE 7.15

Transfection efficiency of mRNA-CAT of vesicles formed in the presence of RNA and after treatment with RNase. In this experiment, the mRNA-CAT was added to the surfactant mixture prior to the vesicle formation. This results strongly suggests that the RNA is internalized within the vesicle aqueous space and it thus protected by the nucleolytic attack. Interestingly, vesicles not treated with RNase (last two bars to the right) exhibit a higher efficiency than Lipofectamine. LIPO (Lipofectamine); V+E (Vesicles + RNase); V (Vesicles not treated with RNase); CAT (naked CAT mRNA). The numbers at the bottom of the bar indicate the vesicle concentration (μM).

This strongly suggests that actually the RNA molecule is internalized and protected within the vesicle. Subsequent to trasfection, the CAT-mRNA is released in the cytoplasm where is translated into protein. The last set of experiments discussed the role the storage temperature from previous evidence from our laboratory [68, 72, 73] implicates that vesicles are quite stable in a temperature range of 15-25 °C. Actually freezing damages the molecular integrity of the vesicles, thus abolishing their transfection efficiency. Freezing almost abrogates the transfection capacity of the SDS-CTAB vesicles since the translation of the CAT-mRNA drops almost to the same level as the one exhibited by the naked RNA (Figure 7.16, first bar to the left).

Therefore, it is reasonable assuming that the freezing process disrupts the supra-molecular organization of the vesicles. Consequently their role as potential molecular bio-machines for the delivery of bioactive polymers is abrogated [91].
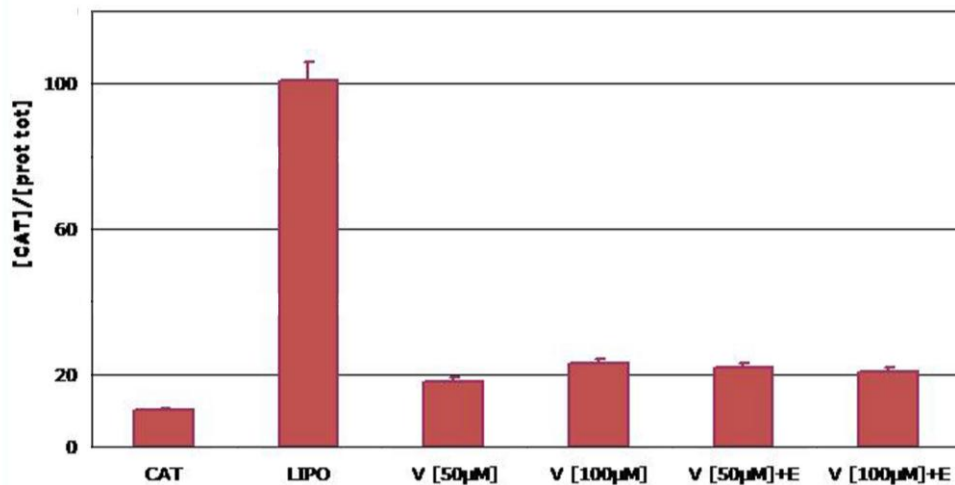
FIGURE 7.16
Effect of freezing on the transfection efficiency. Vesicles formed in the presence of mRNA-CAT and kept frozen at -20 °C for 24 hours. After thawing, the aggregates were treated with RNase and transfected into HEK-293 cells. Data clearly indicate that the Rnase treatment almost abolishes the translation of CAT mRNA into protein. LIPO (Lipofectamine); V[25µM] (25 µM vesicle concentration) ; V[50µM] (50µM vesicle concentration) ; V[100µM] (100µM vesicle concentration) ; CAT (naked CAT mRNA).

Conclusions

Data presented in this contribution clearly indicate the strict relations between the structural organization of surfactants to form vesicular carriers and the related biological performances. From a functional point of view, the efficiency in biopolymer binding is directly related to the nature of the reported vesicles, that is their size and surface charge density. The major contribution to the binding efficiency is due to electrostatic effects, which ensures good stability to the resulting lipo-plexes and substantial possibility to their release from vesicles, when the latter are internalized into cells. Toxicity can be modulated by changing the surfactants or lipids to be used in the preparation of effectively biocompatible formulations.

The results obtained indicate that the cell membrane is possibly the main target of SDS-CTAB vesicles. This emerges from the membrane lipoperoxidation assays in which the main product of oxidative stress, MDA, is significantly increased in vesicle-treated cells. The level of DNA damage, the levels of death markers as well as the higher permeability of the mitochondrial membrane, imply that cell death occurs via the activation of the apoptotic pathway. In any case, the cytotoxic effects of SDS-CTAB vesicles are monitored at relatively high concentrations. The possibility of using supra-molecular aggregates in nano-biotechnology for the delivery of diverse molecules, remains still open.

The interaction of CAT-mRNA with the vesicles causes its internalization within the supra-molecular aggregate. This is the first example of an mRNA being delivered within a cell and translated into a properly folded conformation as shown by the data obtained with the experiment of RNA protection.

The ELISA approach in fact evidences the interaction antigen/antibody (CAT-protein/antiCAT antibody) only if the antigen is found in the proper and presumably active molecular structure.

Finally, one interesting aspect, yet to be investigated in detail, is the mode of cell death. Previous evidence from our laboratory indicates that administration of vesicles to cultured causes apoptosis. This is a multi-step and very complex mode for a cell to die. Therefore, the elucidation of the key step(s) in the process of cell death may help the investigators engaged in this field, to set up the best experimental conditions in which, to minimal cell mortality, corresponds an optimal delivery of the cargo molecule of biotechnological interest.

Acknowledgments

Obituary

During the preparation of this manuscript we were informed that Ali Khan (formerly at Phys. Chem. 1, Lund University, Sweden), passed away. Since the end of 80's, he was one of the first scientists involved in cat-anionic vesicular systems (and in many other subjects). Ali generously shared his deep competences and collaborated with many scientists, who are honored to have been his students and collaborators. One author of this contribution (CLM) knew Ali since more than thirty years and was in friendly relations with him since that time; others knew him from his important activity in the field. We remember him friendly and dedicate this manuscript to his memory. Our condolences are for Lena, his wife, and his beloved sons Malek, Jamil, and Omar.

References

1. Richard, A.; Bourel-Bonnet, L. Internalization of a peptide into multi-lamellar vesicles assisted by the formation of an α-oxo oxime bond. *Chemistry- A European Journal*, 2005, *11*, 7315-7321.
2. Samaj, J.; Baluska, F.; Voigt, B.; Volkmann, D.; Menzel, D. Endocytosis and actomyosin cytoskeleton. *Plant Cell Monographs*, 2006, *1*(Plant Endocytosis), 233-244.
3. Liu, Y.-C.; Le N., Anne-Laure M.; Schmidt, J.; Talmon, Y.; Chmelka, B.F.; Lee, C.T. Jr. Photo-Assisted Gene Delivery Using Light-Responsive Cat-anionic Vesicles. *Langmuir*, 2009, *25*, 5713-5724.
4. Jiang, Y.; Li, F.; Luan, Y.; Cao, W.; Ji, X.; Zhao, L.; Zhang, L.; Li, Z. Formation of drug/surfactant catanionic vesicles and their application in sustained drug release. *Int. J. Pharm.*, 2012, *436*, 806-814.
5. Soussan, E.; Cassel, S.; Blanzat, M.; Rico-Lattes, I. Drug delivery by soft matter: matrix and vesicular carriers. *Angew. Chem. Int. Ed.*, 2009, *48*, 274-288.
6. Kwon, G.S.; Kataoka, K. Block copolymer micelles as long-circulating drug vehicles. *Adv. Drug Delivery Rev.*, 1995, 1*6*, 295-309.
7. Kainthan, R.K.; Janzen, J.; Levin, E.; Devine, D.V.; Brooks, D.E. Biocompatibility testing of branched and linear Polyglycidol. *Biomacromolecules*, 2006, *7*, 703-709.
8. Francis, M.F.; Cristea, M.; Winnik, F.M. Polymeric micelles for oral drug delivery: Why and how. *Pure Appl. Chem.*, 2004, *76*, 1321-1335.
9. Hawker, C. J.; Frechet, J.M.J. Preparation of polymers with controlled molecular architecture. A new convergent approach to dendritic macromolecules. *J. Am. Chem. Soc.*, 1990, *112*, 7638-7647.
10. Junping, W.; Takayama, K.; Nagai, T.; Maitani, Y. Pharmacokinetics and antitumor effects of Vincristine carried by microemulsions composed of PEG-lipid, oleic acid, vitamin E and cholesterol. *Intern. J. Pharm.*, 2003, *251*, 13-21.
11. Bhattacharya, S.; De, S.; Subramanianm M. Synthesis and vesicle formation of hybrid bolaphile/amphiphile ion pairs. Evidence of membrane property modulation by molecular design. *J. Org. Chem.*, 1998, *63*, 7640-7651.
12. Barenholz, Y.; Peer, D. Liposomes, lipid biophysics, and sphingolipid research: from basic to translation research. *Chem. Phys. Lipids*, 2012, *165*, 363-364.
13. Kocer, A. Functional liposomal membranes for triggered release. *Methods Mol. Biol.*, 2010, *605*(Liposomes, Vol. 1), 243-255.
14. Kim, S.-H.; Kim, K.-S.; Lee, S.-R.ae; Kim, E.; Kim, M.-S.; Lee, E.-Y.; Gho, Y.S.; Kim, J.-W.; Bishop, R.E.; Chang, K.-T. Structural modifications of outer membrane vesicles to refine them as vaccine delivery vehicles. *Biochim. Biophys. Acta, Biomembranes*, 2009, *1788*, 2150-2159.
15. Kahya, N.; Merkle, D.; Schwille, P. Pushing the complexity of model bilayers: novel prospects for membrane biophysics. *Springer Ser. Fluorescence*, 2008, *4* (Fluorescence of Supermolecules, Polymers, and Nanosystems), 339-359.
16. Marques, E.F.; Brito, R.O.; Silva, S.G.; Rodriguez-Borges, J. E.; do Vale, M.L.; Gomes, P.; Araujo, M.J.; Soderman, O. Spontaneous Vesicle Formation in Cat-anionic Mixtures of Amino Acid-Based Surfactants: Chain Length Symmetry Effects. *Langmuir*, 2008, *24*, 11009-11017.
17. Bonincontro, A.; Spigone, E.; Ruiz Peña, M.; Letizia, C.; La Mesa, C. Lysozyme binding onto cat-anionic vesicles. *J. Colloid Interface Sci.*, 2006, *304*, 342-347.

18. Colomer, A.; Pinazo, A.; Garcia, M.T.; Mitjans, M.; Vinardell, M. P. Infante, M.R.; Martinez, V.; Perez, L. pH-sensitive surfactants from lysine: assessment of Their Cytotoxicity and Environmental Behavior. *Langmuir*, 2012, *28*, 5900-5912.
19. Mukerjee, P.; Mysels, K.J. Critical Micellar Concentrations of aqueous Surfactant Systems. Natl. Bur. Std. Ser., *NSRDS-NBS 36*, Washington D.C. 1971.
20. Israelachvili, J.N.; Mitchell, D. John; Ninham, B.W. Theory of self-assembly of lipid bilayers and vesicles. *Biochim. Biophys. Acta, Biomembranes*, 1977, *470*, 185-201.
21. Kuo, B.J.H.; Jan, M.S.; Chang, C.H.; Chiu, H.W.; Li, C.T. Cytotoxicity characterization of catanionic vesicles in RAW 264.7 murine macrophage-like cells. *Colloids Surf. B: Biointerfaces*, 2005, *41*, 189-196.
22. Colomer, A.; Pinazo, A.; Garcia, M.T.; Mitjans, M.; Vinardell, M. P. Infante, M.R.; Martinez, V.; Perez, L. pH-sensitive surfactants from lysine: assessment of Their Cytotoxicity and Environmental Behavior. *Langmuir*, 2012, *28*, 5900-5912.
23. Cheng LC, Jiang X, Wang J, Chen C, Liu RS. Nano-bio effects: interaction of nanomaterials with cells. Nanoscale. 2013 May 7;5(9):3547-69.
24. Aiello, C.; Andreozzi, P.; La Mesa, C.; Risuleo, G. Biological activity of SDS-CTAB cat-anionic vesicles in cultured cells and assessment of their cytotoxicity ending in apoptosis. *Colloids Surf. B: Biointerfaces*, 2010, 78, 149-154.
25. Nogueira, D. R.; Mitjans, M.; Infante, M.R.; Vinardell, M.P. Comparative sensitivity of tumor and non-tumor cell lines as a reliable approach for in vitro cytotoxicity screening of lysine-based surfactants with potential pharmaceutical applications. *Intern. J. Pharm.*, 2011, *420*, 51-58.
26. Multi-compartmental oral delivery systems for nucleic acid therapy in the gastrointestinal tract. Kriegel C, Attarwala H, Amiji M. *Adv Drug Deliv Rev*. 2013 Jun 15;65(6):891-901.
27. Guo P, Haque F, Hallahan B, Reif R, Li H. Uniqueness, advantages, challenges, solutions, and perspectives in therapeutics applying RNA nanotechnology. *Nucleic Acid Ther*. 2012 *Aug*;22:226-45.
28. Jokela, P.; Jönsson, B.; Wennerström, H. Phase equilibria in a system containing both an anionic and a cationic amphiphile. A thermodynamic model calculation. *Progr. Colloid Polym. Sci.*, 1985, *70*, 17-22.
29. Jokela, P.; Jönsson, B. Phase equilibria of catanionic surfactant-dodecanol-water systems. *J. Phys. Chem.*, 1988, *92*, 1923-1927.
30. Jokela, P.; Jönsson, B.; Eichmueller, B.; Fontell, K. Phase equilibria in the sodium octanoate octylammonium octanoate-water system. *Langmuir*, 1988, *4*, 187-192.
31. Jönsson, B.; Jokela, P.; Khan, A.; Lindman, B.; Sadaghiani, A. Catanionic surfactants: phase behavior and microemulsions. *Langmuir*, 1991, *7*, 889-895.
32. Marques, E.F. Size and Stability of Catanionic Vesicles: Effects of Formation Path, Sonication, and Aging. *Langmuir*, 2000, *16*, 4798-4807.
33. Brasher, L.L.; Herrington, K.L.; Kaler, E.W. Electrostatic effects on the phase behavior of aqueous cetyltrimethylammonium bromide and sodium octylsulfate mixtures with added sodium bromide. *Langmuir*, 1995, *11*, 4267-4277.
34. Yatcilla, M.T.; Herrington, K.L.; Brasher, L.L.; Kaler, E.W.; Chiruvolu, S.; Zasadzinski, J.A. Phase behavior of aqueous mixtures of cetyltrimethylammonium bromide (CTAB) and sodiumoctylsulfate (SOS). J. Phys. Chem., 1996, 100, 5874-5879.

35. Brasher, L.L.; Kaler, E.W. A small angle neutron scattering (SANS) contrast variation investigation of aggregate composition in catanionic surfactant mixtures. *Langmuir*, 1996, *12*, 6270-6276.

36. Barbetta, A.; Pucci, C.; Tardani, F.; Andreozzi, P.; La Mesa, C. Size and Charge Modulation of Surfactant-Based Vesicles *J. Phys. Chem. B*, 2011, *115*, 12751-12758.

37. Kamenka, N.; Chorro, M.; Talmon, Y.; Zana, R. Study of mixed aggregates in aqueous solutions of sodium dodecyl sulfate and dodecyltrimethylammonium bromide. *Colloids Surf.*, 1992, *67*, 213-222.

38. Söderman, O.; Herrington, K.L.; Kaler, E.W.; Miller, D.D. Transitions from micelles to vesicles in aqueous mixtures of anionic and cationic surfactants. *Langmuir*, 1997, *13*, 5331-5338.

39. Marques, E. F.; Regev, O.; Khan, A.; Grac¸a Miguel, M.; Lindman, B. Vesicle Formation and General Phase Behavior in the Catanionic Mixture SDS-DDAB-Water. The Anionic-Rich Side. *J. Phys. Chem. B*, 1998, *102*, 6746-6758.

40. Marques, E. F.; Regev, O.; Khan, A.; Graca Miguel, M.; Lindman, B. Vesicle formation and general phase behavior in the catanionic mixture SDS-DDAB-water. The cationic-rich side. *J. Phys. Chem. B*, 1999, *103*, 8353-8363.

41. Zumpano, R.C. Cat-anionic vesicles made of dioctyldimethylammonium bromide and Aerosol OT. *Thesis*, 2013, La Sapienza University, Rome, Italy.

42. Pucci C., Salvia A., Ortore M.G.; La Mesa C. The DODAB/AOT/water system: vesicle formation and interactions with salts, or synthetic poly-electrolytes. *Soft Matter*, 2013, *9*, 9000-9007.

43. Jung, H.T.; Coldren, B.; Zasadzinski, J.A.; Iampietro, D.J.; Kaler, E.W. The origins of stability of spontaneous vesicles. *Proc. Natl. Acad. Sci. U.S.A.*, 2001, *98*, 1353-1357.

44. Iampietro, D.J.; Brasher, L.L.; Kaler, E.W.; Stradner, a.; Glatter, O. Direct analysis of SAXS and SANS measurements of catanionic surfactant mixtures by Fourier transformation. *J. Phys. Chem. B*, 1998, *102*, 3105-3113.

45. Youssry, M.; Coppola, L.; Marques, E.F.; Nicotera, I. Unravelling micellar structure and dynamics in an unusually extensive DDAB/bile salt catanionic solution by rheology and NMR diffusometry. *J. Colloid Interface Sci.*, 2008, *324*, 192-198.

46. Barran-Berdon, A.L.; Munoz-Ubeda, M.; Aicart-Ramos, C.; Perez, L.; Infante, M.-R.; Castro-Hartmann, P.; Martin-Molina, A.; Aicart, E.; Junquera, E. Ribbon-type and cluster-type lipoplexes constituted by chiral lysine based cationic gemini lipid and plasmid DNA. *Soft Matter*, 2012, *8*, 7368-7380.

47. Lozano,N.; Pinazo, A.; La Mesa, C.; Perez, L.; Andreozzi, P.; Pons, R. Catanionic Vesicles Formed with Arginine-Based Surfactants and 1,2-Dipalmitoyl-*sn*-glycero-3-phosphate Monosodium Salt. *J. Phys. Chem. B*, 2009, *113*, 6321–6327.

48. Caria, A.; Khan, A. Phase Behavior of Catanionic Surfactant Mixtures: Sodium Bis(2ethylhexyl) sulfosuccinate-Didodecyldimethylammonium bromide-Water System. *Langmuir*, 1996, *12*, 6282-6290.

49. Karukstis, K.K.; Zieleniuk, C.A.; Fox, M.J. Fluorescence Characterization of DDAB-AOT Catan-ionic Vesicles. *Langmuir*, 2003, *19*, 10054-10060.

50. Hartley, G.S. "*Aqueous Solutions of paraffin chain salts*." Herman, Paris, 1936.

51. Tanford, C. "*The hydrophobic effect: formation of micelles and biological membranes.*", 2nd Ed.; 1980, Wiley, New York.

52. Israelachvili, J.N.; Mitchell, D.J.; Ninham, B.W. Theory of self-assembly of hydrocarbon amphiphiles into micelles and bilayers. *J. Chem. Soc. Faraday Trans. 2*, 1976, *72*, 1525-1568.

53. Ninham, B.W.; Evans, D.F. The Rideal Lecture: Vesicles and molecular forces. *Faraday Disc. Chem. Soc.*, 1986, *81*, 1-17.
54. Parker, A.; Fieber, W. Viscoelasticity of anionic wormlike micelles: effects of ionic strength and small hydrophobic molecules. *Soft Matter*, 2013, *9*, 1203-1213.
55. Kamaya, Hi.; Matubayasi, N.; Ueda, I. Biphasic effect of long-chain n-alkanols on the main-phase transition of phospholipid vesicle membranes. *J. Phys. Chem.*, 1984, *88*, 797-800.
56. Kokot, Z. Effect of NaCl and temperature on sodium dodecyl sulfate mixed micelles. *Chemia Analityczna*, (Warsaw, Poland), 2001, *46*, 823-829.
57. Soubeyrand, V.; Luparia, V.; Williams, P.; Doco, T.; Vernhet, A.; Ortiz-Julien, A.; Salmon, J.-M. Formation of micelles containing solubilized sterols during rehydration of active dry yeasts Improves their fermenting capacity. *J. Agric. Food Chem.*, 2005, *53*, 8025-8032.
58. Srinivasan, V.; Blankschtein, D. Effect of Counterion Binding on Micellar Solution Behavior: 1. Molecular-Thermodynamic Theory of Micellization of Ionic Surfactants. *Langmuir*, 2003, *19*, 9932-9945.
59. Stigter, D.; Dill, K.A. Free Energy of electrical double layers: entropy of adsorbed ions and the binding polynomial. *J. Phys. Chem.*, 1989, *93*, 6737-6743.
60. Zasadzinski, J.A.; Jung, H.-T.; Coldren, B.; McElvey, C.; Kaler, E.W. The origins of stability of equilibrium vesicles. *221st ACS Natl. Meeting,* San Diego, CAL, U.S.A., 2001, COLL. 053.
61. Safran, S.A.; Pincus, P.A.; Andelman, D.; MacKintosh, F.C. Stability and phase behavior of Mixed surfactant vesicles. *Phys. Rev. A*, 1991, *43*, 1071-1078.
62. MacKintosh, F.C.; Safran, S.A. Stability and phase behavior of mixed-surfactant vesicles. *Mater. Res. Soc. Symposium Proc.*, 1992, *248* (Complex Fluids), 11-21.
63. Andreozzi, P.; Funari, S.S.; La Mesa, C.; Mariani, P.; Ortore, M.G.; Sinibaldi, R.; Spinozzi, F. Multi- to Unilamellar Transitions in Catanionic Vesicles. *J. Phys. Chem. B*, 2010, *114*, 8056-8060.
64. Silva, B.F.B.; Marques, E.F. Thermotropic behavior of asymmetric chain length catanionic surfactants: The influence of the polar head group. *J. Colloid Interface Sci.*, 2005, *290*, 267-274.
65. Regev, O.; Backov, R.; Faure C. Gold nanoparticles spontaneously generated in onion-type multilamellar vesicles. Bilayers particle coupling imaged by cryo-TEM. *Chem. Mater.*, 2005, *16*, 5280-5285.
66. Marques, E.F.; Regev, O.; Khan, A.; Lindman, B. Self-organization of double-chained and
a. pseudodouble-chained surfactants: counterions and geometry effect. *Adv. Colloid Interface Sci.*, 2003, *100-102*, 83-104.
67. Bordi, F.; Cametti, C.; Diociauti, M.; Gaudino, D.; Gili, T.; Sennato, S. Complexation of anionic polyelecrolytes with cationic liposomes: evidence of reentrant condensation and lipolexes formation. *Langmuir*, 2004, *20*, 5214-5222.
68. Letizia, C.; Andreozzi, P.; Scipioni, A.; La Mesa, C.; Bonincontro, A.; Spigone, E. Protein Binding onto Surfactant-Based Synthetic Vesicles. *J. Phys. Chem. B*, 2007, *111*, 898-908.
69. Stilbs, P. Fourier transform pulsed-gradient spin-echo studies of molecular diffusion. *Progr. NMR Spectrosc.*, 1987, *19*, 1-45.
70. Stejskal, E.O.; Tanner, J.E. Spin diffusion measurements: spin echoes in the presence of a time dependent field gradient. *J. Chem. Phys.*, 1965, *42*, 288-292.
71. Pucci, C.; Scipioni, A.; La Mesa, C. Albumin binding onto synthetic vesicles. *Soft Matter*, 2012, *8*, 9669-9675.

72. Bonincontro, A.; La Mesa, C.; Proietti, C.; Risuleo, G. A Biophysical Investigation on the Binding and Controlled DNA Release in a Cetyltrimethylammonium Bromide-Sodium Octyl Sulfate Cat-Anionic Vesicle System. *Biomacromolecules*, 2007, *8*, 1824-1829.

73. Bonincontro, A.; Falivene, M.; La Mesa, C.; Risuleo, G.; Ruiz Peña, M. Dynamics of DNA Adsorption on and Release from SDS-DDAB Cat-Anionic Vesicles: a Multitechnique Study. *Langmuir*, 2008, *24*, 1973-1978.

74. Stevens JB, Abdallah BY, Liu G, Horne SD, Bremer SW, Ye KJ, Huang JY, Kurkinen M, Ye CJ, Heng HH. Heterogeneity of cell death. *Cytogenet Genome Res*. 2013;*139*:164-73.

75. McIlwain DR, Berger T, Mak TW. Caspase functions in cell death and disease. *Cold Spring Harb Perspect Biol*. 2013;*5*:a008656.

76. Kaczmarek A, Vandenabeele P, Krysko DV. Necroptosis: the release of damage-associated molecular patterns and its physiological relevance. *Immunity*.2013;*38*:209-23.

77. Tekpli X, Holme JA, Sergent O, Lagadic-Gossmann D. Role for membrane remodeling in cell death: implication for health and disease. *Toxicology*. 2013;*304*:141-57.

78. Chaabane W, User SD, El-Gazzah M, Jaksik R, Sajjadi E, Rzeszowska-Wolny J, LosMJ. Autophagy, apoptosis, mitoptosis and necrosis: interdependence between those pathways and effects on cancer. *Arch Immunol Ther Exp (Warsz)*. 2013;*61*:43-58.

79. Mosmann, T., Rapid colorimetric assay for cellular growth and survival: application to proliferation and cytotoxicity assays. *J. Immunol. Methods* 1983, *65*:55-63.

80. Draper, H.H.; Hadley, M. A review of recent studies on the metabolism of exogenous and endogenous malondialdehyde. *Xenobiotica* 1990, *20*: 901-910.

81. Chancerelle, Y.; Kergonou; J.F.. Immunologic relevance of malonic dialdehyde. *Ann Pharm Fr.* 1995;53241-250.

82. Cazzola R, Russo-Volpe S, Cervato G, Cestaro B. Biochemical assessments of oxidative stress, erythrocyte membrane fluidity and antioxidant status in professional soccer players and sedentary controls. *Eur J Clin Invest.* 2003;*33*:924-30.

83. Bonincontro, A; Di Ilio, V.; Pedata, O.; Risuleo G. . Dielectric properties of the plasma membrane of cultured murine fibroblasts treated with a nonterpenoid extract of Azadirachta indica seeds. *J. Membr. Biol.* 2007, *215*:75-79.

84. Cosimati R,Milardi GL,Bombelli C,Bonincontro A,Bordi F,Mancini G,Risuleo G. Interactions of DMPC and DMPC/gemini liposomes with the cell membrane investigated by electrorotation. *Biochim Biophys Acta.*2013;*1828*:352-6.

85. Milardi GL, Stringaro A, Colone M, Bonincontro A, Risuleo G. The Cell Membrane is the Main Target of Resveratrol as Shown by Interdisciplinary Biomolecular/Cellular and Biophysical Approaches. *J Membr Biol.* 2013. [Epub ahead of print] PubMed PMID: 24166779.

86. Berardi V, Aiello C, Bonincontro A, Risuleo G. Alterations of the plasma membrane caused by murine polyomavirus proliferation: an electrorotation study. *J Membr Biol.* 2009;*229*:19-25.

87. Andrabi SA, Dawson TM, Dawson VL. Mitochondrial and nuclear cross talk in cell death: parthanatos. *Ann N Y Acad Sci.* 2008;*1147*:233-41.

88. Li, J.; Yuan, J. Caspases in apoptosis and beyond *Oncogene* (2008) *27*, 6194–6206.

89. Van Blitterswijk W. J., Van Hoeven R. P. and Van Der Meer B. W., Lipid structural order parameters (reciprocal of fluidity) in biomembranes derived from steady-state fluorescence polarization measurements. *Biochim Biophys Acta.* 1981;*644*:323-32.

90. Van Blitterswijk W. J., in: Physiology of membrane fluidity, CRC Press, Taylor & Francis Group, London UK. Vol. II, 1984

91. Shinitzki M., in: Physiology of membrane fluidity, CRC Press, Taylor & Francis Group, London UK. Vol. I, 1984.

92. Russo L, Berardi V, Tardani F, La Mesa C, Risuleo G. Delivery of RNA and its intracellular translation into protein mediated by SDS-CTAB vesicles: potential use in nanobiotechnology. *Biomed Res Int.* 2013; *2013*:734596.

8

Nanoscale drug delivery systems: An updated view

Khan Farheen Badrealam and Mohammad Owais*

Interdisciplinary Biotechnology Unit, Aligarh Muslim University, Aligarh, Uttar Pradesh, India

Outline:

Introduction

Nanomaterials are the cornerstone of the rapidly advancing field of nanotechnology having potentials to revolutionise diagnostics and therapeutics. The National Nanotechnology Initiative defines nanoscale materials as particle approximately in the 1 -100 nm size regime in at least one dimension. Generally these structures are up to several hundred nanometers in size being fabricated by top-down or bottom-up approaches [1]. Compared to their conventional counterpart, nanoparticulate entities have distinctive physicochemical and biological properties [2]. Many of their properties such as size, shape, chemical composition, surface structure, charge, aggregation and solubility influence their interactions with biomolecules and cells; concomitantly influence the way the encapsulated/attached entity (drugs) behave in the biological system [2]. Owing to their nanoscale effects, increased surface area and other desirable attributes, they are promising tools for the advancement of diagnostic biosensors, drug and gene delivery, and biomedical imaging [3].

In the recent scenario, developments of newer drugs are high on pharma agenda; however, widespread clinical applications of these efficacious drugs are limited. All drugs face several enroute barriers during their journey from their site of introduction to their molecular site of action. Important amongst them includes rapid filtration by the renal system, premature clearance via the reticulo-endothelial system (RES) and their tortuous transport from the bloodstream to target cells within tissues. Basically, at the tissue or cellular target, the drug must overcome the selectively permeable membrane barrier. Within the cell, it must escape the harsh acidic environment of endolysosomes within which biomolecular drugs may be inactivated or degraded and they must also overcome the nuclear membrane barrier and blood-brain barrier (BBB) (in circumstances viz. nuclear acting and CNS drugs). Further, the poor solubilities and poor stabilities of various drugs in the biological milieu represent another daunting challenges [4]. Not surprisingly, recent studies have illustrated particularly promising ways by which nanomaterials can assist in navigating these unformidable barriers. In fact, the application of nanomaterials to drug delivery is broadly expected to change the panorama of pharmaceutical and biotechnological industries [5].

In the present chapter, we have highlighted the prospects of nanomaterials for drug and gene delivery. The current state of the art nanomaterial based platforms for drugs and gene delivery has also been discussed. Moreover, at the end of the chapter, a great deal of discussion describing toxicity issues related with various existing nanoparticles have been collated.

Nanocarriers: Potentials for drug/gene delivery

Nanomaterials have gained great impetus particularly in medicine; in fact the practice of supplanting conventional medical procedures has been set into motion. Formulating therapeutic agents with biocompatible nanocarriers (liposomes, polymers, Inorganic Nanoparticles (NPs) and carbon nanotubes etc.) can subdue many of the associated stumbling blocks. Infact, Nanotechnology enables the innovative utilization of drugs under practices or that has been stalled under various issues. Employing nanomaterials as drug delivery platforms, it may be possible to achieve improved delivery of poorly water-soluble drugs thereby increasing their bioavailability in the biological systems [6,7]. Another unique feature of nanomaterial based drug delivery is their ability to achieve targeted delivery of drugs in cell or tissue specific manner [8]. Generally this is achieved either through passive targeting of drugs to the site of action or by active targeting of the drug employing tailored systems sensitive to different stimuli (e.g. pH, temperature, light, etc.) or systems harbouring tissue/cell specific ligands as detailed in

the text. Basically, owing to their miniature size they can efficiently penetrate through small capillaries to tumors and inflamed tissues, and accumulate at the target site, this indirectly leads to reduction in the unwanted side effects and the toxicity of the therapeutic agent; in parallel enhancing their therapeutic efficacy. They also embody features such as delivery of macromolecular drugs to intracellular sites of action [9,10]. Moreover, they could also mediate controlled release of drugs which not only prolongs action but also attempts to maintain drug levels within the therapeutic window to avoid potentially hazardous peaks in drug concentration following administration of the drugs and thereby maximizes therapeutic efficiency [6,7]. Further, they also provide avenues for co-delivery of two or more drugs or therapeutic modality for combination therapy or systems for simultaneous therapeutic and diagnostic applications [11, 12]; cumulatively imparting several potential advantages including synergistic effects, suppressed drug resistance, and the ability to tune the relative dosage of various drugs to the level of a single nanoparticle (NP) carrier and also leads towards newer therapeutic regimen such as hyperthermia and photodynamic therapy (Figure 8.1). Seemingly, these are just a few of the many compelling reasons that nanomaterials hold enormous promise for improving therapeutic efficacies of drugs by subduing their enroute barriers.

FIGURE 8.1
Advantages of nanomaterial based drug delivery platforms as detailed in the text.

The emergence of nanotechnology has nurtured new prospects for the field of genetic medicine as well. It is well documented that gene therapy has the potential to benefit many untamed diseases. Despite the curability of diseases by restoring or rectifying missing or altered functionalities, as of yet no technically feasible method for gene therapy has been established. Albeit, viral vectors owes potentials to overcome most of their stumbling blocks; besides high transduction efficiency, one

critically important advantage of viral vectors is their appreciable DNA packaging capability. Inspite these advantages, their usage has been of limited application due to their various associated issues such as activation of unwanted immune responses, extreme risk of insertional mutagenesis, high cost of their preparation, safety concerns and constraints in specific tissue targeting [13]. To overcome these shortcomings, synthetic non-viral nanocarriers (lipids and polymer based systems) despite their low transfection efficiency have emerged as potential safer alternatives due to their various desirable attributes to modify the current gene therapeutic regimen including, such as targeted delivery, ease of synthesis, protection in systemic circulation and intracellular delivery etc.

Nanomaterials voyage for drug and gene delivery

Both organic and inorganic materials have been investigated for drug delivery (Figure 8.2), each with its own set of advantages and disadvantages.
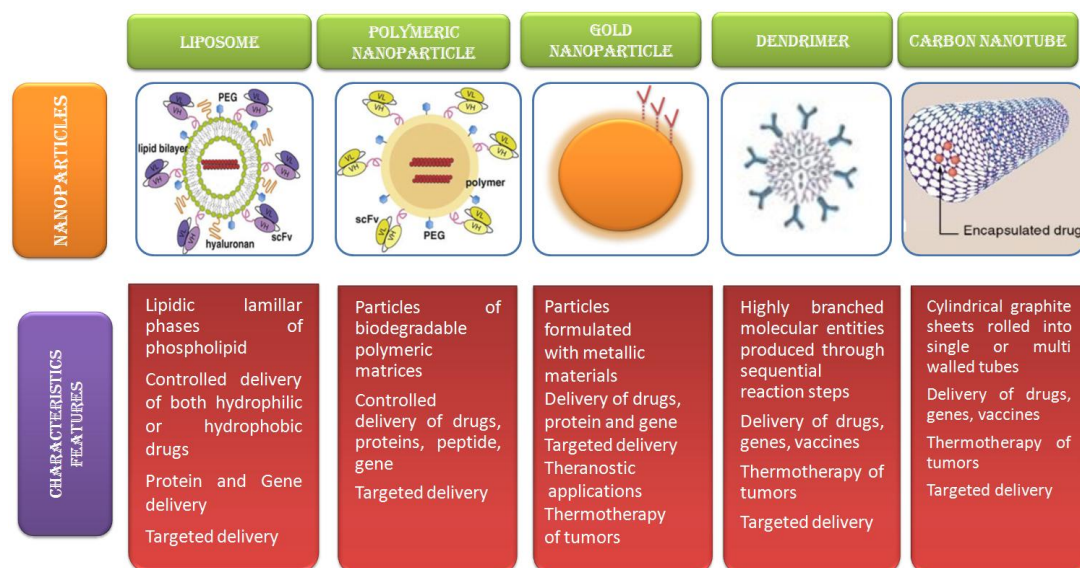
FIGURE 8.2
Representative examples of various types of nanomaterial based drug delivery platforms.

Lipid based nanoparticulate system

The lipid based systems offer diverse delivery platforms comprising of liposomes, micelles, emulsions, solid lipid NPs etc. Apparently, their various features such as biocompatibility, biodegradability, ease of scale-up, capacity to encorporate both lipophilic and hydrophilic drugs, production of fine dispersions of poorly water soluble drugs and cost effective nature compared to polymer based system have enabled them to enjoy the status of the most sought after drug delivery system; moreover, the

application of lipid based systems as drug delivery platforms has been favoured owing to the GRAS (Generally Recognized as Safe) status and their conventional usage in food and pharmaceutical products [14].

Conventional Liposomes

Liposomes are hydrated lipidic lamellar phases comprising of lipid bilayer encapsulating an aqueous core. The tendency of liposomes to deliver the payload (i.e. drugs, antigens, proteins and nucleotides), their relative simplicity, tunable size, charge and their pharmaceutical properties have made these systems the most promising for successful delivery of therapeutic agents. Intriguingly, the first nanomaterial drug delivery systems were lipid vesicles, which were described in the 1960s and later became known as liposomes. Liposomes are one of the most successful delivery systems currently in clinical use for various ailments including cancer, inflammatory, dermatological diseases etc.; of note, Abelcet, Epaxal, Myocet, Doxil represent approved liposomal formulations.

It is in general consensus that the inherent anatomical structures of some tissues especially tumor offers unique advantages for NP targeting; basically, the tumor vasculature is leaky and their lymphatic system is derailed which allows egress of molecular entities of appropriate sizes and their subsequent accumulation inside the tumor, a phenomenon known as Enhanced Permeation Retention (EPR)[15]. To this end, nanoparticulate entities owes competitive advantages while the free drug diffuse non-specifically, they passively accumulate into tumors exploiting EPR effect. Though still exploited in clinics, these passive modes of targeting are not healthier avenues to attain sufficiently desired level of nanoparticle concentration [16]. Although poor lymphatic drainage in the tumors facilitate enrichment of NPs in the tumor interstitium, the EPR phenomenon also induces NPs outflow from the tumor as a result of elevated osmotic pressure in the interstitium and most importantly not all tumors exhibit EPR effect. These issues have motivated the search for active targeting and in the recent scenario targeted drug delivery system (TDDS) are looked upon as more promising strategies. Accordingly, the first example of cell specific targeting of liposomes was described in 1980. Thereafter, there has been flurry of major advancement in the field which simultaneously lead to the developments of various efficacious homing ligands viz. ScFv, Fab, aptamers etc. to be innovatively employed to achieve specific targeting to specific sites which would certainly end up in improved therapeutic outcomes.

Amphotericin B (Amp B), a potent antifungal drug is amongst the one most benefitted by nanomaterial based drug delivery approaches. Researchers have demonstrated that their toxicity issues are considerably reduced upon encapsulating them in nanoparticles especially lipid based system (*AmBisome, Fungisome, Abelcet, Amphotec* represents approved lipid based formulations of AmpB). On this line, we further tried to increase the scope of liposomised Amp B (Lip-Amp B) formulations for the treatment of fungal infections by attaching tuftsin (an immunomodulator) onto their surfaces; the system demonstrated significant improvement over the conventional Lip-AmpB system, as the formulations besides reducing drug toxicity were also anticipated to activate the host's macrophages (important line of host defence against pathogenic fungi) owing to the presence of the tuftsin on their surfaces [16]. Furthermore, we performed elaborative studies to confirm the better efficacy of tuf-Lip-Amp B nanoformulations in enhancing the antifungal activity of amphotericin B [17,18,19,20]; indirectly providing a proof of concept of the better efficacy of the advanced nanoformulations. Moreover, we also demonstrated that tufstin embedded nanoformulations augments the antitumor activity of liposomized etoposide (Lip-ETP) in Swiss albino mice with fibrosarcoma; presumably by nonspecific activation of the host immune system [21].

Further, it is a well known fact that the potential adsorption of antibodies and other immune complex proteins onto these nanoparticulate entities in biological milieu leads to opsonisation and facilitate

their sequestration by the component of the host immune system viz. the reticulo-endothelial system (RES)/mononuclear phagocytic system (MPS). Nevertheless, these innate immunity phenomenon of uptake of nanoparticles (NPs) by the RES may be considered advantageous, providing avenues for targeting macrophages which could be beneficial in the treatment of various ailments including leishmaniasis and candidiasis wherein the pathogen have intracellular abode, residing in the macrophages. There is thus hope for nanotechnology based therapeutic interventions for intracellular pathogens. On the other hand, they also lead to compromise targeted delivery to requisite site. Accordingly, for accomplishing targeted drug delivery, it is enviable to edge uptake by the RES, indirectly interaction with the serum component. Although the surface adaptations of NPs employing hydrophilic and flexible polyethylene glycol (PEG) and other surfactant copolymers (eg poloxamers, polyethylene) have been extensively employed to overcome elimination by MPS [22]. Ironically, they are not free from downsides and there are few limitations that preclude their wide spread application. In case of PEG, issues of polydispersity inside the body and excretion from the body are the main concern in their wide applicability[22]. Though with the commercialisation of advanced purification procedures, PEGs in the market are less polydisperse, but unfortunately the monodisperse PEGs are limited to low molecular weights (< 1000Da only). It is argued that with availability of higher molecular weights analogs, the field of PEGylation chemistry will gain more impetus. Further, there are evidences that the PEG moieties of liposomes maybe immunogenic and evokes antibody responses against second administration. This anticipates that any PEGylated liposomal formulation may display unexpected pharmacological characteristics upon repeated administrations; thereby raising much concern on their utility [23,24, 25].

Furthermore, it is well known that the blood capillaries are lined by a layer of endothelial cells which differ according to the tissue type giving rise to continuous, fenestrated, or discontinuous type of vasculatures. In view of the structural (continuous, fenestrated, and discontinuous) and functional differences (marked by differences in the molecules they express) in the vasculatures of different organ system, NP transport show remarkable differences in various organs and accordingly provides opportunity to aptly design the nanoparticulate formulation to achieved delivery to the requisite organ/tissue. Interestingly, it has been found that liposomes passively accumulate in liver tissues and these phenomenons have been exploited for targeting to liver tissues[25]. Furthermore, poly(vinylpyrrolidone-codimethyl maleic anhydride) co-polymer formulations viz. Poly(VP-co-DMMAn) tailored superoxide dismutase has been found to populate kidneys after intravenous administration [26]. This is another compelling illustration of ability of nanomaterials to improve efficacy of drugs by harnessing the advantages offered by the biological system. However, it still remains a daunting challenge for nanotechnologists to satisfactorily harness the opportunities presented by the biological system. Moreover, with advances in the material science, newer drug delivery systems are being introduced embodying attributes to overcome the enroute barriers along with harnessing the benefits offered by the biological system; however, it would be more rationalistic to fine tune the present nanomaterials in voyage to achieve the same. Our laboratory has been extensively working on nanoparticle based drug delivery platforms for the treatment of cancer and a number of infectious diseases. Moreover, we have also deciphered the antimicrobial and anticancerous activity of various natural and synthetic compounds [6-8, 27]. Earlier, we and others have unequivocally demonstrated that several plant based compounds possess strong anti-microbial and anti-cancerous activity. However, their efficacious translation in clinical setting has been hindered due to various aforementioned reasons. Therefore, it is important to address their solubility, palatability, and sustained/controlled release in systemic circulation prior translating the suitability of these potential anti-microbial and anti-cancerous agents in clinical setting. We and others have shown the potentials of one such plant based product viz. garlic as anti-microbial, anti-oxidant and anti-carcinogenic agents. For

skin ailments, topical application is the most desirable approach amongst the avenues available for the administration of medications. Ironically, administration of drugs by this route leads to extensive diffusion particularly of small-sized molecules; thereby leading to low bioavailability and simultaneously reducing efficacy. This advocates development of formulations that can fine tune the bioavailability issues; paving ways towards their effective utilization against skin ailments. In this regards, various drug delivery platforms including micro-emulsion, nano-emulsion, nanoparticles, liposomes and niosomes etc. have been demonstrated to advance delivery of the active drug to the skin. Intriguingly, amongst these, the liposome-based formulations are most promising and leads to enhanced drug penetration, improved pharmacological properties, reduced adverse effects, controlled drug release, and, their biodegradability and non-immunogenecity further adds to their potentials. Keeping into consideration the suitability of lipid vesicles in targeted delivery, we developed pH-sensitive liposomal formulation of the garlic constituent diallylsulphide (DAS) (pH-Lip-DAS) and compared their chemo-preventive potentials with traditional liposomes (Lip-DAS) against dimethyl benz (a) anthracene (DMBA)-induced skin cancer in animal models [28]. In general, both the system viz. Lip-DAS and pH-Lip-DAS were efficacious in suppressing tumor burden compared to the free form of the drug; however, pH-Lip-DAS had an upper edge over the former. Seemingly, the better efficacy of DAS nanoformulations were anticipated to its ability to mediate a depot effect providing sustained release and higher accumulation of the drug at the tumor site and by improving their solubilities issues; and the superiority of pH-Lip-DAS was anticipated to its enhanced ability to deliver the content to the cytosol of the tumor cells. It is well known that DAS mediate its chemotherapeutic effect by altering apopotic factors populating the cytosolic compartment of the cell; in this regard its association with the cytosolic compartment is desirable for exhibiting its action. To this end, pH sensitive liposomal formulation owing to the presence of dioleoyl phosphatidyl ethanolamine (DOPE) exhibit phosphatidyl-ethanolamine (PE) mediated phase transition at acidic pH thereby mediating cytosolic delivery of the entrapped cargos. Of note, the phospholipid PE not only facilitates the close proximity of approaching bilayers, it is speculated to be directly involved in the merging process. Additionally, the application of liposomes as nanocarrier of anticancer agents including DAS has added benefit as fatty acyl chains of phospholipids may also offer anticancerous effect against various cancers. Recently, oleic acid has been shown to be the key factor responsible for BAMLET/HAMLET mediated killing of cancer cells [29]. Furthermore, to boost their potency as anti-microbial agents; we developed liposomized formulation of DAS for potential application in treating disseminated infection caused by the intracellular opportunistic pathogen *Candida albicans* [30]. The rationale behind the study was to develop a system which could increase their bioavailability in biological system along with providing specific targeting to macrophages wherein intracellular pathogens such as *C. albicans* seek shelter. Interestingly, encapsulating DAS in liposomal formulation would overcome their solubility issues and moreover in doing so they also acquire particulate nature ensuing in avid uptake up by MPS wherein *C. albicans* abode. To translate, these amendments synergistically modulate the activity the molecular drug, inturn increasing their efficacy in treating macrophage resident intracellular opportunistic pathogen *C. albicans.*

With advances in the field of newer generations of drug delivery platforms, liposomal formulation responsive to external or environmental stimuli (e.g., pH, temperature, enzymes) have been fabricated to modulate spatio-temporal release. ThermoDox is a representative example, which are temperature-sensitive nanoliposomal formulation of doxorubicin employed in combination with hyperthermic treatment for cancer therapy [31]; moreover, our next generation immunoliposomes viz. liposomes decorated with infected mouse erythrocyte-specific antibody also represent another non limiting example of advanced TDDS [8]. As it is well documented that the diverse conjugation linkers employed for conjugating antibodies with liposomes not only influence antibody conjugation efficacy but also the

physicochemical behaviour of the formulation; so as to give a deeper sight into the matter Chen et al. provided a glimpse of the influence of different conjugation derivatives on the functionalties of these formulations. They fabricated two variants of anti-EGFR-Fab conjugated immunoliposomal formulations possessing DSPE-PEG-COOH and DSPE-PEG-MAL as conjugation linker and delineated their targeting ability and efficacy in mediating siRNA delivery to SMMC-7721 hepatocarcinoma cells. Both the systems were efficacious in mediating RNAi, with the latter being more effective [32]. This certainly substantiate that the conjugation derivatives should be precisely selected for formulating better targeted drug delivery systems, additionally also corroborates the higher efficacy of targeted systems over nontargeted system.

As mentioned that non-viral vectors are safer and simpler alternatives for gene delivery. Accordingly, liposome and polymer based formulations have been increasingly focused to mediate gene delivery; intriguingly, the lately described liposomal formulations LPD (lipoosmes/protamine/DNA) have displayed superiority over traditional liposomes and DNA polyplexes. Liposome mediated gene delivery was first reported by Felgner in 1987 and as of yet is one of the key method for gene delivery and has been used in human clinical trials. On the contrary, lipid based systems also have various limitations when used for gene delivery as the structures of DNA–lipid complexes are inadequately understood and there arises variations during fabrication step. Cationic liposomal formulation though efficacious and a gold standard for gene delivery in *in vitro* system, their *in vivo* systemic application were rendered inefficient mainly due to their toxicity constraints. With the realization that severe dismal outcomes are associated with the systemic application of cationic liposomes, neutral liposomal formulations revisited their status to mediate systemic delivery of genetic medicines into the cells. Hoffmann and group have innovatively highlighted the feasibility of neutral liposomal formulations to selectively target hair follicles to delivery molecular entities including genes; and their subsequent study illustrated that highly specific targeted and safe gene therapy is indeed viable for hair [33]. Liposomes are still most widely utilized nanomaterial based drug delivery platform in biomedical research endeavours; nevertheless, the system owes several limitations including instability of the carrier, burst release, rapid oxidation of some phospholipids which inturn changes the characteristics of the particular liposomal formulation and non specific uptake by MPS system.

Niosomes

Niosomes are another bilayered vesicular entities composed mainly of non-ionic surfactants being exploited as carrier for lipophilic and hydrophilic drugs. They have the potential to increase the efficacy of the associated drugs [34]. They are biodegradable, biocompatible, non-immunogenic with little toxicity, and structurally and functionally analogous to liposomes [35]. However, unlike liposomes, whose constituents (phospholipids) are more vulnerable to heat and oxidative degradation, they do not impose such reticences. They are formulated on hydration of synthetic non-ionic surfactants with or without incorporation of cholesterol or other lipids which are generally economical than the naturally occurring phospholipids employed in the fabrication of conventional liposomes.

Reckoning with the solubility issues of garlic components and their strong antimicrobial activity; we developed myriads of niosomal formulation of DADS, each differing in their ability to encapsulate DADS to surmount their solubility issues [36]. Interestingly, all niosomal formulations were competent enough to overcome their associated stumbling blocks; albeit those harbouring Span80 were found to be most efficient in encapsulating DADS (size dimensions in the range of 140 ± 30 nm and zeta potential of −30.67 ± 4.5). Furthermore, on evaluating the toxicity of these niosomal formulations, both liver/kidney function tests as well as histopathologic studies suggested that noisome-based DADS

formulations were safe at the dose investigated. Finally, when examined for their efficacy in clearing fungal burden in model animals, it was found that the formulation cleared the fungal burden and increased their survival much efficiently as compared to the free form of the drug. Studies from various groups have provided elaborate overview of niosomes as drug delivery platforms [37].

Further advancements were the introduction of proniosomes which owed attributes to overcome the shortcomings of both liposomes and niosomes. They are basically liquid crystalline compact niosome amalgams which on hydration give rise to niosomes. A recent review by Kuppusamy and group enlighten the various facets of proniosomes [38].

Bacteriosomes

Escheriosomes are lipidic lamellar phases or liposomes being articulated from fusogenic lipids of *Escherichia coli*. Bacteria and yeast have preponderance of unique fusogenic phospholipids within their membranes, presumably to cope with the high multiplication rate. Such lipids seem to facilitate the fusion of the two opposite sites of inner leaflets under physiological conditions. Earlier, we have demonstrated that nanovesicles fabricated from lipid of lower organisms mediate membrane-membrane fusion and thereby offers a novel strategy for effective delivery of the macromolecular drug to the intracellular compartment of the target cells under physiological conditions [39,40]. Considering the potentials of RNAi based therapeutic strategies and the need to achieve safer delivery of RNAi modulators to the cytoplasmic domain of the cell viz. site of their processing and function. In our recent study; we have developed an escheriosomes encapsulated Polo Like Kinase-1-siRNA (PLK-1-SiRNA) nanoformulation and evaluated their efficacy in the treatment of cancer. The nanoformulation delivered the siRNA into the cytosol of the fusing cell; moreover, their near neutral zeta potential and ability to camoflague siRNA inside their bi-layer during the systemic circulation offered safe and efficient intracellular delivery of the intact siRNA cargo with negligible toxicity and widen their therapeutic window, making it more possible to potentialize the effectiveness of siRNA, allowing their usage thereof in various therapeutic arenas in an efficacious manner. The efficacy of whose has been assessed in in vitro and *in vivo* models [9]. Furthermore, we also demonstrated that escheriosomes encapsulating DNA vaccine co-expressing Cu-Zn superoxide dismutase and IL-18 conferred protection against *Brucella abortus* [10]; while escheriosomized propofol–linoleic acid (anti-cancer agent) nanoformulation bestowed protection against murine hepatocellular carcinoma [41]. These were some of the non limiting paradigm where escheriosomes have displayed their efficacy in subduing various daunting challenges faced by various treatment stratagems. Whilst their potentials in mediating protection against intracellular pathogens by acting as desirable adjuvant eliciting strong cell mediated and humoral immune responses against encapsulated antigen in analogy with saccharosomes (lipidic lamellar phases or liposomes being articulated from fusogenic lipids of *S. cerevisiae*), leptosomes(lipidic lamellar phases or liposomes being articulated from fusogenic lipids of *Leptospira biflexa*) subtilosomes(lipidic lamellar phases or liposomes being articulated from fusogenic lipids of *Bacillus subtilis*) and archaeosomes (lipidic lamellar phases or liposomes being articulated from lipids of *Archaebacteria*)are another worthmentioning aspects [39,42,43].

Archaeosomes

As mentioned above, they are liposomes being fabricated from archaebacterial polar lipids [43]. Extensive efforts have appraised their potentials in drug and vaccine delivery. They possess various advantages over conventional liposomes owing to their attributes of ether lipids. This unique characteristics of archaeal polar lipids viz. ether lipids on contrary to ester lipids present in other

liposomal formulation bestow improved physico-chemical stability including enhanced thermal stability, systemic stability, stability at extremes of pH range, resistance to oxidative stress and action of lipases and bile salts compared to their conventional counterparts. They also display safety profile as revealed by intensive *in vitro* and *in vivo* studies [43].

Generally administration of drug via oral route represents the most promising route of drug delivery. However, the formulations for oral delivery should not only have to overcome the low acidic pH of the stomach but also have to defy the deteriorating effects of lipases and bile salts present in the GI tract. Though, conventional liposomal formulations exhibits stability at neutral and acidic pH; however, they are vulnerable to lipases and bile salts. To this end, archaeosomes with their added virtues offers various advantages over the traditional systems. Interestingly, encapsulation of Coenzyme Q_{10} in archaeosomes resulted in an increased appearance of the marker in the blood upon oral administration [44]. Moreover, they also exhibit improved thermo-stability over a range of temperature 4–65^{0}C compared to traditional liposomal systems, which could be further enhanced by increasing the ratio of caldarchaeol lipids in the total polar lipids, they open avenues for fabrication of sterile formulations, especially if the encapsulated cargo is also acquiescent to high temperature [45]. Convincingly, they show good prospect for drug delivery applications paving way for their appraisal for actual commercial exploration.

These bacteriosomes technology have advanced rapidly in pre-clinical settings but requires exhaustive scientific evidences to establish their standing as safer and efficacious *in vivo* drug delivery platforms.

Solid lipid nanoparticles

Solid lipid nanoparticles (SLN) were introduced in the 1990s as an alternative to the conventional carrier systems including emulsions, liposomes and polymeric nanoparticles. They are the newer class of drug delivery system with a solid lipid core possessing various competitive advantages over the conventional drug delivery platforms such as better targeting, higher physical stability, lower toxicity, biocompatibility, and ease of scale up [46]. Moreover, being fabricated from lipids present in our system, they could be easily metabolized via the metabolic pathways already present in the system. Owing to their ready metabolism by the body, they do not accumulate in the body thereby ensuing in lower toxic manifestations; infact their lower toxicities issues have been thoroughly validated with various *in vitro* and *in vivo* SLN toxicity studies [47]. Various lipids employed in the preparation of SLN includes triglycerides such as tricaprin, trilaurin, tripalmitin, hard fat types lipids including glycerol behenate and glycerol palmitostearate, and waxes such as cetyl palmitate and different methodology exists for their fabrication such as high pressure homogenisation, microemulsion based methods and solvent emulsifications and more importantly their fabrication methodology avoids usage of harmful organic chemicals. It has been reported that they can be applied through any parenteral route where polymeric systems are tolerable. Intriguingly, SLN based nanoformulation of paclitaxel displayed efficacy equivalent to commercially available Cremophor EL-based paclitaxel formulation against human ovarian and breast cancer cell lines and were physically stable as well. The systems were prepared employing trimyristin (TM), egg phospholipids (ePC) and pegylated phospholipids (PEG2000–PE) through high-pressure homogenization followed by rapid cooling, wherein TM forms the solid core whilst ePC and PEG2000–PE acted as stabilizers [48]. Another important efficacious drug of plant origin is curcumin. Curcumin (difruloyl methane), a constituent of turmeric (*Curcuma longa*) possess strong antioxidant, anti inflammatory and anti cancerous properties. Despite these desirable properties, widespread clinical applicability of this relatively efficacious drug against cancer and other dreadful ailments are limited due to their poor systemic bioavailability. Considerable efforts have been diverted to increase their bioavailability; consequently, myriads of nano material based formulations have been

developed conferring improved bioavailability and efficacy. Wang et al. developed a curcumin-SLN nanoformulation for the treatment of lung cancer. The system was fabricated employing sol-gel method with size range from 20 to 80nm. The preferential lung tumor targeting lead to efficacious tumor inhibition, paving way towards novel method for new anticancer agents development [49]; further to provide a glimpse of their attributes, Qi et al. detailed the pharmacological behaviour of SLNs [50].

Though, SLNs are versatile agent with many desirable features, they also have limitations including low drug loading competence, ambiguity in purity of SLNs; moreover they may undergo transition during storage which may leads to size increment and release of the encapsulated entity [51]. Despite these, they display various competitive advantages over the traditional drug delivery platforms, hence owes merit for future exploration.

Taken together, though lipid based nanoparticulate systems have reputed standing amongst the drug delivery systems, they are susceptible to alteration in temperature and osmotic pressure and other external agents. These issues together with their intrinsic instability (of some lipid based systems) make it necessary to augment stability using hybrid system viz. Lipid–Polymer hybrid nanoparticulate system, which encompasses the unique attributes of both polymeric and liposome systems, while defying some of their limitations.

Polymers

The first controlled release polymer system for delivery of macromolecules was described in 1976. Amongst the largely employed biodegradable and biocompatible polymers, poly(lactic-co-glycolic acid) (PLGA) represent the most sought after material due to their FDA approval. PLGA system comprises of glycolic and lactic acid in various stiochiometric ratio. Their degradation period and release of the encapsulated cargo are dependent on the ratio of glycolic and lactic acid and can be adapted by varying these ratios. In general, system consisting of equal ratio of lactide and glycolide (50:50) degrade much faster than those comprising higher proportions of either of the two monomers [52]. Their hydrolysis products are easily metabolized in the body via the citric acid cycle and are easily eliminated, therefore adverse toxic manifestations with PLGA based drug delivery platforms are low. They have been widely exploited in the niche of efficacious chemotherapeutic drug delivery reservoirs. Taxol are commercially available PLGA nanoformulation of paclitaxel for the treatment advanced prostate cancer whereas Genexol-PM, a polymeric micelle formulation of paclitaxel is approved for the treatment of breast and lung cancers in Korea. Basically, it is composed of block copolymers of PEG and PLGA [53] and the formulation (20-50 nm) is completely soluble having a maximum tolerated dosage (MTD) of 390 mg/m^2 (50) in phase I clinical trial and exhibited good response rates in subsequent trials.

Apart from their role in improving the efficacy of known chemotherapeutic drugs; increasing interest has emerged to advance the efficacy of biologically active molecular entities that were earlier considered fallow through conventional approaches. In this regard, perillyl alcohol (POH), a monoterpene and constituent of essential oils from a number of plants possess strong anti-cancerous properties against several types of cancer including breast, pancreatic, and liver cancers; however, its therapeutic use is limited due to their various associated challenges. To this end, we developed a PLGA-POH microparticle based systems to address their undesirable issues and evaluated their efficacy against the skin epidermoid cancer cell line (A253) and di-methyl benzo anthracene (DMBA) induced tumors in Swiss albino mice. The formulation when administered to tumor-bearing animals caused greater tumor regression and increased survival rate (~80%) as compared to the free form of POH (survival rate 40%). The superiority of POH-PLGA microparticles over free form of POH could be

attributed to their ability to circumvent the associated stumbling blocks of POH along with bestowing other desirable features [7].

On the same line, we also developed a microcell based system of curcumin. With a view to overcome its solubility, faster degradability and bioavailability constraints; we developed a dual delivery system (810 ±188nm dimension and -82.6±2.3 zeta potential) viz. PLGA microparticle encapsulating curcumin co-entrapped in PC liposomes to control release of curcumin in regulated manner. Furthermore, we evaluated the biodistribution of this system and finally assessed their anti-cancerous potentials against di ethyl nitrosamine induced hepatocellular carcinoma in model animals. Intriguingly, the system was efficacious in mediating regulated release of curcumin and displayed time depended release pattern and were free from toxicity issues; inturn the system reduced tumor burden in model animals exemplifying the efficacy of the prepared formulation of the undeveloped drug curcumin [54]. We also developed amoxicillin bearing poly-lactic-glycolic acid (PLGA) microsphere formulation for treatment of experimental listeriosis to boost the potency of the molecular drug "amoxicillin". Interestingly, PLGA microspheres bearing amoxicillin provided a sustained release of encapsulated drug over extended time period, successfully cleared bacterial burdens in vital organs (kidney, spleen, and brain) and also increased survival rate of treated animals in comparison to free form of the drug. The higher efficacy of microsphere based novel formulation of amoxicillin could be accredited to its targeted delivery to infected macrophages as well as to sustained release over an extended period of time [6].

Various important lipid–polymer hybrid nanoparticulate systems viz. lipid-decorated polymeric nanoparticles consisting of a PLGA core, a PEG shell, and a lipid monolayer have also been developed [55]. In this formulation, the PLGA interior incorporates the hydrophobic entities, whilst the PEG coating promotes retention in the systemic circulation and lipid monolayer being present at the interface of polymers promotes sustain release of the entrapped cargo. The system allowed improved drug encapsulation, sustained drug release over an extended period and good systemic stability.

Additionally, Zhang and group developed a biologically inspired system consisting of PLGA NPs surrounded with natural RBCs which owed attributes of long-circulatory half life greater than the gold standard stealth NPs. Besides, in their subsequent studies, they formulated biomimetic nanosponge that functions as a toxin decoy *in vivo*; the system comprising of a PLGA-NPs core encapsulated into RBCs effectively absorbs toxins and in doing so can promisingly addresses various dismal outcome associated with various toxin secreting dreadful pathogens; and in their proof of concept study in animal model, the system significantly detoxified the staphylococcal alpha-haemolysin (a-toxin). Conclusively, the study highlights the unique feature of nanomaterial based platform i.e. a detoxifying nanobodies that can address issues of toxin mediated toxicities. [56, 57].

Furthermore, SMANCS, a conjugate of the potent chromoprotein neocarzinostatin (NCS) and polymer poly(styrenecomaleic acid) (SMA) represents the first practical use of polymer therapeutics as anticancer agents and has been approved in Japan for use in hepatoma treatment in the early 90's. The milestone study, for the first time illustrated the implication of passive tumour targeting through the EPR effect [58]. SMANCS represent the first successful theranostic (field of combine therapy and diagnostics) application, in a sense being administered with a constrast agent lipiodal, they allows X-ray detection of liver tumor nodules as well.

PLGA based formulations have also been exploited for gene therapy with reasonable success. We formulated PLGA-Cox-2 siRNA nanoparticulate system to evaluate their efficacy against experimental skin papilloma(unpublished data). The system with their added virtues displayed efficacy in suppressing tumor burden in experimental animal models. Additionally, reckoning with the fact that cationically modified nanoparticulate entities bind and condense negatively charged oligonucleotides (plasmid, antisense RNA, RNAi modulators etc.) more efficiently and also offers other benefits including

intracellular delivery; various group have connotated the importance of chitosan modified PLGA nanoparticles (CHT-PLGA-NPs). Chitosan, a biodegradable linear polysaccharide comprising of β-(1‑4)-linked D-Glucosamine (deacetylated unit) and N-acetylated-D-glucosamine (acetylated unit) embody important advantage to enhance penetration of large molecular entities across mucosal surfaces. Interestingly, Nafee et al. fabricated chitosan coated PLGA nanoparticles with desirable physiochemical features (size in the range 135.95-514.3 nm and surface charges 13.5-60.4 mV) for mediating efficacious gene delivery and for providing proof of concept, the efficacy of the system was evaluated by ensuing efficient delivery of antisense oligonucleotides to lung tumor [59]. Likewise, Yuan et al. highlighted the efficacy of CHT-PLGA NPs for effective and safer siRNA delivery [60].

Dendrimers

Dendrimers are extensively branched molecular entities produced through sequential reaction steps. With virtue of distinct architecture alongwith tunable molecular weight, considerable number of accessible terminal groups as well as capacity to encapsulate cargo molecules, they are forseen as promising delivery platform. Moreover, as the intricacies of dendrimer structure, biocompatibility, retention, and delivery has been increasingly illuminated; novel analogs could be fabricated for better targeting and functionality. It has been unequivocally advocated that an aptly fabricated dendrimer structure can be altered concurrently for desire biocompatibility, bioavailability, and pharmacological properties [61].

Cationic dendrimers including poly(amidoamine) dendrimers and poly(propylamine)(PPI) have been studied not only as an efficient scaffold for the therapeutic drugs but also for delivery of genetic medicines. Cationic groups (specially primary amine) at their surfaces participate in the oligonucleotide (negatively charged) binding, their condensation, cellular uptake and triggering proton sponge in endosomes which enhance their release into the cytoplasm. Zhou and co-worker reported an effective siRNA delivery system based on structure flexible polycationic PAMAM dendrimers; which condenses the siRNA into nanoscale particles, moreover protecting them from enzymatic degradation while mediating substantial release of siRNA over an extended period of time for efficient gene silencing [62]. Studies have also illustrated the potency of various generations of poly(propylenimine) (PPI), carbosilane, polylysine and other dendrimeric analogues for delivery of macromolecular drugs[63,64,65]. McCarroll et al. have fabricated single-walled carbon nanotubes functionalized with polylysine dendrimers for delivery of anti-ApoB siRNA. The formulation demonstrated effective reduction in ApoB mRNA thereby causing reduction in serum cholesterol levels while reducing the toxicity and immunogenicity of SWNTs as detailed below [65]. In the arsenal of dendrimer analogues, PAMAM represent the most widely employed system mainly due to their wide commercial availability. Although, these dendrimers impose toxicity issues, but as more is gleaned about their safety issue along with ease of synthesis they could emerge as versatile drug delivery platforms.

Inorganic NPs

With the development in nanotechnology, inorganic nanostructured materials have been designed/discovered or fabricated with important cooperative physical properties to be utilized in the development of delivery systems with both therapeutic and diagnostic modalities [66]. Among the various inorganic particles explored for improving drug delivery efficiency, due to their credits of good biocompatibility, ease of large scale synthesis, high surface-to-volume ratio, monodispersity, and ready

functionalization, amphiphilicity, safe carrier capabilities, tunable shape and size, gold nanoparticles are anticipated as an enticing scaffold for drug delivery [67-70]. Moreover, as efficient release of the cargoes after reaching to the requisite site is prerequisite for effective therapy; the release of the cargoes from the AuNPs could be triggered by internal (e.g. glutathione (GSH), or pH) or external stimuli (e.g. light, temperature etc.) [71-74] providing avenues for spatio-temporal release. By exploiting the phenomenon of surface plasmon resonance (SPR), their complexation with the materials, delivery and distribution within target tissues can be monitored and provides other benefits as well as highlighted below. These unique properties have drawn great attention across the globe for harnessing them in the development of drug delivery platform. Interestingly, the potential application of AuNPs is investigated in phase I & II clinical trials for cancer therapy [75].

Considering the fact that synthesis process plays an important role in maintaining the unique properties of gold nanoformulations; different preparation procedures yield different AuNPs morphology offering an array of AuNPs including spherical gold nanoparticles, gold nanorods, gold nanocages and gold nanostars among others, each with diverse functionalities. Various methods that have been employed for their synthesis includes chemical reduction producing monodisperse spherical AuNPs in the 10–20 nm diameter range [76]; physical reduction producing hollow Au nanostructures [77]; photochemical reduction method giving rise to cubic AuNPs[78]; biological reduction viz. molecular hydrogels of peptide amphiphiles for producing various shapes of AuNPs [79]; solvent evaporation techniques producing 2D Au super lattices [80]; and biomimetic method yielding diverse AuNPs [81] etc. however, the preferred method particularly depends on the ease of synthesis and application required. Considering the global efforts to revolutionize cancer therapeutics, strategies employing nanomaterial based platforms are increasingly exploited in the recent scenario; El-Sayed et al. developed a tamoxifen-PEG-thiol-AuNP conjugates for displaying efficacy against breast cancer treatment. The system selectively targeted estrogen receptor alpha in human breast cancer cells with up to 2.7-times enhanced potency *in vitro* [82]. Moreover, Rotello and group developed gold nanoformulations to incorporate drug into their hydrophobic pocket to display efficacy in cancer treatment. The system was functionalized with a hydrophobic alkanethiol interior and a tetra(ethylene glycol) (TEG) hydrophilic shell that terminated into a zwitterionic head group which reduced nonspecific binding with cell and macromolecular entities in the biological system [83]; interestingly, the system with miniature size and biocompatibility displayed prolonged circulation and inturn better accumulation in tumor tissues by the EPR effect.

Moreover, Elbakry used monodisperse AuNPs as a scaffold for the implementation of layer-by-layer approach to siRNA-AuNP conjugates, forming a system comprising of (polyethylene-imine) PEI/siRNA/PEI-AuNPs [84].The inclusion of PEI rendered opportunities to formulate well defined and homogenously distributed nanocarriers and to mediate endosomal escape besides decreasing the net negative charge of the siRNA-AuNP formulation, which facilitated their cellular uptake as a result of decreased repulsion from the cell membrane. Albeit, the researchers reported successful uptake of siRNA-PEI AuNPs; however, the enhanced stability of the nanoparticles were found to decrease the intracellular release of siRNA, necessitating further concern on the theme. Song et al. fabricated an efficient and safe siRNA delivery system of uniform shape and narrow size composed of PEI-capped gold nanoparticles (AuNPs) which were successfully manufactured using PEI as the reductant and stabilizer. Without causing cytotoxicity, the system exhibited efficient knockdown of the oncogene (PLK-1) and induce enhanced cell apoptosis which was not observed when the cells were treated with PLK-1 siRNA using PEI as the carrier; exemplifying the efficacy of PEI-capped AuNPs to be a suitable carrier for intracellular siRNA delivery [85].Moreover, the system also rendered appreciable intracellular release of siRNA. Although PEI is used as an excipient for imparting various functional attributes to the nanoparticulate systems including AuNPs; however, their toxicity issues has either

lead to the search of other polycatioinic excipients as a safer platform which additionally also imparts other functional attributes, or modulation of PEI ratio such that it is non toxic to the system or have feeble toxicities. Han et al. developed AuNPs being reduced and stabilized by chitosan (CS) onto which (cis-aconitic anhydride-functionalised poly(allylamine) PAH-Cit/PEI and siRNA were electrostatically deposited; the system owed negligible cytotoxicity against HeLa and MCF-7R cells while mediating their efficient protection against nuclease degradation and triggered release of siRNA as a result of charge reversal mechanism [86]. Moreover, Ghosh et al. developed a simple cysteamine-functionalized AuNPs modified with PEG for the delivery of chemically unmodified miRNAs into living cells [87].

As already mentioned, gold nanoparticles embody unique optical properties owing to strong SPR absorption at visible and NIR wavelengths, thereby exhibits photothermal (PTT)effects which can be exploitated to activate myriads of biological manifestations, providing many avenues for future endeavours. Non-spherical AuNPs have some advantages beyond the spherical-nanoparticle as versatile delivery system. Gold nanorods (AuNRds) and gold nanospheres (AuNSs) consisting of a thin gold wall with a hollow interior exhibits strong SPR tunability in the NIR region. Exploiting this property of gold nanoparticulates, Braun et al. developed a formulation comprising of AuNSs that exhibited controlled spatio-temporal release of siRNA cargo upon excitation with NIR laser. The liberation of siRNA from AuNSs upon NIR laser excitation did not show any significant toxicity and exhibited power and time dependence through surface-linker bond cleavage; though decomplexation occurred at low power excitation, but escape from endosome only occurred at high power irradiation; it was foreseen that more advanced transfection methods overcoming the endosomal barrier would have great impetus in the development of more efficacious NIR laser-controlled drug release systems [88]. Hushka et al. developed AuNSs based spatio-temporal nucleic acids (NAs) delivery system comprising of poly-L-lysine peptide (PLL) epilayer covalently attached to the NS surface. They made inclusion of PLL to mediate electrostatic capture of NAs; while on demand liberation of NAs were achieved by excitation with NIR laser. NIR induced delivery of NAs by the NA-PLL formulations resulted in around 50% downregulation of the targeted GFP expression in H1299 lung cancer cells without any significant cytotoxicity [89].

Considering their efficacious nature in mediating improved RNAi regulator delivery in *in-vitro* system, many reports have foreseen their great clinical potential not only for gene therapy but also for drug delivery, biosensing, and bioimaging in *in-vivo* system; yet, the success in clinical settings depends on how these nano-structures behave in the biological system, with the physiological processes and the anatomical structures influencing their behaviours.

As the blood capillaries forms an intimate contact with almost every cells of the body, as a result, any tissue in the body can be accessed through systemic administration of the nanoformualtion provided they surpass the anatomical barriers offered by them. Functionalised NPs have been utilised to achieve targeted delivery upon systemic administration. However, functionalized AuNPs as other NPs have strong tendency to associate with the blood proteins such as albumin, fibrinogen, insulin etc. Albumin, the most abundant protein of the blood plasma, besides their role in maintaining the colloidal osmotic pressure of blood and interstitial fluids, is equipped to mediate transport of various molecules (fatty acids, some amino acids, peptides, and steroids and drugs); it also help in the trafficking of Au NPs across the endothelium. With reports suggesting that these albumin-Au-NP conjugates were internalized either by transcytosis (90%) or by fluid phase endocytosis (10%) [90, 91]. Reckoning with the fact that albumin adsorption on gold nano-surfaces facilitate their drainage from blood vessels to the interstitial space by transcytosis [90]; in the recent scenario, this phenomenon is foreseen as a new avenue for the delivery of gold nanoformulations to tissues upon systemic administration. However, on

the contrary, the nonspecific nature of this process will be a major challenge for targeted delivery. Of note, the fate of AuNPs *in vivo* is influenced by the serum proteins on their surfaces, which is been seen as an interesting area of research that will have implications in drug delivery.

Endothelial lining in the brain is completely continuous with endothelial cells firmly adhered to each other by tight junctions, while further strengthened by astrocytes forming blood-brain barrier that allows only highly selective permeability to transverse through, representing tremendous challenge for delivery of various moieties. Any exogenous molecular entity to transverse through brain has to breach through the blood–brain barrier. In this regards, Bonoiu et al. developed an excellent approach for the delivery of siRNA to brain utilizing gold nanoparticles (AuNPs) complexed to siRNA, called nanoplexes, for modulation of the dopaminergic signaling pathway in an *in vitro* model [93]; exemplifying the efficacy of AuNPs for therapies of central nervous system disorders by transmigration across Blood brain barrier. Reckoning with the fact that TDDS are looked upon as more promising strategy; AuNPs were decorated with various homing ligands including alpha-tocopherol, cholesterol, or Hyluronic acid (HA), folic acid, and transferrin and others which ferry them to specific sites [94, 95].

Recent reports illustrate that AuNRds and AuNSs with their unique NIR light absorbing feature, elevate the temperature of their local milieu (45-50°C) upon laser irradiation, eventually has been seen to cause apoptosis of the cancerous while sparing normal cells, as cancerous cells being much more vulnerable to increase in temperature; as a result AuNRds when co-administered with the anticancer drugs along with cognate siRNA would exhibit enhanced suppression of tumour growth as also exemplified by recent reports [93,96]. Moreover, as already mentioned that inorganic NPs possess unique physicochemical and optoelectronic properties, they could themselves translate into a better therapeutic molecule.

Carbon nanotubes (CNTs)

Carbon-nanotubes (CNTs) are fibrilous nano-cylinders comprising of single (single-walled CNTs, SWCNTs) or multiple (multi-walled CNTs, MWCNTs) graphine layer(s) with length and diameter ranging from 50 nm to 100 nm of 1–5 nm or 10–100 nm respectively [97, 118]. The tunability of CNT layers bestow attributes of multi-valent binding to cells alongwith conjugating multiple targeting molecules. Despite their advantages, therapeutic applicability of CNTs is accompanied by concerns about their non-solubility in aqueous milieu and possible adverse effects[98]. It has been argued that proper functionalisation of CNTs (f-CNTs) could stimulate solubility of CNTs; consequently, their proper functionalisation by covalent or non-covalent methodology facilitated their solubility in aqueous solutions and also refrained non-specific interactions in biological milieu thereby minimizing toxicity observed in the case of non-functionalized raw particles inturn increasing biocompatibility and circulating half life [99]. Moreover, functionalization of CNTs with cationic groups serves another purpose of binding with anionic nucleic acid moieties by electrostatic interactions which could have great impact in the arena of gene therapy. The shape characteristics of any NPs including CNT could significantly affect their biodistribution. The length and shape of the NPs should be taken into account when it comes to the well-individualized cylindrical CNTs. SWCNTs display strong absorbance in the NIR region, the region being transparent for the biological systems, as a result providing avenues for optical imaging and PTT. Targeted delivery has been achieved by deploying CNTs by exploiting various homing ligands such as folic acid, epidermal growth factor, herceptin etc. Liu et al. demonstrated that CNTs-drug conjugates could effectively accumulates in tumors exploiting EPR effect and several magnitude higher concentration could be achieved than that of plasma. Furthermore, in their follow up studies,

they demonstrated the higher efficacy of SWCNT–paclitaxel conjugate in reducing tumor growth in a murine 4T1 breast cancer model without any toxic manifestations [100, 101].

Zhang et al. fabricated functionalized SWCNTs (SWCNTs+) conjugated to human telomerase reverse transcriptase (hTERT) siRNA to deliver to tumours *in vivo*. The SWCNT-formulated siRNA was injected intratumourally and induced reduction in hTERT mRNA and protein levels leading to inhibition in tumour cells growth in a xenograft mouse model [102]. Krajcik et al. developed functionalized SWCNTs using hexamethylenediamine (HMDA) and poly(diallyldimethylammonium) chloride (PDDA) generating positively charged PDDA–HMDA–SWCNTs which electrostatically interacts with the negatively charged siRNA (against extracellular signal-regulated kinase ERK). The system bypassed the cellular membrane barrier and suppressed the expression of the ERK target proteins in primary cardiomyocytes (a reduction of 75% was observed) and exhibited negligible cytotoxic effects on isolated rat heart cells at concentrations up to 10 mg/l [103].

Furthermore, McCarroll and group developed SWCNTs functionalized with lysine-based dendrimers covalently attached to lipid chains (Tol 7); basically, inclusion of the lipid moiety was made to masks the hydrophilicity of siRNA and facilitates cell binding, whereas the positively charged dendrimer condensed the siRNA into discrete particles. The system was utilized for systemic delivery of anti-ApoB siRNA and showed effectual reduction in ApoB mRNA, which led to reduction in serum cholesterol levels.

It is in general consensus that owing to their fibrillar structure, they could lead to cytotoxic manifestations, inflammation and DNA damage [104 -109, 111]. Generally, SWCNTs and MWCNTs can induce platelet aggregation, mitochondrial dysfunction, ROS generation, lipid peroxidation and oxidative stress resulting in cell death among other manifestations [105,106,111]. Evidence suggests that high concentrations of nanotubes demonstrated chronic lung inflammation, including foreign body granuloma formation and interstitial fibrosis leading to toxic effects [104, 107-110, 111]. These adverse side effects can limit the applicability of CNTs in clinical applications. CNTs with desirable features could be exploited for specific application provided their route of administration are aptly considered in which fibrillar structures don't lead to adverse effects. It is too early to establish CNT for clinical settings, these novel carriers are indubitably interesting and deserve further investigation.

Over the decades, the importance of combination therapy for treatments of diseases has been highlighted. In this regard, administration of combined therapeutic modality directed against different targets can enhance therapeutic efficacy or leads to a system with comparable efficacy but with lower side effects. More innovation could involves piling of different therapeutic modalities onto a single system (nano drug delivery platforms) which would leads to simultaneous administration of both; moreover, besides synergism, the nano drug delivery platforms also provide other benefits including reduce toxicity of the free drug and subduing drug resistance [11]. Concurrent with the recent situation, employing nanomaterial based drug delivery platforms for co-delivery of several agents is promising. To translate, it improves rather enhance the action of the therapeutic agents rendering administration of lower concentration of each entity inturn reducing toxicity issues thereby holds tremendous potential for future. On this line, polymer based drug delivery systems were deployed for co-entrapment of conventional chemotherapeutic agent doxorubicin and curcumin. The system displayed improved efficacy on MDR cells, and follow up studies are investigating their efficacy *in vivo* systems [112]. Additionally, combination of RNAi with chemotherapeutics are also promising strategy; based on this, the anthracycline or taxol drugs along with siRNA (VEGF) were encapsulated in cationic micelles to achieve improve therapeutic outcomes [113,114]. Likewise, the cationic drug mitoxan-trone has been complexed with hydrophobic palmitoleic acid to ferry anti-mcl-1 siRNA; the system was found to be a dependable approach[115]. Despite these promising developments, a comprehensive research

is required to advocate the synergistic dose and ratios of siRNA to chemotherapeutics in animal model [11].

Moreover, despite tremendous potential of RNAi based approaches and role of delivery platforms in realising their potentials as of yet, co-delivery of combinational potent synergistic siRNA employing the same platform is in infancy; a group have employed a biodegradable polymer to transport Mdr-1-shRNA and Survivin-shRNA (gene relating to MDR); the polymer with added virtues to compact oligos at neutral pH and liberate them at acidic pH of the endosomal compartment could overcome MDR in tumor cells when delivered with the molecular drugs [116]. More recently, a siRNA combination system viz. a lipid nanoparticulate system encompassing two siRNA viz. VEGF- A and kinesin spindle protein (KSP) paved its way towards clinics. The first-in–human trial of this system illustrated the pharmacokinetics, RNAi mechanism of action, and clinical anti-cancer activity [117]of the same.

More recently, Eldar-Boock et al. have highlighted the developments of nanomaterial based drug delivery systems for combination therapy. Albeit, combination therapy is undoubtedly more complicated than monotherapy; nevertheless, it is certain that apposite drug combinations together with drug delivery platforms can offer important improvements viz. reduced case-fatality, less chances of drug resistance development and in near future efforts would be made to make them cost effective. The selection of appropriate drug delivery platforms plays crucial roles in maintaining the efficacy of combination therapy. Of note, the preference of drug delivery system should be in accordance with physico-chemical attributes of the cargoes [11].

Toxicity of the nanocarrier systems

The potentials of nanomaterial based drug delivery are encouraging. However, they are not free from downside; there are reports indicating that nanomaterials themselves may pose toxicological risk. De Jong and Borm have documented few of the possible adverse toxicological responses observed over the past decade [118]. However, it is intrigued that various amendments in the nanoparticulate entities could leads towards a safer system and it is forseen that even small changes to the physicochemical characteristics of NPs can have appreciable impact on their behaviour, compelling predictive toxicology impossible. Moreover, considering the toxicity issues of nanomaterials, recently our laboratory has innovatively highlighted the potential of biomimetic synthesis to lead towards novel nanoformultion of the molecular entity itself with the rationale that such advancements would be beneficial to pioneer novel nanoassemblages that will be more efficacious and more importantly free from nanomaterial (excipient) related toxicities. In our follow up studies, we are exploring the efficacies of such novel systems in providing protection against various dreadful ailments including cancer [119].Interestingly, global efforts have been exploiting computational modelling and screening approaches to explore requisite properties of NPs viz. dimensions, hydrophilicity, stability, density of homing ligands on NP surfaces etc. for safer and efficacious therapeutic applications.

Conclusions

The expansion of nanomaterial mediated drug delivery may play an important role in adding a new armamentarium of therapeutics to the pipelines of existing drugs embodying improved efficacy. Efforts are in practice to revisit the status of suboptimal but biologically active molecular entities that were formerly known to be fallow through conventional approaches with field of nanomedicine moving at a

very rapid pace. It is intrigued that the characteristics of NPs that bestow them their therapeutic properties may also lead to toxicity. Thus it is imperative to fine tune the efficacy and adverse effects to fabricate an efficacious system. More elaborate work from various sectors is needed to lead towards the more "smarter", ''advanced'' and yet safer system that could trounce various daunting challenges associated with various pharmacological drugs.

References

1. Farokhzad OC, Langer R. Impact of nanotechnology on drug delivery. ACS Nano. 2009; 3:16-20.
2. Gatoo MA, Naseem S, Arfat MY, Dar AM, Khusro Q, and Zubair S. Physicochemical Properties of Nanomaterials: Implication in Associated Toxic Manifestations. Biomed Res Int 2014:498420.
3. Tiwari PM, Vig K, Dennis VA, Singh SR. Functionalized Gold Nanoparticles and Their Biomedical Applications. Nanomaterials. 2011; 1: 31-63.
4. Rabanel JM, Aoun V, Elkin I, Mokhtar M, Hildgen P. Drug-loaded nanocarriers: passive targeting and crossing of biological barriers. Curr Med Chem. 2012; 19:3070-3102.
5. Wagner V, Dullaart A, Bock AK, Zweck A. The emerging nanomedicine landscape. Nat Biotechnol. 2006;24:1211-1217.
6. Farazuddin M, Chauhan A, Khan RM, Owais M. Biosci Rep. 2011; 31:265-272.
7. Farazuddin M, Sharma B, Khan AA, Joshi B, Owais M.Anticancer efficacy of perillyl alcohol-bearing PLGA microparticles. Int J Nanomedicine. 2012; 7:35-47.
8. Owais M, Varshney GC, Choudhury A, Chandra S, Gupta CM. Chloroquine encapsulated in malaria-infected erythrocyte-specific antibody-bearing liposomes effectively controls chloroquine-resistant Plasmodium berghei infections in mice. Antimicrob Agents Chemother. 1995;39:180-4.
9. Chouhan A, Zubair S, Nadeem A, Ansari SA, Ansari MY, Mohammad O. Escheriosome-mediated cytosolic delivery of PLK1-specific siRNA: potential in treatment of liver cancer in BALB/c mice. Nanomedicine (Lond). 2014; 9:407-20.
10. Singha H, Mallick AI, Jana C, Isore DP, Goswami TK, Srivastava SK, Azevedo VA, Chaudhuri P, Owais M. Escheriosomes entrapped DNA vaccine co-expressing Cu-Zn superoxide dismutase and IL-18 confers protectionagainst Brucella abortus. Microbes Infect. 2008; 10:1089-96.
11. Eldar-Boock A, Polyak D, Scomparin A, Satchi-Fainaro R. Nano-sized polymers and liposomes designed to deliver combination therapy for cancer. Curr Opin Biotechnol. 2013; 24:682-9.
12. Knipe JM, Peters JT, Peppas NA. Theranostic agents for intracellular gene delivery with spatiotemporal imaging. Nano Today. 2013;8:21-38.
13. Oh J, Yoon H and Park JH. Nanoparticle Platforms for Combined Photothermal and Photodynamic Therapy. Biomed Eng Lett. 2013; 3:67-73.
14. Yuan X, Shah BA, Kotadia NK, Li J, Gu H, Wu Z. The development and mechanism studies of cationic chitosanmodified biodegradable PLGA nanoparticles forefficient siRNA drug delivery. Pharm Res. 2010; 27:1285-95.
15. Sahu SK and Prusty AK. Toxicological and Regulatory Consideration of Pharmaceutically Important Nanoparticles. J Cur Pharm Res. 2010; 3: 08-12.
16. Owais M, Ahmed I, Krishnakumar B, Jain RK, Bachhawat BK, Gupta CM. Tuftsin-bearing liposomes as drug vehicles in the treatment of experimental aspergillosis. FEBS Lett. 1993; 326:56-8.

17. Khan MA, Nasti TH, Saima K, Mallick AI, Firoz A, Wajahul H, Ahmad N, Mohammad O. Coadministration of immunomodulator tuftsin and liposomised nystatin can combat less susceptibe Candida albicans infection in temporarily neutropenic mice. FEMS Immunol Med Microbiol. 2004; 41:249-58.

18. Khan MA, Nasti TH, Owais M. Incorporation of amphotericin B in tuftsin-bearing liposomes showed enhanced efficacy against systemiccryptococcosis in leucopenic mice. J Antimicrob Chemother. 2005;56:726-31.

19. Khan MA, Owais M. Immunomodulator tuftsin increases the susceptibility of Cryptococcus neoformans to liposomal amphotericin B in immunocompetent BALB/c mice. J Drug Target. 2005;13:423-9.

20. Khan MA, Ahmad N, Moin S, Mannan A, Wajahul H, Pasha ST, Khan A, Owais M. Tuftsin-mediated immunoprophylaxis against an isolate of Aspergillus fumigatus shows less in vivo susceptibility to amphotericin B. FEMS Immunol Med Microbiol. 2005;44:269-76.

21. Khan A, Khan AA, Dwivedi V, Ahmad MG, Hakeem S, Owais M. Tuftsin augments antitumor efficacy of liposomized etoposide against fibrosarcoma in Swiss albino mice. Mol Med. 2007;13 :266-76.

22. Mishra S, Webster P, Davis ME. PEGylation significantly affects cellular uptake and intracellular trafficking of non-viral gene delivery particles. Eur J Cell Biol. 2004; 83: 97–111.

23. Veronese FM, Pasut G. PEGylation, successful approach to drug delivery. Drug Discov Today. 2005; 10:1451-1458.

24. Ganson NJ, Kelly SJ, Scarlett E, Sundy JS, Hershfield MS. Control of hyperuricemia in subjects with refractory gout, and induction of antibody against poly(ethylene glycol) (PEG), in a phase I trial of subcutaneous PEGylated urate oxidase. Arthritis Res Ther. 2006;8:R12.

25. Schroeder A, Heller DA, Winslow MM, Dahlman JE, Pratt GW, Langer R, Jacks T, Anderson DG. Treating metastatic cancer with nanotechnology. Nat Rev Cancer. 2011; 12:39-50.

26. Kamada H, Tsutsumi Y, Sato-Kamada K, Yamamoto Y, Yoshioka Y, Okamoto, T, Nakagawa S, Nagata S and Mayumi T. Synthesis of a poly(vinylpyrrolidone-codimethyl maleic anhydride) co-polymer and its application for renal drug targeting. Nat Biotechnol. 2003; 21: 399-404.

27. Owais M, Sharad KS, Shehbaz A, Saleemuddin M. Antibacterial efficacy of Withania comnifera (ashwagandha) an indigenous medicinal plant against experimental murine salmonellosis. Phytomedicine. 2005;12:229-35.

28. Khan A, Shukla Y, Kalra N, Alam M, Ahmad MG, Hakim SR, Owais M. Potential of diallyl sulfide bearing pHsensitive liposomes in chemoprevention against DMBA induced skinpapilloma. Mol Med. 2007;13:443-51.

29. Hoque M, Dave S, Gupta P, Saleemuddin M. Oleic Acid May Be the Key Contributor in the BAMLET-Induced Erythrocyte Hemolysis and Tumoricidal Action. PLoS One. 2013; 8:e68390.

30. Maroof A, Farazuddin M, Owais M. Potential use of liposomal diallyl sulfide in the treatment of experimental murine candidiasis. Biosci Rep. 2010;30:223-31.

31. Ronnie TP poon and Nicholas borys. Lyso thermosensitive liposomal doxorubicin : an adjuvant to increase the cure rate of radiofrequency ablation in liver cancer. Future Oncol. 2011; 7: 937-45.

32. Deng L, Zhang Y, Ma L, Jing X, Ke X, Lian J, Zhao Q, Yan B, Zhang J, Yao J, Chen J.Comparison of anti-EGFR-Fab' conjugated immunoliposomes modified with two different conjugation linkers for siRNa delivery in SMMC-7721 cells. Int J Nanomedicine. 2013; 8:3271-83.

33. Hoffman RM. The feasibility of targeted selective gene therapy ofthe hair follicle. Nat Med. 1995;1:705-6.

34. Perini G, Saettone MF, Carafa M, Santucci E, Alhaique F. Niosomes as carriers for ophthalmic drugs: in vitro/in vivo evaluation. Boll Chim Farm. 1996;135:145-6.

35. Sankhyan A and Pawar P. Recent Trends in Niosome as Vesicular Drug Delivery System. J App Pharma Sci. 2012; 02:20-32.

36. Alam M, Zubair S, Farazuddin M, Ahmad E, Khan A, Zia Q, Malik A, Mohammad O. Development, characterization and efficacy of niosomal diallyl disulfide in treatment of disseminated murine candidiasis. Nanomedicine. 2013; 9:247-256.

37. Chandu VP, Arunachalam A, Jeganath S, Yamini K, Tharangini K, Chaitanya G. Niosomes: A Novel Drug Delivery System. Int J Nov Trends In Pharm. 2012; 2: 25-31.

38. Yasam VR, Jakki SL, Natarajan J, Kuppusamy G. A review on novel vesicular drug delivery: proniosomes. Drug Deliv. 2014;21:243-9.

39. Owais M, Masood AK, Agrewala JN, Bisht D, Gupta CM. Use of liposomes as an immunopotentiating delivery system: in perspective of vaccine development. Scand J Immunol. 2001;54:125-32.

40. Ahmad N, Masood AK, Owais M. Fusogenic potential of prokaryotic membrane lipids: implication in vaccine development. Eur J Biochem. 2001;268:5667–75.

41. Khan AA, Jabeen M, Khan AA, Owais M. Anticancer efficacy of a novel propofol-linoleic acid-loaded escheriosomal formulation against murine hepatocellular carcinoma. Nanomedicine (Lond). 2013; 8:1281-1294.

42. Faisal SM, Yan W, McDonough SP, Chang CF, Pan MJ, Chang YF. Leptosome-entrapped leptospiral antigens conferred significant higher levels of protection thanthose entrapped with PC-liposomes in a hamster model. Vaccine. 2009;27:6537-45.

43. Ansari MA, Zubair S, Mahmood A, Gupta P, Khan AA, Gupta UD, Arora A, Owais M. RD antigen based nanovaccine imparts long term protection by inducing memory response against experimentalmurine tuberculosis. PLoS One. 2011;6:e22889.

44. Omri A, Makabi-Panzu B, Agnew BJ, Sprott GD, Patel GB. Influence of coenzyme Q10 on tissue distribution of archaeosomes, and pegylated archaeosomes, administered to mice by oral and intravenous routes. J Drug Target. 2000;7:383-92.

45. Patel GB and Chen W. Archaeosomes as drug and vaccine nanodelivery systems. Nanocarrier Technologies, Springer, Netherlands, 2006; pp.17-40.

46. Almeida AJ, Souto E. Solid lipid nanoparticles as a drug delivery system for peptides and proteins. Adv Drug Deliv Rev. 2007;59:478-90.

47. Zhang H, Zhang FM, Yan SJ. Preparation, in vitro release, and pharmacokinetics in rabbits of lyophilized injection of sorafenib solid lipid nanoparticles. Int J Nanomedicine. 2012;7:2901-10.

48. Lee MK, Lim SJ, Kim CK. Preparation, characterization and in vitro cytotoxicity of paclitaxel-loaded sterically stabilized solid lipid nanoparticles. Biomaterials. 2007;28:2137-46.

49. Wang P, Zhang L, Peng H, Li Y, Xiong J, Xu Z. The formulation and delivery of curcumin with solid lipid nanoparticles for the treatment of on non-small cell lung cancer both in vitro and in vivo. Mater Sci Eng C Mater Biol Appl. 2013;33:4802-8.

50. Qi J, Lu Y, Wu W. Absorption, disposition and pharmacokinetics of solid lipid nanoparticles. Curr Drug Metab. 2012;13:418-28.

51. Almeida AJ, Souto E. Solid lipid nanoparticles as a drug delivery system for peptides and proteins. Adv Drug Deliv Rev. 2007;59:478-90.

52. Jain RA. The manufacturing techniques of various drug loaded biodegradable poly(lactide-coglycolide) (PLGA) devices. Biomaterials. 2000; 21:2475–2490.

53. Kim TY, Kim DW, Chung JY, Shin SG, Kin SC, Heo DS, Kim NK, Bang YJ. Phase I and pharmacokinetic study of Genexol-PM, a cremophor-free, polymeric micelle-formulated paclitaxel, in patients with advanced malignancies. Clin Cancer Res. 2004;10:3708–16.

54. Farazuddin M, Dua B, Zia Q, Khan AA, Joshi B, Owais M. Chemotherapeutic potential of curcumin bearing microcells against hepatocellular carcinoma in model animals. Int J Nanomedicine. 2014; 9:1139-52.

55. Zhang L, Chan JM, Gu FX, Rhee JW, Wang AZ, Radovic-Moreno AF, Alexis F, Langer R, Farokhzad OC. Self-assembled lipid--polymer hybrid nanoparticles: a robust drug delivery platform. ACS Nano. 2008;2:1696-702.

56. Hu CM, Zhang L, Aryal S, Cheung C, Fang RH, Zhang L. Erythrocyte membrane-camouflaged polymeric nanoparticles as a biomimetic delivery platform. Proc Natl Acad Sci U S A. 2011;108:10980-5.

57. Hu CM, Fang RH, Copp J, Luk BT, Zhang L. A biomimetic nanosponge that absorbs pore-forming toxins. Nat Nanotechnol. 2013;8:336-40.

58. Matsumura Y and Maeda H. A new concept for macromolecular therapies in cancer chemotherapy: mechanism of tumouritropic accumulation of proteins and the antitumour agent SMANCS. Cancer Res.1986; 6:6387–6392.

59. Nafee N, Taetz S, Schneider M, Schaefer UF, Lehr CM. Chitosan-coated PLGA nanoparticles for DNA/RNA delivery: effect of the formulation parameters on complexation and transfection of antisense oligonucleotides. Nanomedicine. 2007;3:173-83.

60. Yuan X, Shah BA, Kotadia NK, Li J, Gu H, Wu Z. The development and mechanism studies of cationic chitosanmodified biodegradable PLGA nanoparticles forefficient siRNA drug delivery. Pharm Res. 2010;27:1285-95.

61. Gillies ER, Frechet JM. Dendrimers and dendritic polymers in drug delivery. Drug Discov Today. 2005;10:35-43.

62. Zhou J, Wu J, Hafdi N, Behr JP, Erbacher P, Peng L. PAMAM dendrimers for efficient siRNA delivery and potent gene silencing. Chem Commun (Camb). 2006; 22:2362-4.

63. Weber N, Ortega P, Clemente MI, Shcharbin D, Bryszewska M, de la Mata FJ, Gomez R, Munoz-Fernandez MA. Characterization of carbosilane dendrimers as effective carriers of siRNA to HIV-infected lymphocytes. J Control Release. 2008;132:55-64.

64. Taratula O, Garbuzenko OB, Kirkpatrick P, Pandya I, Savla R, Pozharov VP, He H, Minko T. Surface-engineered targeted PPI dendrimer for efficient intracellular and intratumoral siRNA delivery. J Control Release. 2009;140:284-293.

65. McCarroll J, Baigude H, Yang CS, Rana TM. Nanotubes functionalized with lipids and natural amino acid dendrimers: a new strategy to create nanomaterials for delivering systemic RNAi. Bioconjug Chem. 2010; 21:56-63.

66. Li S, Meng Lin M, Toprak MS, Kim do K, Muhammed M. Nanocomposites of polymer and inorganic nanoparticles for optical and magnetic applications. Nano Rev. 2010;1.

67. Papasani MR, Wang G and Hill RA. Gold nanoparticles: the importance of physiological principles to devise strategies for targeted drug delivery. Nanomedicine. 2012; 8:804-814.

68. Shan Y, Luo T, Peng C, Sheng R, Cao A, Cao X, Shen M, Guo R, Tomás H, Shi X.Gene delivery using dendrimer-entrapped gold nanoparticles as nonviral vectors. Biomaterials. 2012;33:3025-35.

69. Shukla R, Bansal V, Chaudhary M, Basu A, Bhonde RR, Sastry M. Biocompatibility of gold nanoparticles and their endocytotic fate inside the cellular compartment: a microscopic overview. Langmuir. 2005;21:10644-54.

70. Connor EE, Mwamuka J, Gole A, Murphy CJ, Wyatt MD. Gold nanoparticles are taken up by human cells but do not cause acute cytotoxicity. Small. 2005;1:325-7.

71. Ghosh P, Han G, De M, Kim CK, Rotello VM. Gold nanoparticles in delivery applications. Adv Drug Deliv Rev. 2008;60:1307-15.

72. Hong R, Han G, Fernández JM, Kim BJ, Forbes NS, Rotello VM. Glutathione-mediated delivery and release using monolayer protected nanoparticle carriers. J Am Chem Soc. 2006;128:1078-9.

73. Polizzi MA, Stasko NA, Schoenfisch MH. Water-soluble nitric oxide-releasing gold nanoparticles. Langmuir. 2007;23:4938-43.

74. Han G, You CC, Kim BJ, Turingan RS, Forbes NS, Martin CT, Rotello VM. Light-regulated release of DNA and its delivery to nuclei by means of photolabile gold nanoparticles. Angew Chem Int Ed Engl. 2006;45:3165-9.

75. Thakor AS, Jokerst J, Zavaleta C, Massoud TF, Gambhir SS. Gold nanoparticles: a revival in precious metal administration to patients. Nano Lett. 2011;11:4029-36.

76. Frens G. Controlled nucleation for the regulation of the particle size in monodisperse gold suspensions. Nature Phys Sci. 1973; 241:20–22.

77. Sun Y, Mayers B, and Xia Y. Metal Nanostructures with Hollow Interiors. Advanced Materials 2003; 15: 641–646.

78. Kundu S, Panigrahi S, Praharaj S, Basu S, Ghosh SK, Pal A, Pal T. Anisotropic growth of gold clusters to gold nanocubes under UV irradiation.Nanotechnology. 2007;18:075712.

79. Mitra RN and Das PK. In situ preparation of gold nanoparticles of varying shape in molecular hydrogel of peptide amphiphiles. J Phys Chem C. 2008; 112:8159–66.

80. Pyrpassopoulos S, Niarchos D, Nounesis G, Boukos N, Zafiropoulou I, Tzitzios V. Synthesis and self organization of Au nanoparticles. Nanotechnology. 2007;18:485-604.

81. Chauhan A, Zubair S, Tufail S, Sherwani A, Sajid M, Raman SC, Azam A, Owais M. Fungus-mediated biological synthesis of gold nanoparticles: potential in detection of liver cancer. Int J Nanomedicine. 2011;6:2305-19.

82. Dreaden EC, Mwakwari SC, Sodji QH, Oyelere AK, El-Sayed MA. Tamoxifen-poly(ethylene glycol)-thiol gold nanoparticle conjugates: enhanced potency and selective delivery for breast cancer treatment. Bioconjug Chem. 2009;20:2247-53.

83. Duncan B, Kim C, Rotello VM. Gold nanoparticle platforms as drug and biomacromolecule delivery systems. J Control Release. 2010;148:122-127.

84. Elbakry A, Zaky A, Liebl R, Rachel R, Goepferich A, Breunig M. Layer-by-Layer Assembled Gold Nanoparticles for siRNA Delivery Nano Lett. 2009; 9:2059–2064.

85. Song WJ, Du JZ, Sun TM, Zhang PZ, Wang J. Gold Nanoparticles Capped with Polyethyleneimine for Enhanced siRNA Delivery. Small 2010; 6: 239–246.

86. Han L, Zhao J, Zhang X, Cao W, Hu X, Zou G, Duan X, Liang XJ. Enhanced siRNA delivery and silencing gold-chitosan nanosystem with surface charge-reversal polymer assembly and good biocompatibility. ACS Nano. 2012; 6:7340-7351.

87. Ghosh R, Singh LC, Shohet JM, Gunaratne PH. A gold nanoparticle platform for the delivery of functional microRNAs into cancer cells. Biomaterials. 2013; 34:807-16.

88. Braun GB, Pallaoro A, Wu G, Missirlis D, Zasadzinski JA, Tirrell M, Reich NO. Laser-Activated Gene Silencing via Gold Nanoshell-siRNA Conjugates. ACS Nano. 2009; 3:2007-15.

89. Huschka R, Barhoumi A, Liu Q, Roth JA, Ji L, Halas NJ. Gene silencing by gold nanoshell-mediated delivery and laser-triggered release of antisense oligonucleotide and siRNA. ACS Nano. 2012 ;6:7681-7691.

90. Papasani MR, Wang G, Hill RA. Gold nanoparticles: the importance of physiological principles to devise strategies for targeted drug delivery. Nanomedicine. 2012; 8:804-14.

91. Ghitescu L, Fixman A, Simionescu M, Simionescu N. Specific binding sites for albumin restricted to plasmalemmal vesicles of continuous capillary endothelium: receptor-mediated transcytosis. J Cell Biol. 1986; 102:1304-11.

92. Menk RH, Schültke E, Hall C, Arfelli F, Astolfo A, Rigon L, Round A, Ataelmannan K, MacDonald SR, Juurlink BH. Gold nanoparticle labeling of cells is a sensitive method to investigate cell distribution and migration in animal models of human disease. Nanomedicine. 2011;7:647-54.

93. Bonoiu AC, Mahajan SD, Ding H, Roy I, Yong KT, Kumar R, Hu R, Bergey EJ, Schwartz SA, Prasad PN. Nanotechnology approach for drug addiction therapy: gene silencing using delivery of gold nanorod-siRNAnanoplex in dopaminergic neurons. Proc Natl Acad Sci U S A. 2009;106:5546-50.

94. Massich MD, Giljohann DA, Seferos DS, Ludlow LE, Horvath CM, Mirkin CA. Regulating immune response using polyvalent nucleic acid gold nanoparticle conjugates. Mol Pharm. 2009; 6:1934-40.

95. Soutschek J, Akinc A, Bramlage B, Charisse K, Constien R, Donoghue M, Elbashir S, Geick A, Hadwiger P, Harboth J, John M, Kesavan V, Lavine G, Pandey RK, Racei T, Rajeev KG, Rohl I, Toudjarska I, Wang G, Wuschko S, Bumcrot D, Koteliansky V, Limmer S, Manoharan M, Vornlocher HP. Therapeutic silencing of an endogenous gene by systemic administration of modified siRNAs. Nature. 2004; 432:173-8.

96. Liu H, Chen D, Li L, Liu T, Tan L, Wu X, Tang F. Multifunctional gold nanoshells on silica nanorattles:a platform forthe combination of photothermal therapy andchemotherapy with low systemic toxicity. Angew Chem Int Ed Engl. 2011; 50:891-5.

97. Moghimi SM, Hunter AC, Murray JC. Nanomedicine: current status and future prospects. FASEB J. 2005;19:311-30.

98. Salvador-Morales C, Flahaut E, Sim E, Sloan J, Green ML, Sim RB. Complement activation and protein adsorption by carbon nanotubes. Mol Immunol. 2006;43:193-201.

99. Murakami H, Nakashima N. Soluble carbon nanotubes and their applications. J Nanosci Nanotechnol. 2006;6:16-27.

100. Liu Z, Sun X, Nakayama N, Dai H. Supramolecular Chemistry on Water-Soluble Carbon Nanotubes for Drug Loading and Delivery. ACS Nano 2007; 1:50–56.

101. Liu Z, Chen K, Davis C, Sherlock S, Cao Q, Chen X, Dai H. Drug delivery with carbon nanotubes for in vivo cancer treatment. Cancer Res. 2008; 68:6652-60.

102. Zhang Z, Yang X, Zhang Y, Zeng B, Wang S, Zhu T, Roden RB, Chen Y, Yang R. Delivery of telomerase reverse transcriptase small interfering RNA in complex with positively charged single-walled carbon nanotubes suppresses tumor growth. Clin Cancer Res. 2006;12:4933-4939.

103. Krajcik R, Jung A, Hirsch A, Neuhuber W, Zolk O. Functionalization of carbon nanotubes enables non-covalent binding and intracellular delivery of small interfering RNA for efficient knock-down of genes. Biochem Biophys Res Commun. 2008; 369:595-602.

104. Radomski A, Jurasz P, Alonso-Escolano D, Drews M, Morandi M, Malinski T, Radomski MW. Nanoparticle-induced platelet aggregation and vascular thrombosis. Br J Pharmacol. 2005; 146:882–93.

105. Sayes CM, Liang F, Hudson JL, Mendez J, Guo W, Beach JM, Moore VC, Doyle CD, West JL, Billups WE, Ausman KD, Colvin VL. Functionalization density dependence of single-walled carbon nanotubes cytotoxicity in vitro. Toxicol Lett. 2006; 161:135–42.

106. Shvedova AA, Castranova V, Kisin ER, Schwegler-Berry D, Murray AR, Gandelsman VZm Maynard A, Baron P. Exposure to carbon nanotube material: assessment of nanotube cytotoxicity using human keratinocyte cells. J Toxicol Environ Health A. 2003; 66:1909–26.

107. Warheit DB, Laurence BR, Reed KL, Roach DH, Reynolds GA, Webb TR. Comparative pulmonary toxicity assessment of single wall carbon nanotubes in rats. Toxicol Sci. 2004; 77:117–25.

108. Ravichandran P, Periyakaruppan A, Sadanandan B, Ramesh V, Hall JC, Jejelowo O, Ramesh GT. Induction of apoptosis in rat lung epithelial cells by multiwalled carbon nanotubes. J Biochem Mol Toxicol. 2009; 23:333–44.

109. Reddy AR, Reddy YN, Krishna DR, Himabindu V. Pulmonary toxicity assessment of multiwalled carbon nanotubes in rats following intratracheal instillation. Environ Toxicol. 2012;27:211-9.

110. Muller J, Huaux F, Moreau N, Misson P, Heilier JF, Delos M, Arras M, Fonseca A, Nagy JB, Lison D. Respiratory toxicity of multi-wall carbon nanotubes. Toxicol Appl Pharmacol. 2005; 207:221–31.

111. Sharma A, Madhunapantula SV and Robertson GP. Toxicological considerations when creating nanoparticle based drugs and drug delivery systems? Expert Opin Drug Metab Toxicol. 2012; 8:47–69.

112. Duan J, Mansour HM, Zhang Y, Deng X, et al., Reversion of multidrug resistance by co-encapsulation of doxorubicin and curcumin in chitosan/ poly(butyl cyanoacrylate) nanoparticles. Int J Pharm. 2012; 426:193-201.

113. Zhu C, Jung S, Luo S, Meng F, Zhu X, Park TG, Zhong Z. Co-delivery of siRNA and paclitaxel into cancer cells by biodegradable cationic micelles based on PDMAEMA-PCL-PDMAEMA triblock copolymers. Biomaterials 2010; 31(8):2408-16.

114. Huang HY, Kuo WT, Chou MJ, Huang YY. Co-delivery of anti-vascular endothelial growth factor siRNA and doxorubicin by multifunctional polymeric micelle for tumor growth suppression. J Biomed Mater Res A. 2011; 330-8.

115. Chang RS, Suh MS, Kim S, Shim G, Lee S, Han SS, Lee KE, Jeon H, Choi HG, Choi Y, Kim CW, Oh YK. Cationic drug-derived nanoparticles for multifunctional delivery of anticancer siRNA. Biomaterials. 2011; 32: 9785-9795.

116. Yin Q, Shen J, Chen L, Zhang Z, Gu W, Li Y. Overcoming multidrug resistance by co-delivery of Mdr-1 and surviving-targeting RNA with reduction-responsible cationic poly(β-amino esters). Biomaterials. 2012. 33: 6495-506.

117. Tabernero J, Shapiro GI, LoRusso PM, Cervantes A, Schwartz GK, Weiss GJ, Paz-Ares L, Cho DC, Infante JR, Alsina M, Gounder MM, Falzone R, Harrop J, White AC, Toudjarska I, Bumcrot D, Meyers RE, Hinkle G, Svrzikapa N, Hutabarat RM, Clausen VA, Cehelsky J, Nochur SV, Gamba-vitalo C, Vaishnaw AK, Sah DW, Gollob JA, Burris HA 3rd. First-in-humans trial of an RNA interference therapeutic targeting VEGF and KSP in cancer patients with liver involvement. Cancer Discov. 2013:406-17.

118. De Jong WH and Borm PJ. Drug delivery and nanoparticles:applications and hazards. Int J Nanomedicine. 2008;3:133-49.

119. Chauhan A, Zubair S, Sherwani A, Owais M. Aloe vera induced biomimetic assemblage of nucleobase into nanosized particles. PLoS One. 2012;7:e32049.